

Atmospheric Mercury in Vermont and New England: Measurement of deposition, surface exchanges and assimilation in terrestrial ecosystems

Final Project Report – Executive Summary – 1/16/2009

PI: Melody Brown Burkins, University of Vermont (UVM)
Co-PIs: Eric K. Miller¹, Ecosystems Research Group, Ltd.; Gerald J. Keeler, University of Michigan; and Jamie Shanley, US Geological Survey
Collaborators: Sean Lawson, VTANR-VMC; Jen Jenkins, Mim Pendelton, Carl Waite and Alan Strong, UVM; Rich Poirot, VTANR-APCD; Alan VanArsdale, USEPA; Mark Cohen, NOAA; Chris Rimmer, Kent McFarland, and Steve Faccio, Vermont Center for Ecostudies; and Robert J. Taylor, Texas A&M.
Project Officer: Eric Hall, USEPA

Executive Summary

Atmospheric mercury research began at the Underhill, Vermont Air Quality Site in 1992 sponsored by EPA and NOAA. The site, hosted by the University of Vermont Proctor Maple Research Center and the Vermont Monitoring Cooperative became a focus for research on the atmospheric chemistry, deposition and ecosystem cycling of mercury in New England. A community of mercury researchers from Vermont and New England contributed to and made effective use of the first decade of wet deposition measurements and ecosystem studies focused on Underhill and the Lake Champlain Basin. In 2003, these researchers worked together to set goals for the second decade of atmospheric mercury research at Underhill that began with this project.

The primary objectives of this project were to 1) continue year-round monitoring of mercury wet-deposition in the Lake Champlain Basin; 2) establish measurements of speciated (GEM, RGM, HGP) ambient atmospheric mercury; 3) conduct measurements of surface-atmosphere exchanges of gaseous elemental mercury (GEM) over a New England forest; and 4) evaluate possible pathways for assimilation of atmospheric mercury into the biota of terrestrial ecosystems of the region. The project investigators established collaborations and institutional support from a variety of partners to augment the core EPA-ORD funding provided by this project. The additional support allowed us to achieve the majority of objectives set forth by the group and to facilitate information transfer between this core project and related mercury research (Figure 1). The original project scope was reduced due to a Congressional EPA budget rescission that resulted in the elimination of funding for the final 2 years of the project. Below we briefly summarize the major results of EPA-ORD funded atmospheric mercury research from 2004 through 2008.

The revised project scope was broken down into the following subprojects:

- Long-term record of event-based precipitation mercury concentration and deposition at Underhill, VT
- Initial Characterization of precipitation methyl-mercury concentration and deposition
- Characterization of ambient atmospheric mercury speciation and concentrations (GEM, RGM, and HGP) and identification of potential sources
- Identification of source regions and meteorological conditions giving rise to elevated wet and dry mercury deposition
- Initial measurements of GEM exchanges over a forest canopy
- Mercury assimilation in a terrestrial food web
- Coordination with national, regional, and state mercury research

¹ Corresponding author for the final project report. Email: ekmiller@ecoystems-research.com Voice: 802-649-5550

Scope of VMC Atmospheric Mercury Studies

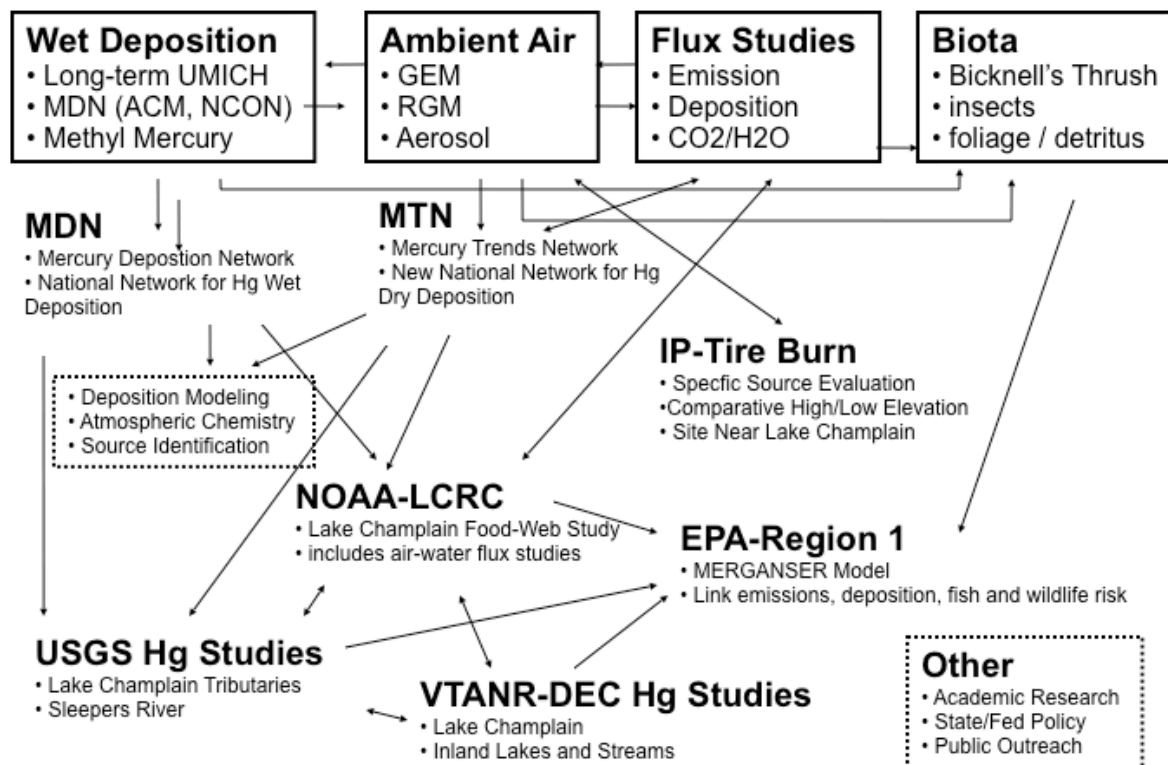


Figure 1. Scope of atmospheric mercury studies coordinated by the Vermont Monitoring Cooperative (VMC) centered on the core EPA-ORD funded atmospheric mercury project (top row of boxes).

Long-term record of event-based precipitation mercury and identification of potential mercury wet-deposition sources

Event-based wet deposition sampling at Underhill, VT was continued for the project duration and continues uninterrupted, maintaining the longest, continuous record of event-based atmospheric mercury deposition *in the world*. We conducted an intensive comparison of collector systems and protocols used for the measurement of mercury in precipitation. The results of this study were used to transition the long-term record at Underhill from the University of Michigan Air Quality Laboratory protocol (deployed from December 1992 through December 2006) to the national NADP-MDN network protocol (deployed at the site since 2004). This project provided a complete 2 calendar-year overlap between the records using different collectors, protocols, and laboratories (Figure 2). Wet-deposition measurements are currently being supported by a grant from NOAA through the Lake Champlain Research Consortium and now follow the NADP-MDN network protocol using event-based sampling.

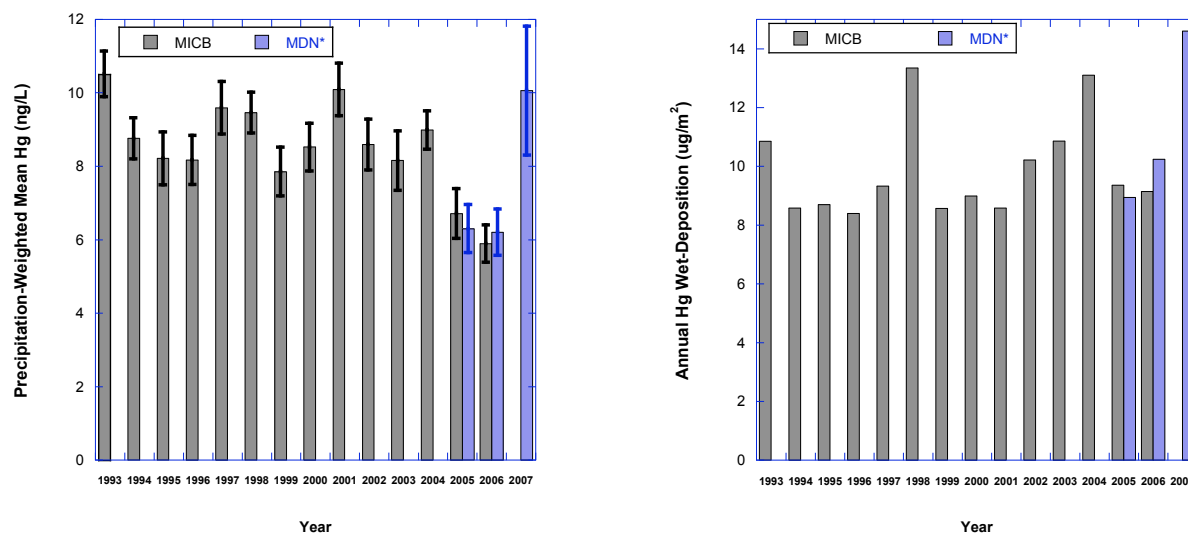


Figure 2. (Left) Annual precipitation-weighted mean Hg concentrations at Underhill, VT as determined by the MICB collector operating the UMAQL protocol with analysis at UMAQL (1993-2006) and the MDN ACM collector operating the MDN event protocol with analysis at Frontier Geosciences (2005-2007). MDN raw concentration values were adjusted by a factor of 1.22 (MDN*) as established by a 1-year collector comparison study. This factor compensates for different collector and sample train performance as well as a persistent laboratory bias. (Right) Annual wet-deposition of Hg at Underhill, VT as determined by the MICB (1993-2006) and the MDN ACM (2005-2007) collectors. The MDN deposition values were calculated from the corrected MDN concentrations and precipitation recorded by the NWS rain gage.

Analysis of the first decade of results obtained with the MICB sampler was conducted by Keeler et al. (2005) and reported in a special issue of the journal *Ecotoxicology*. This analysis demonstrated a strong seasonal pattern to both mercury concentrations and deposition with the highest deposition occurring during the warm season (late spring through early fall) at the peak of terrestrial and aquatic biological activity. Studies of air-mass back trajectories associated with the highest mercury wet-deposition events suggested sources to the west through south were primarily responsible for the largest deposition fluxes.

Annual mercury wet deposition averaged 10.1 ug/m^2 from 1993-2007 with a precipitation-weighted mean concentration of 8.5 ng/L and average precipitation rate of 120 cm/year . There was considerable year-to-year variation in precipitation, mercury concentration (Figure 2), and mercury deposition (Figure 2). Variations in climate (precipitation amount and atmospheric circulation – frequency of storms in air with favored trajectories) explain much of the year-to-year variation in mercury deposition at Underhill, VT.

There were major national (45%) and regional (54%) reductions of estimated mercury emissions during the period of observation. However, neither wet deposition nor the concentration of mercury in precipitation at Underhill declined in response to these reductions. Mercury deposition and concentration at Underhill were correlated with precipitation amount. Deposition was strongly seasonal and event driven with 44% of annual deposition occurring from June through August in conjunction with specific high-deposition events. Analysis of NOAA HYSPLIT model backward air mass trajectories indicated that likely source regions for high deposition events and the majority of

annual deposition were located to the south and west in areas with high densities of coal-fired electric generating units (EGUs) (Figure 3). In contrast to estimated total mercury emissions, estimated EGU emissions have been flat during the period of observation. Variation in precipitation amounts at Underhill and along transport paths appear to be responsible for much of the year-to-year variation in mercury wet deposition at Underhill, VT.

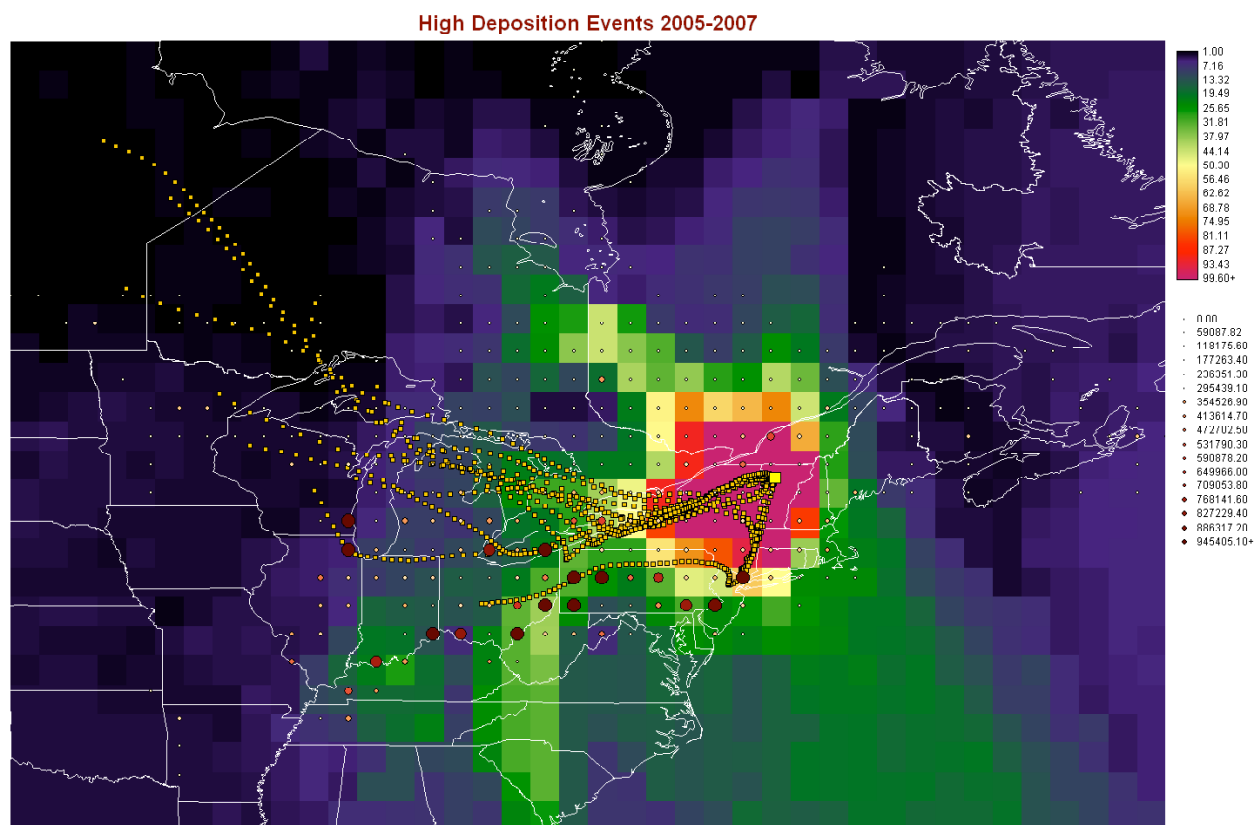


Figure 3. Mercury emissions sampled by air masses reaching Underhill, VT (large yellow square) during “High” deposition type precipitation events 2005-2007 (see text). The frequency of trajectory endpoints falling in a grid cell is shown by the color shading of the grid cells, illustrating the region of potential mercury sources. Overlaid on the grid are circles indicating (by color and size) the annual emissions from each grid cell (g/y). The grid cells with both a high frequency of trajectory crossing and high mercury emissions are the most likely sources for the mercury in wet deposition at Underhill, Vt. Overlaid in small yellow squares are the hourly (72-hours) HYSPLIT backward trajectory endpoints associated with precipitating periods during the event with collection ending on 7/17/2007. This single event provided the highest fraction of annual deposition of any event collected in the 15-year record. Major mercury emissions sources in NJ, central and western PA, OH, and possibly even IL contributed to this extreme event.

Initial characterization of precipitation methyl mercury

As has been observed elsewhere, trace amounts of methyl mercury (range 0.07-3.93%, mean 1.2% of total mercury) are present in precipitation sampled at Underhill, VT. The source of methyl mercury in precipitation is not clearly established and may be varied, but the majority seems quite likely to be the result of aqueous phase methylation of non-particle bound Hg^{2+} (Hammerschmidt et al. 2007). With the exclusion of two outliers (the top 2 high deposition events for total mercury 11.7%

and 7.9% of annual deposition during the methyl mercury sampling period 2005-2007), methyl mercury concentration was positively linearly correlated with total mercury concentration ($r^2 = 0.40$, $p = 0.0005$). This correlation is consistent with Hammerschmidt et al.'s (2007) hypothesis. A provisional estimate of the annual deposition of methyl mercury is $76.5 - 162 \text{ ng/m}^2/\text{y}$ (central estimate $116 \text{ ng/m}^2/\text{y}$) derived by multiplying the monthly volume-weighted mean methyl mercury concentrations by the average monthly precipitation and propagating uncertainties. This flux represents a significant delivery of methyl mercury to terrestrial and aquatic ecosystems in the region.

Characterization of ambient atmospheric mercury speciation and identification of potential sources

Earlier modeling studies indicated that RGM deposition could be nearly equal in magnitude to the wet deposition flux of Hg (Miller et al. 2005). At the outset of this project, there were few measurements of RGM levels in the US (e.g. Lindberg and Stratton 1998) and none in rural northern New England. The Vermont Agency of Natural Resources Air Pollution Control Division (VTANR-APCD) funded the acquisition of a Tekran 1130 RGM module for use with the Tekran 2537A as part of this project. The Tekran 1130 RGM module was deployed with the Tekran 2537A with inlets on the top of the forest canopy observation tower in 2004. This tower was destroyed in a severe storm in the winter of 2004 and equipment was repaired and relocated to the Underhill Air Quality site in the spring of 2005. We acquired and deployed an 1135 particulate mercury module in 2005. We also conducted one short-term deployment of a second system provide by USEPA Region1 at Shoreham, VT, allowing paired observations at a lake-level and mid-elevation site. These measurements were designed to characterize GEM, RGM, and HGP levels in terms of their diurnal, seasonal and spatial variation in the region. The measurements provided necessary information for dry-deposition modeling as well as the opportunity for analysis of potential mercury sources using air-mass back-trajectory methods.

Because of concerns about the comparability of measurements made from the differing inlet locations and heights from 2004 to 2005, the climatology of speciated mercury is presented based on measurements made from the longer record at the Air Quality Site. Measurements are reported from the period May 2005 through June 2008. GEM measurements were made every 5 minutes during the RGM and HGP 2-hour accumulation periods. GEM concentrations presented below are 2-hour averages of the 5-minute observations to be consistent with the 2-hour average concentrations represented by the RGM and HGP measurements.

GEM concentrations ranged from 0.81 to 5.58 ng/m^3 with a period average of 1.45 ng/m^3 . RGM concentrations ranged from 0 to 132.5 pg/m^3 with a period average of 3.56 pg/m^3 . HGP sampling spanned only 44% of the RGM measurement period due to the later acquisition date of the 1135 module, deployment at Shoreham, VT, and minor problems with the module. HGP ranged from 0 to 121 pg/m^3 with a period average of 11.50 pg/m^3 .

The observed concentrations of all three species were dependent on meteorological conditions but in different ways for RGM and HGP than for GEM. There were significant differences in concentrations based on surface wetness state (dry, moist, or wet), time of year, time of day, and in response to different atmospheric conditions. These variations are described in detail in the full report. Of particular note were the correlation of RGM concentrations with relative humidity, the correlation of HGP concentrations with water-vapor mixing ratio, and the tendency for GEM concentrations to rise after first insolation of a moist surface at dawn or after precipitation. The dependence of RGM concentrations on RH may reflect the tendency for that species to be readily scavenged by moist

aerosols at moderate RH. The dependence of HGP on the water vapor mixing ratio may relate to HGP source regions and accompanying seasonal variations in water vapor.

The concentrations of the three mercury species exhibited strong seasonal patterns that were slightly out of phase with each other (Figure). GEM concentrations peak in winter and spring with an early fall minimum, HGP concentrations peak in late winter and RGM concentrations peak in spring (Figure 4). The wintertime peak in HGP may be due, in part, to increased local combustion for home heating. However, trajectory analysis (discussed below) also indicates major out-of-region sources contribute to the observed HGP signal. The spring peak in RGM is likely due to a combination of factors including favored trajectories over major EGU RGM sources and relatively low atmospheric moisture levels at a time when leaves are off of trees along the favored trajectories. As soon as leaves emerge in late spring and early summer, the surface area for dry-deposition removal along the transport pathway increases by a factor of 3 to 4. Atmospheric moisture and relative humidity increase as well, allowing more scavenging by particles and ultimately cloud and rain droplets. As discussed above, summer is the time of peak observed concentrations of Hg in precipitation. The patterns described here suggest more of the ionic mercury in the atmosphere is partitioned into the liquid phase during the summer months.

RGM and HGP concentrations exhibited two distinct temporal patterns that we interpret as driven by either 1) atmospheric mixing processes in conjunction with the balance between deposition and formation reactions and 2) regional transport episodes (Figure 5). The relatively long and continuous record of high-temporal resolution measurements permits unique analysis opportunities for understanding the atmospheric chemistry and regional transport of mercury. These analyses are discussed in detail in the full report. One example of these types of analyses is summarized here.

We adapted existing methods of potential source contribution analysis in order to make full use of the extensive data collected during this study. Our approach, continuous potential source contribution analysis (CPSCA) was developed to take advantage of the very large number of samples produced by semi-continuous high-time resolution analyzers (5-minute to hourly or 2-hour samples) for pollutants such as fine particles, O₃, SO₂, NO_x, and mercury. In addition to the increased number of samples provided by semi-continuous analyzers, each sample can be directly associated with a specific air-mass back trajectory as back-trajectories rarely differ significantly over the course of such short sample durations.

In the data set considered here there are 8,296 2-hour samples from a 26-month period. A 72-hour air-mass back-trajectory with hourly end-points reported was calculated using the NOAA HYSPLIT model with vertical mixing for the center of each 2-hour sample period. There were 588,285 trajectory end points that could each be associated with a concentration measurement at the receptor (Underhill, VT). Because all samples were used, and because the samples were nearly continuous and evenly spaced in time, multiple trajectories “sampled” or “represented” 2/3 of North America and the eastern Atlantic Ocean.

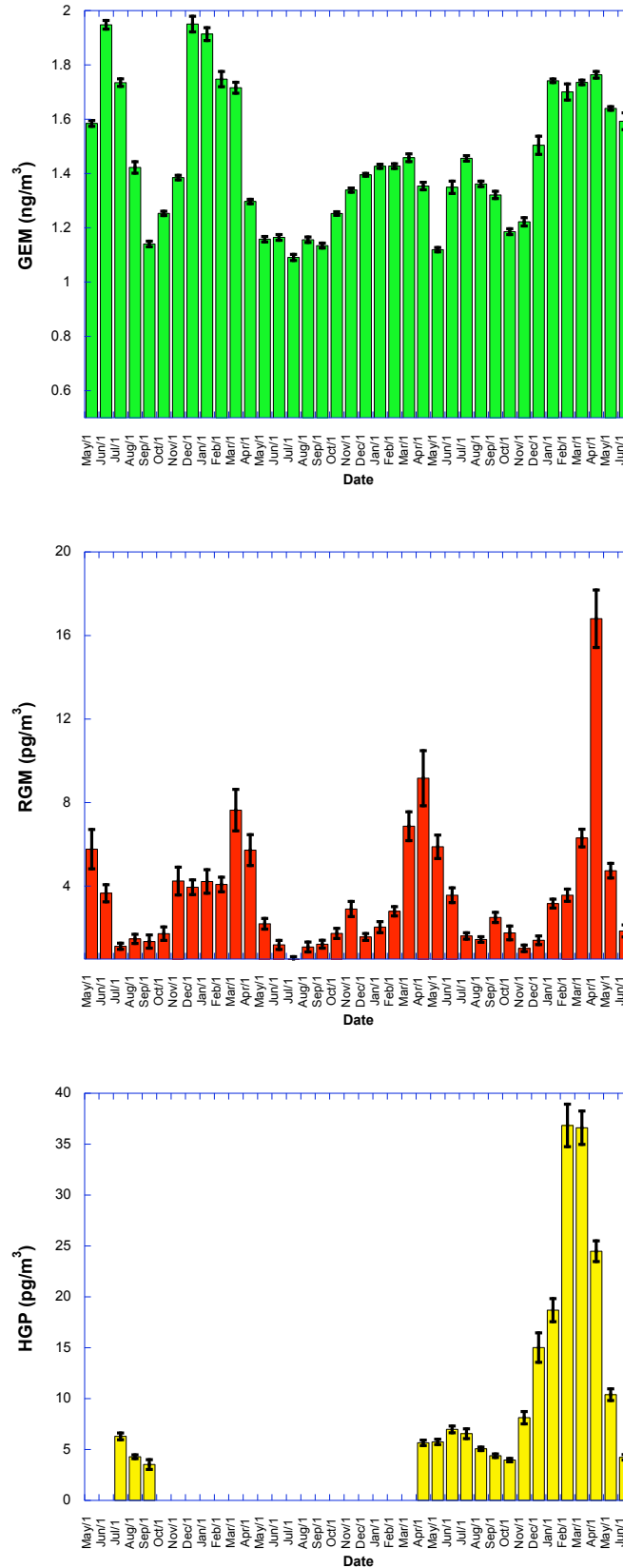


Figure 4. Time series of monthly average concentrations with standard errors for GEM (top), RGM (middle), and HGP (bottom) starting in May of 2005 and ending June 2008. GEM concentrations peak in winter and spring, HGP concentrations peak in late winter and RGM concentrations peak in spring.

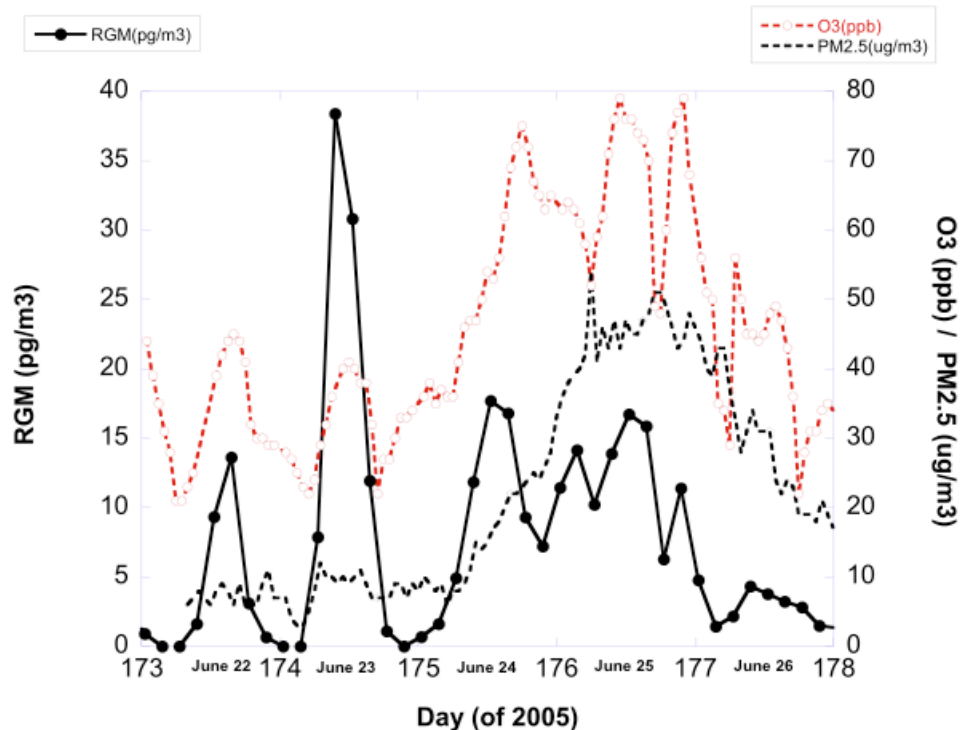


Figure 5. Example of the two primary temporal patterns of RGM and HGP (RGM only shown here). On June 22nd and 23rd, the strong diurnal cycle with concentrations returning to near zero a night suggest that dry-deposition processes outpace replenishment via production reactions or mixing of upper-level air during conditions of low atmospheric mixing at night. During the day, mixing (and/or production processes) outpace the deposition rate and allow surface air concentrations to increase. Ozone and PM levels are moderate on these two days and O₃ follows the same pattern as RGM for the same reasons. The record from June 24th through June 26th illustrates a typical regional transport episode with O₃, and RGM rising together and PM increases lagging slightly. The transport-event signature is the maintenance of moderate to high concentrations overnight. The daytime peaking during a transport event likely indicates additional production during those hours due to photochemistry or the mixing down to the surface of higher concentrations being transported at higher levels in the atmosphere.

The CPSC map for the average RGM at Underhill indicates potential major sources in a corridor from Tennessee through West Virginia and Pennsylvania (Figure 6). Important sources are also indicated in New Jersey and Southern New York. A potential significant source is indicated as far away as northeast Texas. A major potential marine source region is indicated in the western Atlantic Ocean east of Cape Cod. A less significant marine source is indicated from the region of Hudson Bay. Speciated mercury emissions data provided by Mark Cohen of NOAA-ARL representing 1999 emissions inventories for the US and Canada were used to determine the spatial and emissions magnitude correspondence with receptor concentrations associated with a given potential source location. Incinerator (municipal waste and medical) emissions, which are known to have been reduced dramatically since 1999, were excluded to avoid confounding the analysis.

There was an excellent spatial correspondence between emissions source locations and intensity and the potential source areas for a given average RGM concentration at the receptor (Figure 6). The different densities and intensities of sources appear clearly related to the average RGM

concentration arriving at the receptor attributable to a given source field. It is noteworthy that very large and very distant sources (NE Texas, base-metal smelter in Manitoba are indicated as potential sources by the CPSC map for mean RGM concentration. Additional CPSC maps shown in the full report (FR-sec3a-AmbHgSpec-2009-01-16.pdf) further serve to pinpoint the contribution of specific sources to the highest concentration events or “plume hits”.

CPSC maps were prepared for HGP and GEM and identify the different spatial distribution and intensities of anthropogenic HGP and GEM emissions. These analyses demonstrate that out-of-region and even very distant sources are significant contributors to the mercury burdens in New England’s terrestrial and aquatic ecosystems. These observations and source identification analyses will assist the air-quality modeling community in improving emissions transport models. Air-quality planners will make use of the information to target specific sources for emissions reductions.

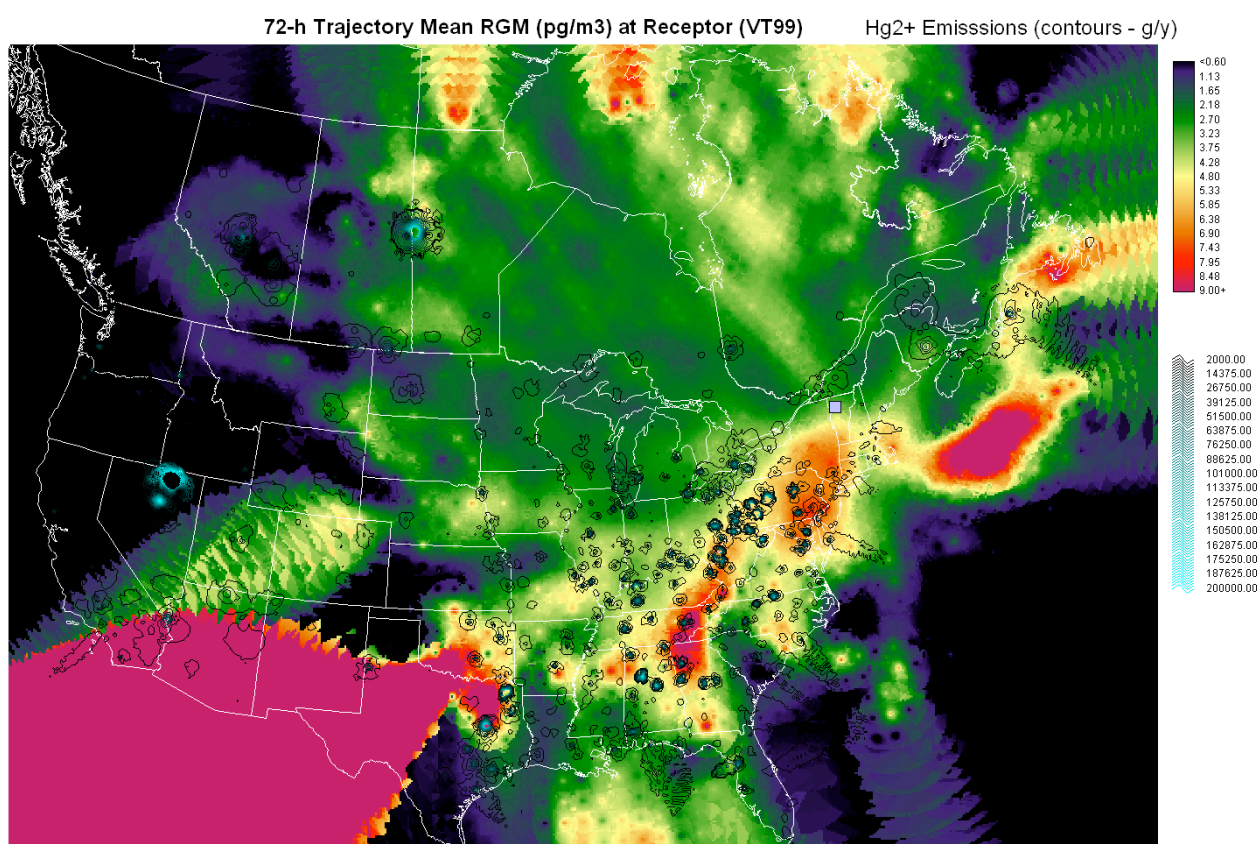


Figure 6. Overlay of 1999 US and Canada Hg²⁺ emissions (courtesy of Mark Cohen, NOAA-ARL) on the CPSC map for mean RGM at Underhill, VT. Emissions (g/y) are contoured with light blue indicating the highest emission rates. *SPECIAL NOTE: this report reflects work in progress. As this material is revised for publication figures will be improved. We plan to mask these figures at a specific value of number of trajectory endpoints per grid cell. This will eliminate the visual artifacts such as the large red area extending from western Texas where only a few trajectories endpoints were located (see Figure 12 in Final Report section 3a). The analysis discussed in this report ignores or discounts these artifacts. Please try to not be distracted by them. We did not have time to remake all the figures by the report submission deadline.*

Several potential “natural process²” sources are also indicated by the analysis, but cannot be compared with emissions data as the anthropogenic sources can. An example is the significant marine source of RGM in the western Atlantic Ocean east of Cape Cod. High halogen concentrations enhance the production of RGM in the marine boundary layer and this potential source location is consistent with the frequent inflow of Atlantic air into New England.

Measurements of GEM exchanges over a forest canopy

At the outset of the project there was tremendous uncertainty about the magnitude and the mechanisms governing net-gaseous Hg assimilation by forest canopies (Miller 2002, Lindberg et al. 1998). The most widely used inferential model for GEM deposition at the time (Lindberg et al. 1992) did not represent the known bi-directional nature of the GEM flux. It was clear from limited direct observations that at times GEM deposits and at times it is emitted from the forest canopy (Lindberg et al. 1998). It was also impossible to reconcile the large GEM fluxes implied by the Lindberg et al. (1992) model with the much smaller fluxes indicated by measurements of leaf-assimilated Hg (see Miller 2002, 2005). It appeared likely that Hg deposition/emission is governed by a compensation point, an ambient concentration above which deposition occurs and below which emission occurs (Hansen et al. 1995). Direct measurements of atmosphere-forest exchanges of GEM were needed to resolve this discrepancy, identify a potential field compensation point and to help elucidate the physical and physiological processes regulating GEM deposition or emission.

Direct, micrometeorological measurements of atmosphere-canopy exchanges of GEM were made using the modified Bowen-ratio method (Lindberg et al. 2002, Lindberg and Meyers 2001, Lee et al. 2000). Briefly, this method involves measuring the concentration gradient of mercury-vapor above the surface while concurrently measuring the gradient of either temperature (Lee et al. 2000) or water-vapor (Lindberg et al. 2002) and the turbulent flux of sensible or latent heat over the same height interval. The turbulent transfer coefficient derived from, for example, the latent heat flux and the water-vapor gradient is then assumed to apply to mercury vapor (Lindberg and Meyers 2001). The turbulent fluxes of latent and sensible heat were measured using the Bowen-ratio method and confirmed with sensible heat-fluxes measured by the eddy correlation method. The mercury gradient was measured with a Tekran 2537A. The GEM flux measurements were conducted from the VMC forest canopy observation tower at the Proctor Maple Research Center.

Bi-directional fluxes (both emission and deposition) were observed (Figure 7). Net emission and deposition fluxes ranged up to 1000 ng/m²/h. Deposition was typically observed during the day with high solar fluxes, while emission typically occurred at night or during cloudy periods. Companion measurements of CO₂ and water-vapor exchanges suggested peak deposition values occurred in conjunction with strong photosynthesis (Figure 8).

GEM exchange measurements and their analysis were limited by the rescission of funding for years 4 and 5 of the project and due to the unfortunate collapse of the forest canopy tower in the winter of 2004 which caused a significant delay in the measurement program.

² While there is no proximal anthropogenic source at the location for such “natural process” emissions as marine boundary-layer oxidation of GEM to form RGM, these processes must be understood to be at least partially, if not largely, anthropogenic sources. They convert previously largely anthropogenically emitted GEM to RGM.

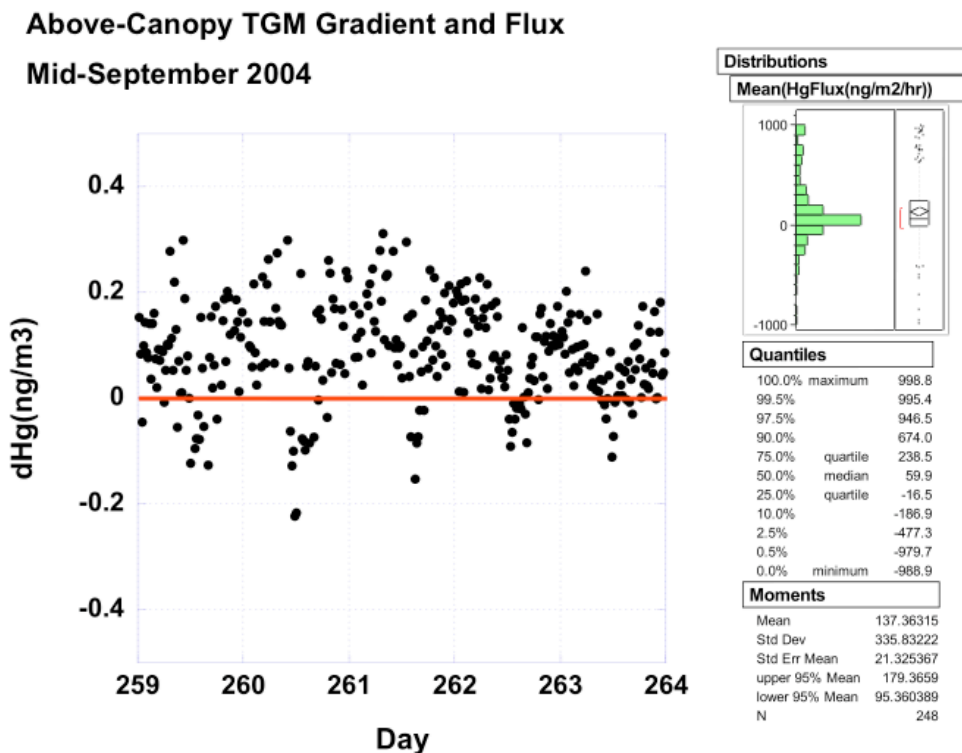


Figure 7. (Left) Example of diurnal and multi-day pattern of above-canopy mercury gradient. Positive values indicate emission of GEM and negative values indicated deposition to the forest canopy. (Right) Frequency distribution of fluxes.

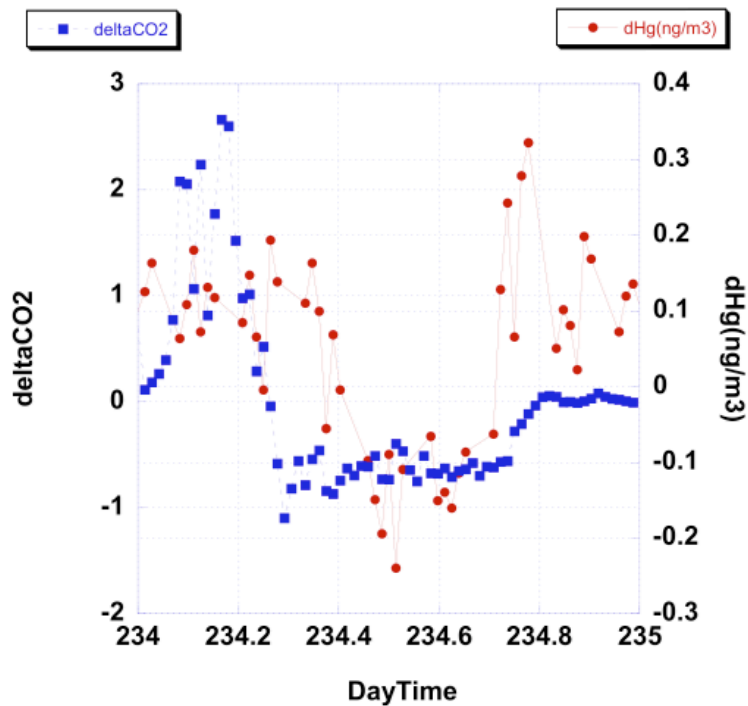


Figure 8. Example diurnal cycle of GEM and CO₂ gradients measured above the forest canopy. GEM deposition is indicated by the negative GEM gradients (red). GEM deposition is strongest at mid-day during intense photosynthesis (indicated by the strong negative CO₂ gradient - blue).

Mercury assimilation in a terrestrial food-web

Methylmercury (MeHg), the bioavailable form of mercury (Hg), is a neurotoxin with well-documented, adverse impacts on natural systems and wildlife populations. Most investigations of Hg bioaccumulation and biomagnification in the northeastern U.S. have focused on freshwater aquatic ecosystems, where conditions promoting methylation are common and Hg concentrations in upper trophic level consumers may be high (e.g., Bank et al. 2005, 2007; Chen et al. 2005; Evers et al. 2005; Yates et al. 2005). Research has increasingly demonstrated that Hg impairs reproductive performance, lifetime productivity, growth and development, behavior, motor skills, and survivorship in aquatic birds and other wildlife (Wolfe et al. 1998; Evers 2004, 2008; Scheuhammer et al. 2007). Despite the recent documentation of elevated Hg exposure in terrestrial biota (summary in Driscoll et al. 2007), relatively little is known about pathways for Hg uptake and transfer in upland ecosystems, or about Hg risk thresholds for terrestrial organisms.

In montane areas of northeastern North America, anthropogenic Hg deposition is 2-5 X higher than in surrounding low elevation areas (Miller et al. 2005). Although mechanisms that drive methylation in montane forests are poorly understood, Hg has recently been documented to bioaccumulate in montane fauna of the Northeast (Bank et al. 2005, Rimmer et al. 2005, Evers and Duron 2008). Bicknell's Thrush (*Catharus bicknelli*), in particular, has been shown to exhibit elevated Hg blood and feather concentrations among all age and sex classes across its breeding range (Rimmer et al. 2005). Understanding of Hg burdens in this species and in other components of its food web could contribute to species-specific and ecosystem-based conservation planning.

As part of long-term demographic research on montane forest bird populations in the northeastern U.S., we investigated the bioaccumulation and trophic transfer of Hg on Stratton Mountain (43° 05' N, 72° 55' W) in southern Vermont. From late May through late July in 2004-2006, we sampled discrete compartments in the terrestrial food web, using an established study site between 1075-1180 m elevation. To reflect a range of trophic levels, we sampled foliage, leaf litter, folivorous and carnivorous arthropods, a terrestrial salamander, an insectivorous passerine bird, two carnivorous raptors, and an omnivorous rodent. Salamanders, birds and rodents were sampled across a study area of c. 25 ha between 1075-1180 m elevation, while we collected foliage, leaf litter and arthropod samples at two sites 50 m apart at 1100 m elevation. Samples were analyzed at the Texas A&M University Trace Element Research Laboratory (TERL) by element-specific cold vapor atomic absorption.

Overall, Hg concentrations showed a pattern of biomagnification at successive trophic levels in the montane forest food web (Figure 9). Mercury concentrations increased from autotrophic organisms to herbivores < detritivores < omnivores < carnivores. Within the carnivores studied, raptors had higher blood mercury concentrations than their songbird prey. The Hg concentration in the blood of the study focal species Bicknell's thrush varied over the course of the summer. Upon arrival on the breeding ground Bicknell's thrush blood Hg increased above the levels carried over from the wintering grounds (Figure 10). By mid-June Bicknell's thrush blood Hg levels began a decline that continued through the end of observations (Figure 10).

The within-season changes in Bicknell's thrush blood Hg levels were consistent with a diet switch from the more abundant Hg rich prey of the detrital-based food-web dominant in early summer to a relatively lower Hg content prey of the foliage-based food web that was relatively more abundant in mid to late summer (Figure 11). There were significant year effects in different ecosystem compartments indicating a possible connection between atmospheric Hg deposition, detrital-layer Hg

concentrations, arthropod Hg concentrations, and passerine blood Hg levels. This project has accomplished possibly the first extensive characterization of mercury in a terrestrial food web.

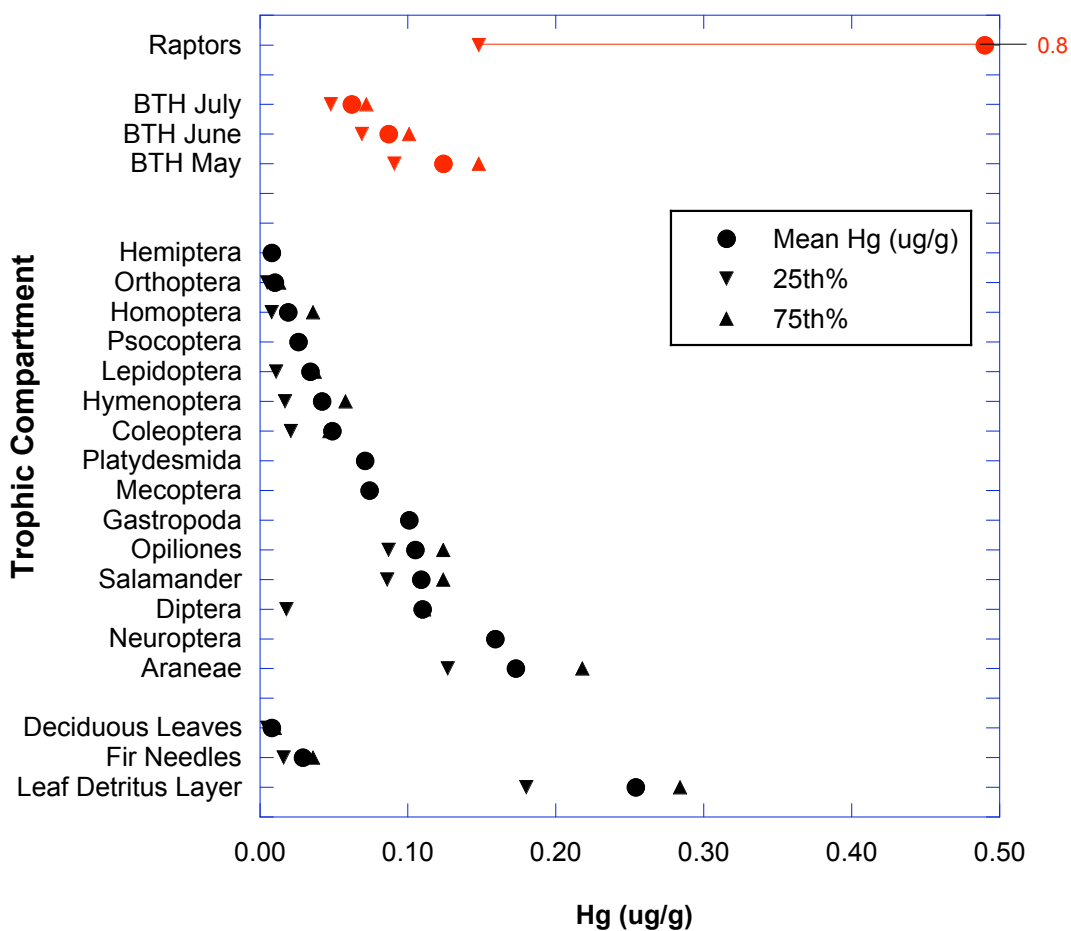


Figure 9. Mean, 25th, and 75th percentile Hg concentrations for leaf litter and biota sampled on Stratton Mountain, Vermont in 2004-2007. BTH = Bicknell’s thrush, the focal species of this study.

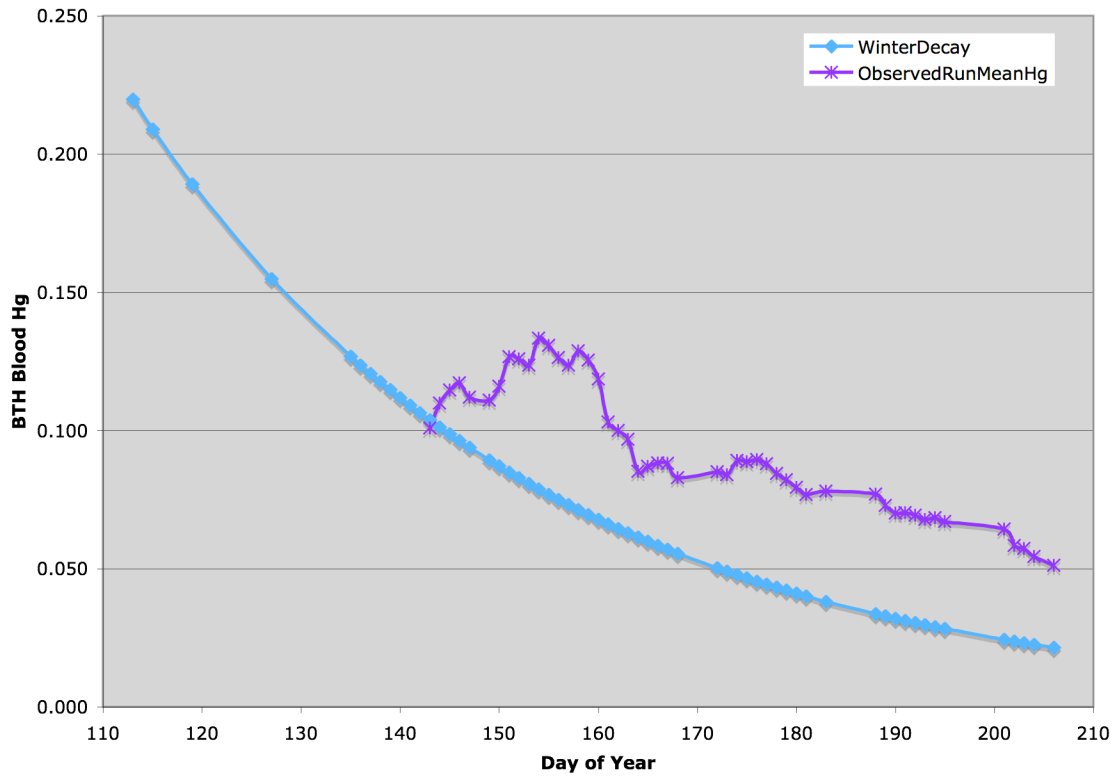
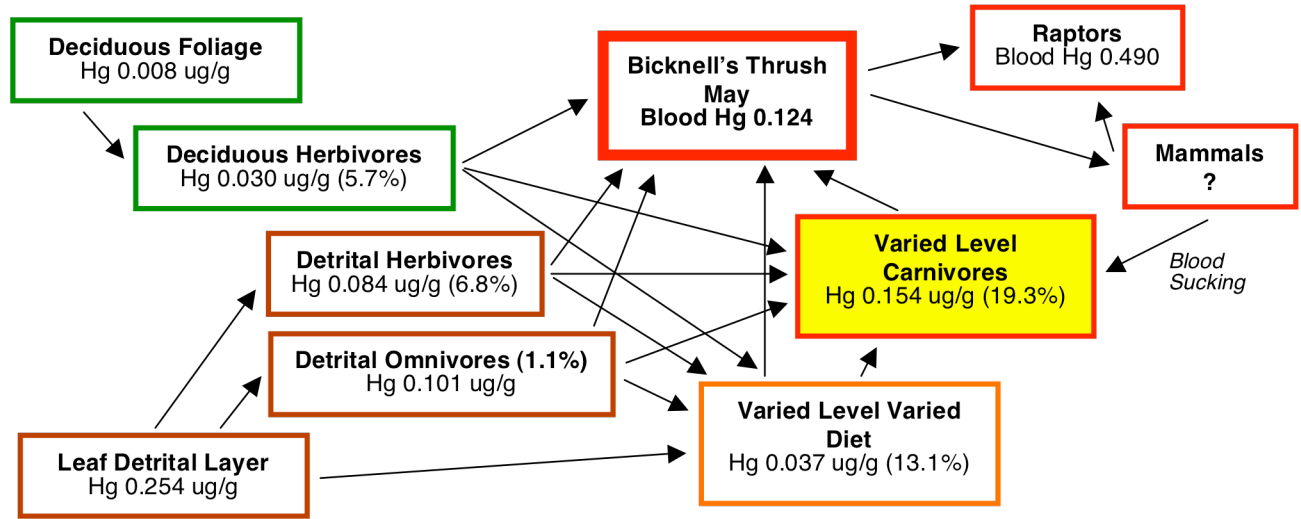


Figure 10. Exponential decay model (light blue) of the dissipation of wintering ground Hg burden and observations (purple) of Hg blood concentrations (ug/g) on the breeding ground in Bicknell’s thrush. Due to the fluctuations in number of birds captured and sampled daily, the observed blood levels are presented as the 10-day moving average. Bicknell’s thrush blood Hg initially increased after reaching the breeding ground. A decline in blood Hg levels began about mid-June.

Early Season Food Web



Late Season Food Web

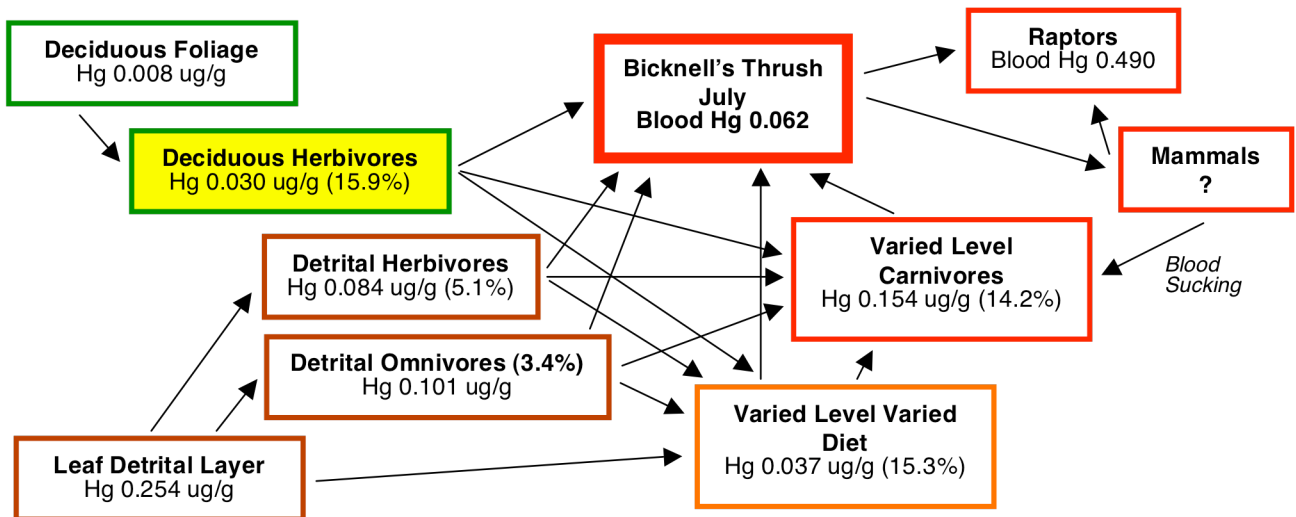


Figure 11. Shifts in food web structure from early to late summer in a montane ecosystem. The relative abundance of different arthropod feeding guilds (as percents in parentheses) and each compartment's mean Hg level are indicated. Food items from a detrital-based food web dominate the early season, while a canopy-based food web organisms increase in relative importance during the late summer season. Bicknell's Thrush (red) is the focal species in this study.

Coordination with national, regional, and state mercury research

The project personnel successfully coordinated with other mercury research efforts at local, regional and national levels. We used the new Hg information from the Underhill site and this project to estimate mercury deposition not only to the forested watersheds of Vermont, but also specifically to Lake Champlain in collaboration with researchers supported by the NOAA funded, Lake Champlain Research Consortium. More broadly, Drs. Miller and Keeler participated in the Northeast Mercury Research Group, a regional research group funded by the USDA Forest service (www.briloon.org/mercury). The three-way, west-east (WA-VT), precipitation mercury collector intercomparison was a collaboration designed to inform the national MDN program on potential improvements to collector design as well as to facilitate Underhill's transition from the UMAQL to the MDN system.

Observations and analyses of mercury concentrations and fluxes at Underhill are providing benefits to several mercury research groups working to model emissions-transport-deposition cycles at regional, national and global scales. The results of our trend analysis (no trend detected) for wet deposition and our source identification efforts for wet and dry deposition have informed state, regional, national, and international air-quality planning bodies about the identity of sources contributing mercury to the biologically sensitive New England region. Our pioneering assessment of mercury in a terrestrial food-web has highlighted the need for expanded consideration of the risks posed by atmospheric mercury deposition to terrestrial environments.

Dr. Miller participated in the technical working group designing protocols and operations standards for the proposed MTN (Mercury Trends Network), a new mercury dry deposition network being established by NADP. Dr. Miller provided detailed information on our operating procedures and data management process for use in developing the network SOP. Underhill served as demonstration site for the network and we hosted a field trip for NADP personnel to observe our operations in 2007. The Underhill site was one of the initial four sites funded by EPA-OAR-CAMD for start-up of the network in January of 2008.

Scientific communication and public outreach

In addition to the research coordination activities described above project personnel made numerous presentations about project activities and results at regional and national meetings. Dr. Miller produced a public-outreach overview document describing mercury research activities at Underhill in conjunction with the VMC. Interviews were granted to print and radio media to convey project results to the public. Several peer-reviewed scientific publications were prepared, accepted and published that made use of project data. Additional manuscripts are currently being prepared for submission by the project team. The final results of the project (which are the subjects of these manuscripts) will be presented at national meetings and communicated to the air-quality management community.

Organization of the Final Report and document file names

Section 0 – **Executive Summary** – “FR-sec0-ExecSum-2009-01-16.pdf”

Section 1 – **Introduction** – “FR-sec1-Introduction-2009-01-16.pdf”

Section 2a – **Event-Based Wet Deposition** – “FR-sec2a-Event-Wet-2009-01-16.pdf”

Section 2b – **Collector Comparison Manuscript** – “FR-sec2b-Collector-Comparison-2009-01-16.pdf”

Section 2c – **Long-Term Wet Deposition Manuscript** – “FR-sec2c-Long-Term-Record-2009-01-16.pdf”

Section 3a – **Ambient Air Mercury Speciation Studies** – “FR-sec3a-AmbHgSpec-2009-01-16.pdf”

Section 3b – **Shorham, VT Short-term Study** – “FR-sec3b-Shoreham-2009-01-16.pdf”

Section 4 – **GEM Flux Measurements** – “FR-sec4-GEMFlux-2009-01-16.pdf”

Section 5 – **Terrestrial Food-Web Study** – “FR-sec5-Food-Web-2009-01-16.pdf”

Section 6 – **Additional Project Activities** – “FR-sec6-EndSections-2009-01-16.pdf”

References

- Bank, M. S., C. S. Loftin, and R. E. Jung. 2005. Mercury bioaccumulation in northern two-lined salamanders from streams in the northeastern United States. *Ecotoxicology* 14:181–191.
- Bank, M. S., J. Crocker, B. Connery, and A. Amirbahman. 2007. Mercury bioaccumulation in green frog (*Rana clamitans*) and bullfrog (*Rana catesbeiana*) tadpoles from Acadia National Park, Maine, USA. *Environmental Toxicology and Chemistry* 26:118-125.
- Chen, C. Y., R. S. Stemberger, N. C. Kamman, B. M. Mayes, and C. L. Folt. 2005. Patterns of Hg bioaccumulation and transfer in aquatic food webs across multi-lake studies in the northeast US. *Ecotoxicology* 14:135-147.
- Driscoll, C. T., Y.-J. Han, C. Y. Chen, D. C. Evers, K. F. Lambert, T. M. Holsen, N. C. Kamman, and R. K. Munson. 2007. Mercury contamination in forest and freshwater ecosystems in the northeastern United States. *BioScience* 57:17-28.
- Evers D.C., O. P. Lane, L. Savoy, and W. Goodale. 2004. Assessing the impacts of methylmercury on piscivorous wildlife using a wildlife criterion value based on the Common Loon, 1998–2003. Gorham (ME): Maine Department of Environmental Protection, BioDiversity Research Institute. BRI Report 2004-05.
- Evers D. C., N. M. Burgess, L. Champoux, B. Hoskins, A. Major, W. M. Goodale, R. J. Taylor, R. Poppenga, and T. Daigle. 2005. Patterns and interpretation of mercury exposure in freshwater avian communities in northeastern North America. *Ecotoxicology* 14: 193–221.
- Evers, D. C. and M. Duron. 2008. Assessing the availability of methylmercury in terrestrial breeding birds of New York and Pennsylvania, 2005–2006. BRI Report 2008-15.
- Evers, D. C., L. J. Savoy, C. R. DeSorbo, D. E. Yates, W. Hanson, K. M. Taylor, L. S. Siegel, J. H. Cooley, Jr., M. S. Bank, A. Major, K. Munney, B. Mower, H. S. Vogel, N. Schoch, M. Pokras, M. W. Goodale, and J. Fair. 2008. Adverse effects from environmental mercury loads on breeding common loons. *Ecotoxicology* 17:69-81.
- Hammerschmidt, C. R., C.H. Lamborg, and W.F. Fitzgerald. (2007) Aqueous phase methylation as a potential source of methylmercury in wet deposition. *Atmos. Environ.* 41:1663-1668.
- Hanson, P.J., S.E. Lindberg, T.A. Tabberer, J.G. Owens, K.-H. Kim. 1995. Foliar exchange of mercury vapor: evidence for a compensation point. *Water, Air, and Soil Pollution* 80:373-382.
- Keeler, G.J., L.E. Gratz, and K. Al-Wali. (2005) Long-term Atmospheric Mercury Wet Deposition at Underhill, Vermont. *Ecotoxicology* 14, 71 –83.
- Lee, X., G. Benoit, X. Hu. 2000. Total gaseous mercury concentration and flux over a coastal saltmarsh vegetation in Connecticut, USA. *Atmos. Environ.* 34: 4205-4213.
- Lindberg, S.E., T.P. Meyers, G.E. Taylor, R.R. Turner, and W.H. Schroeder (1992) Atmosphere-Surface Exchange of Mercury in a Forest: Results of Modeling and Gradient Approaches. *Journal of Geophysical Research* 97:2519-2528.
- Lindberg, S.E. and T.P. Meyers. 2001. Development of an automated micrometeorological method for measuring the emission of mercury vapor from wetland vegetation. *Wetlands Ecology and Management* 9:333-347.
- Lindberg, S.E., W. Dong, and T. Meyers. 2002. Transpiration of gaseous mercury through vegetation in a subtropical wetland in Florida. *Atmos. Environ.* 36:5200-5219.
- Lindberg, S.E., P.J. Hanson, T.P. Meyers, and K.-Y. Kim. 1998. Micrometeorological studies of air/surface exchange of mercury over forest vegetation and a reassessment of continental biogenic mercury emissions. *Atmos. Environ.* 32:895-908.
- Lindberg, S. E., and W.J. Stratton. 1998. Atmospheric mercury speciation: Concentrations and behavior of reactive gaseous mercury in ambient air. *Environ. Sci. & Technol.* 32:49-57.
- Miller, E.K. 2000. Atmospheric Deposition to Complex Landscapes: HRDM – A Strategy for Coupling Deposition Models to a High-Resolution GIS. Proceedings of the National

Atmospheric Deposition Program Technical Committee Meeting, October 17-20, 2000, Saratoga Springs, New York.

- Miller, E.K. 2002. Estimation and Mapping of Wet and Dry Mercury Deposition Across the VT-NH Region. Project report submitted to Neil Kamman, VTDEC, Water Quality Division, 103 South Main St., Building 10 North, Waterbury, VT 05671-0408. Ecosystems Research Group, Ltd., Norwich, VT.
- Miller, E. K., A. VanArsdale, J. G. Keeler, A. Chalmers, L. Poissant, N. C. Kamman, and R. Brulotte. 2005. Estimation and mapping of wet and dry mercury deposition across northeastern North America. *Ecotoxicology* 14:53-70.
- Rimmer, C.C., K.P. McFarland, D.C. Evers, E.K. Miller, Y. Aubry, D. Busby, and R.J. Taylor. 2005. Mercury concentrations in Bicknell's Thrush and other insectivorous passerines in montane forests of northeastern North America. *Ecotoxicology* 14:223-240.
- Scheuhammer, A.M., Meyer, M.W., Sandheinrich, M.B. and Murray, M.W. 2007. Effects of environmental methylmercury on the health of wild birds, mammals, and fish. *Ambio* 36:12-19.
- Wolfe, M., Schwarzbach, F.S. and Sulaiman, R.A. 1998. Effects of mercury on wildlife: a comprehensive review. *Environmental Toxicology and Chemistry* 17: 146-60.
- Yates, D. E., D.T. Mayack, K. Munney, D. C. Evers, A. Major, T. Kaur, and R. J. Taylor. 2005. Mercury levels in mink (*Mustela vison*) and river otter (*Lontra canadensis*) from northeastern North America. *Ecotoxicology* 14:263-274.

Atmospheric Mercury in Vermont and New England: Measurement of deposition, surface exchanges and assimilation in terrestrial ecosystems

Final Project Report – Introduction – 1/16/2009

Investigators and Institutions:

Principal Investigator Melody Brown Burkins, PhD
The Rubenstein School of Environment and Natural Resources
University of Vermont
Burlington, Vermont 05405
Voice: 802-656-2982; email: melody.burkins@uvm.edu

Co-Principal Investigator Eric K. Miller, PhD
Ecosystems Research Group, Ltd. (ERG)
Aldrich House, 16 Beaver Meadow Road
Norwich, Vermont 05055
Voice: 802-291-0831; email: ekmiller@ecosystems-research.com

Co-Principal Investigator Gerald J. Keeler, PhD
University of Michigan
109 Observatory Street
Ann Arbor, Michigan 48109
Voice: 734-936-1836; email: jkeeler@umich.edu

Co-Principal Investigator Jamie Shanley, PhD
US Geological Survey
87 State Street
Montpelier, Vermont 05601
Voice: 802-828-4466; email: jshanley@usgs.gov

Collaborating / Cooperating Institutions:

Vermont Monitoring Cooperative
Vermont Agency of Natural Resources
Vermont Center for Ecostudies / Vermont Institute of Natural Sciences
Dartmouth College Trace-Element Analysis Facility
Texas A&M University Trace Element Research Lab
USGS Mercury Research Laboratory
NOAA - ARL

Overall Project Duration: June 1, 2003 to August 31, 2008

Full Funding Period: June 1, 2003 to August 31, 2006

EPA Project Officer:

Mr. Eric S. Hall
Exposure Modeling Research Branch, HEASD, NERL, ORD, USEPA
109 T.W. Alexander Drive, MD E205-2, Research Triangle Park, NC 27711
Hall.EricS@epa.gov (919) 541-3147

Project Overview

The primary objectives of this project were to 1) continue year-round monitoring of mercury wet-deposition in the Lake Champlain Basin; 2) establish measurements of speciated (GEM, RGM, HGP) ambient atmospheric mercury; 3) conduct measurements of surface-atmosphere exchanges of gaseous elemental mercury (GEM) over a New England forest; and 4) evaluate possible pathways for assimilation of atmospheric mercury into the biota of terrestrial ecosystems of the region.

The project was designed as part of an integrated program of research and monitoring of atmospheric deposition in the Lake Champlain Basin coordinated with NOAA, the Lake Champlain Research Consortium, The Vermont Agency of Natural Resources, and the Vermont Monitoring Cooperative. The project investigators participated in several major regional mercury research initiatives providing a connection between mercury research at Underhill, VT and regional efforts. The characterization and analysis of mercury deposition, surface exchanges, and assimilation in terrestrial ecosystems provided by this study has provided critical understanding of potential mercury response to regional and national reductions in atmospheric mercury emissions. The observational results and analysis provided by this study have applicability to regional assessments of mercury deposition, ecosystem mercury retention and the extent to which atmospherically deposited mercury is transferred to high trophic-level organisms in terrestrial environments.

Project Description

1. Background

Atmospheric mercury research began at Proctor Maple Research Center in Underhill, Vermont in 1992. Sponsored by EPA and NOAA, in collaboration with the University of Vermont and University of Michigan, the station embarked on an event-based sampling program for mercury in precipitation, aerosol particles and mercury vapor. Collecting rain and snowfall storm by storm, rather than the more common weekly sampling, allowed the investigators to relate the mercury concentration patterns in individual storms to specific air mass trajectories. In this way, geographic sources of atmospheric mercury emissions were more easily isolated. Underhill has the longest continuous running event-based mercury wet-deposition station *in the world*. This project provided a crucial comparison and critical evaluation of the 3 major types of mercury wet-deposition collectors used in regional and national wet-deposition networks. This comparison and analysis provided the information needed to transition the long-term mercury observations at Underhill using the University of Michigan MICB collector to the national Mercury Deposition Network monitoring protocol and collector. Inclusion of the Underhill site in the national network was an important step needed to provide national representation and evaluation of mercury risks to Vermont and Northern New England.

Vermont has also been a locus for pioneering research on the fate and transport of mercury in terrestrial and aquatic environments. Because of its quality high temporal-resolution data and its location in the Lake Champlain basin, estimates of atmospheric mercury deposition derived from the measurements at Underhill have been and continue to be used by scientists investigating mercury in terrestrial and aquatic environments. These programs have fostered a community of researchers including atmospheric scientists, hydrologists, limnologists, ecologists and biogeochemists who actively collaborate on the study of the impact of mercury on Vermont's and New England's ecosystems.

This consortium of researchers identified critical areas requiring research in order to advance understanding of the mercury exchanges between ecosystems and the atmosphere, the redistribution of mercury in the landscape, and the transfer of atmospherically deposited mercury to biota. The group formulated research questions that would provide substantial new insights in a short period of time and that would provide information useful for the assessment of mercury risks and impacts throughout the Northeastern USA. Eight priority tasks identified by the group were the focus of this project.

- 1) Extend the long-term record of mercury concentration in precipitation and gas-phase mercury (TGM) in air at Underhill, VT.
- 2) Characterize reactive gas phase mercury (RGM) concentrations at Underhill and other locations.
- 3) Characterize diurnal and daily variations in TGM and RGM within different seasons at Underhill.
- 4) Obtain measurements of vapor-phase mercury exchanges between the atmosphere and the landscape over several different landscape elements. And use these flux measurements to:
 - a. properly parameterize and validate micrometeorological models for atmosphere-surface mercury exchanges.
 - b. assess the magnitude of mercury remission from soils and plant canopies.
- 5) Use the refined and validated micrometeorological models together with the ambient TGM and RGM observations at Underhill to make improved estimates of net mercury deposition.
- 6) Measure rates of mercury accumulation in plant foliage and canopy throughfall over several growing seasons for comparison with model-based estimates of net TGM and RGM deposition.
- 7) Improve confidence in estimates of mercury retention within different landscape elements by comparing measured soil mercury inventories with inventories predicted by net deposition hindcasts using models for atmosphere-surface mercury exchanges and observations of mercury exports.
- 8) Make initial assessments of the potential transfer of atmospherically deposited mercury from plant foliage to high trophic level biota in terrestrial ecosystems.

The project attempted to address each of these objectives. Unfortunately, due to a Congressional rescission of the EPA budget and subsequent program budget decisions at EPA, the project did not receive funding for years 4 and 5 of the planned project. Thus we were not able to address all of the objectives to the extent described in the project proposal. Tasks 1-3 were deemed foundation tasks essential for developing reliable estimates of total atmospheric mercury deposition for Vermont and other northeastern states. Tasks 1-3 were completed as anticipated with support from funding partners and EPA-ORD. Research directed to Task 4 was more limited in scope than envisioned in the project proposal due to both the budget shortfall and due to an accident which disabled the forest-canopy observation tower during early stages of the project. The budget shortfall limited our ability to construct and deploy the planned mobile mercury measurement facility and to conduct flux measurements over different surface types. However, with supplementary funding from NOAA and VTANR we were able to conduct some short-term observations primarily for ambient-air speciation measurements near lake-level in the Lake Champlain Basin. Task 5 (incomplete due to funding rescission) we expect to address in the near future under separate funding despite the limited observations achieved under Task 4. Tasks 6 and 7 were eliminated due to the budget shortfall. Task 8 was satisfactorily addressed despite reduced activity due to the budget shortfall.

During the study, Task 2 was modified to include characterization of particulate-bound mercury (PBM, also referred to as HGP). This measurement was added after acquisition of a Tekran 1135 continuous particulate mercury measurement module, allowing more complete characterization of ambient atmospheric mercury. Task 3 was subsequently modified to include analysis and characterization of GEM, RGM, and HGP. An additional Task 9 was added during the project as the potential importance of atmospheric sources of methyl-mercury was recognized through the food-web study segment of the project (Task 8). We added measurements of methyl-mercury in monthly composite samples of precipitation in order to characterize the potential wet flux of methyl-mercury to both terrestrial and aquatic ecosystems. Late in the project, supplemental funds from NOAA allowed the analysis of event precipitation samples for methyl-mercury during the warm season. This provided the possibility to evaluate meteorological and transport conditions that might give rise to elevated methyl-mercury concentrations and wet-deposition.

As modified during the project, the principal objectives and tasks break down into the following subprojects:

- Long-term record of event-based precipitation mercury concentration and deposition at Underhill, VT
- Initial Characterization of precipitation methyl-mercury concentration and deposition
- Characterization of ambient atmospheric mercury speciation and concentrations (GEM, RGM, and HGP) at Underhill and other locations
- Identification of source regions and meteorological conditions giving rise to elevated wet and dry mercury deposition
- Initial measurements of GEM exchanges over a forest canopy
- Mercury assimilation in a terrestrial food web
- Coordination with national, regional, and state mercury research

Results from these projects have been transferred to natural resource management and human health communities via participation by project-affiliated scientists in the Governor's Task Force on Mercury, regional, national, and international meetings, and scientific publications.

Project Results

Results will be reviewed by subproject in separate documents. The methodologies employed will be briefly reviewed for each task.

Section 0 – **Executive Summary** – “FR-sec0-ExecSum-2009-01-16.pdf”

Section 1 – **Introduction** – “FR-sec1-Introduction-2009-01-16.pdf”

Section 2a – **Event-Based Wet Deposition** – “FR-sec2a-Event-Wet-2009-01-16.pdf”

Section 2b – **Collector Comparison Manuscript** – “FR-sec2b-Collector-Comparison-2009-01-16.pdf”

Section 2c – **Long-Term Wet Deposition Manuscript** – “FR-sec2c-Long-Term-Record-2009-01-16.pdf”

Section 3a – **Ambient Air Mercury Speciation Studies** – “FR-sec3a-AmbHgSpec-2009-01-16.pdf”

Section 3b – **Shorham, VT Short-term Study** – “FR-sec3b-Shoreham-2009-01-16.pdf”

Section 4 – **GEM Flux Measurements** – “FR-sec4-GEMFlux-2009-01-16.pdf”

Section 5 – **Terrestrial Food-Web Manuscript** – “FR-sec5-Food-Web-2009-01-16.pdf”

Section 6 – **Additional Project Activities** – “FR-sec6-EndSections-2009-01-16.pdf”

Atmospheric Mercury in Vermont and New England: Measurement of deposition, surface exchanges and assimilation in terrestrial ecosystems

Final Project Report – Event-Based Wet Deposition – 1/16/2009

PI: Melody Brown Burkins, University of Vermont (UVM)
Co-PIs: Eric K. Miller¹, Ecosystems Research Group, Ltd.; Gerald J. Keeler, University of Michigan; and
Jamie Shanley, US Geological Survey
Collaborators: Sean Lawson, VTANR-VMC; Jen Jenkins, Mim Pendelton, Carl Waite and Alan Strong, UVM;
Rich Poirot, VTANR-APCD; Alan VanArsdale, USEPA; Mark Cohen, NOAA;
Project Officer: Eric Hall, USEPA

Event-based precipitation mercury concentration and deposition at Underhill, VT

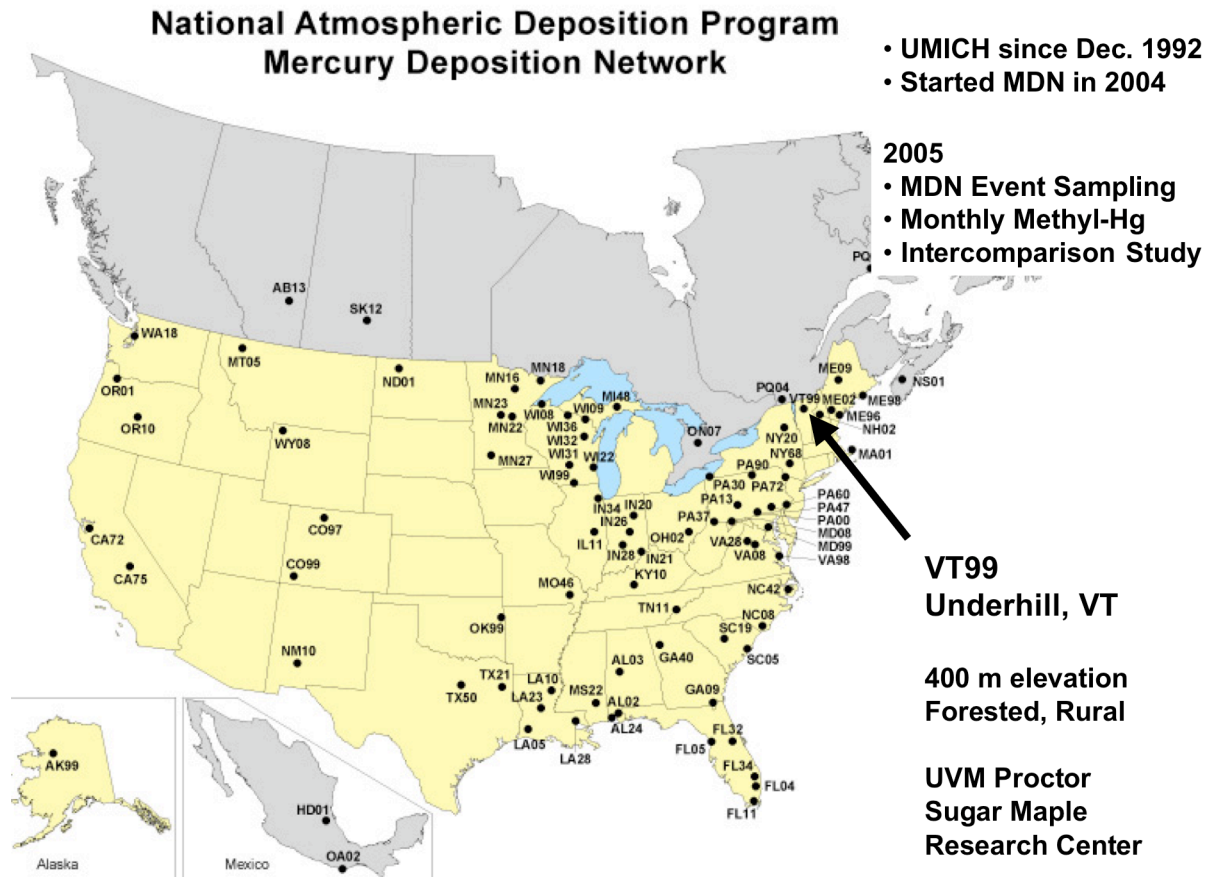
Event-based wet deposition sampling at Underhill, VT was continued for the project duration and continues uninterrupted, maintaining the longest, continuous record of event-based atmospheric mercury deposition *in the world*. These measurements are currently being supported by a grant from NOAA through the Lake Champlain Research Consortium and now follow the NADP-MDN network protocol using event-based sampling. The Underhill site (VT99) is currently a full member of MDN.

A principal goal of the project was to continue event collection and analysis of mercury in wet deposition following the UMAQL protocols that had been in place since the initiation of sampling at Underhill in 1992 (Burke et al. 1995) and were used by EPA elsewhere in New England (Alter 2000). At the outset of the project the University of Michigan expressed reluctance to continue precipitation analysis at the available funding level. Thus, we agreed as a group to analyze archived samples at UMAQL while new samples were to be directed to the Dartmouth College Trace Element Analysis Facility. We conducted an inter-laboratory comparison study using blind analysis of split precipitation samples (described below). After establishing the capability of the local (Dartmouth) laboratory to perform precipitation analyses, the University of Michigan agreed to continue serving as the precipitation analysis laboratory, so the services of the Dartmouth Lab were not required for the duration of the project. This was a better result, as we were able to maintain a consistent laboratory and protocol as well as maintain the interest and involvement of Dr. Keeler in the project.

Mid-way through the project it was made clear to the investigators that future funding of mercury wet deposition at Underhill through NOAA channels (EPA could not commit to long-term funding) would only be possible through the NADP MDN network. The investigators (with input from the broader mercury research community) agreed to begin NOAA-funded mercury wet-deposition measurements following the NADP, MDN protocols. MDN accepted VT99 (an already established NTN and AIRMoN site) into the network as a weekly sample site in 2004. VT99 transitioned to an MDN event-basis site beginning in 2005. The investigators requested and received additional support from MDN, NOAA, USGS and this project to conduct a comparison of the relative performance of the University of Michigan modified MICB, NCON and ACM samplers.

¹ Corresponding author for the final project report. Email: ekmillier at ecoystems-research.com Voice: 802-649-5550

The collector-comparison project facilitated the successful transition from wet-deposition measurements using the University of Michigan modified-MICB collector and the University of Michigan Air Quality Laboratory to wet-deposition measurements using the NCON collector and the Frontier Geosciences Mercury Analytical Facility as part of the national NADP Mercury Deposition Network (MDN). There were considerable challenges to overcome in transitioning between collectors, protocols, laboratories, and networks. As part of this project and in conjunction with NOAA, USGS and MDN we conducted a 3-way wet-deposition collector comparison. This trial characterized the relative performance of the MICB, NCON and ACM collectors for mercury wet-deposition. We identified strengths and weaknesses of each collector and protocol which lead to changes in collector design and network practices. The results of this study have been used to improve the performance and reliability of the MDN-sanctioned systems. We developed transfer functions that can be used to combine wet-deposition records developed using the three different collectors. A supplemental study in we conducted in 2007 suggested the persistent bias between the MICB collector and University of Michigan Protocol and the MDN collectors and MDN protocol is due in large part to differential sample train performance and an approximately 6% laboratory bias.



MICB – MDN (NCON, ACM) Collector Comparison

In partnership with MDN, the USGS, and NOAA, we initiated (August 2005) a 1-year precipitation mercury collector inter-comparison study. This study was the first to make scientific comparisons of the MIC-B (UMICH), MDN and NCON (USGS) collectors for event-based assessment of precipitation mercury deposition. All three types of collectors were in use in the Northeastern US at the start of the project. Data from these different collectors and networks could not readily be pooled and coordinated. This project developed transfer functions allowing data from the three collector types to be merged for regional analyses. This study also informed mercury researchers about the strengths and weaknesses of each collection system, guiding long-term mercury monitoring and upgrade efforts throughout the country. A manuscript for peer-review was produced (included below) but submission has been held up pending receipt of data from University of Michigan from paired deployment of the MDN and University of Michigan sample trains in the MICB collector. The MICB can hold up to 4 sample trains. We exposed multiple pairs of each type of sample train and sent one of each to each laboratory for processing and analysis. This experiment was designed to identify and eliminate and laboratory bias as well as to test the relative performance of each sample train when deployed in the same collector. The experimental design allowed us to separate the overall collector-protocol-laboratory bias into components of 1) collector, 2) sample-train, and 3) laboratory bias.

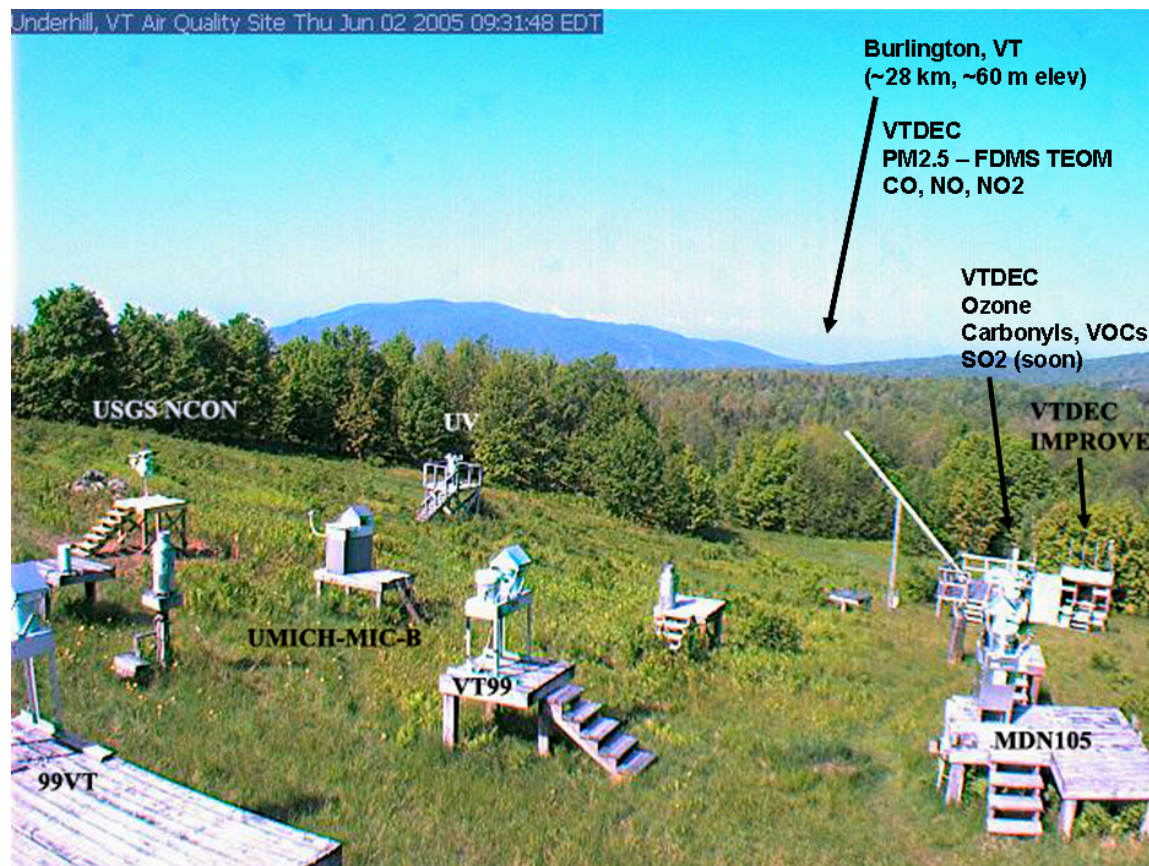


Figure 1. Location of mercury collectors for intercomparison study (left-to-right: USGS NCON, UMICH-MIC-B, MDN-ACM [MDN105]) at the Underhill, VT Air Quality Site. The locations of other air quality instrumentation are also noted.

PLEASE SEE THE SEPARATE DOCUMENT “FR-sec2b-Collector-Comparison-2009-01-16.pdf” FOR THE FULL REPORT ON THE COLLECTOR COMPARISON STUDY.

Dartmouth / University of Michigan Air Quality Laboratory Comparison

Ten precipitation samples spanning the range of generally observed concentrations at Underhill were split for analysis by both labs. There was good agreement between the two labs (Table and Figure 2, $r^2 = 0.97$, $p < 0.0001$). Individual samples showed a mean difference between the two labs of 0.42%, with a range of -10% to +17% $[(\text{Dartmouth} - \text{UMAQL}) / (\text{UMAQL}) * 100]$. There was no significant correlation of bias with concentration. There was no significant difference between the two labs as determined by a paired T-test. Dartmouth results were non-significantly higher (mean apparent bias +0.18 ng/L) while the median apparent bias was (0.08 ng/L). The maximum exhibited a deviation was 1.22 ng/L (Dartmouth higher). Dartmouth was never lower than Michigan by more than 0.33 ng/L.

Table. UMAQL / DARTMOUTH Laboratory Comparison for Mercury in Precipitation

| Samp# | Reps | DARTMOUTH | | | | UNIVERSITY OF MICHIGAN | | | | %Diff |
|-------|------|-----------|-------|-------|--------|------------------------|-------|-------|-------|-------|
| | | Mean | Min | Max | SE | Mean | Min | Max | SE | |
| 335 | 3 | 6.73 | 6.55 | 6.89 | 0.0987 | 6.17 | 6.14 | 6.2 | 0.03 | 6.16 |
| 339 | 3 | 4.04 | 3.98 | 4.09 | 0.0318 | 4.35 | 4.29 | 4.41 | 0.06 | -8.51 |
| 341 | 3 | 3.48 | 3.41 | 3.51 | 0.0333 | 3.775 | 3.73 | 3.82 | 0.045 | -9.67 |
| 345 | 3 | 3.71 | 3.59 | 3.82 | 0.0664 | 3.62 | 3.61 | 3.63 | 0.01 | -0.83 |
| 346 | 3 | 9.62 | 9.51 | 9.73 | 0.0636 | 9.215 | 9.14 | 9.29 | 0.075 | 3.20 |
| 348 | 3 | 4.88 | 4.85 | 4.93 | 0.0267 | 4.59 | 4.58 | 4.6 | 0.01 | 5.66 |
| 359 | 3 | 12.17 | 12.04 | 12.27 | 0.0681 | 12.105 | 12.08 | 12.13 | 0.025 | -0.54 |
| 362 | 3 | 7.86 | 7.73 | 7.99 | 0.0751 | 6.58 | 6.51 | 6.65 | 0.07 | 17.48 |
| 363 | 3 | 3.87 | 3.82 | 3.93 | 0.0318 | 3.85 | 3.81 | 3.89 | 0.04 | -0.78 |
| 364 | 3 | 4.18 | 4.15 | 4.21 | 0.0173 | 4.51 | 4.5 | 4.52 | 0.01 | -7.98 |

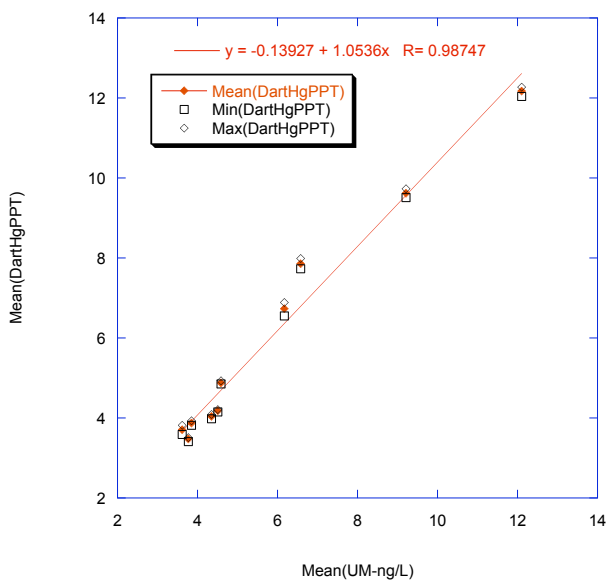


Figure 2. Correspondence between Dartmouth (Dart) and University of Michigan (UM) analyses of mercury in split precipitation samples.

Long-Term Record of Mercury Wet Deposition

The initial year of funding for this project allowed the University of Michigan to complete analysis of archived samples, extending the precipitation record through 2003. Keeler et al. (2005) analyzed the resulting ten-year record and determined that there had been no trend in average-annual mercury concentration (Fig. 3) or deposition (Fig. 4) over the period. The annual volume-wtd mean mercury concentration ranged from 7.8 – 10.5 ng/L during 1993 to 2003. Average annual deposition was 9.7 $\mu\text{g}/\text{m}^2/\text{y}$ during 1993 to 2003. NOAA HYSPLIT model back trajectories of the highest-deposition events were predominantly from the southwest and south (Fig. 5).

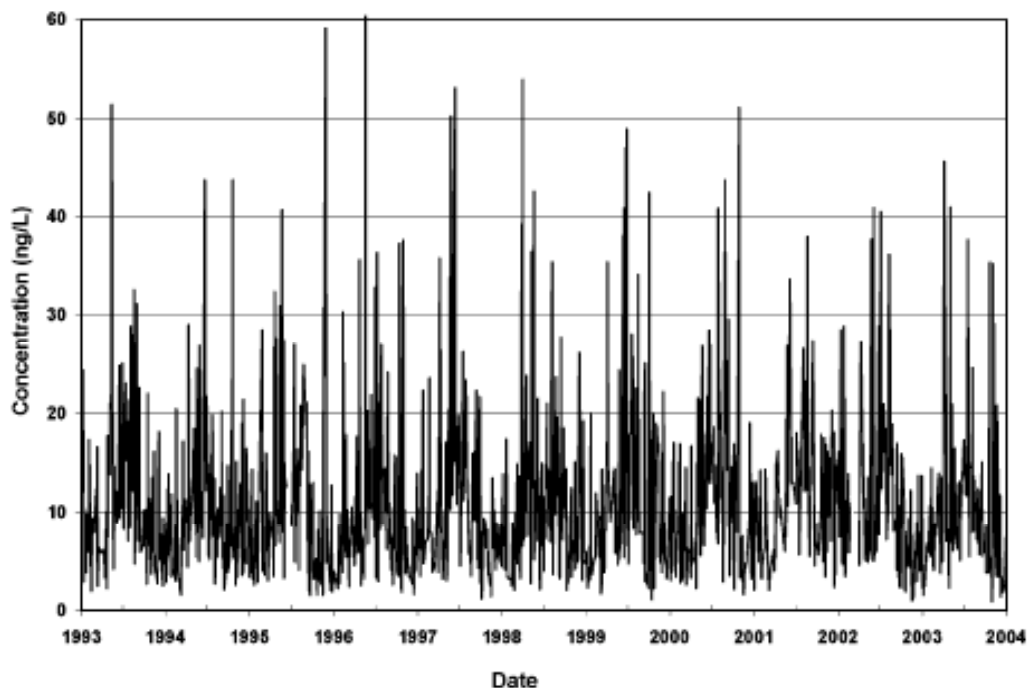


Figure 3. Mercury event precipitation concentrations 1993 thru 2003 from Keeler et al. 2005 – *Ecotoxicology*, 14:71-83.

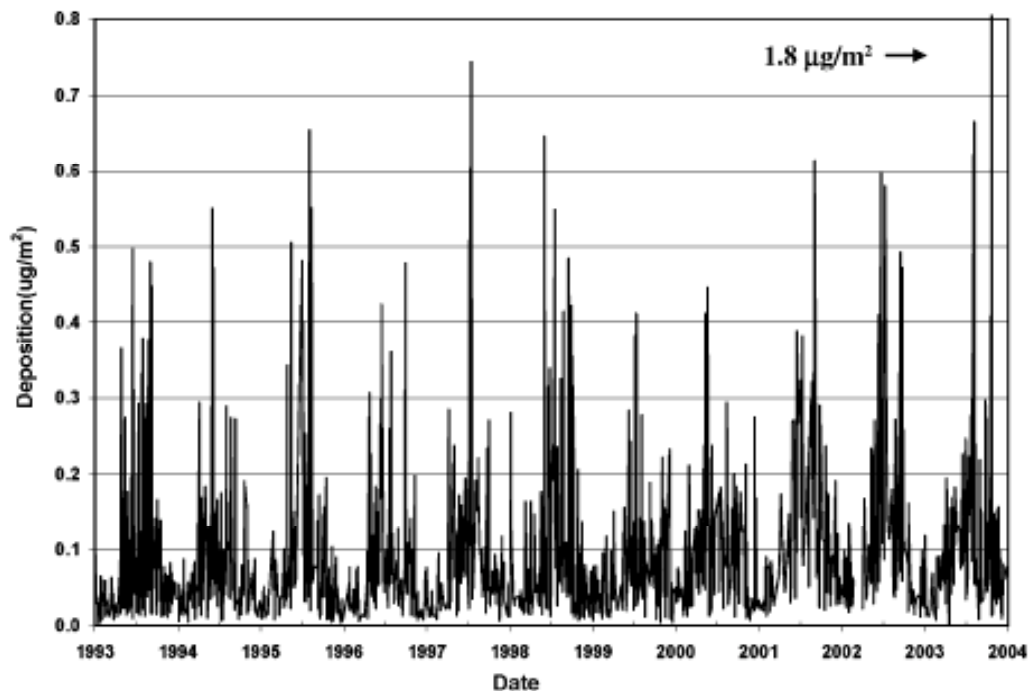


Figure 4. Mercury event wet-deposition 1993 thru 2003 from Keeler et al. 2005 – *Ecotoxicology*, 14:71-83.

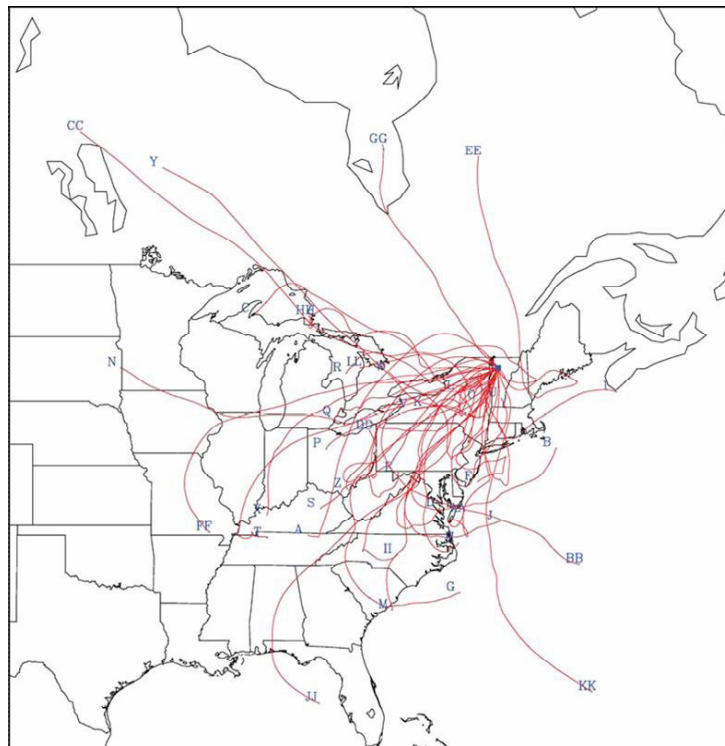


Figure 5. NOAA HYSPLIT Model 72-hour back-trajectories for high mercury deposition events from 1993-2003 from Keeler et al. 2005 – *Ecotoxicology*, 14:71-83

An additional 3 years (2004, 2005, and 2006) of event data were collected with the MICB as part of this project. Years 2005 and 2006 provided overlap with the start up of the MDN sampler. The event record continued in 2007 using the MDN sampler, while operation of the MICB was discontinued at the end of the sample train comparison study.

The transfer functions described in section 2b were used to correct the low-biased MDN results to an “MICB-basis” for analysis and plotting in order to extend the long-term event record. There was good agreement of the annual volume-weighted mean Hg concentration between the MICB and corrected MDN records in both 2005 and 2006 (Figure 6). There was also good agreement between the annual wet mercury depositions determined using the MICB and corrected MDN values (Figure 7).

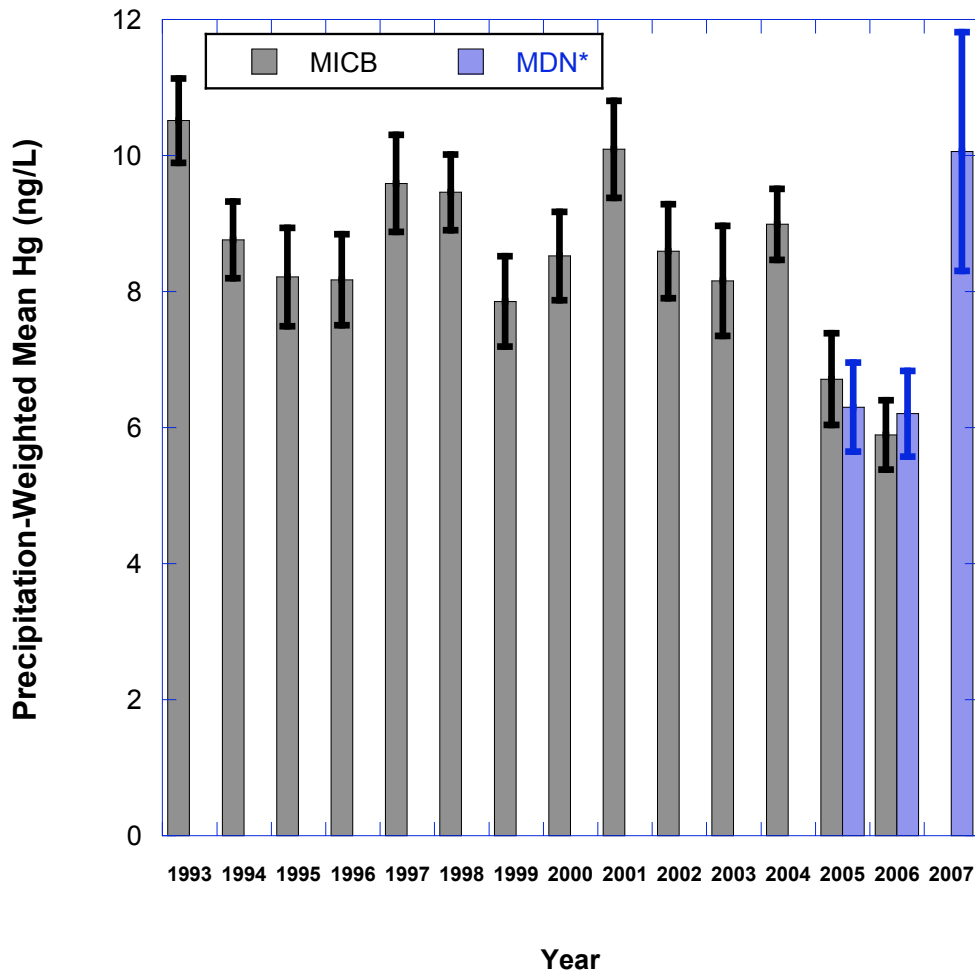


Figure 6. Annual precipitation-weighted mean Hg concentration at Underhill, VT as determined by the MICB collector operating the UMAQL protocol with analysis at UMAQL (1993-2006) and the MDN ACM collector operating the MDN event protocol with analysis at Frontier Geosciences. MDN concentration values were adjusted by a factor of 1.22 (MDN*) as established by a 1-year collector comparison study. This factor compensates for different collector and sample train performance as well as a persistent laboratory bias.

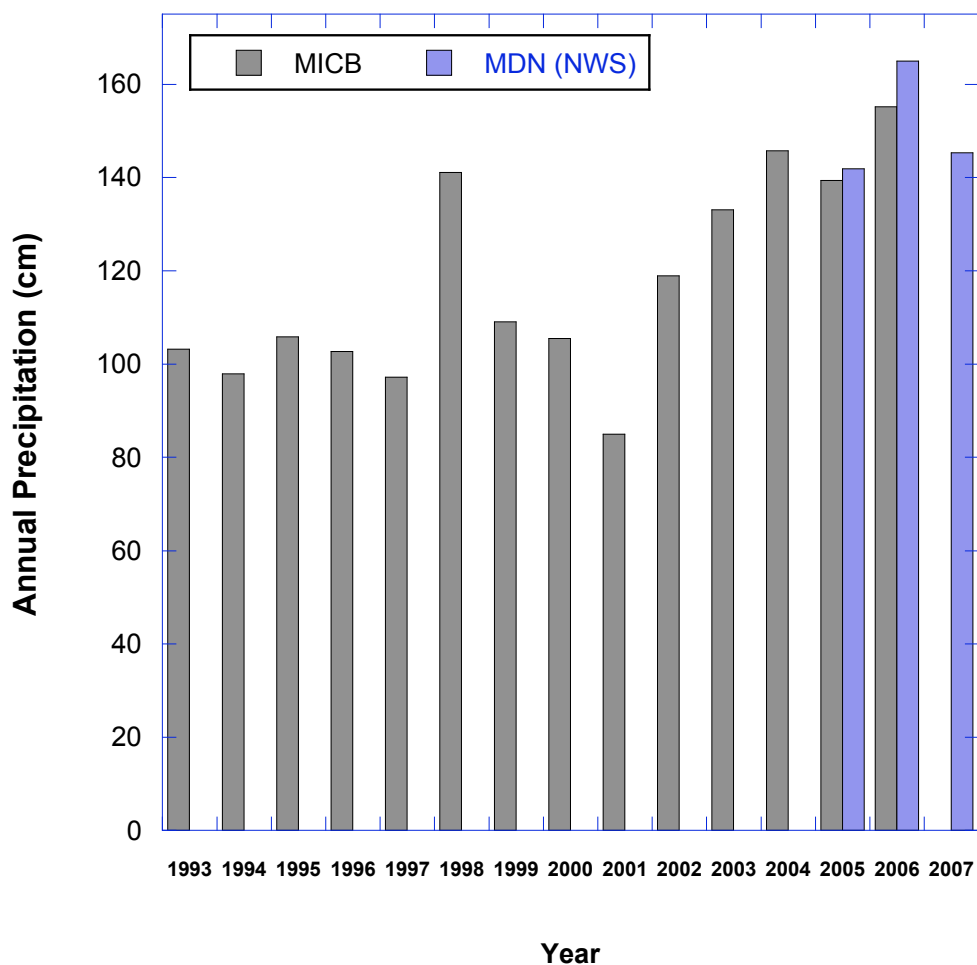


Figure 7. Annual precipitation at Underhill, VT as determined by the MICB collector (1993 – 2006) and the NWS 8-inch rain gage (2005 – 2007). As the result of the 1-year collector comparison study, it was determined that both the ACM collector and the Belfort recording precipitation gage used by MDN significantly under-report precipitation, while the MICB collector and the NWS gage agreed within 1%. Therefore, VT99 MDN reports precipitation amounts and wet-deposition based on the NWS gage precipitation readings.

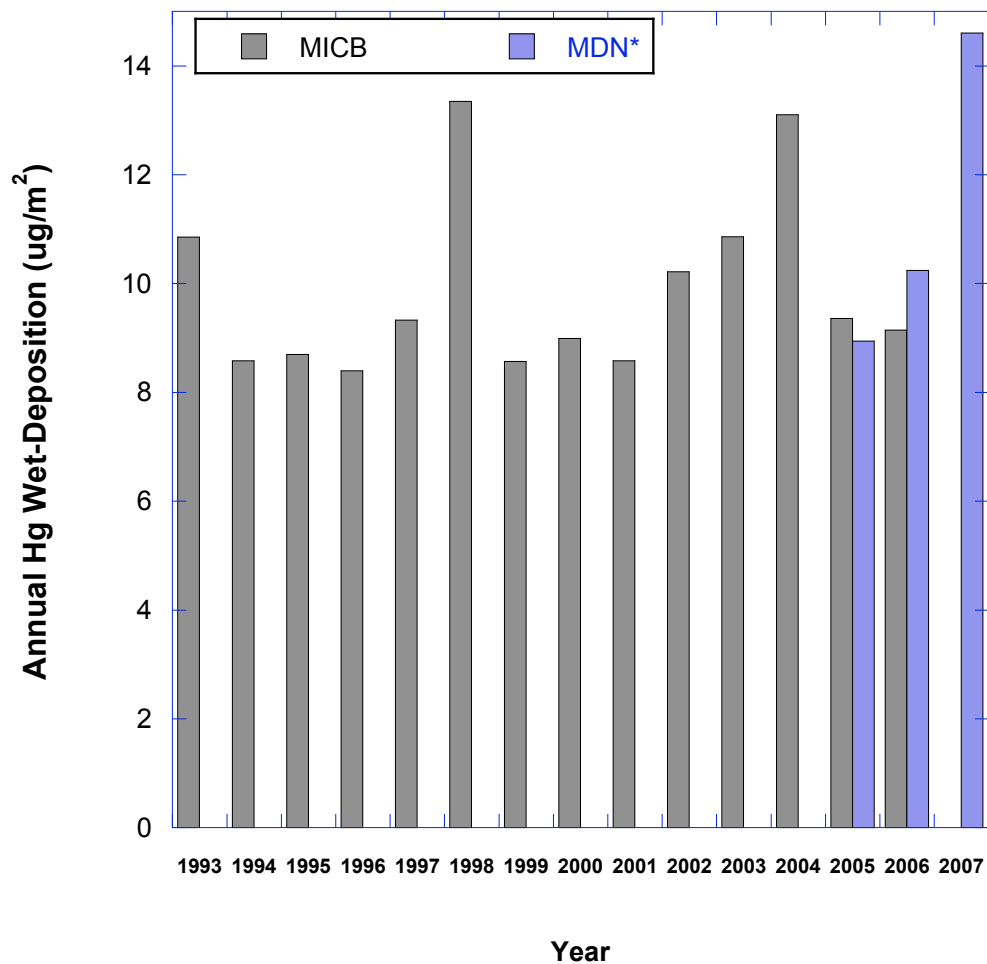


Figure 8. Annual wet-deposition of Hg at Underhill, VT as determined by the MICB collector operating the UMAQL protocol with analysis at UMAQL (1993 - 2006) and the MDN ACM collector operating the MDN event protocol with analysis at Frontier Geosciences (2005 – 2007). MDN concentration values were adjusted by a factor of 1.22 (ACM collector) as established by a 1-year collector comparison study. This factor compensates for different collector and sample train performance as well as a persistent laboratory bias. The MDN deposition values were calculated from the corrected MDN concentrations and precipitation recorded by the NWS rain gage.

A detailed analysis of the wet deposition data from the combined record and methyl-mercury measurements is presented in a separate document “FR-sec2c-Long-Term-Record-2009-01-16.pdf”. Please see this document for additional information.

Continuing the Long-Term Record of Mercury Wet Deposition

Through this project, we have successfully transitioned from the UMAQL program the MDN program. We established and tested transfer functions enabling us to link the long historical record developed with the MICB collector to the ongoing record with either an ACM or NCON collector. Event-based precipitation sampling continues at Underhill (VT99) with the MDN NCON and ACM collectors under funding from the NOAA Lake Champlain Research Consortium Program.

References

- Alter, L. 2000. Mercury Deposition and Atmospheric Concentrations in New England: Year 1 Data and Quality Assurance Report to Ray Thompson, REMAP Coordinator, USEPA, New England Region. North East States for Coordinated Air Use Management, Boston, MA.
- Burke, J., M. Hoyer, G. Keeler, and T. Scherbatskoy. 1995. Wet deposition of mercury and ambient mercury concentrations at a site in the Lake Champlain Basin. *Water Air and Soil Pollution* **80**:353-362.
- Keeler, G.J., L.E.Gratz, and K. Al-Wali. (2005) Long-term Atmospheric Mercury Wet Deposition at Underhill, Vermont. *Ecotoxicology* **14**, 71 –83.

Atmospheric Mercury in Vermont and New England: Measurement of deposition, surface exchanges and assimilation in terrestrial ecosystems

Final Project Report – Wet-Deposition Collector Comparison – 1/16/2009

PI: Melody Brown Burkins, University of Vermont (UVM)
Co-PIs: Eric K. Miller¹, Ecosystems Research Group, Ltd.; Gerald J. Keeler, University of Michigan; and
Jamie Shanley, US Geological Survey
Collaborators: Sean Lawson, VTANR-VMC; Jen Jenkins, Mim Pendelton, Carl Waite and Alan Strong, UVM;
Rich Poirot, VTANR-APCD; Alan VanArsdale, USEPA; Mark Cohen, NOAA;
Project Officer: Eric Hall, USEPA

MICB – MDN (NCON, ACM) Collector Comparison

In partnership with NOAA, MDN, the USGS, and EPA, we conducted a 1-year precipitation mercury collector inter-comparison study. We conducted a short-term follow on direct comparison of MDN and UMICH sample trains in 2007. This experiment was designed to identify and eliminate laboratory bias as well as to test the relative performance of each sample train when deployed in the same collector. The experimental design allowed us to separate the overall collector-protocol-laboratory bias into components of 1) collector, 2) sample-train, and 3) laboratory bias. We also analyzed laboratory quality assurance data provided by MDN and USGS. This study was the first to make scientific comparisons of the MIC-B (UMICH), MDN and NCON (USGS) collectors for event-based assessment of precipitation mercury deposition. All three types of collectors were in use in the Northeastern US at the start of the project. Data from these different collectors and networks could not readily be pooled and coordinated. We identified and quantified substantial uncertainties that must be taken into account when mercury wet-deposition data are used together with mercury measurements in other media (e.g. water, sediment, fish) in ecosystem studies and modeling.

This project developed transfer functions allowing data from the three collector types to be merged for regional analyses. This study also informed mercury researchers about the strengths and weaknesses of each collection system, guiding long-term mercury monitoring and upgrade efforts throughout the country. Most-probable value or “best-estimate” functions were developed to adjust data from different labs and collectors to a common sampling efficiency and NIST-referenced basis.

A manuscript for peer-review was produced (draft included below). Submission of the manuscript is pending discussions by the authors and their institutions. You are receiving this draft as part of your role in reviewing EPA-ORD’s Vermont Atmospheric Mercury Program. ***Please do not cite or distribute this manuscript without permission from the corresponding author.***

¹ Corresponding author for the final project report. Email: ekmillier at ecoystems-research.com Voice: 802-649-5550

Comparison of the MDN Standard Aerochem, proposed MDN NCON, and University of Michigan Air Quality Lab modified MICB precipitation collectors for mercury deposition.

Eric K. Miller*, David Gay, Mark Nilles, Gerald Keeler, Clyde Sweet, Rick Artz, Sean Lawson, Mim Pendleton, and James Barres

*Corresponding Author ekmiller@ecosystems-research.com

Note: Bob Brunette and Gerard Van der Jagt of Frontier Geosciences made significant contributions to this study by generating and providing data as well as contributing to the discussion of results. The authors have extended the opportunity for co-authorship to both scientists and hope they will join the paper after institutional review.

Abstract

We conducted a 1-year study (August 2005 – July 2006) of the event-based relative collection performance of the MDN modified Aerochem (ACM) sampler, the University of Michigan modified MICB sampler, and the NCON Systems mercury deposition sampler. The samplers were deployed at the Underhill, VT Air Quality Research Facility (VT99). The study was designed to assess the effects of differential rain sensor performance, sampling trains, and collector geometry on sampled mercury concentrations and deposition. Extensive data on collector lid status and meteorological conditions including rainfall rate, surface wetness, and humidity were collected. National Weather Service standard 8-inch precipitation gages were monitored as the reference for precipitation amount. Samples from the MICB were analyzed at the University of Michigan Air Quality Laboratory. Samples from the ACM and NCON were analyzed at the MDN HAL.

All three collectors experienced mechanical and other failures during the study. Drive systems failures compromised the results from each of the samplers at one time or another. The MICB collector overflowed during 3 rain events. Heater problems and collector geometry resulted in poor snow collection performance for the ACM and NCON collectors. Approximately 20% of precipitation events and ~24% of precipitation volume were either disqualified or classified as questionable results for each of the samplers. All 3 collectors simultaneously functioned satisfactorily (according to respective protocol QA standards) during 69% of events and 68% of the precipitation measured by the NWS gage during the study period. Because failures occurred more frequently during the colder months, lower fractions of observed snow (33%) and mixed precipitation (62%) were represented in the valid comparison data set than rain (74%).

Compared to the NWS gage, all three collectors under collected snow (NCON < ACM < MICB). The ACM and NCON collectors under collected mixed precipitation (ACM < NCON). The MICB was within 1% of the NWS gage catch for mixed events. All three samplers collected +/- 2.7% of the NWS gage catch for rain events. Part of the observed difference in collection efficiency can be attributed to the precipitation sensing logic of each collector. The MICB lid cycled 3302 times, the NCON 3186 times, and the ACM only 1190 times during the valid comparison period. The NCON lid was open for 1248 hours, the MICB for 789.6 hours, and the ACM for 617 hours during the valid comparison period. The NCON opened immediately in response to any rain shower activity. The MICB was slightly less responsive and did not open for all minor shower events detected by the NCON and an independent wetness sensor. The ACM was often delayed in opening relative to the NCON and MICB for light precipitation and did not stay open as long. The NCON and ACM collectors frequently failed to melt snow rapidly enough to prevent “blow-out” or “knock-off” (when lid closing displaced snow accumulated on the funnel).

The MICB and the NCON collected more Hg than the ACM during the comparison period. Differences in MDN and University of Michigan sample train performance as well as a 6% bias between the laboratories contribute to the discrepancies between measurements obtained by the different collectors.

Background

Three different types of automated wet-only precipitation samplers have been widely used for the collection of mercury in precipitation in North America. Previous studies have identified that there can be substantial differences in the estimates of mercury concentrations and deposition made with each type of collector (Miller et al. 2005). This study was undertaken in order to simultaneously assess the relative performance of 3 collector types in a rural location in Northeastern North America which experiences considerable snow and mixed precipitation. A primary objective of the study was to identify the most suitable collector for long-term monitoring of mercury in precipitation in the Lake Champlain Basin. Secondary objectives were to identify reasons for differences in collector performance that could lead to improved collector designs and to develop transfer functions for normalizing data obtained from the different collector types and laboratories.

Description of Collectors

In 1992, the University of Michigan (UM) developed a modified version of the Canadian MIC-B sampler for simultaneous collection of mercury and trace metals in precipitation (MICB). UM selected the MIC-B platform due to the superior performance of its heated, conductivity/wetness sensing grid relative to other collectors available at that time (Landis and Keeler 1997). The UM version of the MICB (Figure 1a) uses a borosilicate glass, nominally 199-cm² area, straight-sided, 18.5-cm deep collection funnel for the mercury sampling train (Figure 2a). Precipitation is collected in a 1-liter Teflon® bottle precharged with 20 ml of ultra-pure HCl. The funnel and sample bottle are connected by means of a Teflon® adaptor that contains a glass vapor lock. The chamber holding the sample bottle is heated with a 1500-watt thermostatically controlled ceramic heater. Conduction of heat upward through the sample train rapidly melts frozen precipitation accumulated at the base and on the sides of the funnel. The UM-MICB has been deployed at more than 25 sites in the upper Midwest, New England States, Maryland, and Florida.

In 1995 Frontier Geosciences developed a modified version of the Aerochemetrics precipitation sampler for collection of mercury and trace elements in precipitation for use in the NADP Mercury Deposition Network (MDN). The ACM sampler (Figure 1b) was selected because it was widely deployed as the standard wet-only precipitation sampler for the NADP network monitoring major ions in precipitation. The ACM also uses a heated, conductivity/wetness sensing grid; however, the grid is much coarser than the one found on the MICB. The MDN-ACM uses a glass, 120.2-cm² area, 10-cm deep, conical funnel. The sample is collected in a 2-liter glass bottle precharged with 20-ml of ultra-pure HCl. The funnel and sample bottle are connected by means of a glass thistle tube which, by virtue of its length and small diameter, prevents substantial vapor loss (Figure 2b). The chamber holding the sample bottle is heated with a 1500-watt thermostatically controlled ceramic heater. Conduction of heat upward through the thistle tube and chimney is intended to melt frozen precipitation accumulated in the funnel. The MDN-ACM has been deployed at 95 sites as part of the international NADP/MDN.

Recently, Frontier Geosciences and the USGS jointly developed a modified version of the NCON Systems automated precipitation sampler for collection of mercury in precipitation (NCON). The NCON sampler (Figure 1c) was selected by USGS because of its superior screw-type lid motor drive which was expected to be more durable than the ACM sampler's motor drive. In contrast to the MICB and ACM samplers, the NCON sampler uses an infrared-scattering optical precipitation sensor to control lid opening and closing. This sensor has a more immediate response to changes in precipitation than conductivity sensing grids. The NCON sampler uses the same sample train as the MDN-ACM with the exception of a slightly shorter thistle tube to accommodate the collector geometry. The chamber holding the sample bottle is heated with a combination of a 500-watt plate heater and a 200-watt fan heater. Conduction of heat upward through the thistle tube and chimney is intended to melt frozen precipitation accumulated in the funnel. The NCON mercury sampler has been deployed at 8 sites as part of USGS investigations of mercury deposition and cycling.

UMICH-MICB



MDN-ACM



USGS-NCON



Figure 1. a) University of Michigan modified MIC-B collector, b) MDN modified Aerochem collector, and c) USGS NCON collector.

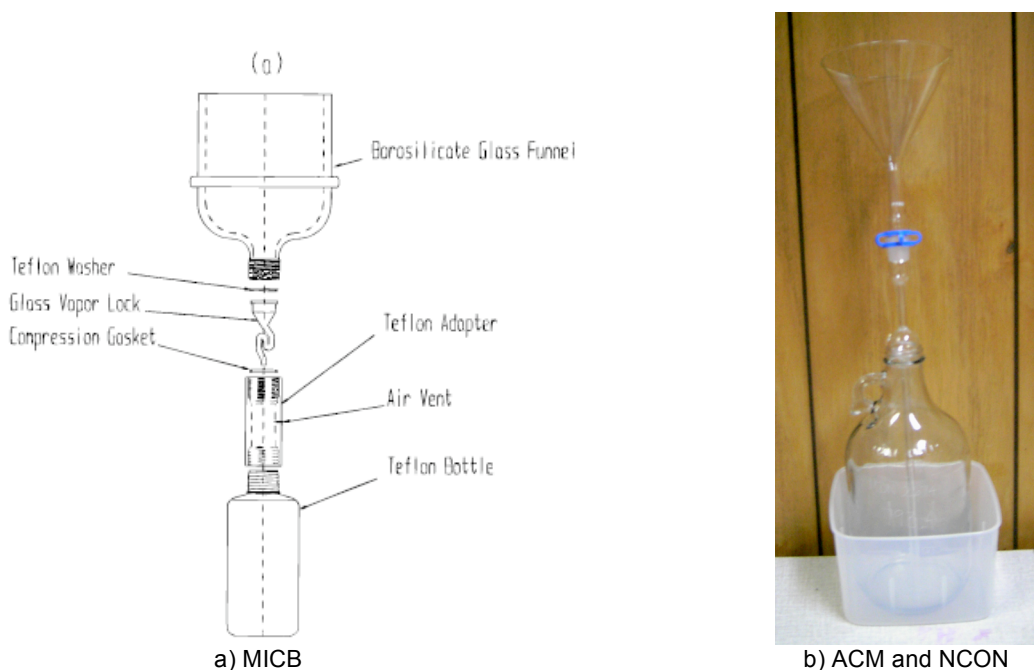


Figure 2. a) MICB, b) ACM and NCON sample trains.

Methods

The three automated collectors were deployed at the Underhill, VT Air Quality Research Facility (VT99) following standard NADP criteria. Figure 3 shows the locations of the samplers, recording rain gages and tipping bucket rain gage. A National Weather Service (NWS) standard 8-inch gage located just to the north of the ACM was monitored throughout the study as the “gold standard” for precipitation amount. Two additional NWS 8-inch gages were deployed east of the MICB and NCON samplers in May 2006 to provide an estimate of the variance in NWS precipitation amount. All samplers and gages were on the same contour with orifice heights +/- 1 meter. The automated samplers were fitted with reed switches to allow recording of lid opening and closing times. A tipping bucket rain gage was located east of the MICB. Temperature, RH, global solar radiation, and surface wetness sensors were located on a tower at the northeast corner of the collector field. The time of each tip of the TBRG or change in status of lid positions was recorded with a data logger. The signal from the surface wetness sensor was also recorded at the time of a lid status change.

The sample trains of the automated collectors were changed on an event basis following the protocol in use at VT99 since 1993. The site is visited daily between 8:30am and 10am. If a precipitation event has concluded in the past 24 hours, the sample trains are changed. If precipitation is occurring, but expected to stop before 3pm, the site operator returns after the end of precipitation to change the sample trains. When precipitation continues steadily or lightly for more than 48 hours, the operator attempts to change sample trains during periods of minimal precipitation in conjunction with air mass changes or to prevent overflow of the MICB collector. Sample trains are changed after 7 days without precipitation. MICB sample trains were prepared and samples analyzed at the University of Michigan Air Quality Laboratory. ACM and NCON sample trains were prepared and samples analyzed at the MDN Mercury Analytical Lab (HAL), Frontier Geosciences, Seattle, WA.

A standard definition of collector area was adopted for all collectors based on the measurement of funnel diameters from mid-rim to mid-rim of the funnel. Recent measurements of funnels were used to calculate funnel areas.

Data, flags, and notes from the two laboratories for the 3 collectors were compiled along with notes and flags from the site operator’s log into a common data set. Each record in the data set represented a common deployment period for all 3 sample trains. Field and laboratory QA flags were used to disqualify records where any one of the 3 samplers experienced failures or QA exceptions. A second category of “questionable” records was identified where either the laboratory or field notes identified potential problems with samples such as leaks during shipment, but the responsible laboratory had not disqualified the sample. Additional screening of the remaining records was conducted to uncover QA problems that were missed by the laboratories.

A follow-on comparison of the MDN and University of Michigan sample trains deployed simultaneously in the MICB collector was conducted from May through October of 2007. Due to funding limitations, this study could only address the relative performance of the sample trains for rain events.

Laboratory quality-assurance data provided by the HAL for 2004-2006 as well as data from a multi-laboratory blind sample exchange coordinated by USGS were analyzed to constrain the potential for stable laboratory-laboratory bias within performance standards of EPA Method 1631.

Linear regression, ANOVA, and paired t-tests were employed to test hypotheses about relative collector performance. All statistical analyses were conducted with JMP 4.04 (SAS Institute).

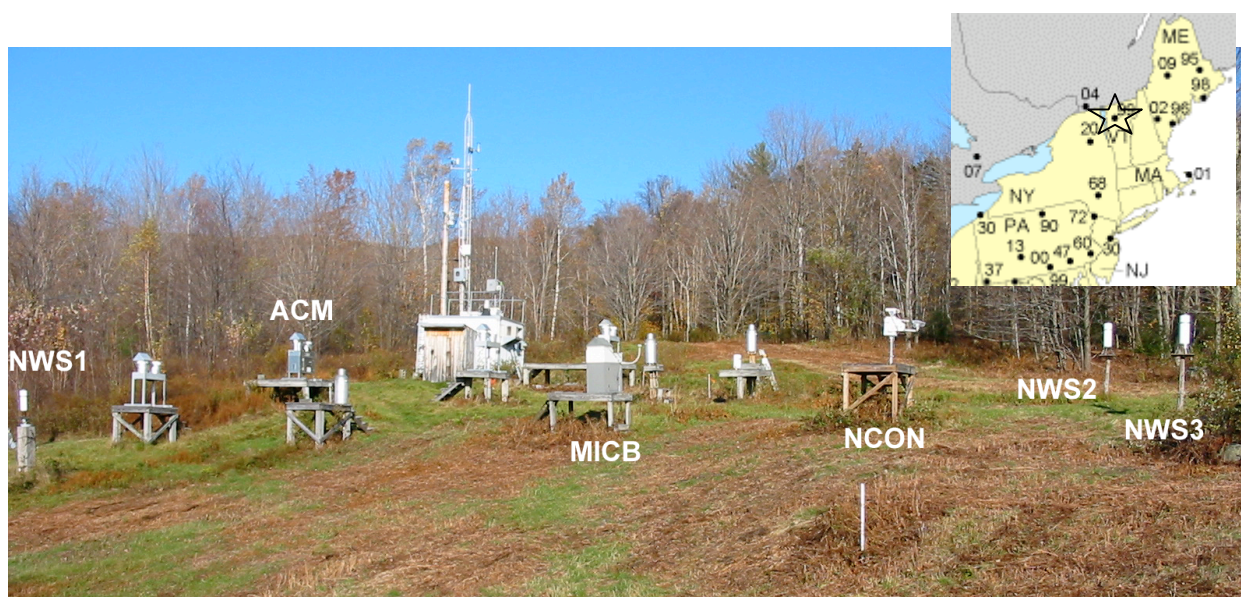


Figure 3. Locations of precipitation samplers at the VT99 NADP site (inset) in Underhill, VT. The NCON is farthest right (south). The MIC-B is in the center of the field. The ACM is on the left (north). The primary NWS 8-inch gage is just slightly downhill (west) of the ACM. Two additional NWS 8-inch gages were located

to the right (south) of the NCON and MICB samplers. The site's 3 Belfort recording rain gages are visible. Two tipping bucket rain gages are located on the platform to the right and behind the MICB.

Results

NWS gage variance

The variance in precipitation sampled by the NWS standard 8-inch gages is summarized in Table 1. On an event basis, we consider the differences between collector catch and NWS gage catch to be meaningful when the difference is $> 22\%$ for low volume events (showers), $> 2.6\%$ for rain, $> 3\%$ for intense rain such as in thunderstorms, and $> 4\%$ for heavy rain events (> 40 mm). NWS gage number 1 (NWS1), used as the standard for the full year of the study, was not significantly different from the mean of the 3 gages or from either of the two other gages when compared gage to gage using paired t-tests. For the sum of the period (May – September 2006), NWS1 = 769.42 mm, NWS2 = 769.74 mm, NWS3 = 762.90 mm, and mean = 767.35. The difference in precipitation measured over the observation period ranged $+0.3\%$ to -0.6% compared to the mean. The much lower percent range for the period compared to the percent range on an event basis indicates that event-to-event differences between gages were random and cancelled out.

Table 1. Summary Results for NWS 8-inch rain gages May 2006 – September 2006.

| Type | N Rows | Mean(NWSmean(mm)) | Mean(StdDev(mm)) | Mean(%CV) | Mean(Range(mm)) | Mean(%range) |
|------------|--------|-------------------|------------------|-----------|-----------------|--------------|
| showers | 9 | 3.55 | 0.11 | 12.16 | 0.21 | 21.99 |
| rain | 18 | 15.09 | 0.20 | 1.58 | 0.33 | 2.63 |
| tstorm | 7 | 18.73 | 0.22 | 1.60 | 0.42 | 3.00 |
| heavy-rain | 6 | 55.46 | 1.10 | 2.08 | 2.12 | 3.97 |

Collector performance and QA exceptions

There were 96 sample train deployments (95 with precipitation) during the 1-year comparison period. Equipment malfunctions and QA exceptions compromised the automated collector results for about 20% of the events sampled for each collector (Table 2). Mechanical failures were greatest for the ACM and least for the MICB. It should be noted that the motor drive failure that occurred in the MICB collector was the first such failure since the collector was deployed at Underhill in December of 1992. There were 9 events where the NCON and 3 events where the ACM collectors failed to completely melt all of the snow captured in the funnels (Figure 3). These records were retained in the data set as they represent the performance of the collectors during snow. The ACM and NCON sample bottles were prone to leakage during shipment (Table 2). These records were retained in the data set because they were not disqualified by the HAL. There were no leaks of the MICB sample bottles during shipment. The MICB sample bottle overflowed during 3 large rain events, including during the passage of the remnants of hurricane Katrina over New England. These records were excluded from the data set because they should have been identified as incomplete samples during standard QA. Additional screening detected an apparent sample contamination for the NCON where debris was noted, but the sample was not disqualified by the HAL. This record was removed from the data set. The remaining “valid comparison set” represents 66 (69%) sample train changes and 1158.5 mm (68%) of the total precipitation observed during the study period (Table 3). Collector performance for capture of precipitation was evaluated with this set of samples.

Additional samples with QA problems were detected by tertiary screening during analysis of collector performance for capture of mercury. Two extremely low-volume (NWS1 < 2.1 mm) snow samples from the MICB were identified as exhibiting mercury concentrations greater than any other snow sample previously analyzed by the UMAQL. These records had been flagged as questionable by the lab and were excluded from the analysis of Hg concentrations and deposition. One low volume rain sample (NWS1 = 2.29 mm) from the ACM exhibited a mercury concentration greater than two times the concentrations measured in samples collected by the NCON and MICB samplers. The ACM exhibited extremely poor collection efficiency for this event (27% of NWS1) while the other two collectors sampled within +/- 3% of the NWS1 gage. The ACM appears to have failed to sample the more dilute portion of the event. This record was excluded from analysis of Hg concentrations and deposition.

Collector openings

During the valid comparison period the NCON sampler was the most responsive to changes in precipitation – opening and closing first and remaining open for the largest number of hours (Table 4). However, there was no statistically significant difference in the number of openings per event between the NCON and MICB collectors (2-sided paired t-test, p=0.859). The ACM collector

opened significantly fewer times per event compared to the NCON (-63%, p=0.0009) and the MICB (-64%, p<0.0001) as assessed by 1-sided, paired t-tests. The NCON sampler was open a significantly greater number of hours per event than both the MICB (+58%, p<0.0001) and the ACM (+103%, p<0.0001) as assessed by 1-sided, paired t-tests. The ACM collector was open for significantly fewer hours per event (-22%) than the MICB (1-sided paired t-test, p=0.002).

Table 2. Summary of equipment and QA exceptions.

| VT99 Sampler Comparison (8/1/2005 - 7/31/2006) | Precipitation Sampled (mm) | | | | | Number of Precipitation Events | | | | |
|--|--------------------------------|--------------|---------------|---------------|--------------|--------------------------------|-----------|-----------|-----------|--------------|
| | snow | mixed | rain | all | %all | snow | mixed | rain | all | %all |
| NWS Standard 8" Gage | 124.7 | 426.5 | 1159.0 | 1710.1 | 100.0% | 18 | 22 | 55 | 95 | 100.0% |
| | | | | | | | | | | |
| | Precipitation NOT Sampled (mm) | | | | | Number of Events NOT Sampled | | | | |
| ACM | snow | mixed | rain | all | %all | snow | mixed | rain | all | %all |
| Mechanical Failure* | 42.7 | 106.4 | 6.6 | 155.7 | 9.1% | 3 | 3 | 1 | 7 | 7.4% |
| Sample Train Failure* | | | 9.1 | 9.1 | 0.5% | | | 1 | 1 | 1.1% |
| Power Failure* | | | 14.5 | 14.5 | 0.8% | | | 1 | 1 | 1.1% |
| Leak DQed by HAL* | | | 30.2 | 30.2 | 1.8% | | | 1 | 1 | 1.1% |
| Shipping Leak NOT DQed by HAL** | 10.4 | 50.8 | 138.4 | 199.6 | 11.7% | 1 | 2 | 4 | 7 | 7.4% |
| Snow not melted** | 7.9 | 66.6 | | 74.4 | 4.4% | 1 | 2 | | 3 | 3.2% |
| All Disqualified* | 42.7 | 106.4 | 60.5 | 209.5 | 12.3% | 3 | 3 | 4 | 10 | 10.5% |
| All DQ* + Questionable** | 61.0 | 223.8 | 198.9 | 483.6 | 28.3% | 5 | 7 | 8 | 20 | 21.1% |
| | 48.9% | 52.5% | 17.2% | | | 27.8% | 31.8% | 14.5% | | |
| | | | | | | | | | | |
| | Precipitation NOT Sampled (mm) | | | | | Number of Events NOT Sampled | | | | |
| NCON | snow | mixed | rain | all | %all | snow | mixed | rain | all | %all |
| Mechanical Failure* | 50.9 | 30.7 | 29.7 | 111.3 | 6.5% | 4 | 3 | 2 | 9 | 9.5% |
| Sample Train Failure* | 8.9 | | | 8.9 | 0.5% | 1 | | | 1 | 1.1% |
| Power Failure* | | 83.8 | 14.5 | 98.3 | 5.7% | | 1 | 1 | 2 | 2.1% |
| Debris Contam. Missed by HAL* | | | 25.4 | 25.4 | 1.5% | | | 1 | 1 | 1.1% |
| Shipping Leak NOT DQed by HAL** | | 85.1 | 104.9 | 190.0 | 11.1% | | 3 | 3 | 6 | 6.3% |
| Snow not melted** | 22.1 | 86.9 | | 109.0 | 6.4% | 3 | 3 | | 6 | 6.3% |
| All Disqualified* | 59.8 | 114.6 | 69.6 | 243.9 | 14.3% | 5 | 4 | 4 | 13 | 13.7% |
| All DQ*+ Questionable** | 81.9 | 286.5 | 174.5 | 542.9 | 31.7% | 8 | 10 | 7 | 25 | 26.3% |
| | 65.7% | 67.2% | 15.1% | | | 44.4% | 45.5% | 12.7% | | |
| | | | | | | | | | | |
| | Precipitation NOT Sampled (mm) | | | | | Number of Events NOT Sampled | | | | |
| MICB | snow | mixed | rain | all | %all | snow | mixed | rain | all | %all |
| Mechanical Failure* | 20.8 | 48.5 | 6.6 | 75.9 | 4.4% | 5 | 5 | 1 | 11 | 11.6% |
| Overflow* | | | 198.1 | 198.1 | 11.6% | | | 3 | 3 | 3.2% |
| Power Failure* | | 83.8 | 14.5 | 98.3 | 5.7% | | 1 | 1 | 2 | 2.1% |
| Operator Error* | | | 9.1 | 9.1 | 0.5% | | | 1 | 1 | 1.1% |
| Possible Contam. noted by lab** | 3.3 | | | 3.3 | 0.2% | 2 | | | 2 | 2.1% |
| All Disqualified* | 20.8 | 132.3 | 228.3 | 381.5 | 22.3% | 5 | 6 | 6 | 17 | 17.9% |
| All DQ*+ Questionable** | 24.1 | 132.3 | 228.3 | 384.8 | 22.5% | 7 | 6 | 6 | 19 | 20.0% |
| | 19.3% | 31.0% | 19.7% | | | 38.9% | 27.3% | 10.9% | | |
| | | | | | | | | | | |
| Notes | | | | | | | | | | |
| All single asterisk "*" items reflect samples that normal QA at the site or lab level either did disqualify or should have disqualifyed. | | | | | | | | | | |
| All double asterisk "**" items reflect samples that normal QA at the site or lab level did or should have identified as questionable. | | | | | | | | | | |
| The final line in each table combines all of the disqualified "DQ" and questionable samples. | | | | | | | | | | |
| The amount of precipitation not sampled is the NWS measured precip corresponding to the disqualified or questionable samples. | | | | | | | | | | |



Figure 3. NCON sampler with unmelted snow in funnel. A portion of the snow extending above the funnel rim was knocked off when the lid closed.

Precipitation collection efficiency

Data were available for the NWS1 and Belfort gages for the full year comparison period. The NWS1 gage recorded 1710.11 mm of precipitation for the year. The Belfort gage (charts interpreted by the site operator) recorded 1632.7 mm or 4.5% less (1-sided t-test, $p < 0.0001$) than the NWS gage for the year.

During the valid comparison period the precipitation catches of the MICB and NCON samplers were not significantly different from the NWS1 catch (paired t-tests) and both differed from the NWS gage less than the percent difference noted between the 3 NWS gages (- 0.6 to +0.3%). The precipitation catch of the ACM was biased significantly lower (-5.0%) than the NWS1 gage (1-sided paired t-test, $p=0.016$). When analyzed by precipitation type, all collectors were significantly biased low (1-sided paired t-tests: MICB, -46% $p=0.046$; NCON, -66% $p=0.021$; ACM, -46% $p=0.007$) compared to the NWS1 gage for collection of snow (Table 3). The ACM was significantly biased low (1-sided paired t-test: -10.6% $p=0.054$) compared to NWS1 for mixed precipitation. There was no significant difference in precipitation catch between any of the collectors and NWS1 for rain events. Because snow and mixed precipitation are severely underrepresented in proportion to their occurrence relative to rain in the valid comparison set (Table 2), it is possible that all 3 collectors could be biased low on annual basis if these precipitation types were fully represented in the data set.

The frequency distributions of event collection efficiencies (%CE, Figure 4) show that there can be substantial departures from the NWS1 gage catch on an event basis for all 3 collectors. The standard deviations of the distributions of event errors (mm) were 3.8 mm for the NCON, 3.3 mm for the ACM, and 2.9 mm for the MICB. The errors (mm) were strongly positively correlated between the NCON and ACM samplers ($r^2 = 0.7$, $p < 0.0001$) and weakly positively correlated between the MICB and the other two collectors ($r^2 = 0.2$, $p < 0.0001$).

Relative performance for collecting mercury

For the 63 sample train deployments valid for comparison of mercury concentrations, the 3 samplers collected significantly different amounts of mercury as determined by paired t-tests. The ACM sampler collected significantly less mercury than the NCON (-7.3%, 1-sided t-test, $p = 0.023$) and the MICB (-21.4%, 1-sided t-test, $p < 0.0001$). The NCON sampler also collected significantly less mercury than the MICB (-15.3%, 1-sided t-test, $p = 0.002$). Mercury concentrations were well correlated ($p < 0.0001$) among all three samplers with coefficients of determination ranging from 0.8 to 0.86.

Precipitation type had a profound influence on the relative collection of mercury between the collectors. There were smaller, but significant differences between collectors for rain-only events (ACM -6.0% of NCON, $p = 0.037$; NCON -14.5% of MICB, $p = 0.006$; ACM -19.7% of MICB, $p = 0.0001$) than for all snow events (ACM -46% of NCON, $p = 0.059$; NCON -23% of MICB, ns; ACM -59% of MICB, $p = 0.050$). Mixed precipitation events produced mixed results with the NCON and ACM (+/- 1.5%, ns) sampling similar amounts of mercury but about 15% less than the MICB ($p = 0.081$ and 0.037 , respectively). The degrees of freedom were much lower (4) for the analyses of all snow events than for the analyses of mixed (12) or rain (44) events.

Table 3. Summary of precipitation catch relative to NWS 8-inch gage by precipitation type.

| | ACM | NCON | MICB |
|------|--------|--------|--------|
| snow | -48.3% | -66.0% | -46.4% |
| mix | -10.6% | -7.3% | -0.5% |
| rain | -1.2% | 2.4% | 2.7% |
| all | -5.0% | -2.2% | 0.2% |

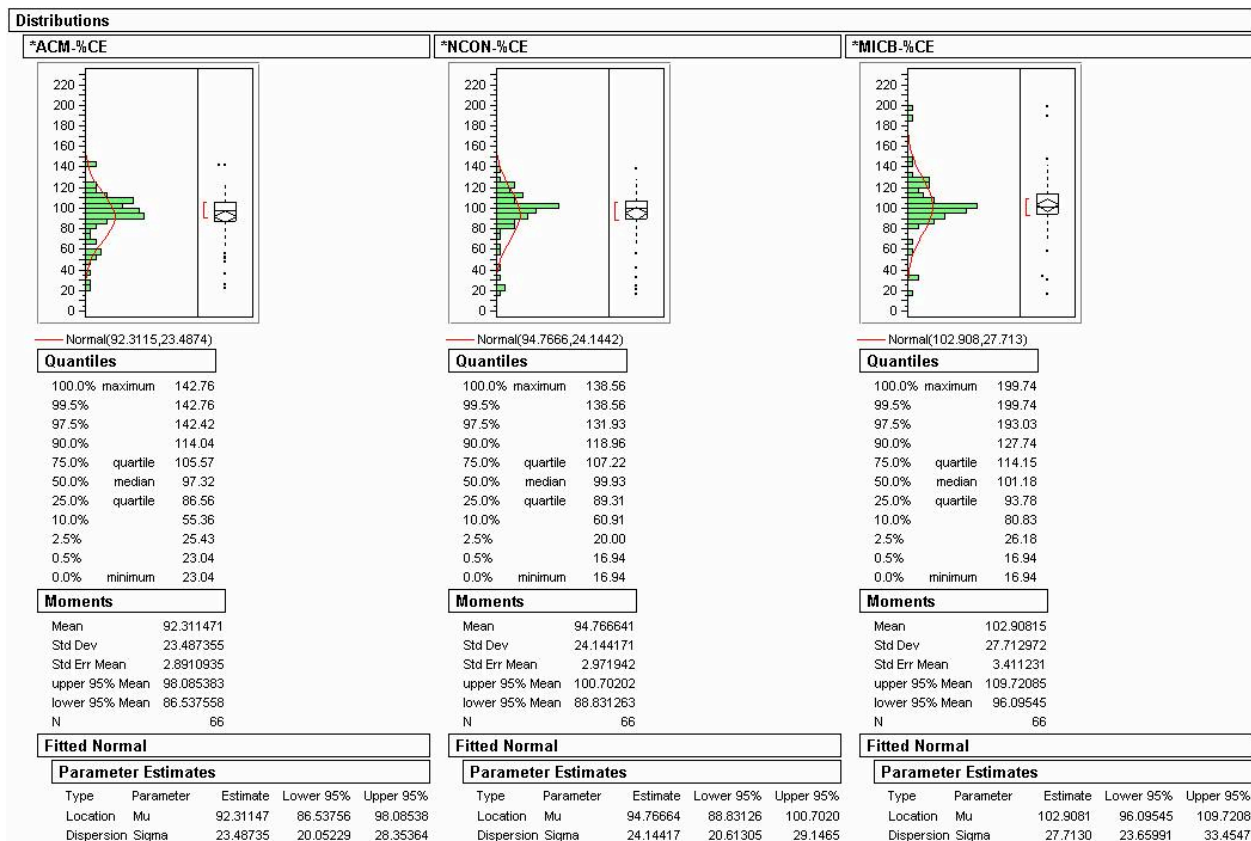


Figure 4. Frequency distributions of event precipitation collection efficiency compared to the NWS1 gage.

Table 4. Summary of collector lid openings.

| Number of Collector Openings and Closings | | | | |
|--|-------------|--------------|-------------|------------------|
| | Snow | Mixed | Rain | All Valid |
| ACM | 363 | 300 | 527 | 1190 |
| NCON | 155 | 642 | 2389 | 3186 |
| MICB | 786 | 765 | 1751 | 3302 |
| Number of Hours Collector was Open | | | | |
| | Snow | Mixed | Rain | All Valid |
| ACM | 51.3 | 145.3 | 420.5 | 617.0 |
| NCON | 247.4 | 301.0 | 699.5 | 1248.0 |
| MICB | 57.8 | 186.7 | 545.1 | 789.6 |

Paired deployment of replicate MDN and UMICH sample trains in the MICB collector

A total of 16 paired-deployments were achieved. For 8 events a pair of MDN sample trains were deployed along side a University of Michigan (UMICH) sample train. Frontier Geosciences analyzed one of the MDN sample trains while the UMICH sample train and one MDN sample train were shipped for analysis by the UMAQL. For an additional 8 events a duplicate UMICH sample

train was deployed with one of the duplicates analyzed by Frontier Geosciences and one by UMAQL. This design allowed comparison of sample train performance (e.g. catch, evaporation) as well as a comparison of laboratory processing of the sample trains. Due to funding limitations, data were only returned by the UMAQL for the UMICH sample trains, partially limiting the laboratory comparison. For the data reported below the reference UMICH sample train was always analyzed by UMAQL (UMAQL-UMICH: LAB-SAMPLETRAIN) while the replicate MDN or UMICH sample trains were always analyzed by Frontier Geosciences (Frontier-MDN, or Frontier-UMICH).

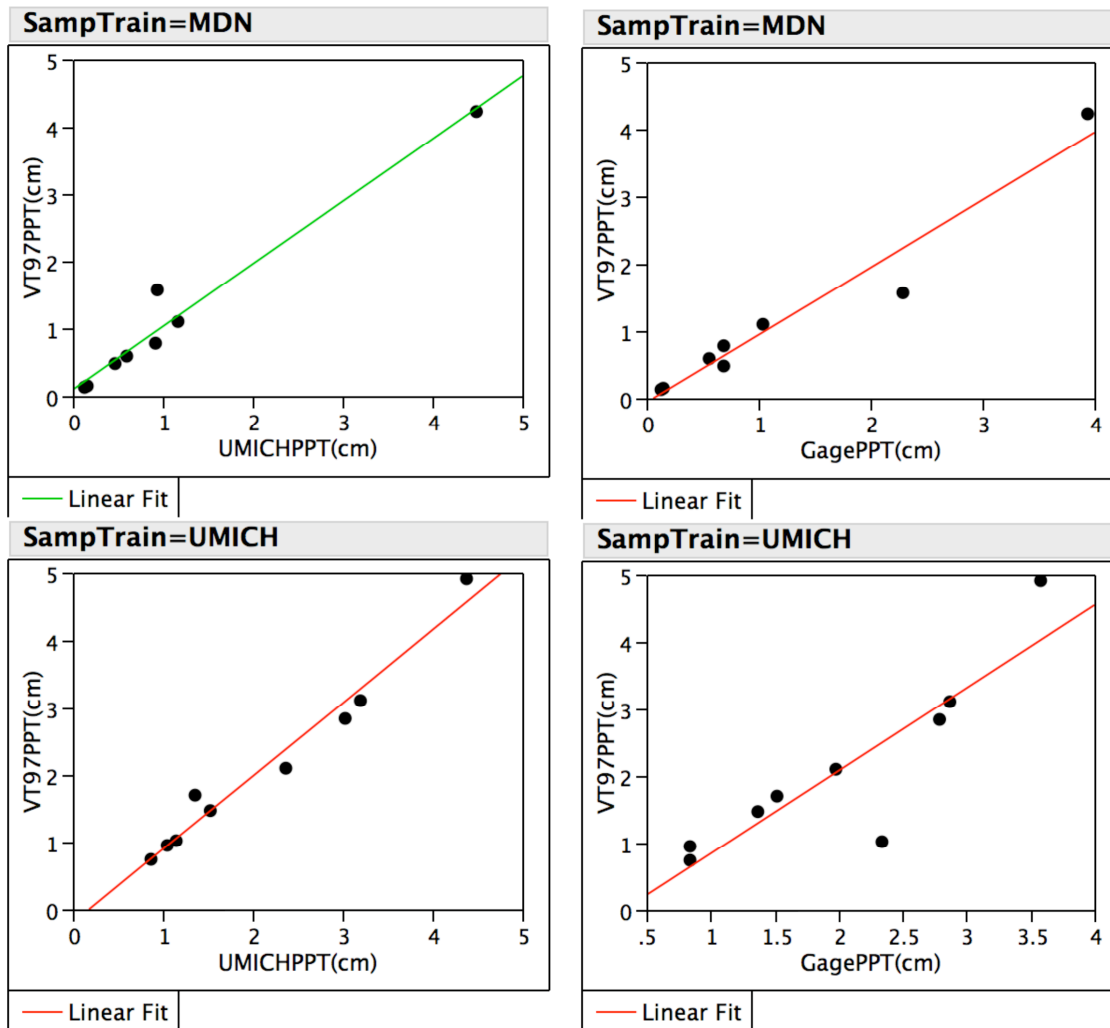


Figure 5. Correlations between redundant co-deployed sample trains (VT97 = MDN at top or UMICH at bottom) and the reference co-deployed UMICH sample train (left-side) and the Belfort rain gage (right-side).

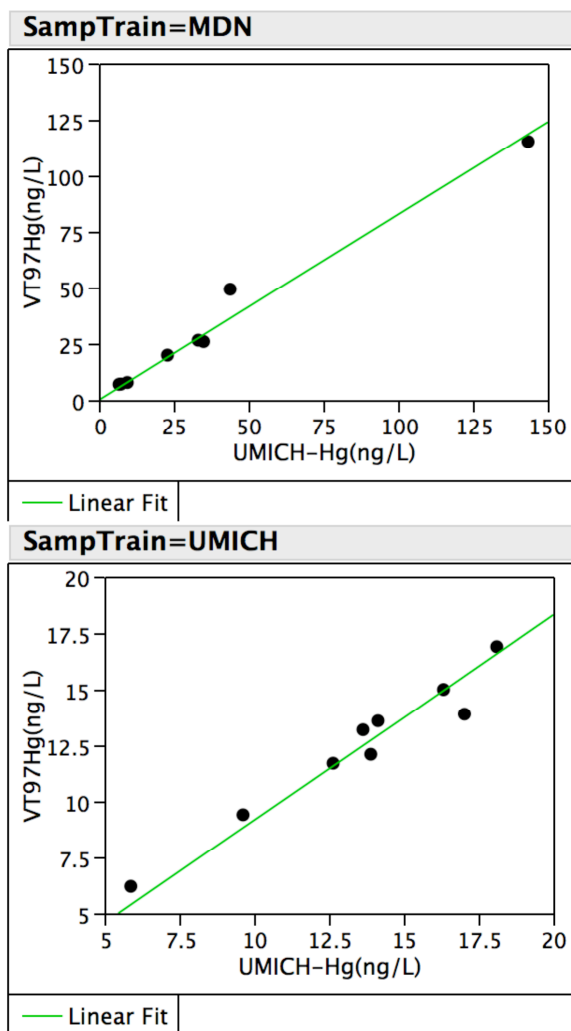


Figure 6. Correspondence between mercury concentrations measured in samples collected by redundant co-deployed sample trains (VT97 = MDN at top or UMICH at bottom) and the reference co-deployed UMICH sample train.

Precipitation amounts sampled during the sample-train comparison ranged from 0.13 to 3.94 cm as measured by the Belfort gage and were distributed over nearly this full range for each sample train. Precipitation sampled by both redundant sample trains correlated well with the co-deployed reference UMAQL-UMICH sample train (Frontier-MDN $r^2=0.96$ or Frontier-UMICH $r^2=0.96$) and somewhat less well with the Belfort gage (Frontier-MDN $r^2=0.94$ or Frontier-UMICH $r^2=0.75$) (Figure 5). Best-fit lines constrained to an intercept of zero produced slopes of 0.97 ± 0.05 for the Frontier-MDN vs. UMAQL-UMICH; 1.02 ± 0.04 Frontier-UMICH vs. UMAQL-UMICH; 0.98 ± 0.06 Frontier-MDN vs. Belfort; and 1.07 ± 0.10 Frontier-UMICH vs. Belfort.

Mercury concentrations ranged from 5.9 to 143 ng/l as measured by the normally deployed reference UMICH sample train and analyzed by UMAQL (UMAQL-UMICH). Mercury sampled by both redundant sample trains correlated well with the co-deployed UMAQL-UMICH sample train (Frontier-MDN $r^2=0.98$ or Frontier-UMICH $r^2=0.95$, Figure 6). Best-fit lines constrained to an intercept of zero produced slopes of 0.83 ± 0.03 for the Frontier-MDN vs. UMAQL-UMICH and

0.92+/-0.02 Frontier-UMICH vs. UMAQL-UMICH. The apparent mercury concentration bias with respect the reference UMICH sample train analyzed by UMAQL averaged -10.6% (median -15.6%) for the MDN sample train ($[\text{Frontier-MDN} - \text{UMAQL-UMICH}] / \text{UMAQL-UMICH}$) and averaged -6.2% (median -5.3%) for the UMICH sample train ($[\text{Frontier-UMICH} - \text{UMAQL-UMICH}] / \text{UMAQL-UMICH}$).

Laboratory Quality Assurance Data

EPA Method 1631 performance data from Frontier Geosciences (HAL) for 2004-2006 are summarized in Table 5. The HAL demonstrated excellent performance with respect to the Method 1631 criteria. Mean recovery of the CRM by the HAL was 95.2% with an RSD of 4.1%.

The USGS conducted a multi-laboratory blind sample analysis program (Gregory Wetherbee, U.S. Geological Survey, written communication, 2008). Data from 6 participating labs with adequate numbers of samples were analyzed to assess the relative bias observed between laboratories when all laboratories meet the Method 1631 performance criteria. There were adequate data for 4 dilutions of NIST CRM prepared by USGS. Because of anticipated error in the method of preparation of the NIST dilutions to rain water levels, USGS did not report an expected concentration for the dilutions (Gregory Wetherbee, U.S. Geological Survey, personal communication, 2008). Dilutions were prepared and shipped to the laboratories monthly. Periodic batch-to-batch preparation variability was detected by ANOVA. Batches that were significantly different in mean concentration from the majority of batches were eliminated from further analysis. A small number of outlier values beyond Method 1631 performance criteria were also removed. The means, 95% confidence intervals about the means, and median values for each of the 4 solutions are presented in Table 6.

There were significant differences among laboratories as indicated by ANOVA² for all 4 solutions. Means comparisons using the Tukey-Kramer Highly Significant Difference test indicated that the HAL was consistently biased low (average - 5.2%) relative to other laboratories and the Northern States Analytical Laboratory was consistently biased high (average +3.9%). The spread (stable bias) between these two EPA 1631 performance-compliant laboratories was 9.1%. Taking the mean value of all analyses for all laboratories as a good estimate of the true value of each solution, then the mean percent recovery of blind USGS-prepared NIST CRM dilutions indicated for the HAL (94.8%) is consistent with the HAL's own internal NIST performance data (mean recovery 95.2%).

² While only one of the 4 solutions produced a normal distribution as determined by the Shapiro-Wilk test, normal quantile plots indicated that the measurements of each solution were nearly normally distributed with only minor tailing. In a normal distribution the median and mean are equal. The observed median values were typically within about 1% of the mean for the 4 solutions. In all cases the medians were within the 95% confidence envelope of the means. Thus, it is reasonable and appropriate to use parametric techniques such as ANOVA to investigate these data.

Table 5. HAL CRM (NIST1641d) recovery 2004-2006.

| | |
|--------------------------|--------------|
| EPA Method 1631 | |
| Minimum | 71.0% |
| HAL Minimum | 75.0% |
| HAL 2.5% Quantile | 86.5% |
| HAL 10% Quantile | 90.0% |
| HAL 25% Quantile | 93.3% |
| HAL Mean | 95.2% |
| HAL Median | 95.7% |
| HAL 75% Quantile | 97.5% |
| HAL 90% Quantile | 99.7% |
| HAL 97.5% Quantile | 104.9% |
| HAL Maximum | 106.4% |
| EPA Method 1631 | |
| Maximum | 125.0% |
| HAL Precision (CV) | 4.1% |
| HAL Inter-Quartile Range | 4.5% |
| HAL 95%-Probability | |
| Range | 18.4% |
| HAL Range | 33.0% |
| HAL Number of Samples | 1073 |

Table 6. Summary table of the current study's interpretation of USGS Inter-lab comparison data for 2004-2007. Data for Northern States Analytical Laboratory (NSA) are provided to illustrate the possible spread (bias) between the HAL and another EPA Method 1631 – compliant laboratory.

| Solution | QA Solution Most Probable Value Estimates | | | | | | Individual Lab Performance | | | | |
|----------|---|--------|--------|------|--------|-----------|----------------------------|----------|--------|----------|--------|
| | N | L95%CI | Median | Mean | U95%CI | Med-Mean% | HAL Mean | HAL Bias | HAL CV | NSA Bias | NSA CV |
| MP1 | 134 | 6.36 | 6.40 | 6.47 | 6.59 | -1.1% | 6.10 | -5.72% | 9.2% | +2.8% | 7.3% |
| MP2 | 122 | 9.06 | 9.10 | 9.19 | 9.32 | -1.0% | 8.94 | -2.70% | 7.2% | +3.5% | 7.9% |
| MP3 | 113 | 15.1 | 15.4 | 15.4 | 15.8 | 0.0% | 14.2 | -7.80% | 12.3% | +5.2% | 9.5% |
| MP4 | 122 | 21.4 | 21.4 | 21.7 | 22.0 | -1.4% | 20.7 | -4.61% | 4.7% | +4.1% | 6.4% |

Discussion

Multiple working hypotheses were developed that might explain the observed differences in collector performance for sampling of precipitation and mercury. Below we review information gathered in this study and others that either supports or refutes each working hypothesis.

1. Differences between precipitation sensors were responsible for the -5% bias of the ACM as compared to the NCON and MICB collectors which were not significantly different in precipitation catch from the NWS gage.

The significantly lower number of lid openings and significantly lower time open for the ACM compared to the NCON and MICB are consistent with this hypothesis.

2. Rain splash from the large surface area pan, lid, or lid screen of the MICB collector augmented the precipitation collected by the MICB.

If rain splash was augmenting the collector catch of the MICB we might expect the following conditions to be true [result is provided in brackets]:

- Mean MICB %CE > 100% [not significantly different (nsd) from 100% by t-test]
- Mean MICB %CE significantly greater than both NCON and ACM [nsd from NCON]
- Mean MICB %CE positively correlated with average rainfall intensity (mm/hr) [ns]
- Mean MICB %CE > ACM and NCON for the top-5 rainfall intensity events [nsd]
- Mean MICB %CE positively correlated with maximum event rain intensity (mm/hr) [ns]

Landis and Keeler (1997) reported that the MICB collector under collected (98%) a co-located MICB sample train that was manually exposed on event basis on a simple ring stand which had no opportunity for sample splash.

3. Differing heater efficiencies lead to different collection efficiencies for snow and mixed precipitation events among the 3 collectors.

The ACM and MICB both had 1500 W heaters while the NCON had only 700 W of combined plate and fan-type heating capacity. The sample funnel is farthest from the heated area in the ACM and closest in the MICB. The NCON had the lowest %CE for snow but is similar to the ACM for mixed precipitation. The MICB had the highest %CE for both snow and mixed precipitation. There were multiple observations of unmelted precipitation in the NCON (6) and ACM (3) at the time of collection (Figure 3).

4. Differences in funnel geometry are responsible for different precipitation collection efficiencies among the 3 collectors.

The MICB funnel was the widest and had deep (18.5 cm), straight sides making it most similar to the geometry of the NWS 8-inch gage. A deep, cylindrical catch basin would be expected to be more efficient at preventing wind-entrainment of deposited snow and bounce out of high kinetic energy rain drops. If wind-entrainment were a significant problem, we might expect to see an inverse relationship between average or peak wind speeds and the %CE of the NCON and ACM. The mean %CE for snow events was markedly lower for the NCON (48%) and the ACM (55%) than for the MICB (80%). If bounce-out of high-energy rain droplets were a problem for the

shallow funnels, we might expect the %CE of the NCON and ACM to be negatively correlated to average or instantaneous rainfall intensity (mm/h) [contrary result, see below]. The mean %CE of the 5 most intense rain events was not significantly different (paired t-tests) between the NCON (99%), ACM (98%), and MICB (96%) collectors. The NCON had the lowest %CE for snow but was similar to the ACM for mixed precipitation. The MICB had the highest %CE for all precipitation types. Thus it seems likely that funnel geometry may influence collection efficiency for snow. The effect is less clear for rain (see #8 below).

5. Laboratory differences were responsible for a portion of the difference in mercury concentrations among samplers.

Processing of field samples for this study was conducted similarly by UMAQL and Frontier Geosciences following EPA Method 1631. Both laboratories demonstrated compliance with the Method 1631 performance criteria. Unfortunately, there were no direct comparisons between the laboratories during the time period of this study. Sample exchanges between Frontier Geosciences and the University of Michigan Air Quality Laboratory (UMAQL) in 1999 demonstrated that laboratory differences in analyses of pre-digested samples should not exceed 5% (Keeler, personal communication). The duplicate sample-trains analyzed at the two different laboratories were consistent with this earlier study, yielding an average difference between the laboratories of 6.2% (median 5.3%). The internal NIST recovery data for the HAL and the USGS multi-laboratory comparison indicate the HAL is biased low on average by 4.8% and 5.2%, respectively. The apparent 6.2% spread between the laboratories is less than the spread observed between the HAL and NSA (9.1%) in the USGS 6-lab comparison data. In a recent (2006) exchange of pre-digested samples between the UMAQL and the Dartmouth College Trace Element Research Facility agreement averaged 5.4% (slope of linear regression = 1.054, intercept=ns, $r^2 = 0.97$, $p < 0.0001$, Dartmouth biased high). The available information suggests that laboratory results from the HAL are generally 5% below NIST values while UMAQL results may be ~1.2% above NIST values. Therefore, it is reasonable to attribute 6.2% of the 22% difference between the MICB and ACM collector and 6.2% of the 13% difference between the MICB and NCON collector in this study to laboratory bias that is permitted to exist within the EPA Method 1631 performance criteria.

6. Rain splash from the large surface area pan, lid, or lid screen of the MICB collector contaminated the MICB samples leading to the observed greater Hg amount collected by the MICB relative the NCON and ACM samplers.

In the discussion of hypothesis 2 (above) we have explained why it is unlikely that rain splash makes a significant contribution to the MICB samples. Even if rain splash does not add significant volume to the sample, dry-deposited mercury on collector surfaces could still be picked up and added to the sample by minor rain splash. If this were the case, we would expect to observe the following:

- The difference in Hg collection between the MICB and NCON should increase with increasing rainfall amount [ns]
- The difference in Hg collection between the MICB and NCON should increase with increasing average rainfall intensity [ns]
- The difference in Hg collection between the MICB and NCON should increase with increasing peak rainfall intensity [ns]

- The difference in Hg collection between the MICB and NCON should be larger for the top-5 rainfall intensity events than for the bottom-5 intensity rainfall events [ns]

Landis and Keeler (1997) reported no statistically significant difference between the concentration of mercury collected using the UM-MICB automated system and a manual system consisting of the same sample train, deployed on an event basis with no possibility of splash contamination (15.8 ng/l and 15.9 ng/l, respectively).

7. The lower precipitation collection efficiency of the ACM sampler relative to the NCON and MICB samplers resulted in lower mercury concentrations being measured in samples from the ACM.

There was a weak but significant positive correlation between the ACM vs. NCON Hg bias and the ACM %CE ($r^2=0.19$, $p=0.0003$, Figure 5a). The Hg bias between the ACM and NCON for all samples with ACM % CE < 100% (mean -1.1 ng/l) was significantly less than the bias (+0.16 ng/l) for all samples with ACM %CE >= 100%.

There was also a weak but significant positive correlation between the ACM vs. MICB Hg bias and the ACM %CE ($r^2=0.07$ $p=0.0364$, Figure 5 b). The Hg bias between the ACM and MICB for all samples with ACM % CE < 100% (mean -2.73 ng/l) was significantly less than the bias (-1.10 ng/l) for all samples with ACM %CE >= 100%.

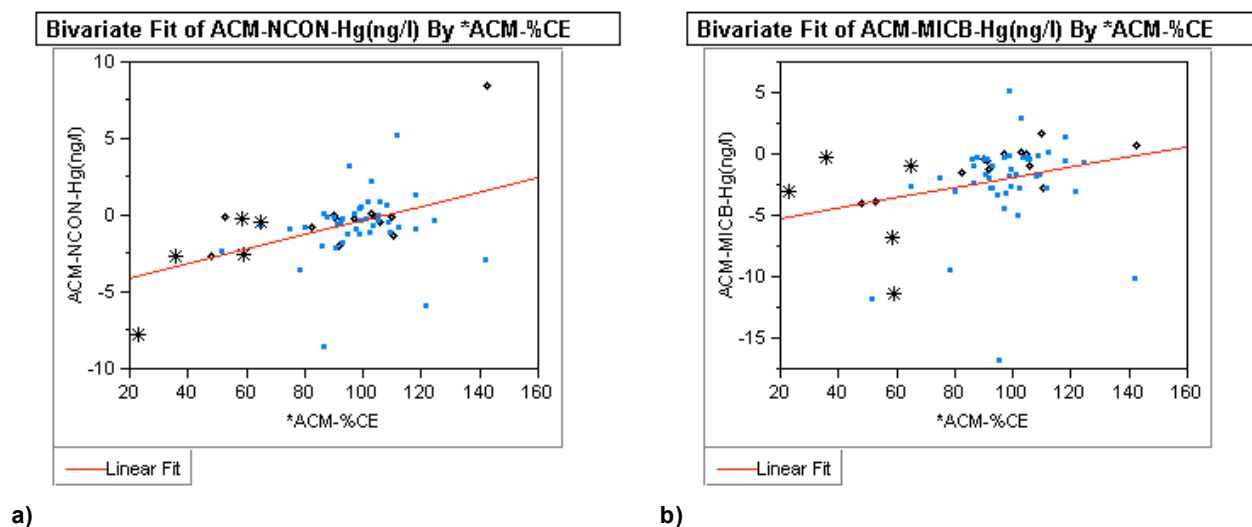
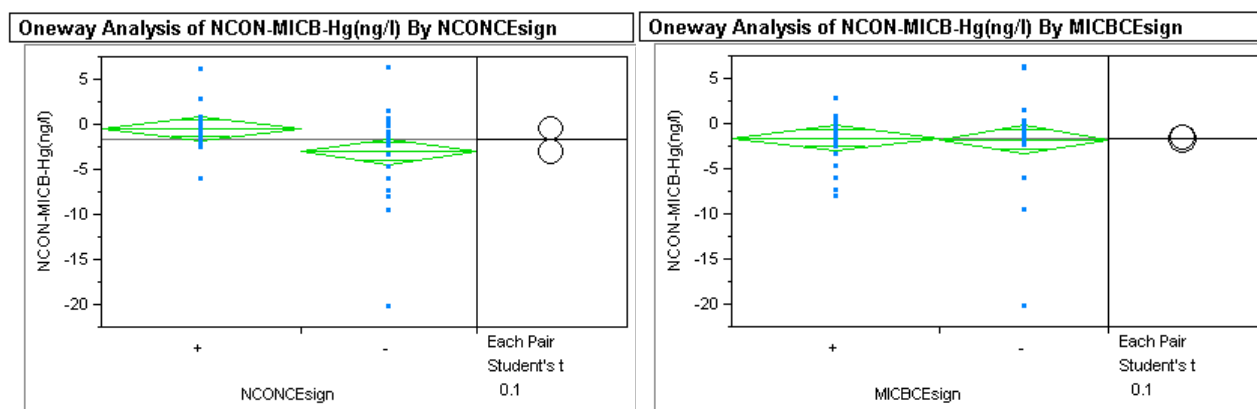


Figure 5. a) The difference in Hg concentration between the ACM and NCON samples was positively correlated with ACM % collection efficiency for precipitation. **b)** The difference in Hg concentration between the ACM and MICB samples was positively correlated with ACM % collection efficiency for precipitation. Stars = snow, diamonds = mixed precipitation, blue squares = rain.

8. Differences in collection efficiency of the NCON sampler relative to the MICB sampler resulted in lower mercury concentrations being measured in samples from the NCON.

Despite the lack of a significant difference between either the NCON or the MICB and the NWS1 gage for the collection of precipitation when analyzed over all 65 samples, there was a significant difference between the %CE of the NCON and MICB collectors for the 62 samples with valid Hg concentrations. The mean %CE for the NCON (95.5 %) was significantly different (1-sided, paired t-test, $p=0.0024$) from the %CE for the MICB (102.3%) including samples of all precipitation types. Mercury concentrations measured in samples of all precipitation types from the NCON were significantly less (t-test, $p = 0.05$) than in samples from the MICB when the %CE of the NCON was $<100\%$ (mean -2.45 ng/l) than when NCON %CE was $\geq 100\%$ (-0.55 ng/l). There was no significant difference (t-test, $p=0.88$) in mercury bias between the two collectors as a function of the MICB %CE with a mean bias of -1.48 ng/l for samples of all precipitation types.

The mean %CE for the NCON (100.4 %) was also significantly different (1-sided, paired t-test, $p=0.0024$) from the %CE for the MICB (104.9%) for rain-only samples. Mercury concentrations measured in samples of rain-only events from the NCON were significantly less (t-test, $p = 0.03$) than in samples from the MICB when the %CE of the NCON was $<100\%$ (mean -2.99 ng/l) than when NCON %CE was $\geq 100\%$ (-0.38 ng/l) (Figure 6a). There was no significant difference (t-test, $p=0.74$) in mercury bias between the two collectors as a function of the MICB %CE with a mean bias of -1.60 ng/l for samples of rain-only events (Figure 6b).



a)

b)

Figure 6. a) The difference in Hg concentration measured in samples from the NCON and MICB collectors was significantly different (t-test, $p = 0.03$) for events where the NCON over (+) or under (-) sampled precipitation relative to the NWS1 gage. The mean difference (NCON-MICB) was -0.38 ng/l for events where the NCON over sampled NWS1 and -2.99 ng/l for events where the NCON under sampled the NWS1 gage. **b)** The difference in Hg concentration measured in samples from the NCON and MICB was not significantly different (t-test, $p = 0.88$) as function of MICB over (+) or under (-) collection relative to the NWS1 precipitation gage.

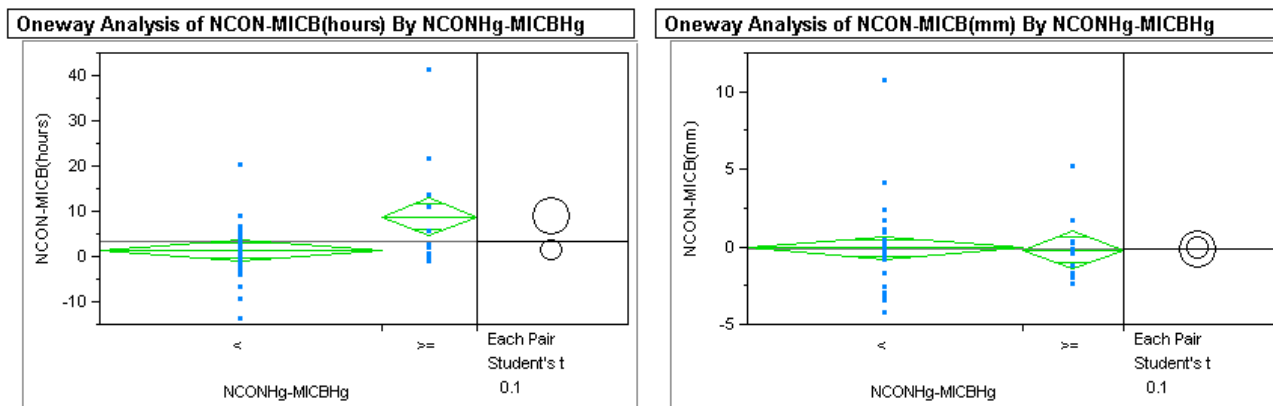
These relationships suggest that the observed differences in mercury concentration between the MICB and NCON collectors could, in part, be the result of the collection of slightly less precipitation by the NCON sampler than by the MICB sampler during rain, snow, and mixed precipitation. This small difference in collection is not enough to be significantly different from the

NWS1 gage collection, but is large enough to produce a significant and meaningful bias in the mercury concentrations measured in samples from the two collectors. However, it is difficult to square this interpretation of the results with lid opening data. The NCON and MICB lid openings were not significantly different and the NCON was consistently open for many more hours than the MICB, thus apparently offering more opportunity to collect precipitation and mercury than the MICB. The NCON was open on average 1.5 hours more than the MICB when measured mercury concentrations were less in the NCON samples than MICB samples. The NCON was open 9 hours longer than MICB on average when concentrations measured in the NCON samples were higher than the MICB. This difference in duration of opening was significant (t-test, $p=0.010$, Figure 7a). There was no significant difference in the amount of precipitation collected as a function of mercury concentration bias (Figure 7b) or as a function of difference in time open (linear regression, $p=0.827$). This may suggest that the additional time of lid opening for the NCON (average +9 hours) allowed dry deposition of Hg to be collected on the funnel that was subsequently incorporated into the sample with continuing rainfall resulting in higher concentrations compared to the MICB for these conditions. Dry deposition appears to be greater than potential volatile losses (see below).

Conversely, the additional amount of time the NCON was open compared to the MICB (average 1.5 hours, Figure 7a) when mercury concentrations measured in samples from the NCON were lower than those measured in samples from the MICB may have lead to a portion of the collected precipitation and mercury volatilizing and escaping from the NCON collector. It is possible that the thistle tube vapor restrictor is less effective than a water trap for preventing evaporation and volatile Hg loss. For the rain events where the measured Hg concentration in samples from the NCON were lower than those from the MICB there was a weak ($r^2=0.13$) but significant ($p=0.037$) positive correlation with the amount of precipitation measured by the NWS1 gage (Figure 8a). This relationship supports the idea of evaporative/volatile loss as an explanation for the lower %CE (Figure 8b) and lower Hg concentrations (Figure 8a) measured in these events relative to the MICB. Smaller volume samples would be more susceptible to evaporative/volatile loss than larger volume samples. It is hard to explain how more hours open would lead to a lower opportunity to catch precipitation. There was no significant correlation ($p=0.44$) between the MICB %CE for precipitation and NWS1 precipitation amount for the same events.

Another possible explanation for both lower %CE and lower Hg concentrations in the NCON collector for smaller precipitation events might be aerodynamic differences between the smaller funnel and chimney of the NCON, relative to the larger funnel and pan of the MICB. In windy conditions it might be possible for small droplets to escape capture by the smaller funnel, while the larger MICB pan and funnel create more drag, stalling airflow enough to allow small droplets to sediment into the collector.

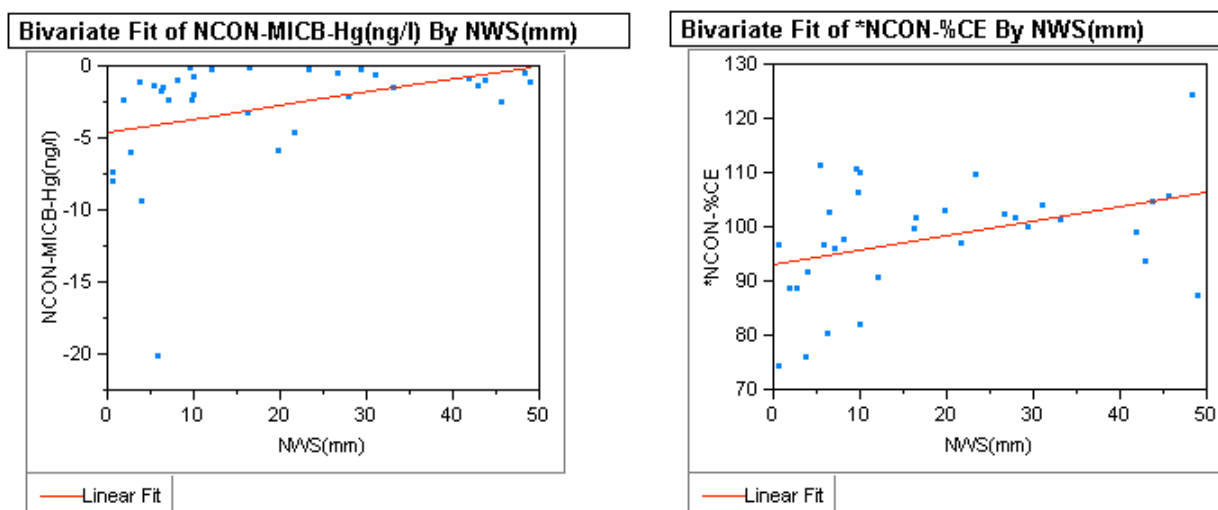
The paired sample-train comparison data suggest the possibility of a sample train bias (MDN 5-6% lower than UMICH). The sample train bias was only evaluated for rain samples. The sum of bias indicated for laboratory and sample-train effects approaches the total bias observed in the 1-year collector comparison. However, sample-train bias could be higher for mixed precipitation and snow (see above). The collector opening performance differences effects on collection efficiency could reasonably account for the remaining bias.



a)

b)

Figure 7. a) The difference in time open for the NCON and MICB collectors was significantly greater (t-test, $p=0.010$, + 9 hours) for events where the Hg concentrations measured in samples from the NCON were greater (\geq) than the Hg concentration in samples from the MICB compared to events where Hg concentrations from the NCON were less ($<$) than from the MICB (+ 1.5 hours). Rain-only events are shown in this figure, but a similar significant difference (t-test, $p=0.027$) was observed for all precipitation types. **b)** The significant difference in time open was not accompanied by a significant difference in precipitation captured by the NCON relative the MICB as a function of mercury concentration bias.



a)

b)

Figure 8. a) Linear correlation ($r^2=0.13$, $p=0.037$) between mercury concentration bias (NCON-MICB) and the amount of precipitation (equivalent to sample volume). The bias was more negative (lower concentrations from the NCON sampler) for lower volume events. This might be suggestive of evaporative/volatile loss. **b)** Linear correlation ($r^2=0.16$, $p=0.022$) between NCON percent precipitation collection efficiency and rainfall amount (equivalent to sample volume).

Mechanical failures of the collectors and sample trains

Each of the collectors had performance problems that compromised samples. The combination of large funnel diameter with a small sample bottle resulted in overflows for the MICB collector during 3 events. Overflow is a serious performance issue because large amounts of the annual deposition are included in large storm events. The MICB failed to sample 11.6% of the total precipitation for the year due to overflows. While mechanical failure of the MICB resulted in the loss of samples for 4.4% of the precipitation during the study period, this was an anomalous situation. The same MICB collector has been deployed at Underhill since 1993 with no prior mechanical failure. The ACM failed to sample 9.1% of the total precipitation for the year due to various mechanical failures. The NCON failed to sample 6.5% of the total precipitation due to mechanical failures. Additional samples from the ACM (17.9% of precipitation) and NCON (17.5% of precipitation) were compromised by sample bottle leaks during shipping and the failure to completely melt snow.

Transfer functions

Transfer functions were developed so that data acquired using each of the three collector types can be directly compared with each of the others. The correlations between collectors on an event basis are too low (only 80 to 86% of variance explained) to produce transfer functions with acceptable error rates (< 10%). However, the correlations between the monthly precipitation-weighted means of the different collectors are suitable for normalizing the data obtained with one collector to the reference frame of another. The NCON-MICB transfer function is very strong (98% of variance explained). The NCON-ACM and MICB-ACM transfer functions are satisfactory (90% of variance explained).

Using monthly precipitation-weighted means where the precipitation amount is on an NWS 8-inch gage basis for all collectors, the transfer functions are as follows:

1. NCON-basis = 1.0789 * ACM %variance explained = 90% (Figure 9a)
2. NCON-basis = 0.8813 * MICB %variance explained = 98%
3. MICB-basis = 1.2232 * ACM %variance explained = 90% (Figure 9b)
4. MICB-basis = 1.1320 * NCON %variance explained = 98% (Figure 9c)

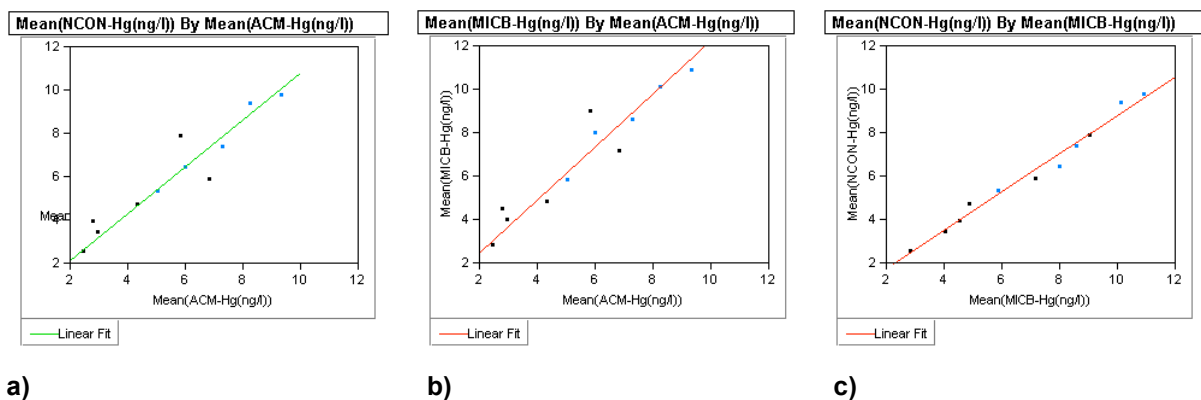


Figure 9. Transfer functions for NWS precipitation-weighted mean monthly mercury concentration.

Additional transfer functions were developed to correct each of the collector types to the best collective estimate of mercury concentration. Following the discussion above, MICB concentrations are reduced 1.2% and MDN (NCON or ACM) concentrations increased 5% to bring them a common NIST-referenced basis that is consistent with the mean performance of 6 laboratories. Thus, accounting for the sampling deficiencies discussed above:

1. Best Estimate = $0.988 * \text{MICB}$
2. Best Estimate = $1.209 * \text{ACM}$
3. Best Estimate = $1.116 * \text{NCON}$

Accounting for the 95% NIST-recovery normalization for the MDN samplers the effective difference between collector systems is 16% between the MICB and ACM sampler and 6.6% between the MICB and NCON sampler. As noted above, the difference between the NCON and ACM sampler is 7.9%. These differences in relative collector performance approximate the expected performance of duplicate ACM samplers (Wetherbee et al. 2008) of 8.6% to 13%. However, the precipitation regimes sampled by Wetherbee et al. (2008) may not be representative of the precipitation regime at VT99. In the discussion above we have demonstrated how differences in collector performance of this magnitude can be explained and accounted for, suggesting corrections that may be applied to account for systematic differences in estimates of precipitation and mercury by different sampling systems.

Summary

Lab-to-lab bias of 6.2% plus performance differences of sample-trains (6%), and collectors (sensors/heaters) explain differences in mercury collection of the NCON sampler with respect to the MICB sampler in rain and mixed precipitation events dominated by rain. Based on the observations in this study, it seems possible that evaporative/volatile losses from the NCON sample train and/or aerodynamic differences in the capture of small droplets between the two types of collectors may account for a portion of the observed difference in precipitation collection efficiencies and Hg concentration bias.

An additional -8% difference (total -23%) in mercury collection observed for the NCON with respect to the MICB during snowfall events is likely due to the demonstrated under sampling of snow by the version of the NCON sampler evaluated here. Under sampling of snow by the NCON is most likely due to a combination of funnel geometry and inadequate heating capacity. Heating capacity has been improved in current models.

Differences in the response of the rain sensors is most likely responsible for the under sampling of precipitation by the ACM relative to the NWS gage and the two other collectors. The under sampling of mercury by the ACM compared to both the NCON and MICB samplers appears to be related to failure to capture complete precipitation samples (fewer hours open, fewer lid openings, lower CE). The laboratory and sample-train differences noted above contribute to the difference between the ACM and the MICB collector as well. A modern rainfall sensor, a deep straight-sided funnel, additional heating of the sample funnel, and an improved motor-drive would significantly improve the performance of the ACM sampler.

Because of its larger funnel area and smaller sample bottle the original UM-MICB is prone to overflow potentially causing the loss of valid mercury data for a meaningful portion (~10%) of annual precipitation. The 2nd-generation UM-MICB sampler with multiple collection bottles addresses this problem.

Precipitation collector designs undergo constant modification and new designs for all three collectors emerged during this study. It is possible that the next generation ACM sampler may overcome some of the problems experienced in this study due to more durable screw-type motor drive and improved conductivity/wetness sensing grid. Current versions of the UM-MICB include the option to split event samples into multiple bottles under computer control or to sample multiple events without operator intervention. We propose modifications to the NCON sampler (larger, deeper, and straight-sided funnel, water trap, and a heated chimney) that may combine the advantages of the original UM-MICB and the NCON sampler designs to produce a low-cost and effective sampler for mercury suitable for wide deployment in North America.

Additional studies could be conducted to clearly identify the factors contributing to the 15% difference in mercury deposition measured by previous and current generation collectors. These investigations might include modifications to each of the collectors (heater, water-trap, straight-sided funnels), and triggering all collectors with a common precipitation sensor, wind-tunnel evaluations, and modeling. Additional raw and prepared sample exchanges between laboratories would be helpful. Because mechanical and power failures caused the amount of precipitation collected as snow or mixed precipitation to be severely underrepresented in this study, additional cold-season sampling should be conducted to better quantify collector limitations and performance differences.

Mercury concentrations estimated using the MICB and NCON collectors are extremely well correlated on a monthly precipitation-weighted mean basis with a consistent ~ 12-13% difference. Modelers and other users of MDN data should know that existing measurements based on the ACM are at least 8% low relative to an NCON collector and potentially as much as 18% low relative to an MICB collector on a monthly precipitation-weighted mean basis. The observed 6.2% difference between the two laboratories is within the range of commonly accepted agreement for trace-level analysis with EPA Method 1631 and within the demonstrated stable spread between the HAL and another laboratory. Thus, data from the two laboratories can be corrected to common NIST-referenced basis. Modelers should consider correcting data from multiple laboratories to a common NIST-referenced basis prior to combined analysis (e.g. atmospheric deposition and lake-water concentrations used in an ecosystem model). Atmospheric modelers should account for both the laboratory and sampler systematic biases prior to comparison of simulation results with wet-deposition observations. Unless these corrections are undertaken, data users should assign significant uncertainty envelopes (up to 54% allowed by EPA Method 1631, plus the additional uncertainty associated with differential collector performance) to the observational data used to drive or evaluate models. End-users of MDN data should also realize that apparent differences in mercury concentrations between locations and over time might be explained, in part, by differences in the amount of snow, rain, and mixed precipitation due to the strong bias of the ACM collector for frozen precipitation. Site operators should be required to provide information on precipitation type for each sample, and this information should be included in the web distribution of MDN data.

Acknowledgements

This research was funded by USEPA-ORD, NOAA-ARL, NOAA-Lake Champlain Research Consortium, NADP/MDN, USGS, and the Vermont Monitoring Cooperative. The University of Vermont Proctor Maple Research Center, Frontier Geosciences, Inc., and Ecosystems Research Group, Ltd. provided facilities, equipment, and additional support. We thank Melody Burkins, Carl Waite, Judy Rosvosky, Heidi Albright and the staff of the Proctor Maple Research Center for their contributions to the project.

References

- Landis, M.S. and G. J. Keeler (1997) Critical Evaluation of a Modified Automatic Wet-Only Precipitation Collector for Mercury and Trace Element Determinations. *Environmental Science and Technology* 31:2610-2615.
- Miller, E.K., VanArsdale, A., Keeler, G.J., Chalmers, A., Poissant, L., Kamman, N., and Brulotte, R. (2005) Estimation and Mapping of Wet and Dry Mercury Deposition across Northeastern North America. *Ecotoxicology* 14, 53-70.”
- Wetherbee, G.A., Latysh, N.E., and Greene, S.M. (2006) External quality-assurance results for the National Atmospheric Deposition Program/National Trends Network and Mercury Deposition Network, 2004, U.S. Geological Survey Scientific Investigations Report 2006-5067, 52 p.
- Wetherbee, G.A., Gay, D.A., Brunette, R.C., and Sweet, C.W. (2008) Estimated Variability of National Atmospheric Deposition Program/Mercury Deposition Network Measurements Using Collocated Samplers. *Environ. Monit. Assess.* DOI 10.1007/s10661-006-9456-6.

Draft Manuscript – 1/14/2009 – Please do not cite or distribute without permission from the first author.

Possible explanations for the lack of trend in wet deposition of mercury at Underhill Vermont during a period of significant estimated mercury emissions reductions

Eric K. Miller, Richard Poirot, Jamie Shanley, Mark Cohen, Lynne Gratz, Miriam Pendelton, Sean Lawson, Melody Burkins, and Gerald Keeler

Abstract

The National Oceanic and Atmospheric Administration, US Environmental Protection Agency, Vermont Monitoring Cooperative, University of Vermont, Ecosystems Research Group, Ltd., University of Michigan, US Geological Survey, and Vermont Department of Environmental Conservation Air Quality Division have collaborated to measure atmospheric mercury deposition at Underhill VT (44.5283N, 72.8684W) on a storm-event basis since 1993. This 15-year event-based record provides unique insights into the climatology of mercury wet deposition in northern New England. There were major national (45%) and regional (54%) reductions of estimated mercury emissions during the period of observation. However, neither wet deposition nor the concentration of mercury in precipitation at Underhill declined in response to these reductions. Mercury deposition and concentration at Underhill were correlated with precipitation amount. Deposition was strongly seasonal and event driven with 44% of annual deposition occurring from June through August in conjunction with specific high-deposition events. Analysis of NOAA HYSPLIT model backward air mass trajectories indicated that likely source regions for high deposition events and the majority of annual deposition were located to the south and west in areas with high densities of coal-fired electric generating units (EGUs). In contrast to estimated total mercury emissions, estimated EGU emissions have been flat during the period of observation. Variation in precipitation amounts at Underhill and along transport paths appear to be responsible for much of the year-to-year variation in mercury wet deposition at Underhill, VT.

Introduction

Mercury is used in industry, medicine and dentistry, and in commercial products such as fluorescent lights, thermostats, switches, and thermometers. Mercury is also present as a trace contaminant in coal and oil. Mercury is released into the atmosphere when metal ores are smelted or coal, oil or municipal and medical wastes are combusted in facilities without proper pollution control technology. Large amounts of mercury have been released into the environment over the last several centuries by human activities, much of which is now stored in soils, vegetation, and lake sediments. Previously deposited anthropogenic mercury is re-emitted to the atmosphere by a process termed evasion and during forest fires.

Once deposited to the land or water a small fraction of mercury pollution is converted to the organic methyl-mercury form by bacteria active in anaerobic conditions. While it was recently thought that this methylation activity was restricted to throughoutly anoxic environments such as lake bottoms during summer stratification, recent research has shown the methylation process occurs widely in anerobic microsities in soils and sediments. Methyl-mercury is a potent neurotoxin and is readily concentrated in animal tissues. Methyl-mercury accumulates in both aquatic and terrestrial food webs (Rimmer et al. in preparation). Higher trophic level organisms with longer life-spans and slower growth rates exhibit the highest total and methyl-mercury burdens. Vermont and many other states have been forced to issue advisories against the consumption of popular fish species due their accumulated mercury levels. Emerging science is recognizing biologically significant mercury burdens in top-level consumer organisms in terrestrial food webs. There is particular concern about mercury impacts on insectivorous birds.

The atmospheric mercury observation program at Underhill, Vermont is designed to provide a comprehensive picture of atmospheric mercury pollution. The areas of investigation range from the temporal patterns of mercury concentration and speciation, to identification of sources of atmospheric mercury pollution arriving in Vermont, to direct measurements mercury deposition and evasion. The Underhill Air Quality Measurement site hosts a wide range of air pollution monitoring programs funded and operated by state and federal agencies. Other measurements include sulfur, nitrogen, and acid deposition, ground-level ozone, toxic substances, trace metals, fine particulate mass, UV-radiation, and meteorology. These additional measurements significantly enhance the ability to interpret the atmospheric mercury observations.

Atmospheric mercury research began at Underhill in 1992 when the University of Vermont and University of Michigan initiated a long-term monitoring program for mercury in precipitation. Precipitation samples are collected by an automated collector, which opens only during a precipitation event (Figure 1). In 2004 the Underhill Air Quality Site joined the NADP Mercury Deposition Network (MDN). Samplers using both the Michigan and MDN protocol were operated simultaneously for a period of 2 years after which event sampling was continued using only the MDN sampler and protocol. The record of mercury concentrations and deposition in individual rain and snow events at Underhill is the longest event-based record of mercury deposition in the world. During the 1990s pioneering studies of mercury accumulation in forest tree leaves, mercury in cloud water, and the wash-off of dry deposited material from tree leaves were conducted by UVM students in cooperation with UMAQL.



Figure 1. The University of Michigan MICB (left) and Mercury Deposition Network ACM (right) automated samplers for collecting mercury in precipitation. Moisture on a wetness-sensing element (on pole at upper right of the Michigan collector – not visible on the MDN collector) causes the lid to automatically open, exposing a clean sample train for collection of rainfall. Site operators exchange sample trains following each rain or snow event.

Several scientific papers have been published describing or using the information on atmospheric mercury collected at Underhill. Burke et al (1995) described the seasonal patterns in atmospheric mercury concentrations and deposition. Mercury concentrations and wet-deposition were highest in summer months and lowest in winter months, particularly when airflow associated with a precipitation event was from the south through west. Subsequent analyses using other wet deposition measurements throughout northeastern North America demonstrated that this seasonal pattern occurs throughout the region (Miller et al. 2005; VanArsdale et al. 2005).

In the late 1990s Lawson et al. (2003) and Malcom et al. (2003) investigated the concentration of mercury in cloud water near the summit of Mt. Mansfield adjacent to Underhill, Vermont. They found that mercury in cloud water was similar to but slightly higher (by a factor of 1.2) than the concentrations observed in precipitation. This difference can be explained by the generally smaller size (and lower water volume) of cloud droplets compared to rain droplets. Mercury does not appear to be as readily enriched in clouds droplets as are other pollutants such as sulfur and nitrogen. This is due to the exceedingly low concentrations of the soluble mercury forms (RGM and HGP) in the atmosphere and the very low water solubility of the dominant form

(GEM). Similar to the earlier results for precipitation (Burke et al. 1995), the highest cloud water concentrations were observed when airflow was from the southwest.

Keeler et al. (2005) described the record of mercury concentration and deposition in precipitation at Underhill measured by the Michigan MICB collector through 2003. Both Keeler et al. (2005) and VanArsdale et al. (2005) – who analyzed the Underhill data in conjunction with additional data from MDN sites in the region – determined that most of the annual mercury deposition in New England is associated with a small number of “high-deposition” periods or events, typically occurring from spring through early fall, when air-masses had traveled from the south and southwest to reach New England. These high deposition events appear to be associated with meteorological conditions that result in air-mass trajectories that bring air from high emissions density regions to the northeast during periods of vigorous convective mixing resulting in moderate to heavy rainfall (Keeler et al. 2005).

This paper analyzes the combined record from the Michigan MICB collector and NADP/MDN ACM collector through 2007. The additional years of observations increase the capability of the record for trend detection or rejection. New observations from the MDN collector from 2005 through 2007 are analyzed using air mass back trajectory methods to obtain further insights on factors controlling the timing and magnitude of mercury wet deposition in northern New England.

Methods

Study site

The Underhill, VT Air Quality Site (44.5283N, 72.8684W, 400-m elevation) is located in a rural setting on the campus of the University of Vermont Proctor Maple Research Center. Collectors are located in a clearing surrounded by northern hardwood forest. Situated on the western shoulder Mt. Mansfield, approximately 30 km east of Burlington, VT, the site is representative of deposition in the Lake Champlain Basin of Northern VT and NY. The site staff has extensive experience with precipitation collection through participation in NADP NTN, AIRMoN, MDN, VTDEC, and UMAQL networks. A site operator visits the site daily to facilitate event collection.

Precipitation collection and analysis using the MICB collector (1993-2006)

From 1993 to 2006 mercury wet deposition was monitored with the University of Michigan Air Quality Laboratory (UMAQL) protocol and UMAQL-modified MICB collector (Figure 1a, Burke et al. 1995, Keeler et al. 2006). Samples were analyzed at UMAQL following EPA method 1631.

Precipitation collection and analysis using the MDN ACM collector (2005-2007)

From 2005-2007 mercury wet deposition was monitored using the NADP Mercury Deposition Network (MDN) ACM (Figure 1b) sampler and protocol. Samples were analyzed following EPA Method 1631 at the MDN Hg Analytical Laboratory (HAL), Frontier Geosciences

in Seattle, WA. The sample protocol and sample processing are very similar to the UMAQL methods and are described in (Wetherbee et al. 2007).

Beginning in 2006 methyl mercury was analyzed in samples obtained with the MDN-ACM collector. Event-based analyses were conducted during the warm (June – October) season while monthly composite analyses were conducted during the remainder of the year. Methyl mercury was analyzed at the MDN HAL (<http://nadp.sws.uiuc.edu/lib/qaplans/HALqap2006.pdf>).

Blending data from two collection systems to create a long-term record

From 2005 to 2006 we operated both the MICB collection and analysis system and the MDN collection and analysis system on an event basis at Underhill (MDN site VT99). We conducted an exhaustive comparative performance analysis of the UMAQL-MICB, the MDN-ACM, and MDN-NCON collectors that is reported elsewhere (Miller et al. in preparation and Miller et al. 2008). From this study we developed transfer functions to relate concentration and deposition measured with each collector to measurements made with another. These transfer functions explained a high proportion of variance in the data ($r^2 = 0.9$) and are used to adjust for differential collection efficiencies of the two systems. We also determined that there was a stable and explainable bias between the MDN HAL and UMAQL laboratories on the basis of internal and external NIST-referenced QA samples provided by MDN and USGS (Greg Wetherbee, USGS personal communication 2008). The observed laboratory-laboratory bias of 9% was well within the performance requirements of EPA Method 1631 (77 -123%, USEPA 2002) to which both laboratories adhere. Still, this level of bias must be accounted for when comparing data from two different laboratories as we do here. To merge the time series, mercury concentrations from each laboratory were adjusted to a NIST recovery value of 100% based on the observed NIST recoveries. This adjustment eliminated the laboratory bias and eliminated the need to arbitrarily establish one laboratory or the other as the “best” measurement of concentration.

The two networks had different approaches to estimating precipitation amount with the UMAQL network using the precipitation catch of the collector (Landis and Keeler, 1997) and MDN using the precipitation measured by a co-located Belfort recording rain gage. Our comparative study demonstrated that the MICB precipitation collection was not significantly different from an NWS standard 8-inch gage, while the Belfort underestimated the NWS gage catch (Miller et al. in preparation). The long-term record was standardized to an NWS 8-inch precipitation gage basis. Deposition was calculated as the product of the NIST-referenced concentrations and NWS-gage referenced precipitation amounts.

Back trajectory analysis and source region identification

Air-mass backward trajectories for the 72 hours preceding air arrival at the receptor site were calculated using NOAA’s HYSPLIT model (Draxler et al. 2003) using EDAS 40-km resolution meteorology archived by NOAA. Trajectories were calculated in this study for a subset of all observations (2005-2007) corresponding to the MDN-network samples and because trajectory analysis for the period 1993-2003 had already been reported elsewhere (Keeler et al. 2005). A difficulty with calculating trajectories associated with precipitation events is associating air-mass arrival with precipitation collected. Earlier studies (e.g. Keeler et al. 2005) often selected a single “representative” trajectory associated with air arrival in the middle of or at the onset of the major precipitation associated with an event. From 2005-2007 we collected data from collector openings, tipping-bucket rain gage activity, relative humidity sensors, and a surface wetness sensor to document the periods of time when precipitation was occurring during the course (start to finish) of

an observed wet deposition event. We included in the analysis trajectories associated with all times of active precipitation during the 3-hour intervals. These trajectories were retrieved from a database of hourly trajectories developed for a companion study of ambient air mercury speciation (Miller et al. in preparation). Trajectory start heights for the primary trajectory data set were set to 500 m asl for the purposes of the ambient air speciation study. It is common practice to start trajectories at $\frac{1}{2}$ the mixed layer depth for precipitation studies (So.-Lai et al. 2007). The location of the Underhill site on the shoulder of Mt. Mansfield at 400 m asl places this site relatively high in the mixed layer – or at times above the mixed layer – and often at or just below cloud base during precipitation. Evaluation of mixed-layer depths during precipitation from the EDAS data indicated that the 500 m start height was appropriate for all 221 events analyzed in the trajectory study. Meteorological conditions (rainfall, air temperature, relative humidity, solar-flux, mixed layer depth) were extracted from the EDAS data for each trajectory endpoint time-location.

All hourly endpoints for trajectories originating at appropriate heights and times associated with each precipitation event were assigned the characteristics of each event at the receptor (concentration, precipitation amount, deposition). Trajectory endpoints with associated receptor conditions were aggregated into 1° degree latitude by 1° longitude grid cells. Descriptive statistics of receptor conditions associated with air passage over each grid cell were calculated. Maps were produced showing the number of times air arriving at the receptor during precipitation traversed each grid cell. Grid cells with fewer than 10 trajectory endpoints were removed from further analysis due to the limited representation of air traversing those locations at the receptor (Poirot and Wishinski, 1985). All GIS operations were conducted using IDRISI image processing software (Clark University <http://www.clarklabs.org>). These maps were used to identify likely source regions for high concentration and deposition events.

The potential source regions indicated by back-trajectory analysis were compared with a mercury emissions inventory (Cohen et al. 2004) to assess correspondence between potential source regions indicated by the trajectory analysis and known anthropogenic mercury emissions sources. The Cohen et al. (2004) inventory represents estimated emissions prior to the major regional reductions (~90%) in municipal waste combustor (MWC) and medical waste incinerator (MWI) emissions that occurred between 1998 and 2003. For this reason MWC and MWI emissions in the inventory were eliminated from this analysis of 2005-2007 precipitation events and trajectories. Because of uncertainty in trajectory endpoint locations due to numerical dispersion (Draxler et al. 2003) and the importance of large point sources to mercury emissions, the emissions data were aggregated into 1° latitude by 1° longitude grid cells for comparison with trajectory frequency. Specific precipitation events were associated with the emissions in a grid cell if any of the of the trajectory endpoints for an event fell within an emissions grid cell. Emissions were only associated with an event if the trajectory height in a given grid cell was below the mixed-layer height. If the trajectory height was above the mixed layer height at a grid cell, then it was assumed that the air mass transited that location without significant incorporation of emissions from within that cell as those emissions would likely be confined to the mixed layer. Emissions associated with specific event trajectories were also normalized for time-of-travel from source to receptor by dividing the emissions in a grid cell by the number of hours required to reach the receptor along the associated trajectory from that location. Time-of-travel normalized emissions were summed along all trajectories contributing to each event. Statistical analysis (described below) was conducted to explore the association of meteorological conditions and emissions along trajectories with deposition of mercury at the receptor.

Statistical analysis

Descriptive statistics, linear regressions, and ANOVA analyses were calculated using JMP 6.03 (SAS institute) statistical software. Data were natural log transformed as appropriate to obtain normal distributions prior to specific parametric analyses. Non-parametric Kendall family of trend tests were performed with the USGS computer program kendall.exe (Helsel et al. 2005 SIR 2005-5275 <http://pubs.usgs.gov/sir/2005/5275>). Seasonal Mann-Kendall p values were adjusted for serial correlation (Helsel et al. 2005) as there were more than 10 years of data available.

Results and Discussion

The NIST-referenced and collector efficiency-adjusted estimates of deposition for the two collector systems were comparable during the two years of overlap (2005:9.3/8.9, 2006:9.0/10.2 MICB/ACM). The difference between the two collector-protocol-laboratory systems (2005:-4.1%, 2006:+12%) was much less than the coefficient of variation for the time series (+/-20%) and within the expected range of agreement for two co-located MDN-ACM collectors as determined by Wetherbee et al. (2007). The adjusted MDN-ACM values obtained for 2005 and 2006 were used for this analysis.

Annual mercury wet deposition averaged 10.1 ug/m² from 1993-2007 with a precipitation-weighted mean concentration of 8.5 ng/L and average precipitation rate of 120 cm/year. There was considerable year-to-year variation in precipitation (Figure 2), mercury concentration (Figure 3), and mercury deposition (Figure 2). This variation was normally distributed (Shapiro-Wilk test) for precipitation amount and the precipitation-weighted mean concentration suggesting random processes influencing each. However, the distribution of annual mercury deposition was skewed slightly (median 9.21 ng/L, mean 10.1 ng/L).

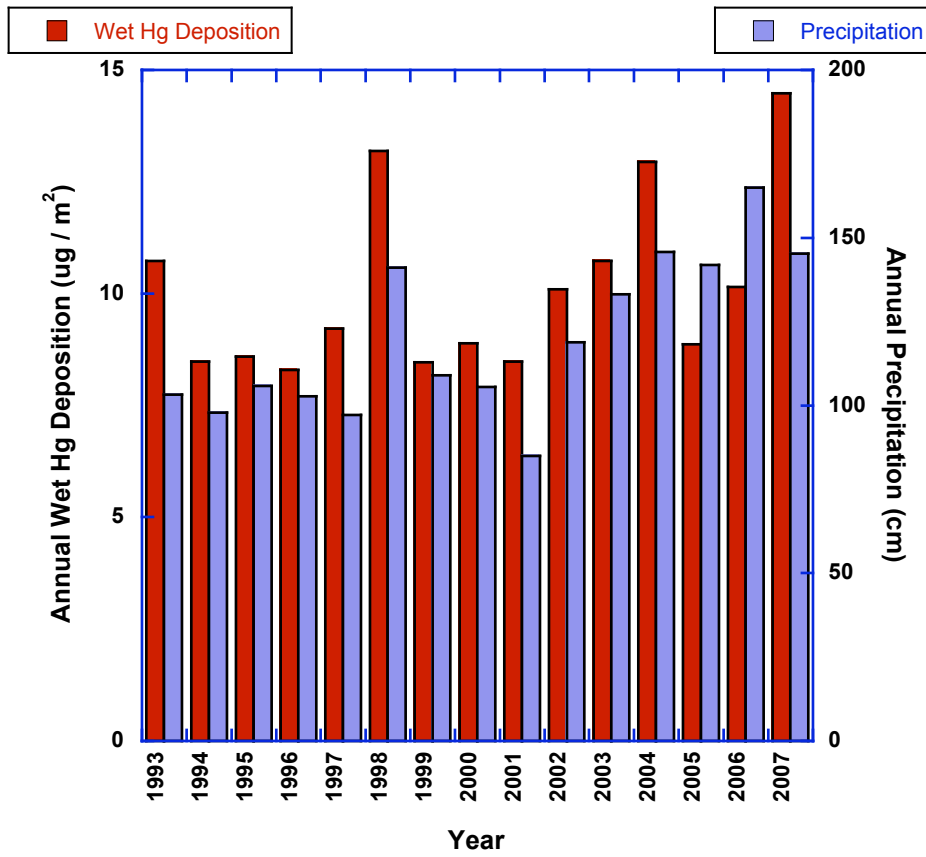


Figure 2. Annual precipitation and mercury wet deposition at Underhill, VT 1993-2007.

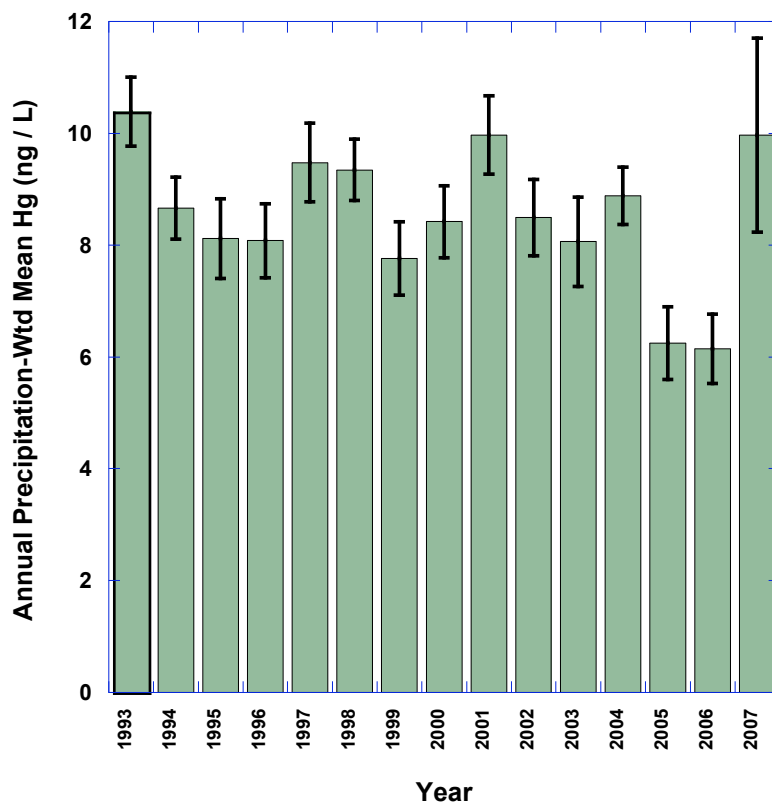


Figure 3. Annual precipitation-weighted mercury concentration in precipitation with standard errors.

Deposition was strongly seasonal with 44% of annual deposition occurring during summer (June-August) while only 10% of annual deposition occurred during winter (December-February) (Figure 4). Precipitation was also seasonal, but less so than mercury deposition (Figure 4). The proportions of precipitation delivered in summer and fall (September-November) precipitation were not significantly different at $p = 0.01$ (Tukey-Kramer HSD) with each season contributing just over 30% of annual precipitation. The proportion of annual precipitation delivered was significantly ($p = 0.01$) lower in winter (15%) and spring (March-May, 22%). Individual high-deposition events were responsible for a significant fraction of annual deposition. Two events (out of 1463) contributed more than 10% of annual deposition in their respective years, 22 events (1.5%) contributed more than 5% of annual deposition, and 498 events (34%) contributed more than 1% of annual deposition. High-deposition events were typically associated with air mass back trajectories to the south through west (Keeler et al. 2005, and discussed in detail below).

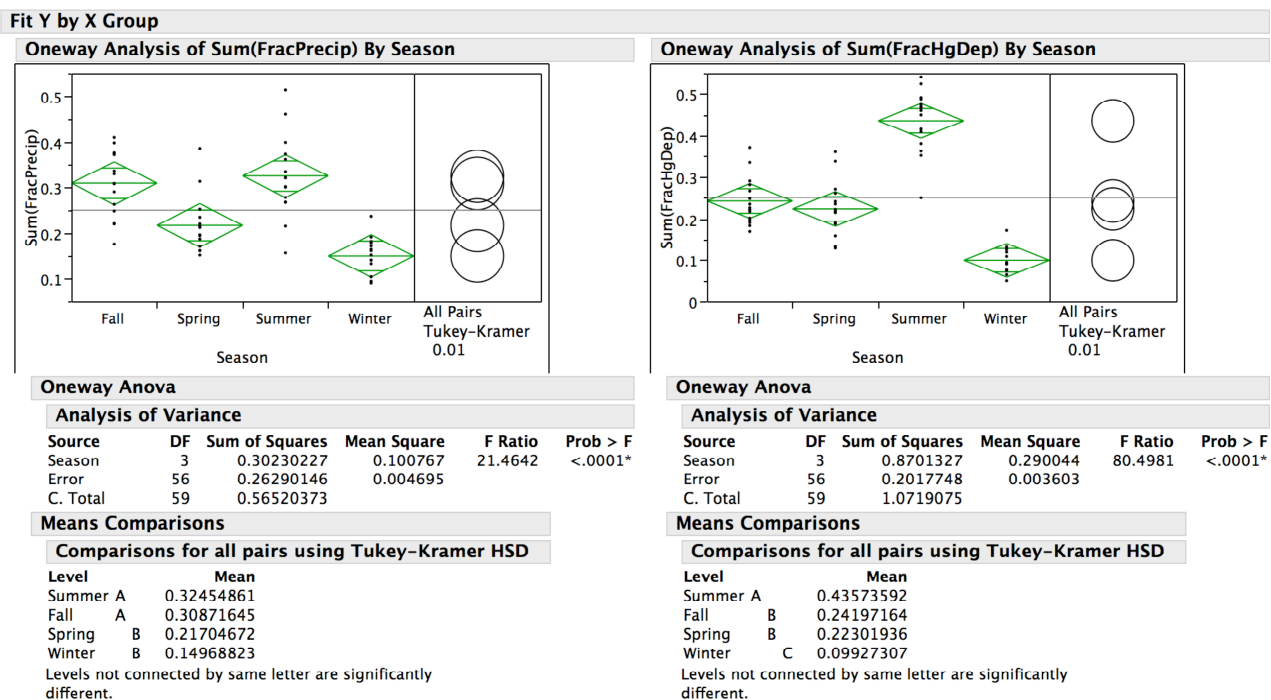


Figure 4. ANOVAs for the fraction of annual precipitation and fractional mercury wet deposition delivered by season (1993-2007).

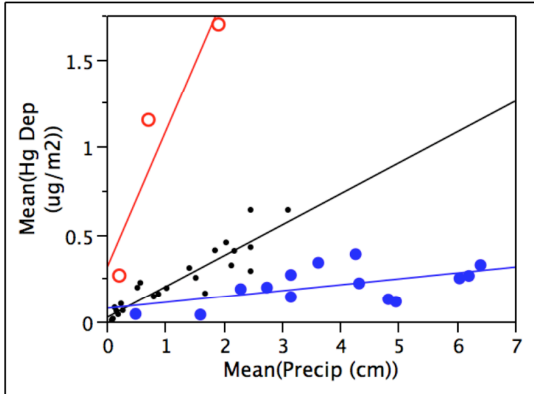
Potential mercury sources and meteorological influences on mercury deposition

There were consistent correlations between mercury wet deposition and precipitation amount by season suggesting stable sources and/or atmospheric production of divalent mercury available for scavenging in a given season. However, there were frequent outliers of either higher or lower apparent scavenging or higher or lower atmospheric Hg^{2+} levels in any given month (Figure 5, Table 1). The high and low outlier groups also showed consistent correlations with precipitation by season with either higher or lower slopes indicated (Figure 5, Table 1). The slopes of the regressions of wet deposition vs. precipitation were highest in summer and lowest in winter months (Figure 6, Table 1), consistent with the observed behavior of the volume weighted mean concentrations. The majority of events follow the intermediate deposition vs. precipitation trend group. We designate this trend (slope) the “normal” deposition dependence on precipitation rate. We designate the events falling on the higher slope trend for each season as the “high” deposition rate events, and the events falling on the lower slope trend for each season as the “low” deposition rate events.

11/18/08 5:32 PM

Data Table=June-July Subset of wet-traj-with-emiss-0d By
(WYear, WMonth, WDay, Season, Collection End Date)

Bivariate Fit of Mean(Hg Dep (ug/m2)) By Mean(Precip (cm))



— Linear Fit
— Linear Fit
— Linear Fit

Linear Fit

$$\text{Mean(Hg Dep (ug/m2))} = 0.0218845 + 0.1764932 \text{ Mean(Precip (cm))}$$

Summary of Fit

| | |
|----------------------------|----------|
| RSquare | 0.827767 |
| RSquare Adj | 0.819938 |
| Root Mean Square Error | 0.078391 |
| Mean of Response | 0.235 |
| Observations (or Sum Wgts) | 24 |

Linear Fit

$$\text{Mean(Hg Dep (ug/m2))} = 0.3020808 + 0.7719432 \text{ Mean(Precip (cm))}$$

Summary of Fit

| | |
|----------------------------|----------|
| RSquare | 0.869812 |
| RSquare Adj | 0.739625 |
| Root Mean Square Error | 0.369003 |
| Mean of Response | 1.038 |
| Observations (or Sum Wgts) | 3 |

Linear Fit

$$\text{Mean(Hg Dep (ug/m2))} = 0.0757006 + 0.0339338 \text{ Mean(Precip (cm))}$$

Summary of Fit

| | |
|----------------------------|----------|
| RSquare | 0.3162 |
| RSquare Adj | 0.259217 |
| Root Mean Square Error | 0.091574 |
| Mean of Response | 0.207 |
| Observations (or Sum Wgts) | 14 |

Figure 5. Example separation of “high”, “normal”, and “low” deposition per unit precipitation trends. This example shows the combined events for June and July 2005-2007. The period 2005-2007 (the MDN record) is used here for consistency with the trajectory analysis presented below.

Table 1. Slopes, standard errors, and coefficients of determination for regressions of event wet mercury deposition ($\mu\text{g}/\text{m}^2$) against event precipitation (cm). The “normal” trend events were regressed by month. Due to the small number of observations of “high” and “low” trend events, these groups were regressed by two seasons (Fall-Winter-Spring and Summer). The values for the seasonal regressions are placed in the corresponding monthly positions in the table if there were events (data points) contributed to the seasonal regressions for a given month.

| Month | HIGH Deposition | | | Normal Deposition | | | Low Deposition | | |
|-----------|-----------------|-------|----------------|-------------------|-------|----------------|----------------|-------|----------------|
| | Slope | SE | r ² | Slope | SE | r ² | Slope | SE | r ² |
| 1 | 0.079 | 0.004 | 0.97 | 0.033 | 0.006 | 0.68 | 0.022 | 0.005 | 0.58 |
| 2 | 0.079 | 0.004 | 0.97 | 0.030 | 0.002 | 0.94 | 0.022 | 0.005 | 0.58 |
| 3 | ne | ne | ne | 0.131 | 0.013 | 0.91 | 0.022 | 0.005 | 0.58 |
| 4 | ne | ne | ne | 0.108 | 0.015 | 0.88 | 0.022 | 0.005 | 0.58 |
| 5 | ne | ne | ne | 0.118 | 0.023 | 0.66 | 0.022 | 0.005 | 0.58 |
| 6 | ne | ne | ne | 0.181 | 0.024 | 0.83 | 0.129 | 0.012 | 0.96 |
| 7 | 0.772 | 0.299 | 0.74 | 0.172 | 0.027 | 0.79 | 0.129 | 0.012 | 0.96 |
| 8 | ne | ne | ne | 0.098 | 0.009 | 0.86 | 0.129 | 0.012 | 0.96 |
| 9 | ne | ne | ne | 0.097 | 0.011 | 0.82 | 0.022 | 0.005 | 0.58 |
| 10 | 0.079 | 0.004 | 0.97 | 0.041 | 0.005 | 0.81 | 0.022 | 0.005 | 0.58 |
| 11 | 0.079 | 0.004 | 0.97 | 0.034 | 0.004 | 0.79 | 0.022 | 0.005 | 0.58 |
| 12 | 0.079 | 0.004 | 0.97 | 0.029 | 0.002 | 0.95 | 0.022 | 0.005 | 0.58 |

*ne - no high deposition events were detected during these months

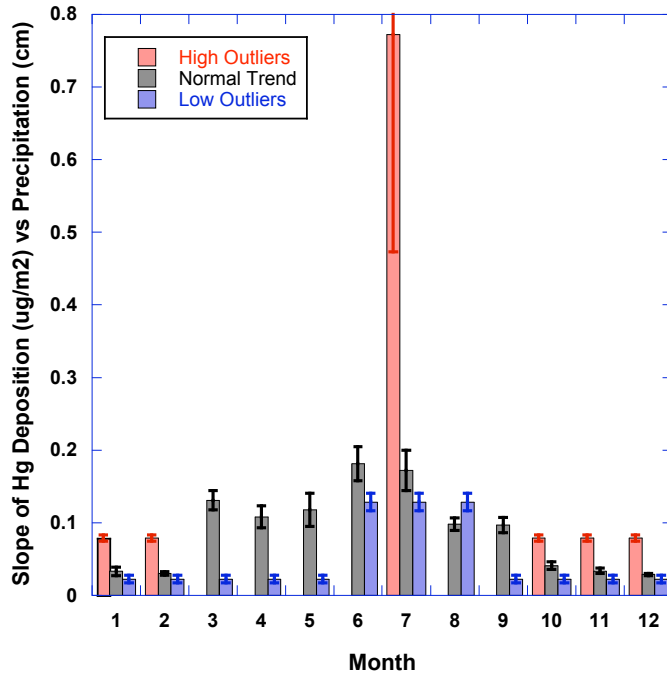


Figure 6. Slopes (with standard errors) of event wet mercury deposition ($\mu\text{g}/\text{m}^2$) against event precipitation (cm) by month (normal trend) and season (high and low trends).

Differences in emissions incorporated into the precipitating air-mass is a possible explanation for the different apparent functions of deposition with respect to precipitation amount (high, normal, low) in each season. Both total and time-of-travel normalized estimated mercury emissions along event back trajectories were higher for events in the group with higher deposition / precipitation slope than for the normal slope group when compared by season (ANOVA $p < 0.0001$, Figure 7). Both the total and normalized estimated emissions along the trajectories for the lower slope events were lower than those for the normal slope events, which in turn were lower than those for the high slope events ($p = 0.01$ means comparison, Figure 7). Back trajectories transited over lower estimated emissions regions during normal and low deposition events during summer than during other seasons (ANOVA $p = 0.01$, Figure 7). This was not true for high-deposition events for which the time-of-travel normalized estimated emissions along the back trajectories were not significantly different between seasons (t-test). These relationships suggest that different emissions levels associated with different transport pathways play a role in the increased or decreased deposition relative to precipitation amount relative to the normal trend in the high and low slope event groups (see additional discussion below).

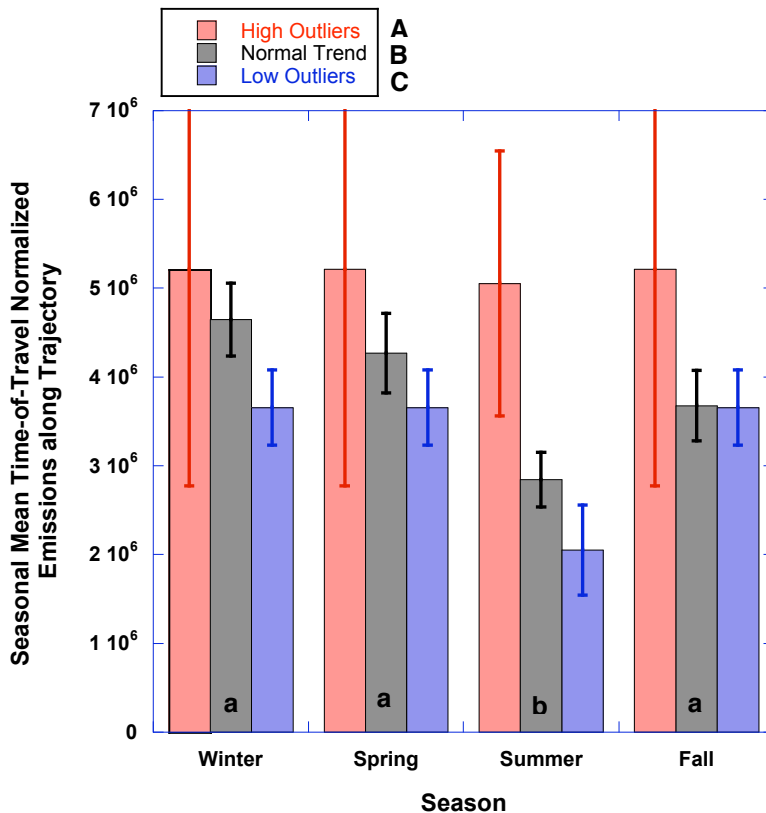


Figure 7. Time-of-travel normalized emissions along the back trajectories associated with precipitation events sampled at Underhill, VT during different seasons 2005-2007. Capital letters indicate significant ($p = 0.01$ means test) differences between event types (High, Normal, Low trends) across seasons using natural log transformed data (ANOVA $p < 0.0001$). Small letters indicate significant ($p = 0.01$ means test) between seasons for a given event type (ANOVA $p = 0.01$).

Low Hg deposition per unit precipitation events were associated with higher average precipitation amounts (mean 4.7 cm vs. 1.45 cm for high and normal trend events, $p=0.01$ means test, ANOVA $p<0.0001$). This relationship suggests a diluting effect of additional rainfall from low Hg trajectories providing a larger fraction of the precipitation than higher Hg trajectories during the event. Meteorological conditions along the back trajectory also differed by event type (high, normal, low slope). Low Hg deposition per unit precipitation events had higher humidity ($p=0.05$ means test, ANOVA $p=0.001$) and higher rainfall prior to arrival at the receptor ($p=0.05$ means test, ANOVA $p=0.029$). This suggests there was greater opportunity for scavenging and removal of atmospheric Hg^{2+} along the transport path prior to commencement of precipitation at Underhill. A general linear model including precipitation at the receptor, event type, trajectory mean solar flux, trajectory mean air temperature, and trajectory sum of emissions explained 83.7% of the variance in Hg wet deposition (Table 2). Thus, meteorological conditions and spatial variation in emissions along transport paths appear to regulate wet deposition rates at Underhill, VT. The substantial proportion of variance explained by the solar flux along the transport path is consistent with current models of photochemically driven oxidation of GEM to Hg^{2+} (Lin and Pekonnen 1999).

Table 2. General linear model results for mercury wet deposition as a function of precipitation amount at receptor site and meteorological conditions along air mass back trajectories for events sampled from 2005-2007. The bulk of the emissions signal is captured by the “Event Type” term (High, Normal, Low – see text).

| 2005-2007 221 Events Variance Explained Effect on Deposition p | PPT-R | TSunFlux | EventType | TSumEmiss | TAirT | Total |
|---|--------------|-----------------|------------------|------------------|--------------|--------------|
| | 55.9% | 17.9% | 8.6% | 0.9% | 0.5% | 83.7% |
| | + | + | H+, L- | + | + | |
| | <0.0001 | <0.0001 | <0.0001 | 0.0003 | 0.0078 | <0.0001 |

A challenge for identification of sources using event precipitation samples with back-trajectory analysis is that most precipitation event samples combine precipitation originating from different air masses arriving at different times over the many hours or days of a typical precipitation event. Therefore, multiple trajectories must be identified for each event and it is likely that only a few will describe the transport of the majority of the mercury contained in any given sample. The other trajectories will likely reflect additional precipitation from a non-source region that is diluting the sample.

A typical frontal-passage type rainfall scenario for Underhill involves low pressure to the north of the site and high pressure to the south both moving east. Initial flow is from the south and southwest sector, with flow shifting to the west and northwest as the front passes with precipitation occurring throughout the period. This general pattern is evident in Figure 8, which shows the frequency of trajectory hourly endpoints intersecting a grid cell for 221 precipitation events sampled at Underhill from 2005-2007. While there is clearly air arriving from eastern sectors associated with precipitation, the dominant pathways are from SSW, SW, W, and NW. Figure 8 also shows the total mercury emissions for each grid cell that was traversed by air arriving at Underhill in

association with precipitation. The largest emissions sources tend to occur in the south through west quadrant. There are no major mercury emission sources within 150 km of Underhill.

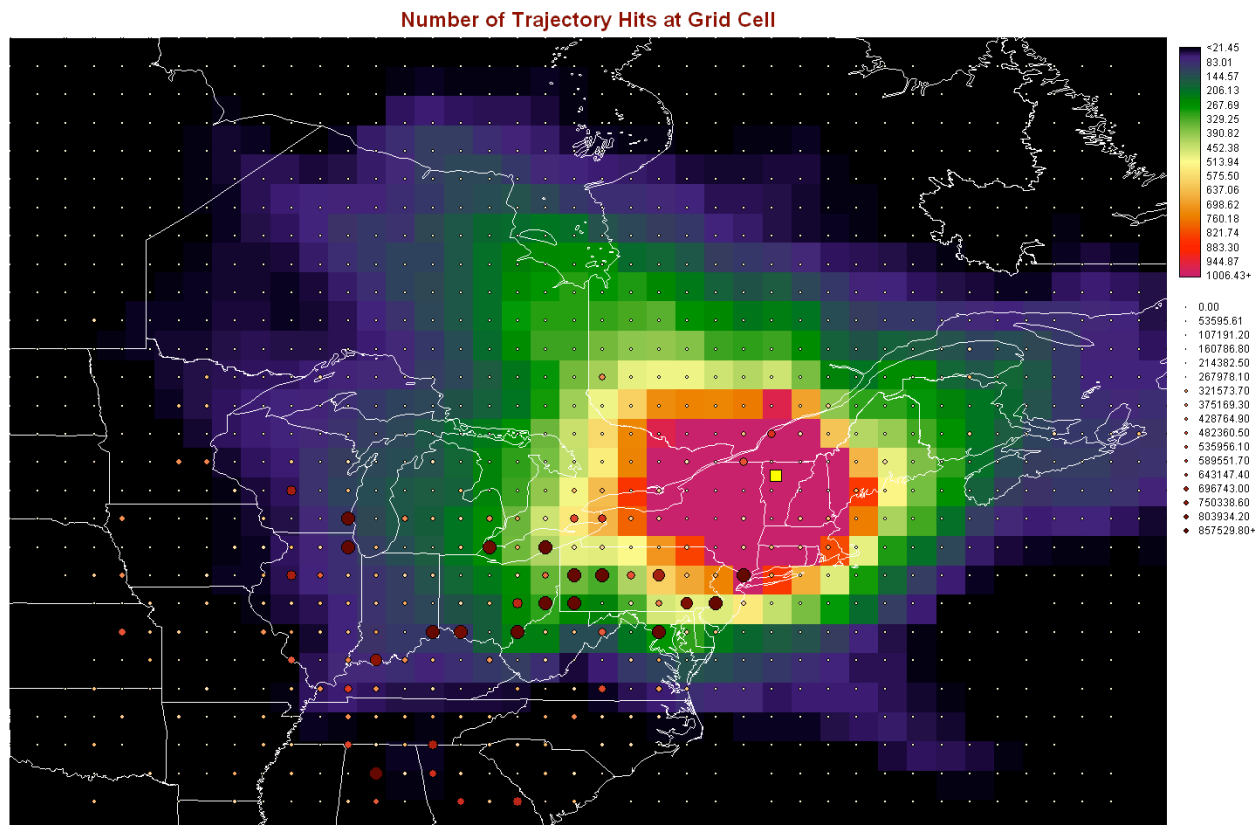


Figure 8. Mercury emissions sampled by air masses reaching Underhill, VT (large yellow square) during wet deposition events 2005-2007. The frequency of 72-hour trajectory endpoints falling in a grid cell is shown by the color shading of the grid cells, delineating the region of potential mercury sources. Overlaid on the grid are circles indicating (by color and size) the annual mercury emissions originating from each grid cell. The grid cells with both a high frequency of trajectory crossings and high mercury emissions are the most likely sources for the mercury in wet deposition at Underhill, Vt.

Figure 9 shows the frequency of air masses transiting grid cells for only the “high” deposition regime events. The SW and NW corridors are dominant transport paths for these types of events. As an example, all of the trajectories associated with precipitation occurring during the event collected on 7/17/2005 are presented in figure 9. This event provided the highest fraction of annual deposition of any event in the full time series (11.7%). It seems likely that the bulk of the mercury in this event was contributed by the major sources in NJ, central and western PA, OH, and possibly from the very large but distant source region near Chicago IL. None of the trajectories associated with this event crossed the much smaller magnitude, but more proximal sources in QC. Similar patterns are evident for the other high deposition events with the W through NW corridor reflecting air arriving during the end of the precipitation events.

There was a significant difference in the location of trajectory endpoints by event type (Table 3). High deposition per unit precipitation events had 47.1% of their trajectory endpoints in

the SW quadrant relative to the receptor, while low deposition events had only 20.4% in the SW sector. Conversely, Low deposition events had 28.8% of trajectory endpoints in the eastern sectors, while high deposition events had only 15.5% in the eastern sectors. All three event types had ~35% of trajectory endpoints in the NW sector. The spatial-mean annual estimated Hg emissions sampled by trajectory endpoints were significantly different by quadrant. Spatial-mean annual estimated emissions sampled by trajectory endpoints in the SW sector were 3 times greater than those from any other quadrant. Thus the high-deposition regime can be characterized as atmospheric circulation conditions that favor precipitation during south to west flow from the high emissions sector with less precipitation contributed to each event in association with flow from much lower emissions sectors to the east. The low deposition regime can be characterized as atmospheric circulation conditions that favor precipitation occurring during flow from the low emissions eastern region with less precipitation contributed in association with flow from the high-emission region (SW).

Table 3. Summary of trajectory endpoint frequency by event type and quadrant relative to receptor location and summary of spatial-mean annual Hg emissions sampled by trajectory endpoints by quadrant relative to receptor. Trajectory endpoint frequency was significantly different by quadrant ($p < 0.00005$). Mean annual estimated emissions were significantly different by quadrant (ANOVA $p < 0.00005$) with each quadrant's estimated emissions significantly different from all others (Tukey-Kramer HSD means test $p = 0.01$).

| Trajectory Quadrant | NE | NW | SE | SW |
|---------------------------------------|-----------|-----------|-----------|-----------|
| Event Type | | | | |
| High Dep/PPT | 9.1% | 37.4% | 6.4% | 47.1% |
| Normal Dep/PTT | 13.3% | 37.5% | 15.5% | 33.8% |
| Low Dep/PPT | 27.7% | 32.9% | 19.1% | 20.4% |
| Mean Estimated Emissions (g/y) | 41,646 | 62,026 | 71,561 | 211,656 |

The attribution of significant wet deposition of mercury at Underhill to the EGU and industrial sources in the S through W quadrant is consistent with the potential source contribution analysis conducted by Miller et al. (in preparation) for ambient vapor-phase mercury measured at Underhill. In the ambient air study, a single trajectory can be associated with each 2-hour integrated sample, thus making plain the dominance of the known sources in the S through W quadrant. S.-o Lai et al. (2007) also identified qualitatively similar source regions contributing to wet deposition of mercury sampled at Pottsdam, NY (44°40'N, 74°59'W, ~170 km almost due west of Underhill) during 2004 and 2005.

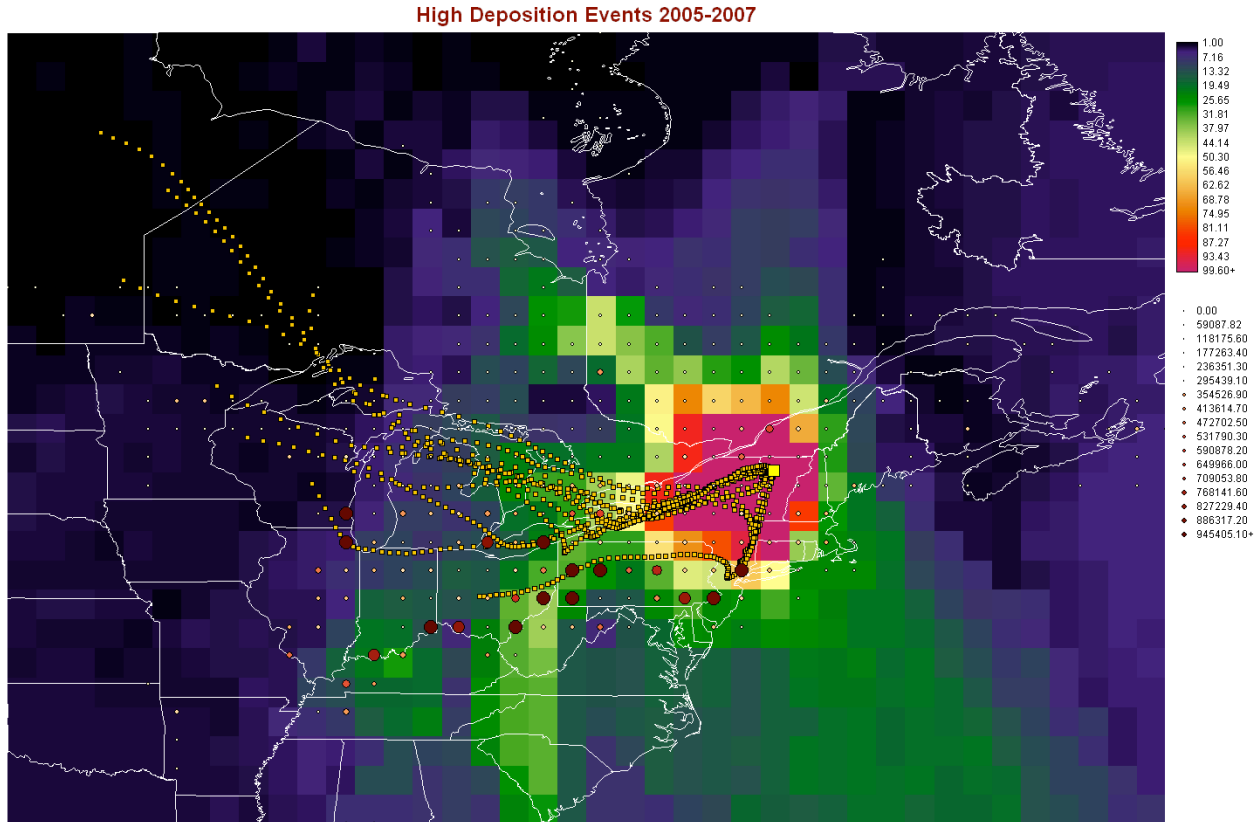


Figure 9. Mercury emissions sampled by air masses reaching Underhill, VT (large yellow square) during “High” deposition type precipitation events 2005-2007 (see text). The frequency of trajectory endpoints falling in a grid cell is shown by the color shading of the grid cells, illustrating the region of potential mercury sources. Overlaid on the grid are circles indicating (by color and size) the annual emissions from each grid cell (g/y). The grid cells with both a high frequency of trajectory crossing and high mercury emissions are the most likely sources for the mercury in wet deposition at Underhill, Vt. Overlaid in small yellow squares are the hourly (72-hours) HYSPLIT backward trajectory endpoints associated with precipitating periods during the event with collection ending on 7/17/2007. This single event provided the highest fraction of annual deposition of any event collected in the 15-year record. Major mercury emissions sources in NJ, central and western PA, OH, and possibly even IL contributed to this extreme event.

No trend in precipitation mercury despite significant estimated emissions reductions

The mercury wet deposition record at Underhill, VT (1993 – 2007) covered an important period when estimated US mercury emissions fell by 45% (1990 – 1999; USEPA, www.epa.gov) and estimated emissions in the Northeastern states and Eastern Canadian Provinces dropped by 54% during 1998-2003 (C. Mark Smith, NESCAUM 2004 Mercury Conference, Portland ME). Despite the apparently significant mercury emissions reductions achieved during the period of observation, there were no significant declining trends in mercury wet deposition or concentration detected by either annual or seasonal Mann-Kendall tests (Figure 2). This is likely due to the apparent significant influence of long-range transport of EGU mercury emissions on a large portion of the annual mercury deposition at Underhill. Estimated EGU emissions were constant both nationally and regionally during the period of observation (USEPA, C. Mark Smith, NESCAUM 2004 Mercury Conference, Portland ME). The apparent emissions reductions were achieved through controls on medical waste incinerators and municipal waste combustors along with the closing of a chlor-alkali plant in Maine.

Alternatively, it is also possible that emissions reductions were overestimated for the period. Also, remission from soils of previously deposited anthropogenic Hg that would be concentrated near large sources could compensate for some of the estimated recent emissions reductions. Others have suggested that increases in emissions sources such as fires in northern peatlands (<http://www.usgs.gov/newsroom/article.asp?ID=1550>) may offset recent estimated emissions reductions. However, the trajectory analysis presented above does not indicate any strong influence from the region of these northern peatlands.

As would be expected from their high correlation on an event basis, annual mercury wet deposition increased linearly with annual precipitation, while concentration decreased linearly with annual precipitation (4 outlier years excluded, Figure 10). The 4 outlier years (1993, 1998, 2004, and 2007) with annual precipitation-weighted mean mercury concentrations above the long-term average dilution line (Figure 4) were also the 4 highest deposition years. These four years had a greater proportion of “high-deposition” type events where the Hg concentration was high relative the precipitation amount (14-19 events as compared to an average of 11 events for the on-trend years). High-deposition events were responsible for 45 to 63% of annual deposition in the outlier years as opposed to 32% of annual deposition for on-trend years. The high deposition years were distributed throughout the record.

Butler et al. (2007) studied the much shorter record (1998-2005) available for NADP/MDN sites and identified a declining trend in precipitation concentration with no trend in wet deposition for the eastern US sites during this shorter period. They attributed this short-term decline in precipitation mercury concentration to declines in anthropogenic mercury emissions nationally and regionally. The much longer record of observation at Underhill indicates that the 1998-2005 decline in precipitation mercury concentration was a short-term cycle within a long-term period with no trend (Figures 2,3). Our analysis suggests that the most plausible explanation for this string of nominally declining concentration years is largely the result of increasing precipitation during the period. The period of 1998-2005 can be seen as typical of the range of variation present over 15 years with no long-period trends (Figures 2,3). Furthermore, the bulk of estimated anthropogenic emissions reductions were accomplished between 1990 and 1999 before the MDN observation

record began. There was no clear signal of these major reductions in the 1993-2007 record at Underhill.

Variations in climate (precipitation amount and atmospheric circulation – frequency of storms in air with favored trajectories) explain much of the year-to-year variation in mercury deposition at Underhill, VT. The high contribution of “high-deposition” events resulting from air masses traversing the high emissions regions to the south and west with multiple EGUs to the annual deposition likely explains the lack of any temporal signal associated with large national and regional estimated mercury emissions reductions from municipal waste combustors and medical waste incinerators during the period of observation.

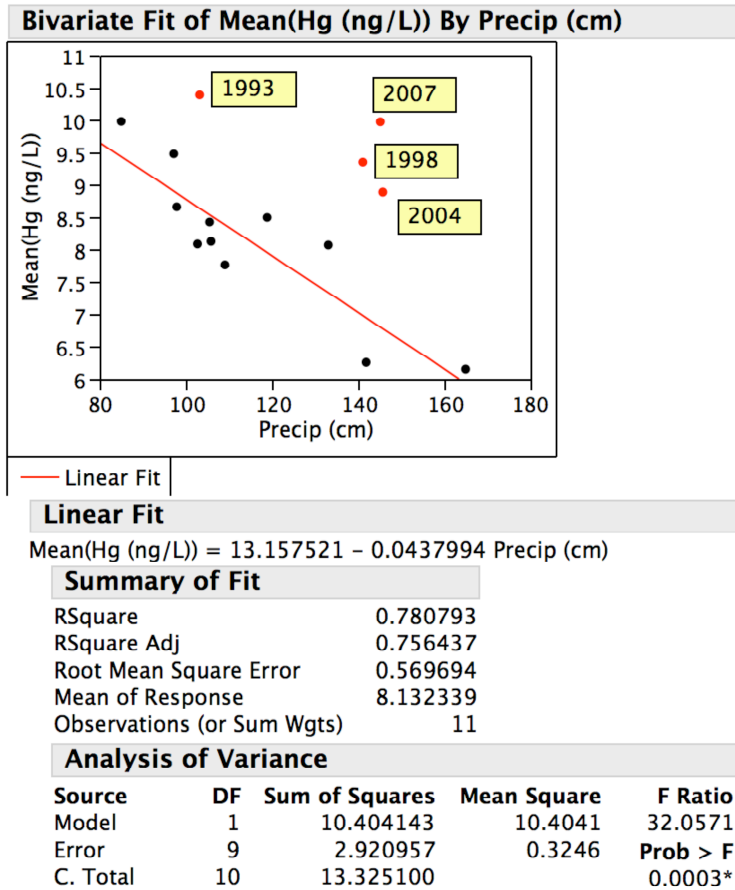
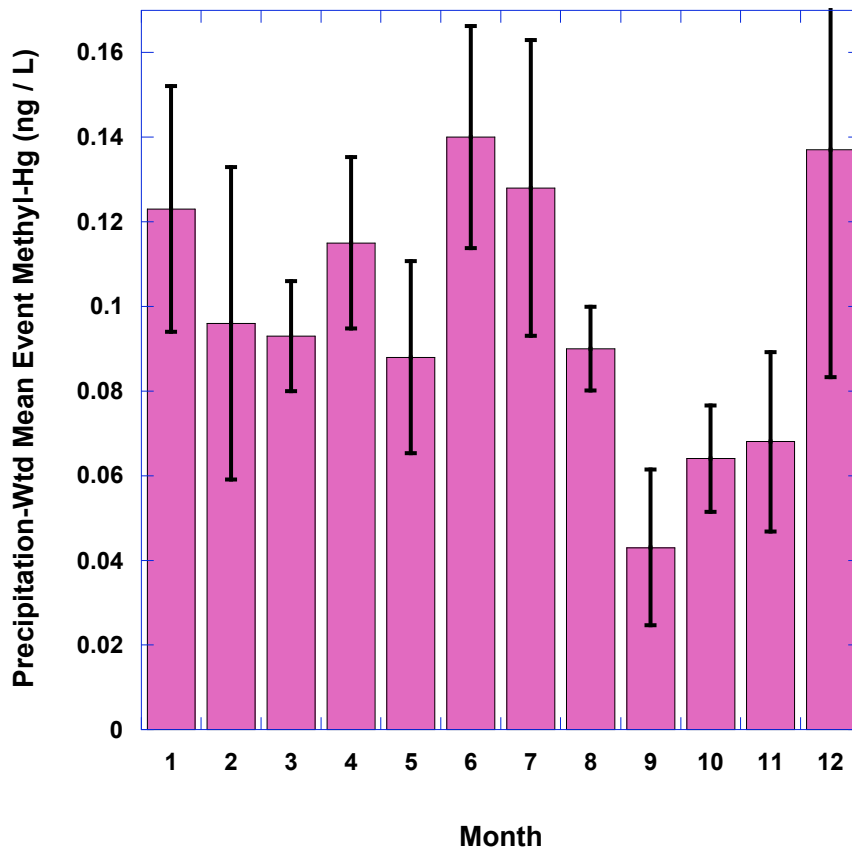


Figure 10. Precipitation “dilution effect” on mean annual mercury concentration in precipitation. The four outlier years (removed from regression) had unusually high mercury concentrations relative to precipitation amounts for the period resulting in the 4 highest deposition years of the record.

Methyl Mercury

As has been observed elsewhere, trace amounts of methyl mercury (range 0.07-3.93%, mean 1.2% of total mercury) are present in precipitation sampled at Underhill, VT (Figure 11). The source of methyl mercury in precipitation is not clearly established and may be varied, but the

majority seems quite likely to be the result of aqueous phase methylation of non-particle bound Hg^{2+} (Hammerschmidt et al. 2007). With the exclusion of two outliers (the top 2 high deposition events for total mercury 11.7% and 7.9% of annual deposition during the methyl mercury sampling period 2005-2007), methyl mercury concentration was positively linearly correlated with total mercury concentration ($r^2 = 0.40$, $p = 0.0005$). This correlation is consistent with Hammerschmidt et al.'s (2007) hypothesis. A provisional estimate of the annual deposition of methyl mercury is $76.5 - 162 \text{ ng/m}^2/\text{y}$ (central estimate $116 \text{ ng/m}^2/\text{y}$) derived by multiplying the monthly volume-weighted mean methyl mercury concentrations (Figure 11) by the average monthly precipitation and propagating uncertainties. This flux represents a significant delivery of methyl mercury to terrestrial and aquatic ecosystems in the region.



Acknowledgements

The atmospheric mercury observation program at Underhill, Vermont would not be possible without the dedicated efforts of VMC staff members Mim Pendleton, Carl Waite, and Judy Rosvosky. These individuals maintain and operate the monitoring equipment and their hard work in all kinds of weather has been responsible for the high quality of the extensive observational record. The authors gratefully acknowledge the NOAA Air Resources Laboratory (ARL) for the provision of the HYSPLIT transport and dispersion model used in this publication. Funding for this research was provided by NOAA, EPA, VTANR, and USGS.

References

- Burke, J., M. Hoyer, G. Keeler, and T. Scherbatskoy. 1995. Wet deposition of mercury and ambient mercury concentrations at a site in the Lake Champlain Basin. *Water Air and Soil Pollution* 80:353-362.
- Butler, T.J., M.D. Cohen, F.M. Vermeulen, G.E. Likens, D. Schmeltz, and R.S. Artz. (2008) Regional precipitation mercury trends in the eastern USA, 1998-2005: Declines in the Northeast and Midwest, no trend in the Southeast. *Atmos. Environ.* DOI:10.1016/j.atmosenv.2007.10.084.
- Cohen, M., R. Artz, R. Draxler, P. Miller, D. Niemi, D., D. Ratte, M. Deslauriers, R. Duvar, R., Laurin, J. Slotnick, T. Nettesheim, and J. McDonald. (2004) Modeling the atmospheric transport and deposition of mercury to the Great Lakes. *Environmental Research* 95:, 247-265.
- Draxler, R.R. and Rolph, G.D., 2003. HYSPLIT (HYbrid Single-Particle Lagrangian Integrated Trajectory) Model access via NOAA ARL READY Website (<http://gus.arlhq.noaa.gov/ready/open/hysplit4.html>). NOAA Air Resources Laboratory, Silver Spring, MD.
- Hammerschmidt, C. R., C.H. Lamborg, and W.F. Fitzgerald. (2007) Aqueous phase methylation as a potential source of methylmercury in wet deposition. *Atmos. Environ.* 41:1663-1668.
- Keeler, G.J., L.E.Gratz, and K. Al-Wali. (2005) Long-term Atmospheric Mercury Wet Deposition at Underhill, Vermont. *Ecotoxicology* 14, 71 –83.
- Lawson, S.T., Cloud water and throughfall deposition of mercury and trace elements in a high-elevation spruce-fir forest at Mt. Mansfield, Vermont. (2003) *Journal of Environmental Monitoring* 5, 578-583.
- Malcom, E.G., G.J. Keeler, S.T. Lawson, and T. Scherbatskoy. (2003) Mercury and trace elements in cloud water and precipitation collected on Mt. Mansfield, Vermont. *Journal of Environmental Monitoring* 5, 584-590.
- Miller, E.K., VanArsdale, A., Keeler, G.J., Chalmers, A., Poissant, L., Kamman, N., and Brulotte, R. (2005) Estimation and Mapping of Wet and Dry Mercury Deposition across Northeastern North America. *Ecotoxicology* 14, 53-70.
- Poirot, R.L. and P.R. Wishinski (1985). Regional apportionment of ambient sulfate contributions to a remote site in northern VT. *Transactions APCA Int. Spec. Conf. on Receptor Modeling: Real World Issues and Applications*, T.G. Pace, Ed., pp. 239-250, Williamsburg, VA.
- Rimmer, C.C., McFarland, K.P., Evers, D.C., Miller, E.K., Aubry, Y., Busby, D., and Taylor, R.J. (2005) Mercury Levels in Bicknell's Thrush and Other Insectivorous Passerines in Montane Forests of Northeastern North America. *Ecotoxicology* 14, 223-240.
- Lai, S.-o , T. M. Holsen, P. K. Hopke, and P. Liu. (2007) Wet deposition of mercury at a New York state rural site: Concentrations, fluxes, and source areas. *Atmos. Environ.* 41:4337-4348.
- USEPA (2002) Method 1631, Revision E: Mercury in Water by Oxidation, Purge and Trap, and Cold-Vapor Atomic Fluorescence Spectrometry. www.epa.gov
- VanArsdale, A., Weiss, J., Keeler, G.J., Miller, E.K., Boulet, G., Brulotte, R., Poissant, L., and Puckett, K. (2005) Patterns of Mercury Deposition in Northeastern North America (1996-2002). *Ecotoxicology* 14, 37-52.

Wetherbee, G.A., D. A. Gay, R.C. Brunette, and C.W. Sweet. (2007) Estimated variability of National Atmospheric Deposition Program/Mercury Deposition Network Measurements using collocated samplers. *Environ. Mon. Assess.* DOI 10.1007/s10661-006-9456-6.

Atmospheric Mercury in Vermont and New England: Measurement of deposition, surface exchanges and assimilation in terrestrial ecosystems

Final Project Report – Ambient Air Mercury Speciation Studies – 1/16/2009

PI: Melody Brown Burkins, University of Vermont (UVM)
Co-PIs: Eric K. Miller¹, Ecosystems Research Group, Ltd.; and Jamie Shanley, US Geological Survey
Collaborators: Sean Lawson, VTANR-VMC; Mim Pendelton, Carl Waite, UVM;
Rich Poirot, VTANR-APCD; Alan VanArsdale, USEPA; Mark Cohen, NOAA
Project Officer: Eric Hall, USEPA

Climatology and potential sources of speciated (GEM, RGM, and HGP) ambient atmospheric mercury in Northern New England

Earlier modeling studies indicated that RGM deposition could be nearly equal in magnitude to the wet deposition flux of Hg (Miller et al. 2005). At the outset of this project, there were few measurements of RGM levels in the US (e.g. Lindberg and Stratton 1998) and none in rural northern New England. The Vermont Agency of Natural Resources Air Pollution Control Division (VTANR-APCD) funded the acquisition of a Tekran 1130 RGM module for use with the Tekran 2537A as part of this project. The Tekran 1130 RGM module was deployed with the Tekran 2537A with inlets on the top of the forest canopy observation tower in 2004. This tower was destroyed in a severe storm in the winter of 2004 and equipment was repaired and relocated to the Underhill Air Quality site in the spring of 2005. We acquired and deployed an 1135 particulate mercury module in 2005. We also conducted one short-term deployment of a second system provide by USEPA Region 1 at Shoreham, VT, allowing paired observations at a lake-level and mid-elevation site (see FR-sec3b). These measurements were designed to characterize GEM, RGM, and HGP levels in terms of their diurnal, seasonal and spatial variation in the region. The measurements provided necessary information for dry-deposition modeling as well as the opportunity for analysis of potential mercury sources using air-mass back-trajectory methods.

Ambient TGM had been characterized at Underhill since 1992 using 24-hour exposures of gold traps every 6th day (Burke et al. 1995). The Tekran system provided continuous hourly (or more frequent) measurements of TGM (or GEM) providing valuable information on TGM/GEM levels allowing us to characterize the diurnal and seasonal variation in this parameter.

GEM and RGM measurements were initiated in 2004 with inlets located at the top of the forest canopy observation tower (Figure 1). Due to the collapse of the forest canopy tower in a severe storm during December 2004, RGM and GEM measurements were relocated to the Air Quality Site (Figure 2). The Air Quality Site is ~1 km from the forest canopy tower site. The basic met package that was previously deployed at the forest canopy tower was redeployed with the vapor-phase mercury instrumentation at the Air Quality Site. A Tekran 1135 particulate mercury sampling head (seen above the 1130 RGM head in Figure 2) for the mercury speciation system was acquired and installed in order to test hypotheses about the influence of PM_{2.5} and humidity on RGM levels. Gathering of this information was necessary to support the deposition-modeling task. The high temporal resolution measurements of mercury speciation also made possible potential

¹ Corresponding author for the final project report. Email: ekmillier at ecoystems-research.com Voice: 802-649-5550

source contribution analysis and identification of likely major anthropogenic emissions sources contributing to mercury deposition in the Lake Champlain Basin and Northern New England.

Because of concerns about the comparability of measurements made from the differing inlet locations and heights from 2004 to 2005, the climatology of speciated mercury is presented based on measurements made from the longer, continuous record at the Air Quality Site. Measurements are reported from the period May 2005 through June 2008. GEM measurements were made every 5 minutes during the RGM and HGP 2-hour accumulation periods. GEM concentrations presented below are 2-hour averages of the 5-minute observations to be consistent with the 2-hour average concentrations represented by the RGM and HGP measurements.

RGM Sampling Head



Figure 1. Initial deployment of RGM sampling head on the forest canopy observation tower in 2004.



Figure 2. Sampling heads for RGM, GEM, and particulate mercury were located on the met tower fixed to the instrument shelter (see inset) at the Underhill, VT Air Quality Site in April of 2005.

Climatology of Speciated Ambient Atmospheric Mercury at Underhill, VT

Because we are still uncertain of the comparability of measurements (primarily an issue for RGM) made from the top of the forest canopy tower and from the Air Quality Site, the climatology of speciated mercury is presented based on measurements from the Air Quality Site only. Measurements are reported from the period May 2005 through June 2008. GEM measurements were made every 5 minutes during the RGM and HGP 2-hour accumulation periods. GEM concentrations presented below are 2-hour averages of the 5-minute observations to be consistent with the 2-hour average concentrations represented by the RGM and HGP measurements.

GEM concentrations ranged from 0.81 to 5.58 ng/m³ with a period average of 1.45 ng/m³ (Figure 3). RGM concentrations ranged from 0 to 132.5 pg/m³ with a period average of 3.56 pg/m³ (Figure 3). HGP sampling spanned only 44% of the RGM measurement period due to the later acquisition date of the 1135 module, deployment at Shoreham, VT, and minor problems with the module (Table 1). HGP concentrations ranged from 0 to 121 pg/m³ with a period average of 11.50 pg/m³ (Figure 3).

Table 1. Numbers of RGM and HGP 2-hour samples.

| Month | N RGM Samples | N HGP Samples | %RGM Samples |
|--------------|----------------------|----------------------|---------------------|
| 1 | 679 | 208 | 30.6 |
| 2 | 622 | 191 | 30.7 |
| 3 | 705 | 194 | 27.5 |
| 4 | 616 | 431 | 70 |
| 5 | 925 | 479 | 51.8 |
| 6 | 906 | 456 | 50.3 |
| 7 | 663 | 366 | 55.2 |
| 8 | 682 | 440 | 64.5 |
| 9 | 621 | 226 | 36.4 |
| 10 | 713 | 242 | 33.9 |
| 11 | 641 | 240 | 37.4 |
| 12 | 523 | 114 | 21.8 |

The observed concentrations of all three species were dependent on meteorological conditions but in different ways for RGM and HGP than for GEM. Observed concentrations of all three species were dependent the surface moisture status (dry, moist, or wet) as determined by a Campbell Scientific, Inc. (Logan, Utah) surface wetness sensing grid (2-m AGL, facing SW, 45°-tilt). Mean RGM and HGP concentrations were significantly different for each surface wetness state (dry > moist > wet) (Figure 4). These differences likely exist, in part, because RGM and HGP are more efficiently removed from the atmosphere during wet or moist conditions. Deposition velocities for both species are greater to moist surfaces. Both species tend to exhibit higher concentrations in drier air masses (Figure 5). RGM was more highly correlated with relative humidity than with water-vapor mixing ratio, whereas HGP was more strongly correlated with water vapor mixing ratio. The dependence of RGM concentrations on RH may reflect the tendency for that species to be readily scavenged by moist aerosols at moderate RH. The dependence of HGP on the water vapor mixing ratio may relate to the coincidence of HGP source regions, low water-vapor source regions and seasonal effects (discussed below).

Mean GEM concentrations were significantly higher during moist conditions than either dry or wet for which GEM concentrations were not significantly different. This different response to surface moisture may exist because GEM appears to be volatilized and emitted from moist surfaces in the presence of sunlight (see further discussion below). Short-term increases in GEM were frequently observed at first insolation of moist surfaces (in morning or after precipitation).

8/28/08 11:32 AM

Data Table=VT99-HG-met-EDAS-tstats72h-2005-2008

Distributions

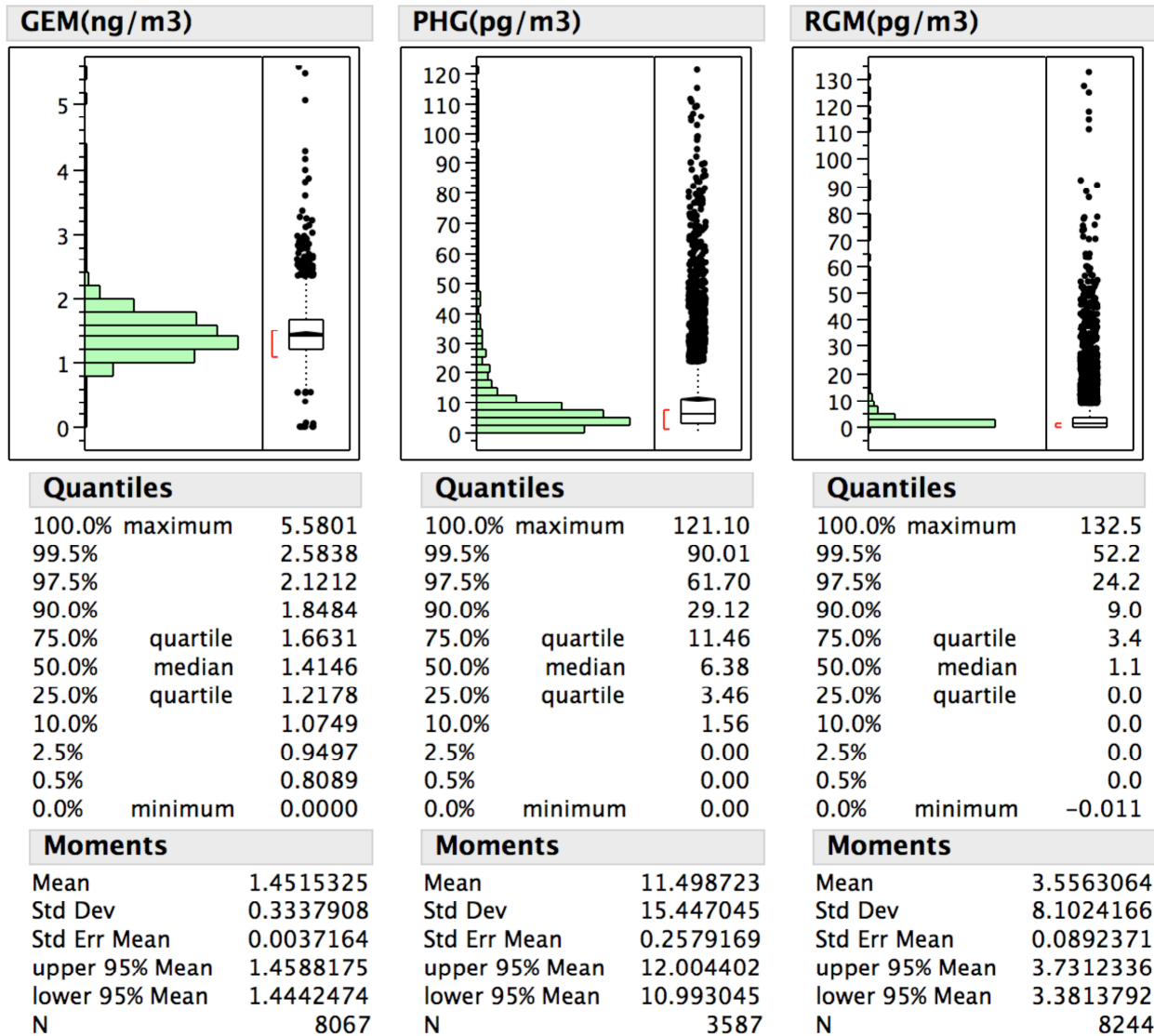
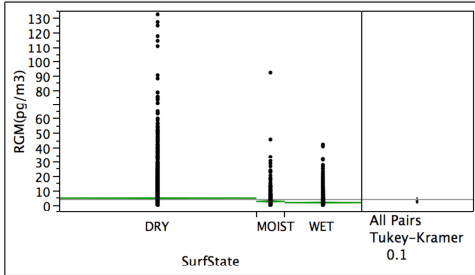


Figure 3. Frequency distributions of ambient atmospheric mercury species measured at Underhill, VT from May 2005 through June 2008.

8/28/08 1:39 PM

Data Table=VT99-HG-met-EDAS-tstats72h-2005-2008

Oneway Analysis of RGM(pg/m3) By SurfState



Missing Rows 756

Oneway Anova

Summary of Fit

| | |
|----------------------------|----------|
| Rsquare | 0.029953 |
| Adj Rsquare | 0.029695 |
| Root Mean Square Error | 7.951066 |
| Mean of Response | 3.568873 |
| Observations (or Sum Wgts) | 7540 |

Analysis of Variance

| Source | DF | Sum of Squares | Mean Square | F Ratio | Prob > F |
|-----------|------|----------------|-------------|----------|----------|
| SurfState | 2 | 14712.80 | 7356.40 | 116.3629 | <.0001* |
| Error | 7537 | 476485.00 | 63.22 | | |
| C. Total | 7539 | 491197.80 | | | |

Means for Oneway Anova

| Level | Number | Mean | Std Error | Lower 90% | Upper 90% |
|-------|--------|---------|-----------|-----------|-----------|
| DRY | 4921 | 4.57467 | 0.11334 | 4.3882 | 4.7611 |
| MOIST | 710 | 2.30429 | 0.29840 | 1.8134 | 2.7952 |
| WET | 1909 | 1.44648 | 0.18198 | 1.1471 | 1.7458 |

Std Error uses a pooled estimate of error variance

Means Comparisons

Comparisons for all pairs using Tukey-Kramer HSD

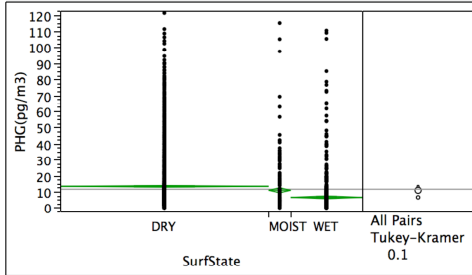
| Level | Mean |
|---------|-----------|
| DRY A | 4.5746653 |
| MOIST B | 2.3042930 |
| WET C | 1.4464767 |

Levels not connected by same letter are significantly different.

8/28/08 1:40 PM

Data Table=VT99-HG-met-EDAS-tstats72h-2005-2008

Oneway Analysis of PHG(pg/m3) By SurfState



Missing Rows 4718

Oneway Anova

Summary of Fit

| | |
|----------------------------|----------|
| Rsquare | 0.035181 |
| Adj Rsquare | 0.034642 |
| Root Mean Square Error | 15.19357 |
| Mean of Response | 11.49329 |
| Observations (or Sum Wgts) | 3578 |

Analysis of Variance

| Source | DF | Sum of Squares | Mean Square | F Ratio | Prob > F |
|-----------|------|----------------|-------------|---------|----------|
| SurfState | 2 | 30092.86 | 15046.4 | 65.1799 | <.0001* |
| Error | 3575 | 825269.65 | 230.8 | | |
| C. Total | 3577 | 855362.51 | | | |

Means for Oneway Anova

| Level | Number | Mean | Std Error | Lower 90% | Upper 90% |
|-------|--------|---------|-----------|-----------|-----------|
| DRY | 2470 | 13.3057 | 0.30571 | 12.803 | 13.809 |
| MOIST | 262 | 10.8214 | 0.93866 | 9.277 | 12.366 |
| WET | 846 | 6.4099 | 0.52237 | 5.550 | 7.269 |

Std Error uses a pooled estimate of error variance

Means Comparisons

Comparisons for all pairs using Tukey-Kramer HSD

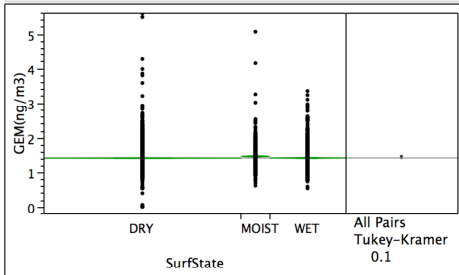
| Level | Mean |
|---------|-----------|
| DRY A | 13.305672 |
| MOIST B | 10.821363 |
| WET C | 6.409908 |

Levels not connected by same letter are significantly different.

8/28/08 1:43 PM

Data Table=VT99-HG-met-EDAS-tstats72h-2005-2008

Oneway Analysis of GEM(ng/m3) By SurfState



Missing Rows 927

Oneway Anova

Summary of Fit

| | |
|----------------------------|----------|
| Rsquare | 0.001996 |
| Adj Rsquare | 0.001725 |
| Root Mean Square Error | 0.327064 |
| Mean of Response | 1.431218 |
| Observations (or Sum Wgts) | 7369 |

Analysis of Variance

| Source | DF | Sum of Squares | Mean Square | F Ratio | Prob > F |
|-----------|------|----------------|-------------|---------|----------|
| SurfState | 2 | 1.57567 | 0.787836 | 7.3649 | 0.0006* |
| Error | 7366 | 787.94846 | 0.106971 | | |
| C. Total | 7368 | 789.52414 | | | |

Means for Oneway Anova

| Level | Number | Mean | Std Error | Lower 90% | Upper 90% |
|-------|--------|---------|-----------|-----------|-----------|
| DRY | 4829 | 1.42579 | 0.00471 | 1.4180 | 1.4335 |
| MOIST | 686 | 1.47671 | 0.01249 | 1.4562 | 1.4973 |
| WET | 1854 | 1.42853 | 0.00760 | 1.4160 | 1.4410 |

Std Error uses a pooled estimate of error variance

Means Comparisons

Comparisons for all pairs using Tukey-Kramer HSD

| Level | Mean |
|---------|-----------|
| MOIST A | 1.4767123 |
| WET B | 1.4285276 |
| DRY B | 1.4257874 |

Levels not connected by same letter are significantly different.

Figure 4. Ambient atmospheric mercury concentrations by surface wetness class.

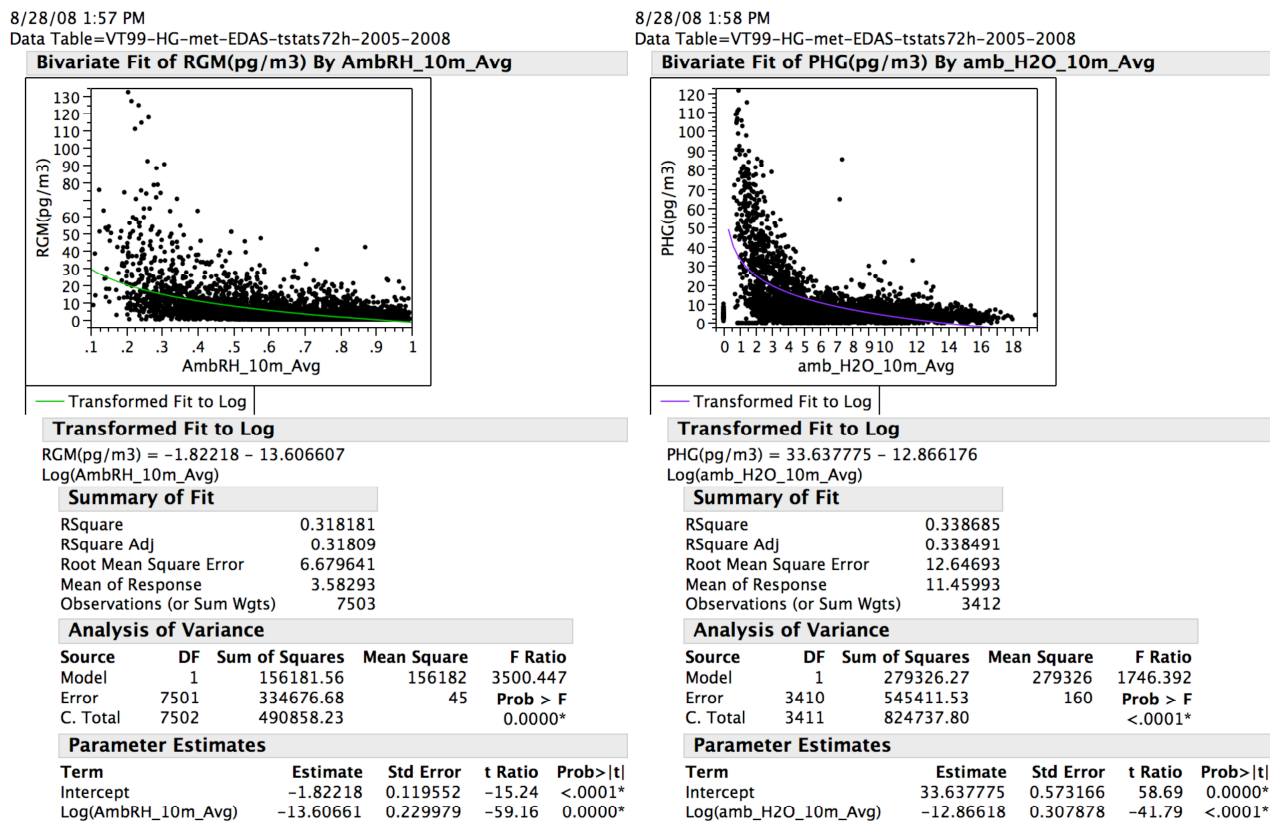


Figure 5. Dependence of RGM (left) and HGP (right) on atmospheric moisture. RGM was more highly correlated with relative humidity than with water vapor mixing ratio whereas HGP was more strongly correlated with water vapor mixing ratio (units in figure are mm/mole).

The concentrations of the three mercury species exhibited strong seasonal patterns that were slightly out of phase with each other (Figure 6). GEM concentrations peak in winter and spring with an early fall minimum, HGP concentrations peak in late winter and RGM concentrations peak in spring (Figure 7). The wintertime peak in HGP may be due, in part, to increased local combustion (wood and oil) for home heating. However, trajectory analysis (discussed below) also indicates major out-of-region sources likely contribute to the observed HGP signal. The spring peak in RGM is likely due to a combination of factors including favored trajectories over major EGU RGM sources and relatively low atmospheric moisture levels at a time when leaves are off of trees along the favored trajectories (Figure 8). As soon as leaves emerge in late spring and early summer, the surface area for dry-deposition removal along the transport pathway increases by a factor of 3 to 4. Atmospheric moisture and relative humidity increase as well, allowing more scavenging by particles and ultimately cloud and rain droplets (Figure 9). As discussed in the section on wet-deposition, summer is the time of peak observed concentrations of Hg in precipitation. The patterns described here suggest more of the ionic mercury in the atmosphere is partitioned into the liquid phase during the summer months.

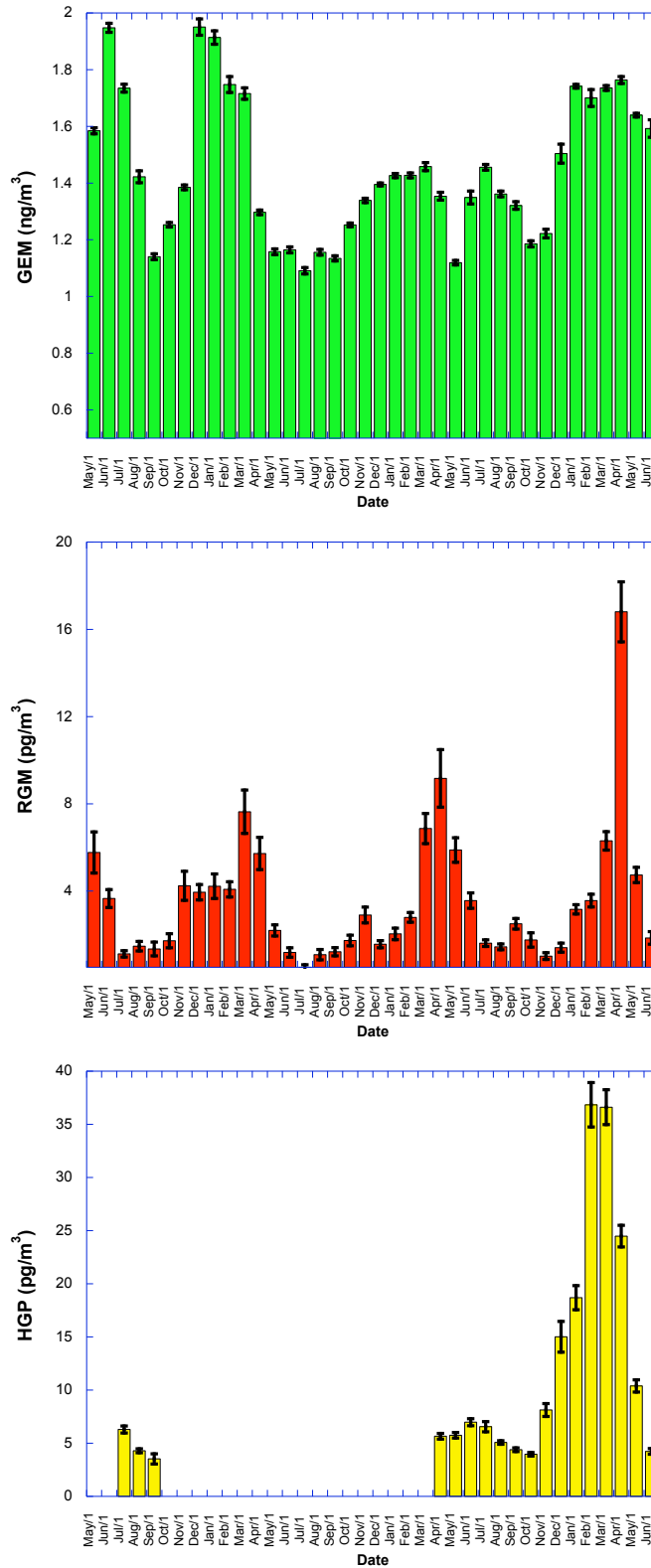


Figure 6. Time series of monthly average concentrations with standard errors for GEM (top), RGM (middle), and HGP (bottom) starting in May of 2005 and ending June 2008. GEM concentrations peak in winter and spring, HGP concentrations peak in late winter and RGM concentrations peak in spring.

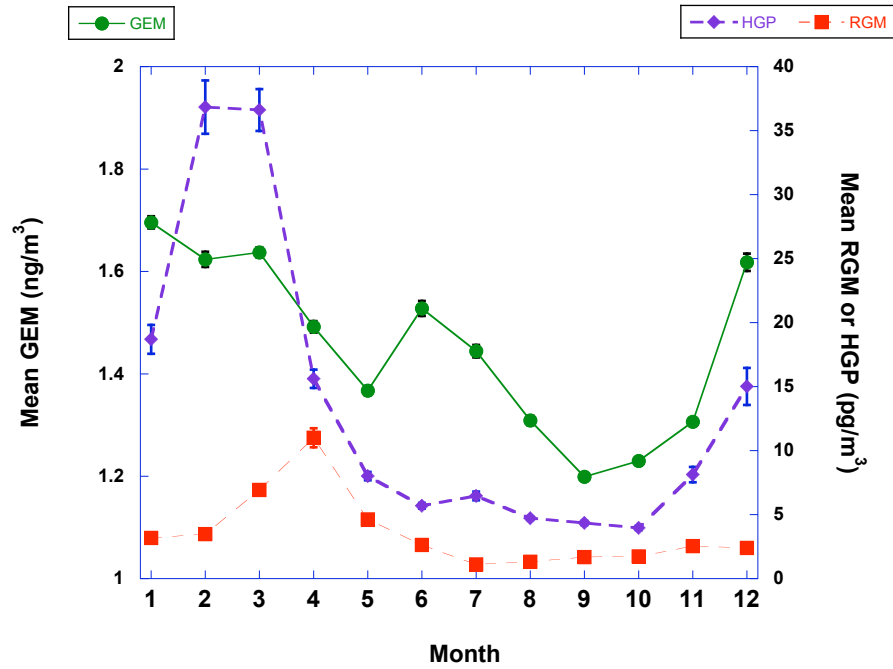


Figure 7. Mean monthly concentrations of atmospheric mercury species over the observation period. GEM concentrations peak in winter and spring with an early fall minimum, HGP concentrations peak in late winter and RGM concentrations peak in spring.

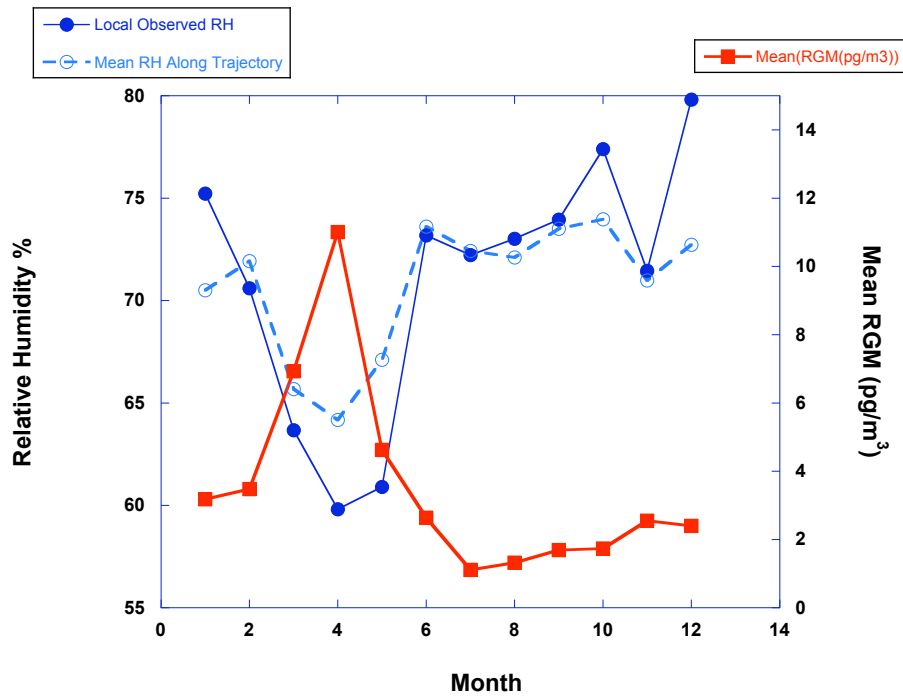


Figure 8. Mean monthly RGM concentrations and mean monthly RH. Both local-observed RH (solid blue line) and the mean of RH values along all back-trajectories for the month (dashed blue line) are shown. Surface-measured RGM concentrations peak during the minima in atmospheric (local and along the transport path) humidity.

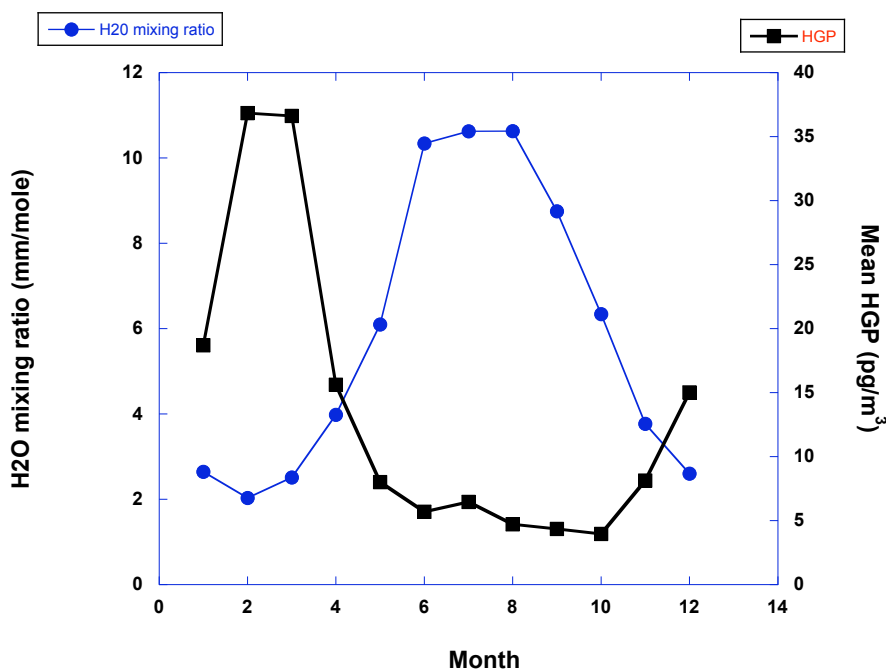


Figure 9. Mean monthly HGP concentrations and the atmospheric water-vapor mixing ratio. HGP concentrations peaked at the minima of atmospheric water vapor. This could indicate that cloud droplets scavenged fewer particles during times of low atmospheric moisture content. Alternatively (see text) this pattern could represent a coincidence between favored trajectories for HGP during winter when the water-vapor mixing ratio is low (in part because of more frequent incursions of polar air with low mixing ratios). In other words, the source regions for low H₂O mixing-ratio air and HGP may be similar. Local combustion sources may also contribute to increased HGP during winter.

RGM and HGP concentrations exhibited two distinct temporal patterns that we interpret as driven by either 1) atmospheric mixing processes in conjunction with the balance between deposition and formation reactions and 2) regional transport episodes (Figure 10). On June 22nd and 23rd 2005, the strong diurnal cycles with concentrations returning to near zero at night suggest that dry-deposition processes outpace replenishment via production reactions or mixing of upper-level air during conditions of low atmospheric mixing at night. During the day, mixing (and/or production processes) outpace the deposition rate and allow surface air concentrations to increase. Ozone and PM levels are moderate on these two days and O₃ follows the same pattern as RGM for the same reasons.

The record from June 24th through June 26th, 2005 illustrates a typical regional transport episode with O₃, and RGM rising together and PM increases lagging slightly (Figure 10). The transport-event signature is the maintenance of moderate to high concentrations overnight. The daytime peaking during a transport event likely indicates additional production during those hours due to photochemistry or the mixing down to the surface of higher concentrations being transported

at higher levels in the atmosphere. These two patterns are repeated again and again throughout the observation record.

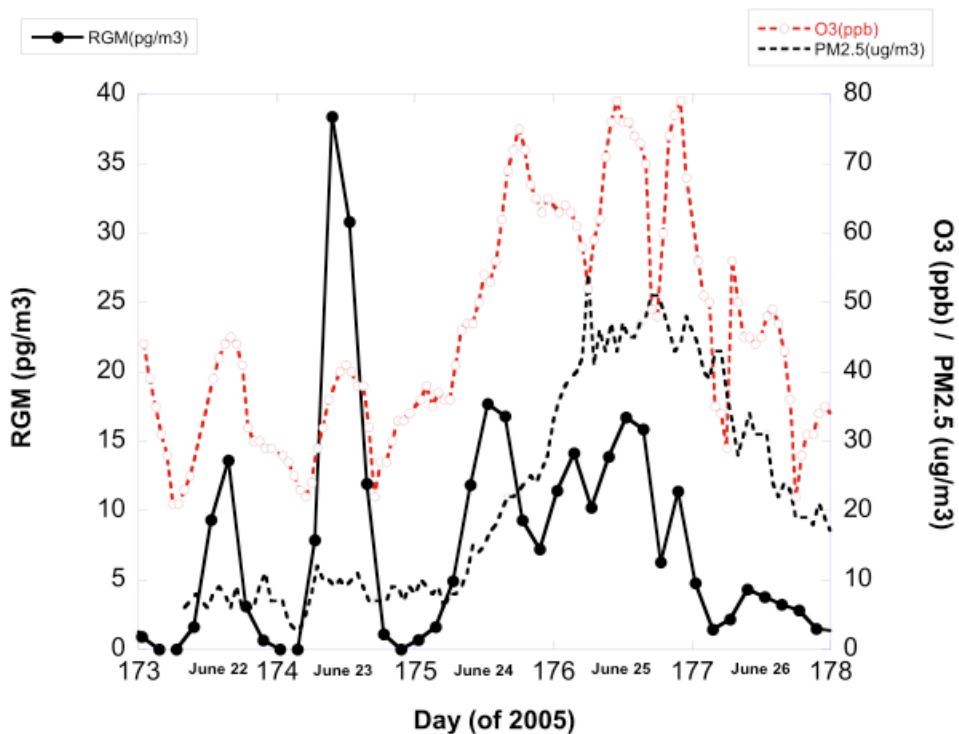


Figure 10. Examples of the two primary temporal patterns of RGM and HGP (RGM only shown here). June 22nd and 23rd illustrate the “mixing/production” pattern, while June 24th through 26th illustrate the patterns associated with regional transport events. Ozone (measured at Underhill) and PM_{2.5} concentrations (measured at Burlington, VT) courtesy of VTANR-APCD.

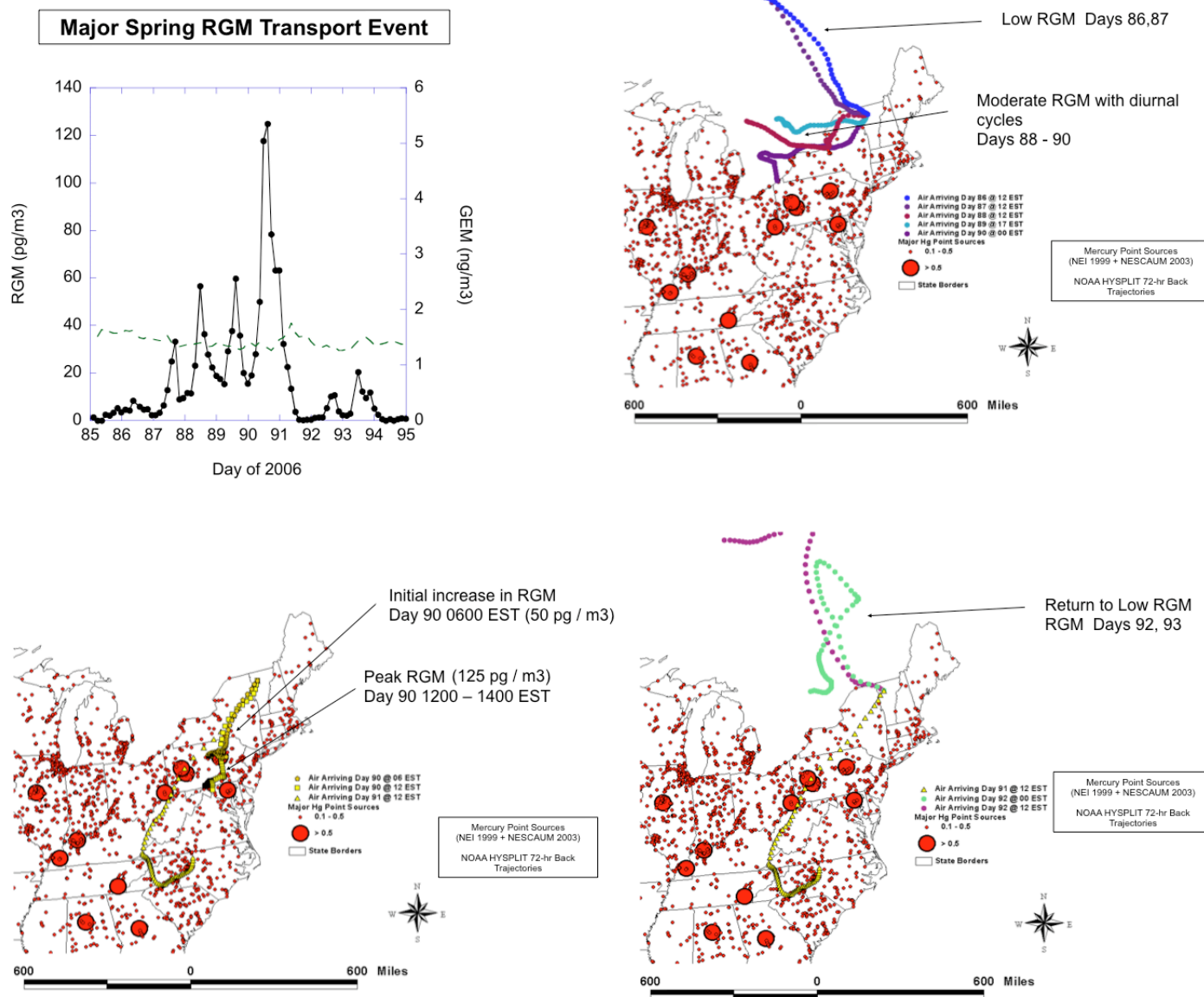


Figure 11. Example of a major RGM transport event in the spring of 2006. The trajectory symbols represent the hourly positions of air in transit to Underhill over the 72-hour preceding collection of a specific air sample. The time course of RGM concentrations at Underhill is shown in the top left panel. Emissions data courtesy of Mark Cohen (NOAA).

Our confidence in the identification of regional transport events contributing mercury from distant sources to Northern New England is strengthened by detailed air-mass back-trajectory studies of individual events. For example, we present the trajectory analysis of a major RGM transport event that occurred in the spring of 2006 (Figure 11). Prior to the event (days 85-87) low RGM values were observed and air-mass back-trajectories calculated with the NOAA HYSPLIT model indicate air arriving at Underhill had traversed Quebec. On days 88-90, air began arriving from southern Ontario and western New York. RGM levels increased, exhibited strong diurnal cycles, and concentrations failed to return to zero during the night. Days 90 and 91 saw some of the highest RGM levels observed at Underhill up to 125 pg/m³ (occurring overnight, rather than during

mid-day). Air arriving at Underhill during these samples had recently traversed the RGM emissions-rich region of PA and NJ (Figure 11). Moreover, the trajectory analysis showed that the arriving air mass dwelled for a considerable length of time over specific known major RGM sources, and then began a fairly rapid movement to the receptor. This analysis strongly suggests that several major stationary RGM emission sources (primarily EGUs) in Pennsylvania are responsible for episodically high RGM concentrations and deposition in Northern New England. As discussed elsewhere in this report, these high concentration episodes are responsible for the majority of annual dry deposition. On days 92 and 93, after the passage of a front, air arriving at the receptor was again coming from Quebec and exhibited much lower RGM concentrations with nocturnal values falling to zero (Figure 11).

The relatively long (26-months) and continuous record of high-temporal resolution (every 3-hours) measurements permits unique analysis opportunities for understanding the atmospheric chemistry and regional transport of mercury. These analyses are discussed in detail in the following section.

Identification of potential sources of atmospheric mercury measured at Underhill, VT using Continuous Potential Source Contribution Analysis (CPSCA)

Potential source area identification using single pollutant data is generally conducted using potential source contribution function analysis (PSCF, e.g. Lai et al. 2007). PSCF was developed in the context of moderate-time integration sampling (e.g. 24-hr accumulated samples) where there may be multiple back trajectories contributing to one sample as meteorological conditions change over a 24-hour period. Often this type of sample is collected infrequently (e.g. IMPROVE every 6th-day 24-hr integrated sample). PSCF analysis quantifies the potential for a source region to contribute to the sample by determining the number of instances that a back-trajectory associated with pollutant concentrations above a criterion value measured at a receptor crosses the source region. The number of trajectory intersections are normalized to create a probability (0 to 1) of the source region contributing to a pollutant concentration measurement above the criterion value at the receptor. Depending on the number of pollutant samples available, length of back-trajectories used, and grid size for the potential source fields, a relatively small number of sample-trajectory pairs contribute to the assessment of the potential contribution of each source-field grid cell. A limitation of conventional PSCF analysis is the selection of the concentration criterion that can be arbitrary. Information from trajectories associated with concentrations less than the criterion value is lost.

We adapted earlier methods of source identification for this study (the “upwind average” Poirot and Wishinski 1985 and the “Kenski” method Kenski 2004) and refer to this method as continuous potential source contribution analysis (CPSCA). CPSCA takes advantage of the very large number of samples produced by semi-continuous high-time resolution analyzers (5-minute to hourly or 2-hour samples) for pollutants such as continuous fine particle, ozone, SO₂, NO_x, and mercury analyzers. In addition to the increased number of samples provided by semi-continuous analyzers, each sample can be directly associated with a specific air-mass back trajectory as such back-trajectories rarely differ significantly over the course of such short sample durations. CPSCA makes use of data from trajectories associated with all samples at all times and all observed concentrations, so no information is lost.

Air-mass back-trajectories of 72-hours duration are calculated with hourly endpoints reported using the NOAA HYSPLIT model (Draxler and Rolph 2003) with vertical mixing and the EDAS 40-km meteorological data. With a large number of samples collected continuously representing several years, trajectory endpoints are well distributed spatially and temporally. Thus most locations on the potential source field grid have been sampled multiple times in multiple seasons (sometimes hundreds or thousands of times) by back-trajectories associated with different samples.

Observed local and extracted EDAS meteorological data, along with the observed pollutant concentrations, are associated with each trajectory endpoint arising from a specific sample. The trajectory endpoint-associated data are summarized by source-field grid cell. The choice of grid-cell size influences both the spatial resolution of potential sources and the number trajectory endpoints representing each grid cell. For this analysis data were aggregated by 1-degree latitude and longitude. Data aggregation by grid cell included the mean and maximum of all receptor concentrations associated with trajectories passing through that grid cell. Additional statistics (e.g. median, quantiles, even measures of variation) may be used. Gridded data are interpolated to a potential surface using the 6 nearest-neighbor cells with linear distance weighting.

When plotted, the aggregated data display a map of receptor conditions associated with air mass passage over the potential source domain. This type of map immediately conveys the average or maximum concentration (or any other appropriate statistic describing the pollutant or meteorological conditions) at the receptor potentially contributed by sources from a given location. The local and EDAS-extracted meteorological data may be used to inform, stratify, or constrain the analysis based on known or suspected influences of meteorology on pollutant concentrations during transport (e.g. washout due to rain, gas-particle partitioning based on humidity, oxidation/reduction based on sunlight, upper-air entrainment, etc.). For example, for a rapidly dry-depositing species such as RGM or HNO₃, where the dry-deposition velocity is strongly dependent on wetness, data from periods with a wet surface may be excluded.

Contoured pollutant emissions values are overlaid on the unconstrained or constrained receptor concentration source-field maps to explore the correspondence between potential source fields for a given receptor concentration and emissions location and magnitude. With appropriate gridding of emissions data and CPSC data, spatial correlations of emissions with receptor conditions can be calculated with image processing tools for specific regions of the domain or along specific transects through the grid.

Summary of CPSCA Method Steps

1. 72-h air-mass back-trajectories with hourly end-points are calculated for every sample (2 hours sample duration or less) representing the mid point in time of each sample. Trajectories are calculated using the NOAA HYSPLIT model with vertical mixing and the EDAS 40-km meteorological data.
2. Trajectory statistics (total rain, solar flux and average T, Theta, height, mixing height, pressure level, etc.) are extracted from each trajectory.

3. EDAS meteorological information such as mixing depth is extracted at the receptor location for every sample.
4. Local surface average meteorological measurements for every sample at the receptor are compiled.
5. Receptor pollutant concentrations and the EDAS and local observed meteorology are assigned to each hourly trajectory endpoint associated with each sample.
6. The trajectory endpoint-associated data are summarized by source-field grid cell. The choice of grid-cell size influences both the spatial resolution of potential sources and the number trajectory endpoints representing each grid cells. Data aggregation by grid cell includes the mean and maximum of all receptor concentrations (or met parameter) associated with trajectories passing through that grid cell. The median or specific quantiles could also be used. Gridded data are interpolated to a potential surface using the 6 nearest-neighbor cells with linear distance weighting.
7. The aggregated data are plotted to display a map of receptor conditions associated with air mass passage over the potential source domain. This type of map immediately conveys the average or maximum (or other statistic) concentration (or met parameter) at the receptor potentially influenced by sources from a given location.
8. Specific pollutant emissions data are then overlaid on the CPSC map to assess spatial correspondence and emissions intensity correspondence between potential source locations and conditions (various statistics of the measured pollutant concentrations) at the receptor.
9. With appropriate gridding of emissions data and CPSC data, spatial correlations of emissions with receptor conditions can be calculated with image processing tools for specific regions of the domain or along specific transects through the grid.

Application of CPSCA to Underhill Ambient Mercury Data

This section describes the application of CPSCA to data collected using the Tekran Ambient Air Mercury Speciation System deployed at the Underhill, VT Air Quality Site. In the data set considered here there are 8,296 2-hour samples from a 26-month period. A 72-hour air-mass back-trajectory with hourly end-points reported was calculated using the NOAA HYSPLIT model (Draxler and Rolph 2003) with vertical mixing for the center of each 2-hour sample period. The starting height was set to 200 m above model terrain height (~300 m for model terrain at the receptor, actual receptor elevation = 400 masl, approximate start height 500 masl). The start height of 500-meters was selected based on prior experience with calculations of trajectories for this receptor location in complex terrain. There were 588,285 trajectory end points that could each be associated with a concentration measurement at the receptor (Underhill, VT). Because all samples were used, and because the samples were nearly continuous and evenly spaced in time, multiple trajectories “sampled” or “represented” 2/3 of North America and the eastern Atlantic Ocean (Figure 12).

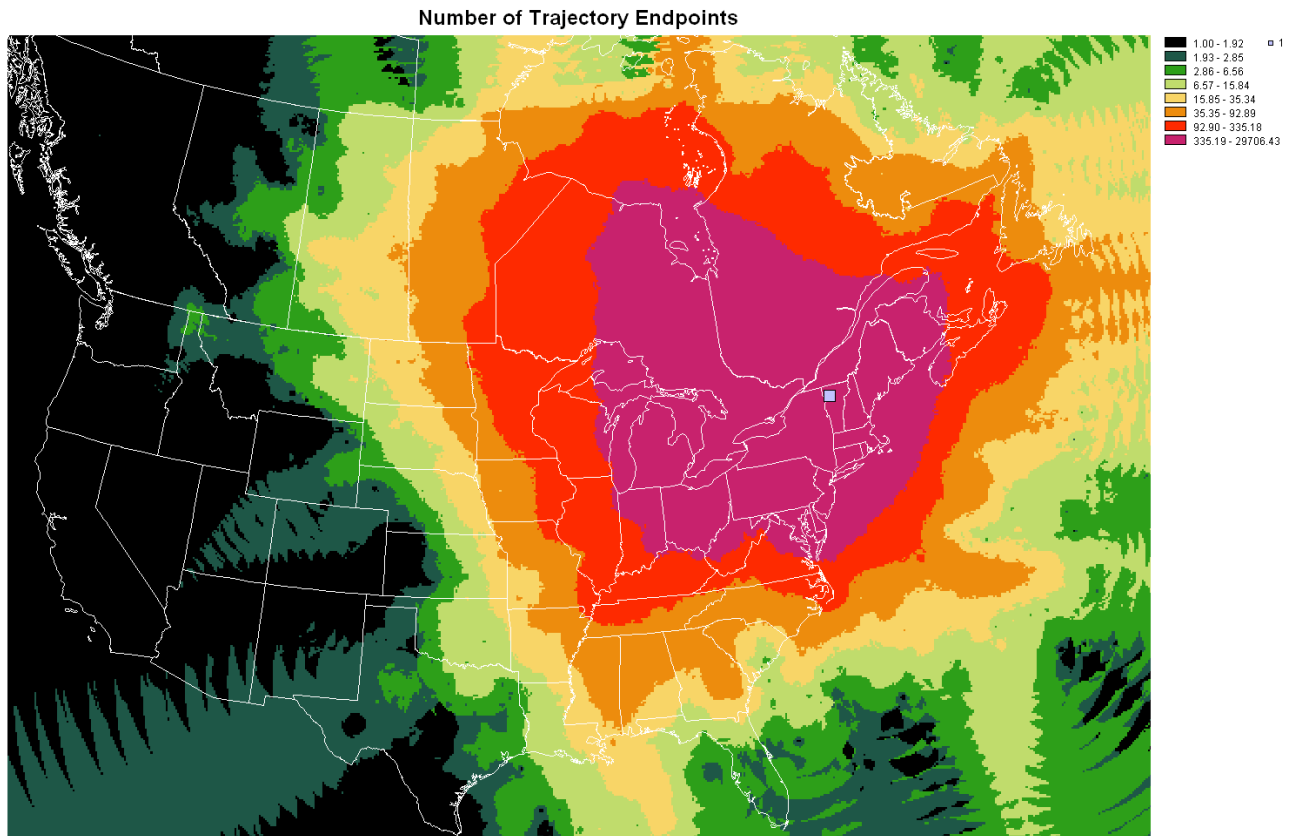


Figure 12. Number of trajectory endpoints at a grid cell location. The blue square represents the receptor location (Underhill, VT). Since trajectories were calculated every 3 hours for a 26-month period, this map shows the frequency (number of endpoints) with which air arriving at the receptor traversed a given location up to 72 hours before arrival.

The CPSC map for the average RGM at Underhill indicates potential major sources in a corridor from Tennessee through West Virginia and Pennsylvania (Figure 13). Important sources are also indicated in New Jersey and Southern New York. A potential significant source is indicated as far away as northeast Texas. While significant emissions sources exist in northeast Texas (discussed below), we remain cautious about assigning importance to potential source contributions indicated in areas sampled by only a small number of trajectories (see Figure 12). A possible major source is indicated in Newfoundland Canada. A major potential marine source region is indicated in the western Atlantic Ocean east of Cape Cod. A less significant marine source is indicated from the region of Hudson Bay. The CPSCA indication of important marine RGM sources is consistent with identification of important marine RGM sources in recent model simulations by Sillman et al. (http://www.htap.org/meetings/2007/2007_01/presentations/Thursday%20afternoon/Sillman_IHTP_Geneva2007.pdf). However, the location of the marine sources identified by this study differs from the locations identified by Sillman. This may be a result of the specific modeling time periods considered.

72-h Trajectory Mean RGM (pg/m3) at Receptor (VT99)

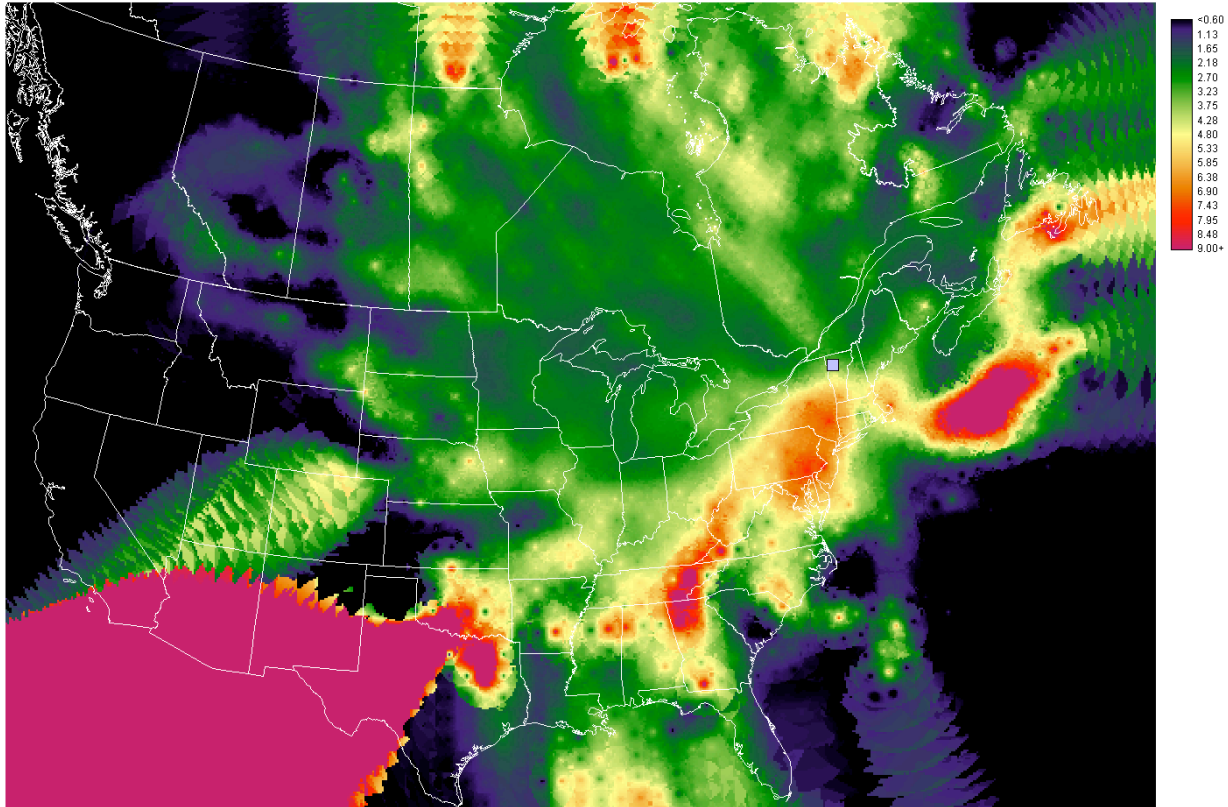


Figure 13. CPSC map for RGM sources depicting the potential contribution of a given location to average concentrations of the indicated value at the receptor (Underhill, VT – indicated by the blue square. Green indicates source areas contributing air arriving with an average concentration of 2-3 pg/m^3 , while red areas indicate source areas contributing air arriving with an average concentration of 7 pg/m^3 or greater. *SPECIAL NOTE: this report reflects work in progress. As this material is revised for publication figures will be improved. We plan to mask these figures at a specific value of number of trajectory endpoints per grid cell. This will eliminate the visual artifacts such as the large red area extending from western Texas where only a few trajectory endpoints were located (see Figure12). The analysis discussed in this report ignores or discounts these artifacts. Please try to not be distracted by them. We did not have time to remake all the figures by the report submission deadline.*

Speciated mercury emissions estimates (Cohen et al. 2004) representing 1999 emissions inventories for the US and Canada were used to determine the spatial and emissions magnitude correspondence with receptor concentrations associated with a given potential source location. Incinerator (municipal waste and medical) emissions, which are known to have been reduced dramatically since 1999, were excluded to avoid confounding the analysis. Emissions (point and area sources) were gridded at 0.1-degree latitude and longitude resolution. Contours of emissions values were generated from the grid and were overlaid on the receptor concentration source-field maps to explore the correspondence between potential source fields for a given receptor concentration and emissions location and magnitude (Figure 14).

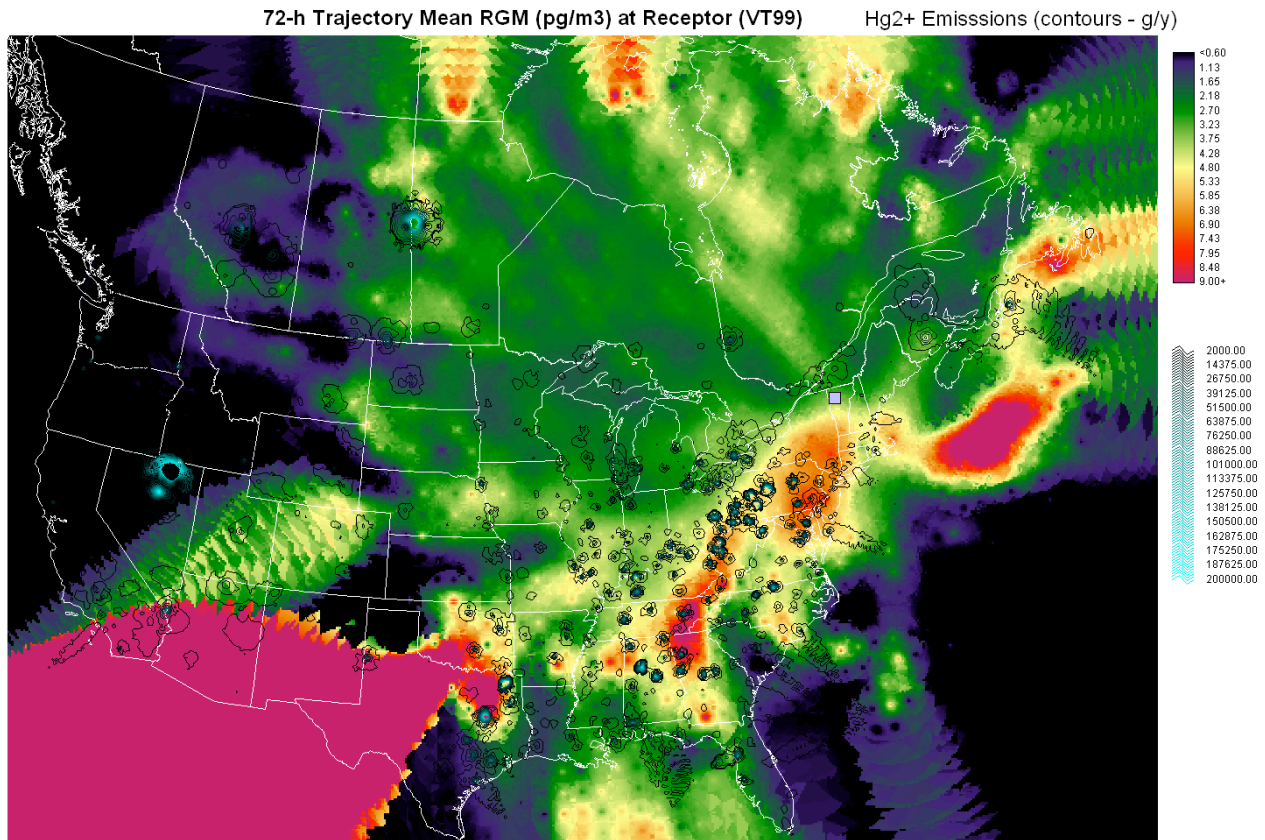


Figure 14. Overlay of 1999 US and Canada Hg^{2+} (RGM) emissions (courtesy of Mark Cohen, NOAA-ARL) on the CPSC map for mean RGM at Underhill, VT. Emissions (g/y) are contoured with light blue indicating the highest emission rates. *SPECIAL NOTE: this report reflects work in progress. As this material is revised for publication figures will be improved. We plan to mask these figures at a specific value of number of trajectory endpoints per grid cell. This will eliminate the visual artifacts such as the large red area extending from western Texas where only a few trajectories endpoints were located (see Figure 12). The analysis discussed in this report ignores or discounts these artifacts. Please try to not be distracted by them. We did not have time to remake all the figures by the report submission deadline.*

There was an excellent spatial correspondence between emissions source locations and intensity and the potential source areas for a given average RGM concentration at the receptor (Figure 14). The different densities and intensities of sources appear clearly related to the average RGM concentration arriving at the receptor attributable to a given source field. It is noteworthy that very large and very distant sources (northeast Texas and the Flin-Flon base-metal smelter in Manitoba) are indicated as potential sources by the CPSC map for mean RGM concentration. The potential contributions from these distant sources is more clearly identified by the CPSC map for the maximum RGM concentrations from a given source-field location (Figure 15). The maximum RGM concentration CPSC map depicts major plume “hits” at Underhill associated with a source field location. It should be noted that because air arriving from any moderate-range or long-range source must traverse the relatively source-free area within a few hundred km of the receptor, this near-receptor area is indicated as potentially “contributing” high concentrations of RGM – especially on the maximum concentration maps. The interpretation of the maximum concentration map display close to the receptor (when there are no known or suspected sources) should be that of a transport route.

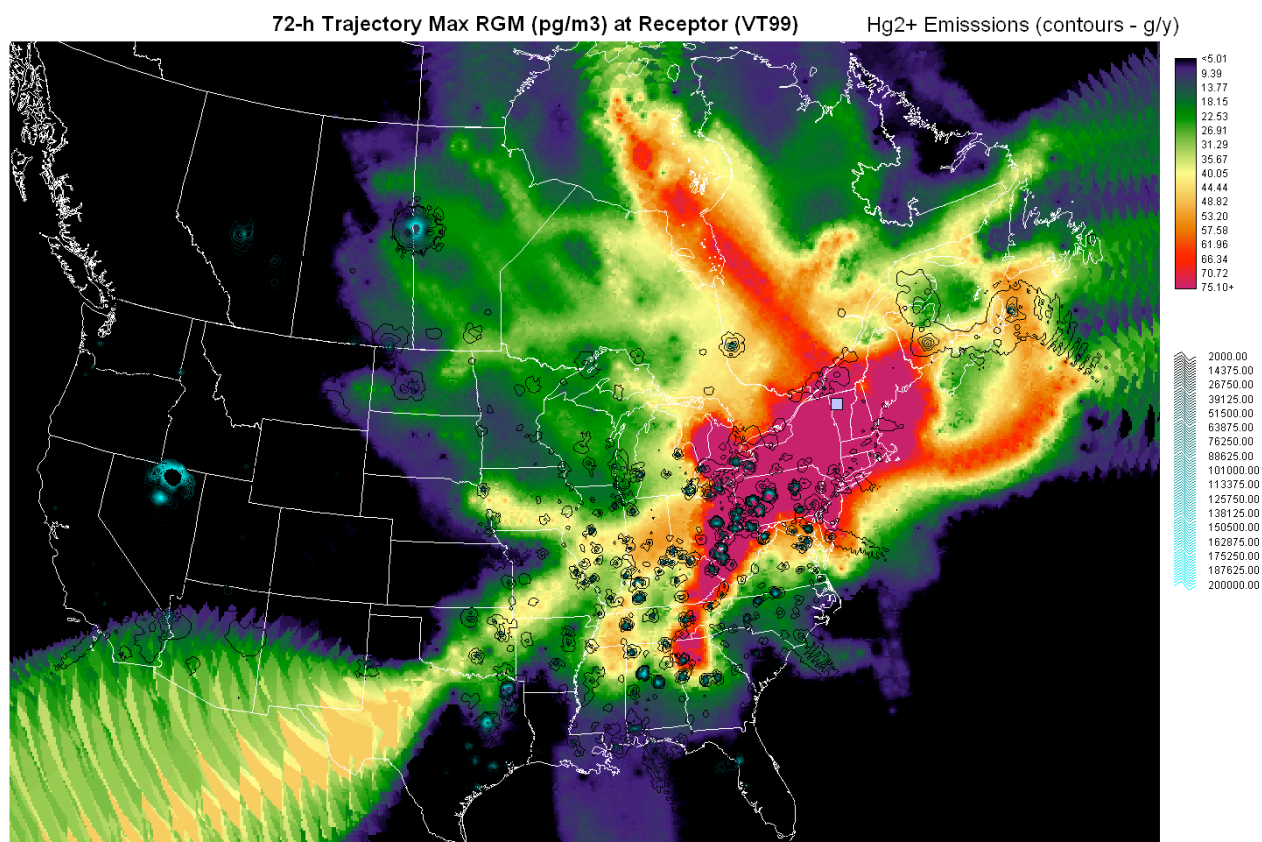


Figure 15. CPSC map of maximum RGM concentration observed at Underhill for air traversing a given location. 1999 US and Canada Hg^{2+} (RGM) emissions (courtesy of Mark Cohen, NOAA-ARL) are overlaid for reference. Using the maximum RGM value highlights specific trajectories associated with major transport events more than the average RGM CPSC map. *SPECIAL NOTE: this report reflects work in progress. As this material is revised for publication figures will be improved. We plan to mask these figures at a specific value of number of trajectory endpoints per grid cell. This will eliminate the visual artifacts such as the large highlighted area extending from western Texas where only a few trajectory endpoints were located (see Figure 12). The analysis discussed in this report ignores or discounts these artifacts. Please try to not be distracted by them. We did not have time to remake all the figures by the report submission deadline.*

The CPSC maps for mean (Figure 16) and maximum (Figure 17) HGP concentrations at Underhill indicate a different set of locations for major particulate mercury source areas consistent with the HGP emissions data. The potential impact of the Flin-Flon base-metal smelter in Manitoba as a source of HGP arriving at Underhill is evident in both maps. HGP sources appear to be mainly to the N and NW of the receptor while RGM sources are predominantly to the S and SW. There are indications of an unknown source along the Mississippi River in eastern Iowa. A possible marine source in the Atlantic is indicated as well for moderate ($50\text{-}75\text{ pg/m}^3$) HGP events.

The CPSC map for mean GEM concentrations at Underhill indicates yet a different pattern of contributing source areas (Figure 18). A more diffuse contributing zone from the W through the S is peppered with industrial and power-generation GEM sources. A potential marine source is indicated along the coast from Florida through the Carolinas. The CPSC map for maximum concentrations (big “hits”) indicates major sources in the emission-rich Ohio-River corridor on through to major sources in eastern Texas are responsible for the highest GEM concentrations observed at Underhill (Figure 19).

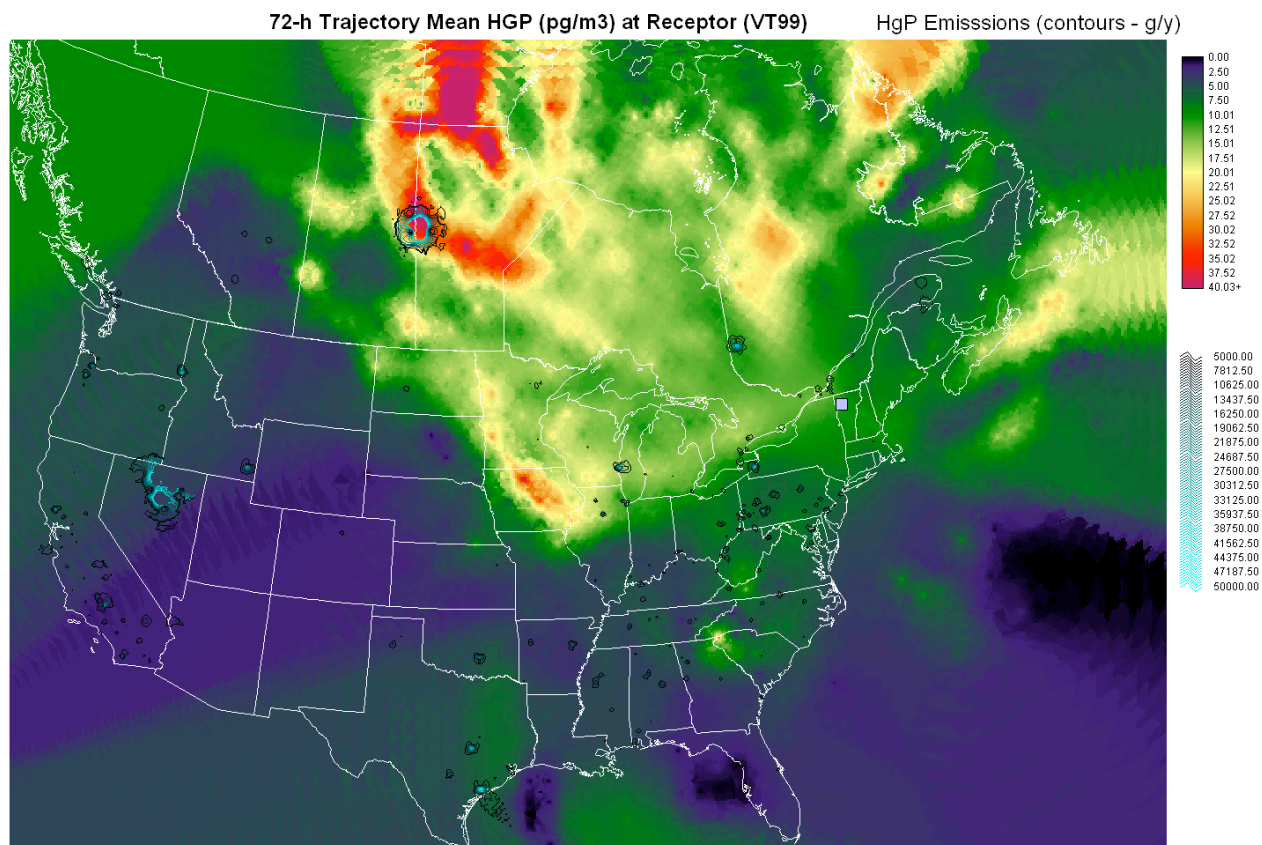


Figure 16. CPSC map for HgP sources depicting the potential contribution of a given location to average concentrations of the indicated value at the receptor (Underhill, VT – indicated by the blue square). Green indicates source areas contributing air arriving with an average concentration of 7-15 pg/m^3 , and red areas indicate source areas contributing air arriving with an average concentration of 30 pg/m^3 or greater. 1999 US and Canada HgP emissions (courtesy of Mark Cohen, NOAA-ARL) are overlaid for reference. *SPECIAL NOTE: this report reflects work in progress. As this material is revised for publication figures will be improved. We plan to mask these figures at a specific value of number of trajectory endpoints per grid cell. This will eliminate the visual artifacts such as the large highlighted area northwest of Hudson Bay where only a few trajectories endpoints were located (see Figure 12). The analysis discussed in this report ignores or discounts these artifacts. Please try to not be distracted by them. We did not have time to remake all the figures by the report submission deadline.*

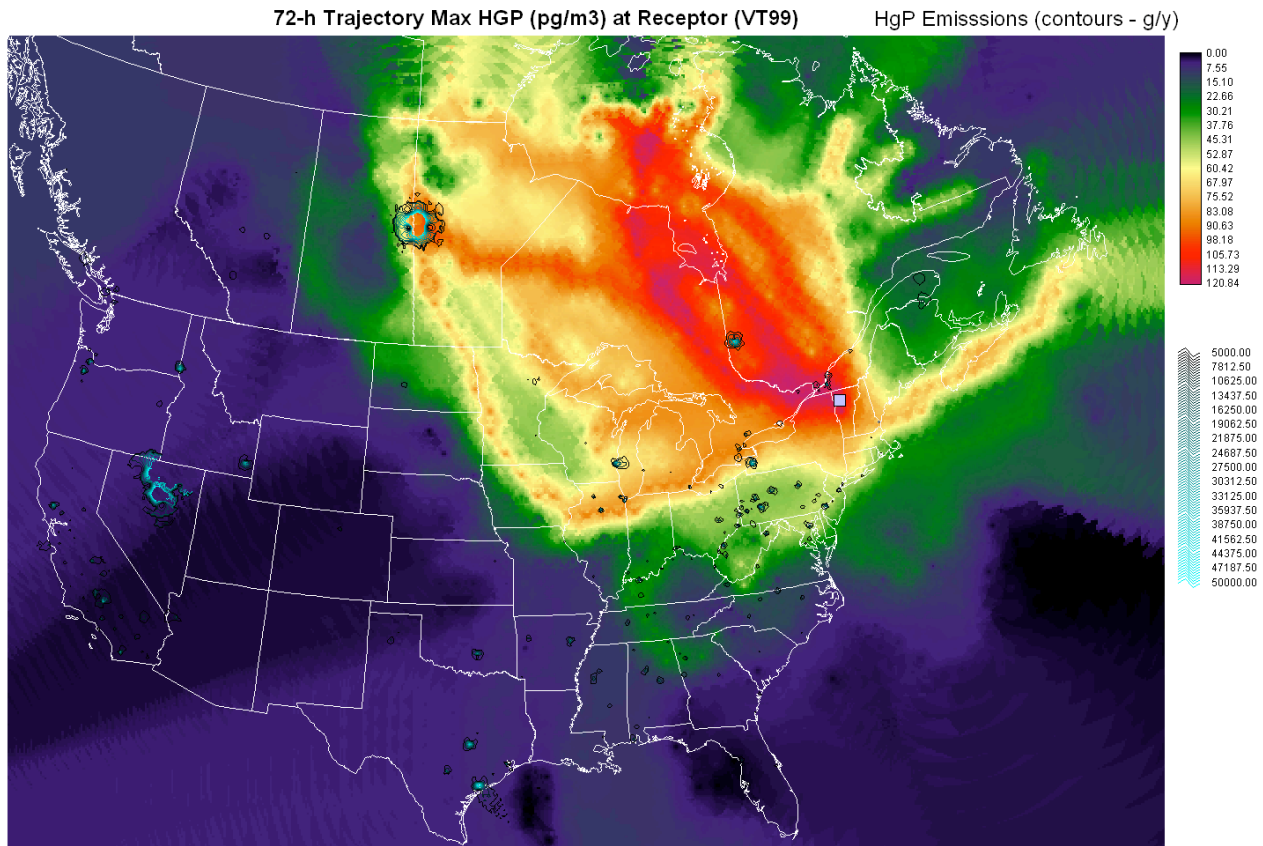


Figure 17. CPSC map of maximum HGP concentration observed at Underhill for air traversing a given location. 1999 US and Canada HGP emissions (courtesy of Mark Cohen, NOAA-ARL) are overlaid for reference. Using the maximum HGP value highlights specific trajectories associated with major transport events more than the average HGP CPSC map. The large Manitoba base-metal smelter is indicated as a major HGP source via multiple transport paths. A possible marine source in the Atlantic is indicated as well for moderate (50-75 pg/m³) HGP events. *SPECIAL NOTE: this report reflects work in progress. As this material is revised for publication figures will be improved. We plan to mask these figures at a specific value of number of trajectory endpoints per grid cell. This will eliminate the visual artifacts such as the large highlighted area northwest of Hudson Bay where only a few trajectories endpoints were located (see Figure 12). The analysis discussed in this report ignores or discounts these artifacts. Please try to not be distracted by them. We did not have time to remake all the figures by the report submission deadline.*

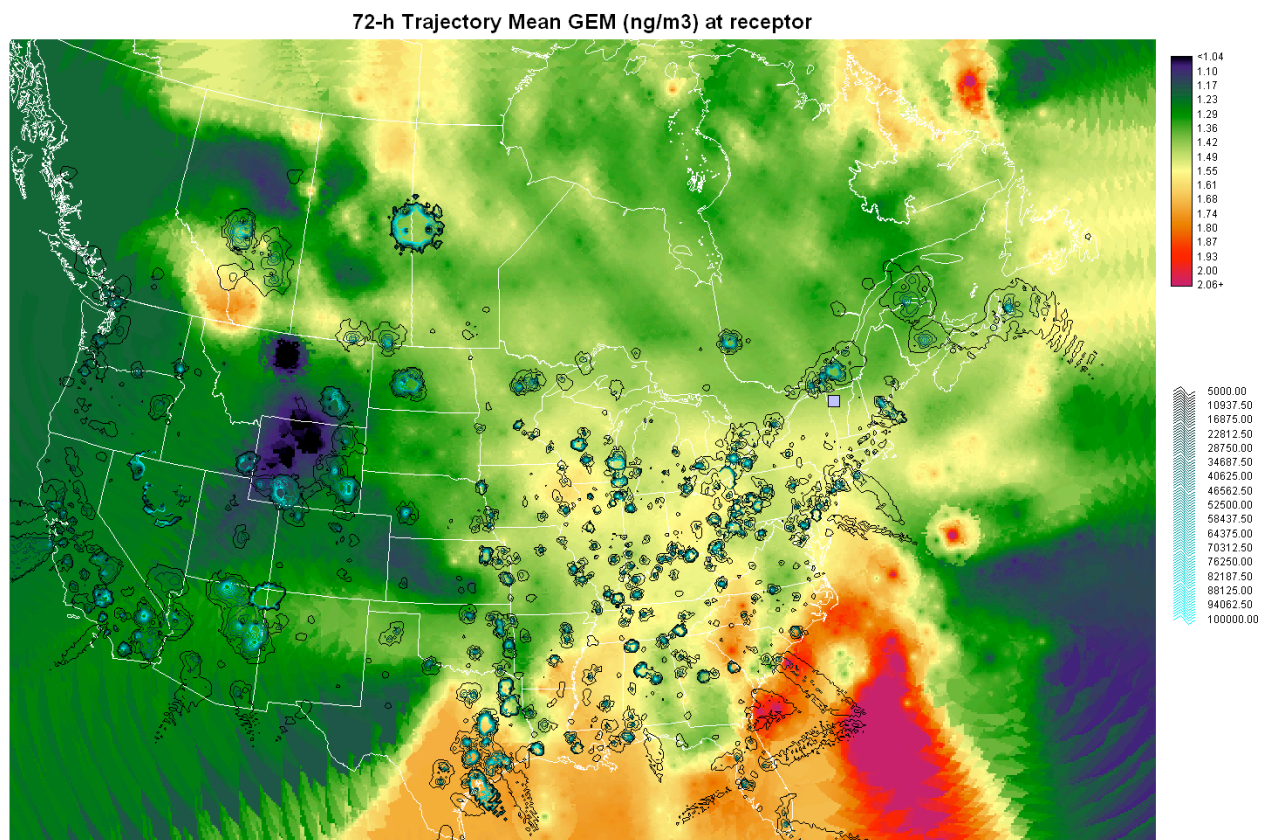


Figure 18. CPSC map for GEM sources depicting the potential contribution of a given location to average concentrations of the indicated value at the receptor (Underhill, VT – indicated by the blue square). Green indicates source areas contributing air arriving with an average concentration of 1.2-1.4 ng/m³ (global background), and red areas indicate source areas contributing air arriving with an average concentration of 1.8 ng/m³ or greater. 1999 US and Canada GEM emissions (courtesy of Mark Cohen, NOAA-ARL) are overlaid for reference. *SPECIAL NOTE: this report reflects work in progress. As this material is revised for publication figures will be improved. We plan to mask these figures at a specific value of number of trajectory endpoints per grid cell. This will eliminate the visual artifacts such as the large highlighted area in the western US where only a few trajectory endpoints were located (see Figure 12). The analysis discussed in this report ignores or discounts these artifacts. Please try to not be distracted by them. We did not have time to remake all the figures by the report submission deadline.*

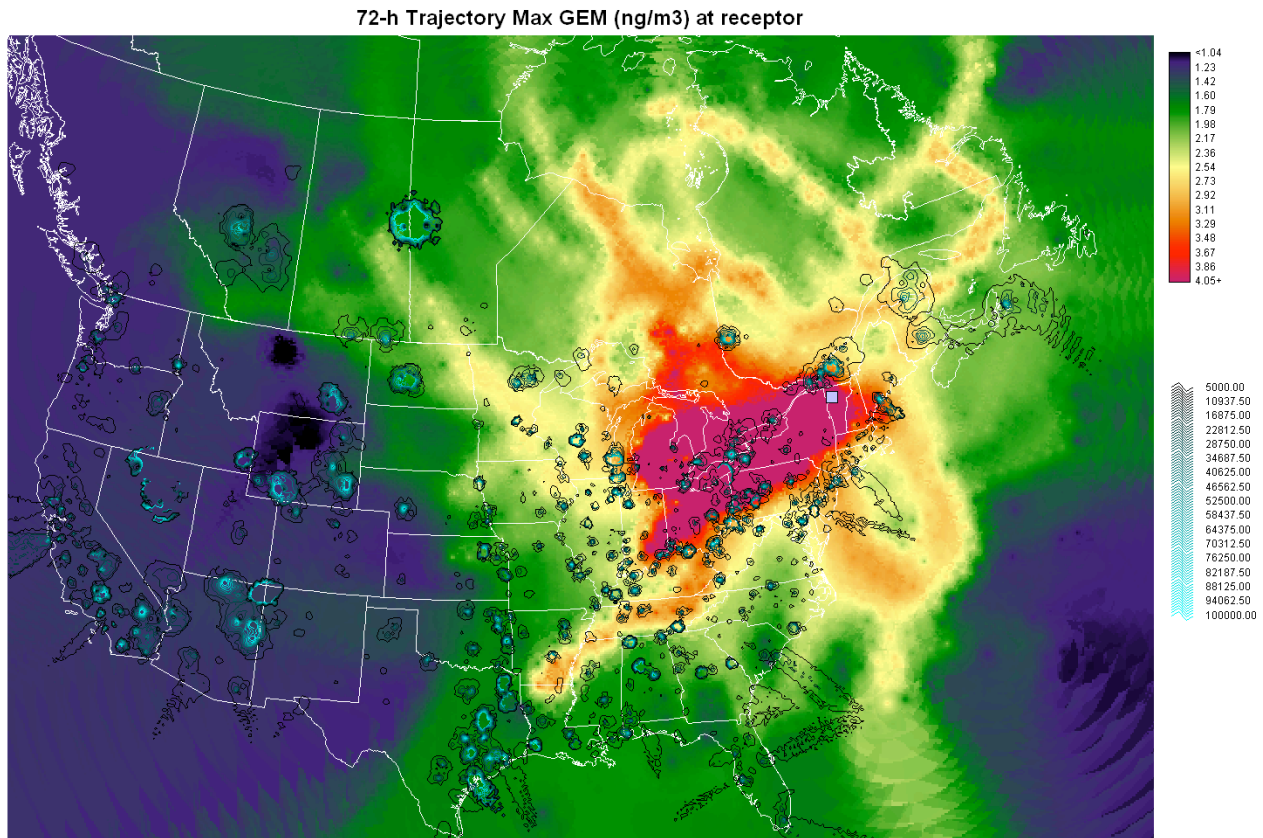


Figure 19. CPSC map of maximum GEM concentration observed at Underhill for air traversing a given location. 1999 US and Canada GEM emissions (courtesy of Mark Cohen, NOAA-ARL) are overlaid for reference. Using the maximum GEM value highlights specific trajectories associated with major transport events more than the average GEM CPSC map. *SPECIAL NOTE: this report reflects work in progress. As this material is revised for publication figures will be improved. We plan to mask these figures at a specific value of number of trajectory endpoints per grid cell. This will eliminate the visual artifacts such as the highlighted areas in the western US where only a few trajectory endpoints were located (see Figure 12). The analysis discussed in this report ignores or discounts these artifacts. Please try to not be distracted by them. We did not have time to remake all the figures by the report submission deadline.*

The analysis described above demonstrates the capability and sensitivity of CPSCA for source identification and attribution of atmospheric mercury. To illustrate the generality of the method, CPSCA was conducted for the ambient water vapor mixing ratio as measured at Underhill for the same set of trajectories as the mercury observations. The CPSC map of potential water vapor sources is intuitively reasonable with major source regions identified off the eastern Atlantic coast and in the Gulf of Mexico (Figure 20). A more modest potential source of water vapor is indicated in the region of the Great Lakes and another moderate source from Hudson Bay. It seems likely this method can be fruitfully applied to other continuous pollutant data (SO_2 , O_3 , $\text{PM}_{2.5}$ by TEOM) from Underhill and other locations.

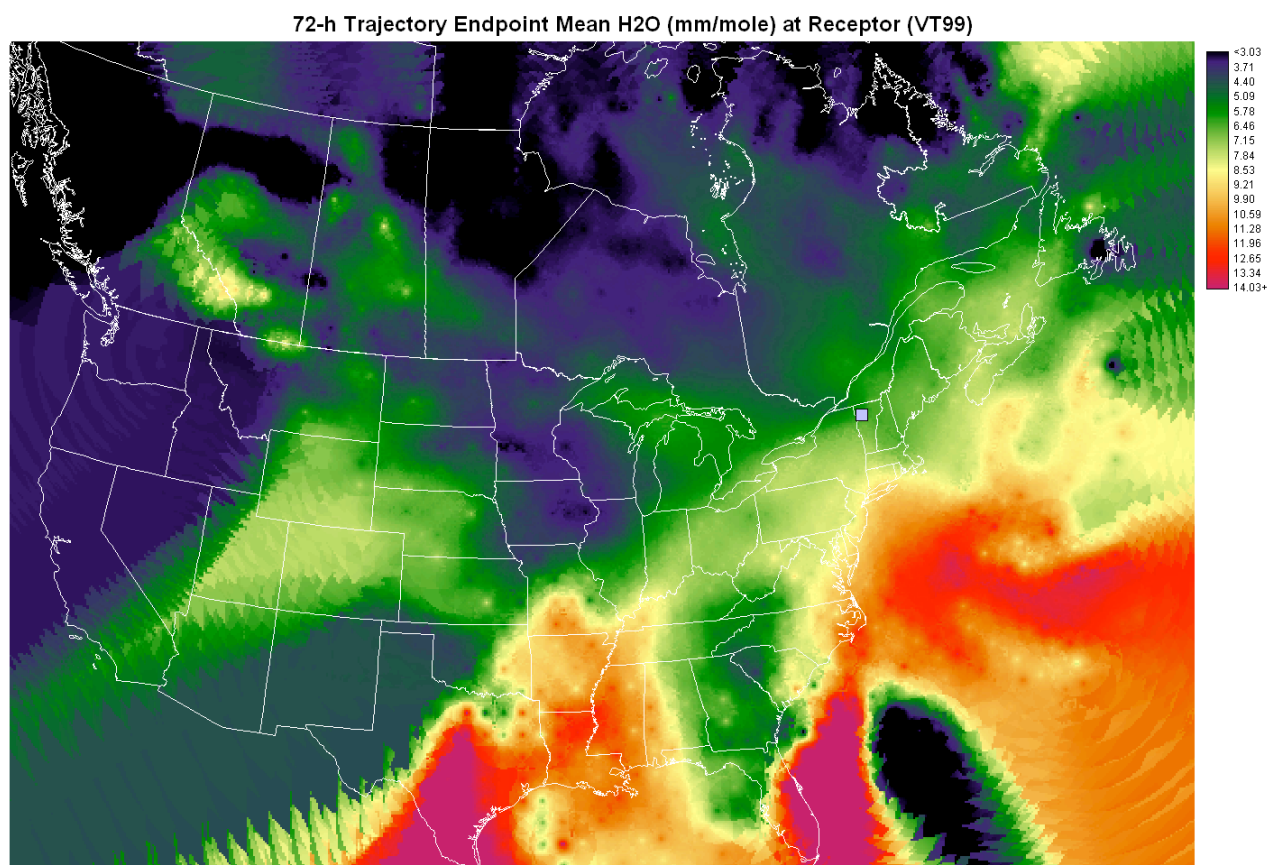


Figure 20. CPSC map for mean water-vapor mixing ratio. The anticipated source regions of the Atlantic Ocean and Gulf of Mexico are clearly indicated. The Great Lakes Region is indicated as a moderate source. *SPECIAL NOTE: this report reflects work in progress. As this material is revised for publication figures will be improved. We plan to mask these figures at a specific value of number of trajectory endpoints per grid cell. This will eliminate the visual artifacts such as the highlighted areas in the western US where only a few trajectory endpoints were located (see Figure 12). The analysis discussed in this report ignores or discounts these artifacts. Please try to not be distracted by them. We did not have time to remake all the figures by the report submission deadline.*

Ambient Atmospheric Mercury Speciation Summary

The ambient concentrations of the 3 major forms of atmospheric mercury GEM, HGP, and RGM were successfully characterized. This information allows improved dry-deposition modeling and dry-deposition estimates for the Lake Champlain Basin. We were able to interpret seasonal and diurnal variations of GEM, RGM and HGP concentrations in terms of observed meteorological influences and regional transport from anthropogenic and natural sources. Both individual transport-event analyses and the CPSC analysis of the full 26-month suggest that out-of-region sources are dominantly responsible for the moderate and highest concentrations of RGM, HGP, and GEM observed at Underhill, Vermont. Thus, reductions of mercury dry deposition will depend on successful reductions of out-of-state and out-of-region sources. The information generated through this project will be of great value to atmospheric modelers attempting to predict changes in mercury deposition from changes in emissions.

References

- Cohen, M., R. Artz, R. Draxler, P. Miller, D. Niemi, D., D. Ratte, M. Deslauriers, R. Duvar, R., Laurin, J. Slotnick, T. Nettesheim, and J. McDonald. (2004) Modeling the atmospheric transport and deposition of mercury to the Great Lakes. *Environmental Research* 95:, 247-265.
- Draxler, R.R. and Rolph, G.D., 2003. HYSPLIT (HYbrid Single-Particle Lagrangian Integrated Trajectory) Model access via NOAA ARL READY Website (<http://gus.arlhq.noaa.gov/ready/open/hysplit4.html>). NOAA Air Resources Laboratory, Silver Spring, MD.
- Kenski, D.M. (2004). Quantifying Transboundary Transport of PM_{2.5}: A GIS Analysis. *Proc. AWMA 97th Annual Conf.*, Indianapolis (June 2004).
- Lai, S.-o , T. M. Holsen, P. K. Hopke, and P. Liu. (2007) Wet deposition of mercury at a New York state rural site: Concentrations, fluxes, and source areas. *Atmos. Environ.* 41:4337-4348.
- Lindberg, S. E., and W.J. Stratton. 1998. Atmospheric mercury speciation: Concentrations and behavior of reactive gaseous mercury in ambient air. *Envir. Sci. & Technol.* 32:49-57.
- Miller, E.K., VanArsdale, A., Keeler, G.J., Chalmers, A., Poissant, L., Kamman, N., and Brulotte, R. (2005) Estimation and Mapping of Wet and Dry Mercury Deposition across Northeastern North America. *Ecotoxicology* 14, 53-70.
- Poirot, R.L. and P.R. Wishinski (1985). Regional apportionment of ambient sulfate contributions to a remote site in northern VT. *Transactions APCA Int. Spec. Conf. on Receptor Modeling: Real World Issues and Applications*, T.G. Pace, Ed., pp. 239-250, Williamsburg, VA.

Atmospheric Mercury in Vermont and New England: Measurement of deposition, surface exchanges and assimilation in terrestrial ecosystems

Final Project Report – GEM Flux Measurements – 1/16/2009

PI: Melody Brown Burkins, University of Vermont (UVM)
Co-PIs: Eric K. Miller¹, Ecosystems Research Group, Ltd.; and Jamie Shanley, US Geological Survey
Collaborators: Sean Lawson, VTANR-VMC; Mim Pendelton, Carl Waite, UVM;
Rich Poirot, VTANR-APCD; Alan VanArsdale, USEPA; Mark Cohen, NOAA
Project Officer: Eric Hall, USEPA

Measurements of GEM exchanges over a forest canopy

At the outset of the project there was tremendous uncertainty about the magnitude and the mechanisms governing net-gaseous Hg assimilation by forest canopies (Miller 2002, Lindberg et al. 1998). The most widely used inferential model for GEM deposition at the time (Lindberg et al. 1992) did not represent the known bi-directional nature of the GEM flux. It was clear from limited direct observations that at times GEM deposits and at times it is emitted from the forest canopy (Lindberg et al. 1998). It was also impossible to reconcile the large GEM fluxes implied by the Lindberg et al. (1992) model with the much smaller fluxes indicated by measurements of leaf-assimilated Hg (see Miller 2002, 2005). It appeared likely that Hg deposition/emission is governed by a compensation point, an ambient concentration above which deposition occurs and below which emission occurs (Hansen et al. 1995). Direct measurements of atmosphere-forest exchanges of GEM were needed to resolve this discrepancy, identify a potential field compensation point and to help elucidate the physical and physiological processes regulating GEM deposition or emission.

Direct, micrometeorological measurements of atmosphere-canopy exchanges of GEM were made using the modified Bowen-ratio method (Lindberg et al. 2002, Lindberg and Meyers 2001, Lee et al. 2000). Briefly, this method involves measuring the concentration gradient of mercury-vapor above the surface while concurrently measuring the gradient of either temperature (Lee et al. 2000) or water-vapor (Lindberg et al. 2002) and the turbulent flux of sensible or latent heat over the same height interval. The turbulent transfer coefficient derived from, for example, the latent heat flux and the water-vapor gradient is then assumed to apply to mercury vapor (Lindberg and Meyers 2001). The turbulent fluxes of latent and sensible heat were measured using the Bowen-ratio method and confirmed with sensible heat-fluxes measured by the eddy correlation method. The mercury gradient was measured with a Tekran 2537A. The GEM flux measurements were conducted from the VMC forest canopy observation tower at the Proctor Maple Research Center (Figures 1 and 2). Simultaneous measurements of the turbulent fluxes of CO₂ and H₂O were made in conjunction with mercury flux measurements over the forest canopy. These measurements provided insight into the physiological and physical mechanisms governing mercury exchange.

Initial flux measurements were begun in late summer of 2004. In December of 2004 a severe windstorm following heavy rains blew over the 100-foot tower that supported the mercury concentration and flux measurements (Figure 3). Shortly after the tower collapsed, typical cold winter weather set in and the ground froze solid. Difficult winter conditions limited salvage operations. After winter conditions eased, equipment was salvaged and repaired. Concentration

¹ Corresponding author for the final project report. Email: ekmiller at ecoystems-research.com Voice: 802-649-5550

measurements were reestablished in April, 2005 based out of an instrument shelter at the NADP/MDN site located ~1km north of the tower site. We were delayed in restarting the flux measurement program at the tower site for several reasons. University of Vermont Facilities Management controlled the schedule of salvage, repair, and insurance claims for the tower damage. There were considerable logistical problems to overcome in designing and constructing new anchors and a new tower. The tower reinstatement was completed on October 4th, 2005.

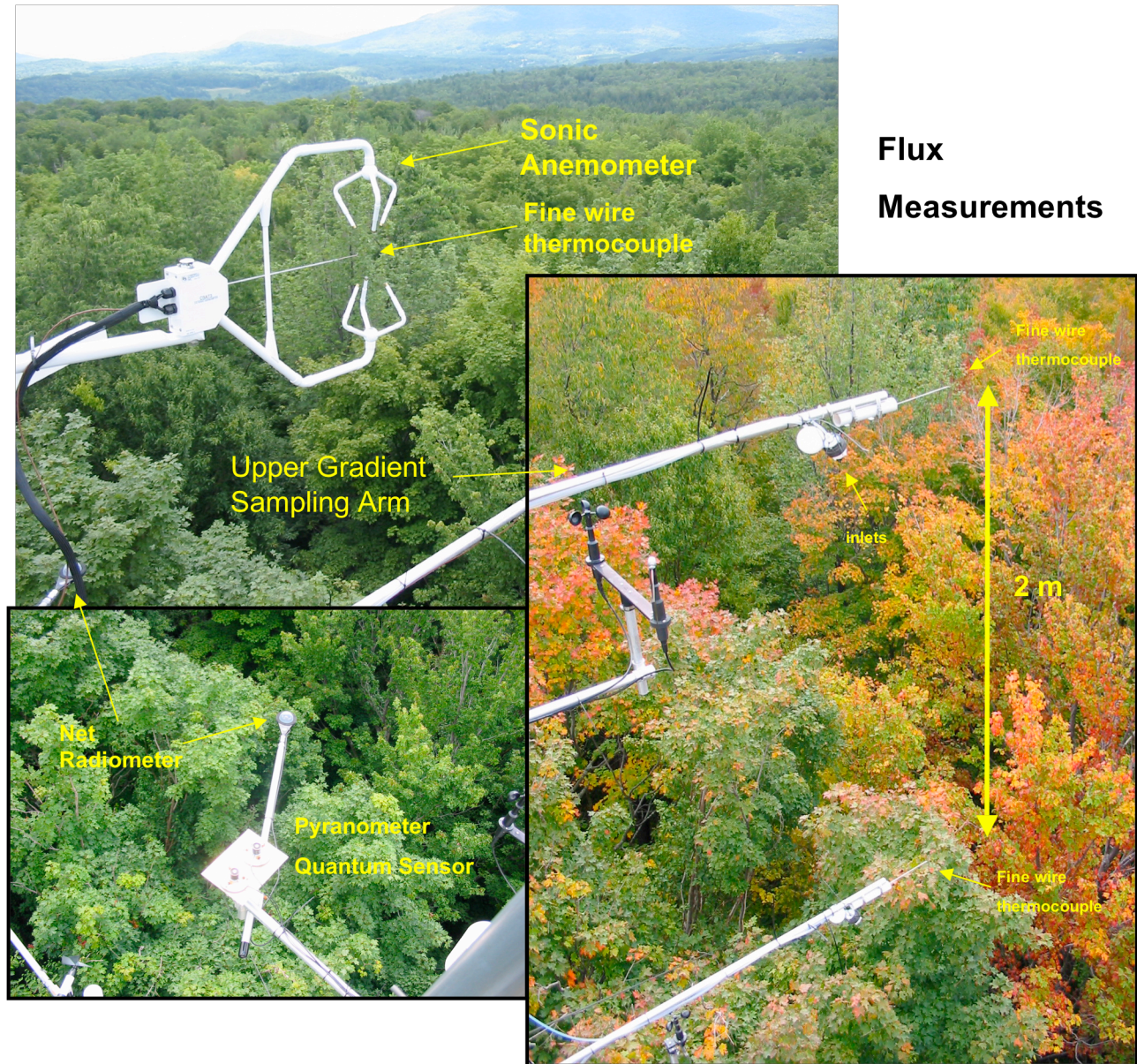


Figure 1. Configuration of inlets and sensors for the GEM flux measurement system deployed on top of the forest canopy observation tower.

Valve Box, CO₂/H₂O and Hg Analyzers

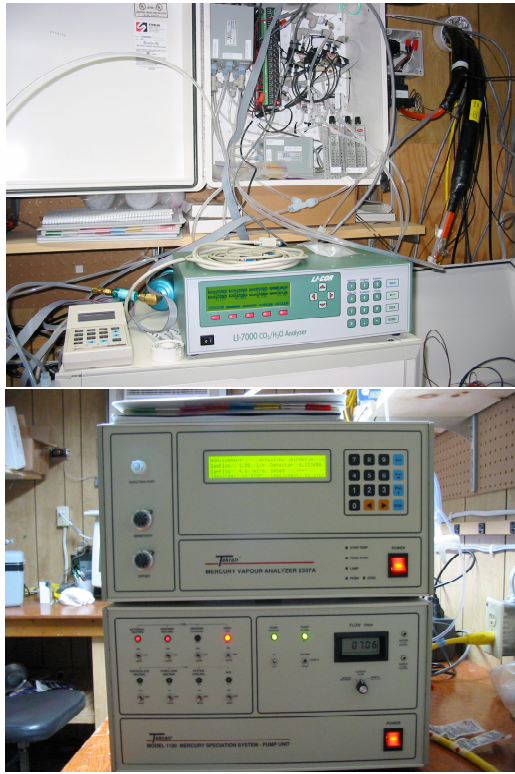


Figure 2. Analytical equipment housed in the trailer at the base of the forest canopy observation tower.



Figure 3. The atmospheric measurement tower after the severe wind storm (left). New forest canopy tower under construction (right).

Bi-directional fluxes (both emission and deposition) were observed (Figure 4). Net emission and deposition fluxes ranged up to 1000 ng/m²/h. Deposition was typically observed during the day with high solar fluxes, while emission typically occurred at night or during cloudy periods. Companion measurements of CO₂ and water-vapor exchanges suggested peak deposition values occurred in conjunction with strong photosynthesis (Figure 5).

GEM exchange measurements and their analysis were limited by the rescission of funding for years 4 and 5 of the project and due to the unfortunate collapse of the forest canopy tower in the winter of 2004 which caused a significant delay in the measurement program. We hope to complete additional analyses of GEM flux measurements in the near future under separate funding.

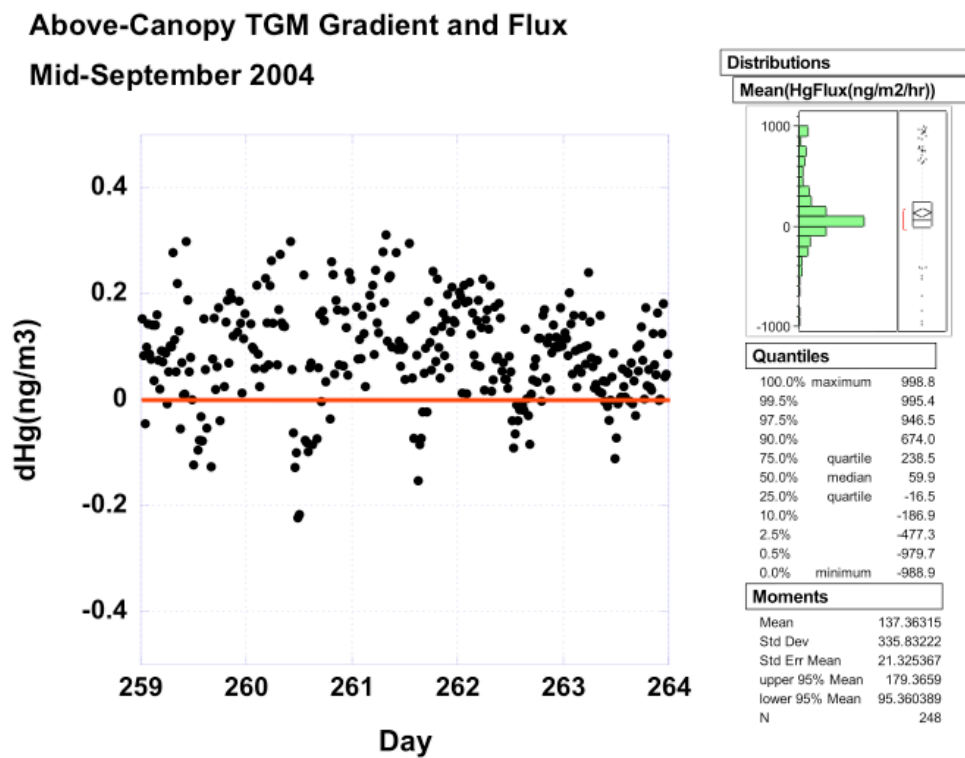


Figure 4. (Left) Example of diurnal and multi-day pattern of above-canopy mercury gradient. Positive values indicate emission of GEM and negative values indicated deposition to the forest canopy. (Right) Frequency distribution of fluxes.

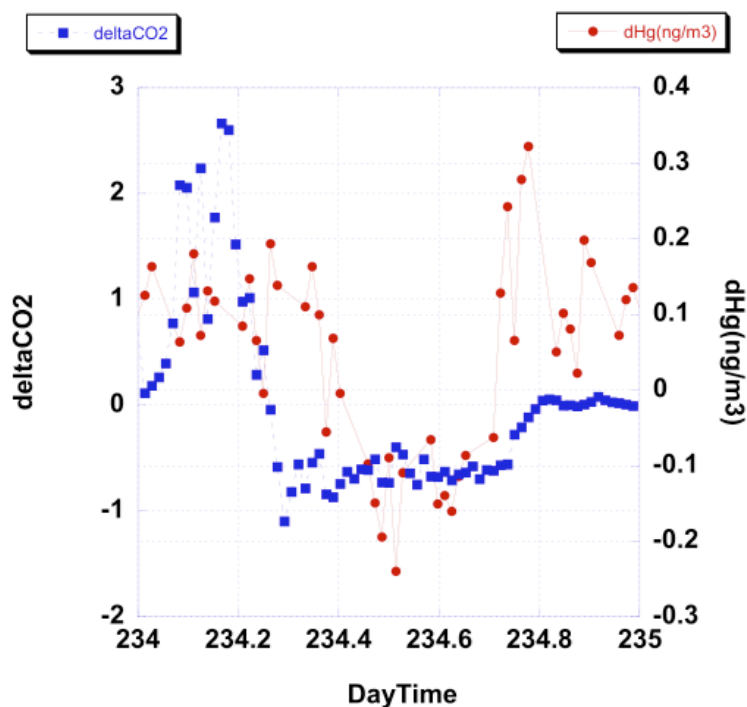


Figure 5. Example diurnal cycle of GEM and CO₂ gradients measured above the forest canopy. GEM deposition is indicated by the negative GEM gradients (red). GEM deposition is strongest at mid-day during intense photosynthesis (indicated by the strong negative CO₂ gradient - blue).

References

- Hanson, P.J., S.E. Lindberg, T.A. Tabberer, J.G. Owens, K.-H. Kim. 1995. Foliar exchange of mercury vapor: evidence for a compensation point. *Water, Air, and Soil Pollution* **80**:373-382.
- Lee, X., G. Benoit, X. Hu. 2000. Total gaseous mercury concentration and flux over a coastal saltmarsh vegetation in Connecticut, USA. *Atmos. Environ.* **34**: 4205-4213.
- Lindberg, S.E., T.P. Meyers, G.E. Taylor, R.R. Turner, and W.H. Schroeder (1992) Atmosphere-Surface Exchange of Mercury in a Forest: Results of Modeling and Gradient Approaches. *Journal of Geophysical Research* **97**:2519-2528.
- Lindberg, S.E. and T.P. Meyers. 2001. Development of an automated micrometeorological method for measuring the emission of mercury vapor from wetland vegetation. *Wetlands Ecology and Management* **9**:333-347.
- Lindberg, S.E., W. Dong, and T. Meyers. 2002. Transpiration of gaseous mercury through vegetation in a subtropical wetland in Florida. *Atmos. Envir.* **36**:5200-5219.
- Lindberg, S.E., P.J. Hanson, T.P. Meyers, and K-Y Kim. 1998. Micrometeorological studies of air/surface exchange of mercury over forest vegetation and a reassessment of continental biogenic mercury emissions. *Atmos. Envir.* **32**:895-908.
- Lindberg, S. E., and W.J. Stratton. 1998. Atmospheric mercury speciation: Concentrations and behavior of reactive gaseous mercury in ambient air. *Envir. Sci. & Technol.* **32**:49-57.

- Miller, E.K. 2002. Estimation and Mapping of Wet and Dry Mercury Deposition Across the VT-NH Region. Project report submitted to Neil Kamman, VTDEC, Water Quality Division, 103 South Main St., Building 10 North, Waterbury, VT 05671-0408. Ecosystems Research Group, Ltd., Norwich, VT.
- Miller, E. K., A. VanArsdale, J. G. Keeler, A. Chalmers, L. Poissant, N. C. Kamman, and R. Brulotte. 2005. Estimation and mapping of wet and dry mercury deposition across northeastern North America. *Ecotoxicology* 14:53-70.

Mercury Bioaccumulation in a Terrestrial Food Web of a Montane Forest

Christopher C. Rimmer¹, Eric K. Miller², Kent P. McFarland¹, Steven D. Faccio¹,
Allan B. Strong³, and Robert J. Taylor⁴

¹ Vermont Center for Ecostudies, P.O. Box 420, Norwich, VT 05055

² Ecosystems Research Group, Ltd., P.O. Box 1227, Norwich, VT 05055

³ Rubenstein School of Natural Resources and Environment, Aiken Center, 81 Carriage
drive, University of Vermont, Burlington, VT 05405

⁴ Trace Element Research Laboratory, Texas A & M University, VMA Building, Room 107,
Highway 60, College Station, TX 77843-4458

Abstract

We investigated mercury (Hg) concentrations in a terrestrial food web in high elevation forests in Vermont. Mercury concentrations increased from autotrophic organisms to herbivores < detritivores < omnivores < carnivores. Within the carnivores studied, raptors had higher blood mercury concentrations than their songbird prey. The Hg concentration in the blood of the study focal species Bicknell's thrush varied over the course of the summer in response to a diet shift related to changing food item availability. The montane food web is more detrital-based (with higher Hg concentrations) in early summer and more foliage-based (with lower Hg concentrations) during late summer. There were significant year effects in different ecosystem compartments indicating a possible connection between atmospheric Hg deposition, detrital-layer Hg concentrations, arthropod Hg concentrations, and passerine blood Hg levels.

Introduction

Methylmercury (MeHg), the bioavailable form of mercury (Hg), is a neurotoxin with well-documented, adverse impacts on natural systems and wildlife populations. Most investigations on Hg bioaccumulation and biomagnification have focused on freshwater aquatic ecosystems, where conditions promoting methylation are common and Hg concentrations in upper trophic level consumers may be high (e.g., Bank et al. 2005, 2007; Chen et al. 2005; Evers et al. 2005; Yates et al. 2005). Research has increasingly demonstrated that Hg impairs reproductive performance, lifetime productivity, growth and development, behavior, motor skills, and survivorship in aquatic birds and other wildlife (Wolfe et al. 1998; Evers 2004, 2008; Scheuhammer et al. 2007). Despite the recent documentation of elevated Hg exposure in terrestrial biota (summary in Driscoll et al. 2007), relatively little is known about pathways for Hg uptake and transfer in upland ecosystems, or about Hg risk thresholds for terrestrial organisms.

Trophic transfer of Hg in a strictly terrestrial food web has not been documented, although Cristol et al. (2008) showed Hg biomagnification in biota from a terrestrial habitat adjacent to a Hg-contaminated river in Virginia. Hg concentrations increased in known avian prey items (Orthoptera [grasshoppers] → Lepidoptera [moths or caterpillars] → Aranea [spiders]) to passerine birds. Nearly 50% of the Hg in spiders, which comprised 20-30% of diet in three focal songbird species, was in the form of bioavailable MeHg. Twelve of 13 avian species sampled had significantly higher Hg blood concentrations at the contaminated site than at uncontaminated reference sites. Cristol et al. (2008) concluded that aquatic Hg moved into and through the terrestrial food web, where avian consumption of predatory invertebrates increased the food chain length and caused Hg to biomagnify.

In montane areas of northeastern North America, anthropogenic Hg deposition from atmospheric sources is 2-5 times higher than in surrounding low elevation areas (Miller et al. 2005). Although mechanisms that drive methylation in montane forests are poorly understood, Hg has recently been documented to bioaccumulate in montane fauna of the Northeast (Bank et al. 2005, Rimmer et al. 2005, Evers and Duron 2008). In particular, Bicknell's thrush (*Catharus bicknelli*), a Nearctic-Neotropical migratory songbird has been shown to exhibit elevated Hg blood and feather concentrations among all age and sex classes across its breeding range (Rimmer et al. 2005). This rare, range-restricted habitat specialist of montane forests is an avian species of high continental conservation concern (Rimmer et al. 2001, Rich et al. 2004). As a higher trophic level consumer, primarily of arthropods, Bicknell's thrush is a potentially valuable bioindicator of montane forest ecosystem health. Understanding of Hg burdens in this species and in trophic compartments of its food web could contribute to species-specific and ecosystem-based conservation planning.

To elucidate trophic transfer of Hg in montane forests, we sampled leaf litter and biota at a long-term study site in the northeastern U.S. Our goals were to examine Hg concentrations and their variability among compartments of a terrestrial food chain during the montane summer.

Study Area and Methods

Field sampling

As part of long-term demographic research on montane forest bird populations in the northeastern U.S., we investigated the bioaccumulation and trophic transfer of Hg on Stratton Mountain (43° 05' N, 72° 55' W) in southern Vermont. From late May through late July in 2004-2007, we sampled discrete compartments in the terrestrial food web, using an established study site between 1075-1180 m elevation. To reflect a range of trophic levels, we sampled leaf litter, foliage, folivorous and carnivorous arthropods, a terrestrial salamander, an insectivorous passerine bird, and two carnivorous raptors. Salamanders and birds were sampled across a study area of c. 25 ha between 1075-1180 m elevation, while we collected leaf litter, foliage and arthropod samples at two sites 50 m apart at 1100 m elevation. One site was situated on the northwest-facing edge of a 30-m wide ski slope, the second 50 m to the west in mature, closed-canopy, fir-dominated forest.

Avian sampling was conducted on a near-daily basis throughout the entire sampling period in each summer, typically between dawn and mid-morning and from late afternoon through dusk, weather permitting. Sampling of litter and other biota was conducted opportunistically in dry and relatively warm weather, both to maximize logistic efficiency and to take advantage of peak activity patterns of exothermic arthropods. Because inclement weather is frequent at high elevations, we were unable to sample litter, foliage and arthropods as frequently as planned.

Care was taken to ensure that samples were not contaminated, especially those that required manual handling (e.g., litter and foliage). We generally used latex gloves during sampling, and we cleaned sampling utensils with distilled water and/or 5% nitric acid. All samples were frozen within 2 hours of collection.

Leaf litter: At both sampling sites, we collected leaf litter and organic soil samples of ~250 cm³ at a depth of 5-10 cm, using a small hand trowel that was wiped cleaned and rinsed with nitric acid and distilled water between individual sampling events. Care was taken not to include any portion of the underlying inorganic soil horizon. We collected three samples per site on 21 July 2004, 6 June 2006, and 15 June 2007; on 13 July 2007, we collected one sample at each site. Each sample was double-bagged in Ziploc® bags.

Foliage: We sampled whole leaves of three dominant deciduous tree species (paper birch [*Betula papyrifera* var. *cordifolia*], American mountain-ash [*Sorbus americana*], and pin cherry [*Prunus pennsylvanica*] and needles from the dominant conifer (balsam fir [*Abies balsamea*]), generally following methods outlined by Rea et al. (2002). Using hand pruners (wiped and cleaned with distilled water between each individual sampling event), we snipped the distal 20-30 cm of branch tips between 2-3 m height. On deciduous species, this yielded samples of 8-12 leaves, while coniferous branch tips generally contained 6-10 branchlets. We sampled and homogenized for analysis the previous 2-3 years of growth of fir needles on each branch, with the exception of three 2007 samples for which we separately clipped and analyzed needles grown in 2005, 2006 and 2007. For each species, we collected three replicates at both sampling sites on five dates: 21 July 2004, 8 and 28 June 2005, and 15 June

and 13 July 2007. All foliage samples were transferred immediately upon collection to Ziploc® plastic bags, double-bagged inside a second Ziploc® bag.

Arthropods: We sampled terrestrial and arboreal arthropods at both sites on six dates: 21 July 2004, 8 and 28 June 2005, 11 July 2006, and 15 June and 13 July 2007. We collected ground-dwelling arthropods (as well as a single sample of small gastropods) primarily through visual searches and gentle probing of the top leaf litter layer. Individuals were collected either with plastic forceps or a rubber aspirator, then transferred immediately to small plastic vials. For flying and arboreal arthropods, we used sweep nets, shook understory branches onto plastic protective sheets, or collected foliage-dwelling individuals with forceps or directly into storage vials. For small and medium-sized arthropods, we typically combined multiple individuals of a distinct taxon (e.g., ants, spiders, opiliones) into single storage vials. Prior to analysis, we identified each sample, whether consisting of a single or multiple individuals, to the lowest possible taxonomic level (usually order), using several references that included Borror and White (1970), Borror et al. (1981), and on-line sources such as BugGuide.Net (Iowa State University 2009). The very small masses of many individual arthropods (below detection limits for Hg determination) required lumping them by identifiable taxon for laboratory analyses. For all taxa for which we collected an adequate number of individuals for analysis, we archived at least one frozen reference sample.

Red-backed salamander: On 26 June 2006, we conducted active searches for red-backed salamanders (*Plethodon cinereus*) in forested habitat on Stratton Mountain by turning over objects (logs, rocks, etc) where salamanders often hide. All salamanders were captured by hand at 1000-1110 m elevation, placed in a moistened plastic bag, and measured (snout-to-vent, and total length). A tissue sample was collected from each individual by clipping a small (~ 5mm) portion of their tail tip using surgical scissors. Hg levels in salamander tail tips have been shown to provide a good correlation with whole body Hg burdens (D. Evers, personal comm.). Salamanders were then immediately released at their point of capture. All samples were immediately stored in Whirl-pak® sample bags and Ziploc® bags.

Birds: Using standard arrays of 6-m and 12-m, 36-mm mesh nylon mist nets throughout our study site, we captured individuals of our focal avian species, Bicknell's thrush, using both passive and broadcast elicitation methods. In the course of this netting, we incidentally captured individuals of two raptorial species, sharp-shinned hawk (*Accipiter striatus*) and northern saw-whet owl (*Aegolius acadicus*). Sharp-shinned hawks are predators on small passerines, and are known to regularly depredate Bicknell's thrush (Rimmer et al. 2001). Northern saw-whet owls primarily feed on small rodents, but they occasionally take passerine birds, including *Catharus* thrushes (Rasmussen et al. 2008) and are thus potential predators of Bicknell's Thrush. All captured birds were banded with uniquely numbered U.S. Fish and Wildlife Service aluminum leg bands, aged and sexed according to standard criteria (Pyle et al. 1997, Collier and Wallace 1988), and weighed prior to release. A series of morphometric measurements was also taken. From each individual of these three species, we collected a 30-50 µl blood sample from the cutaneous ulnar (brachial) vein in a 75 µl heparinized capillary tube, which was sealed on both ends with Crito-seal or Critocaps® and placed in a labeled glass 7 cc vacutainer. We sampled blood from all individuals upon their

initial captures in each year, and we selectively collected subsequent blood samples from individuals captured one week or more after collection of their previous sample.

Laboratory Analyses

All samples were shipped in liquid nitrogen or ice to Texas A&M University Trace Element Research Laboratory (TERL) for analysis by element-specific cold vapor atomic absorption. We measured only total Hg in each compartment, rather than bioavailable MeHg. Although the ratio of MeHg to total Hg may vary temporally and geographically within and among taxa (Cristol et al. 2008, Evers and Duron 2008), total Hg concentrations are commonly used to indicate exposure. All results from TERL are presented in units of parts per million (ppm or ug/g) as wet weight (ww) for avian blood and dry weight (dw) for other compartments.

Statistical Analyses

We examined all Hg data for normality. Non-normal data were log-transformed prior to analysis. Descriptive statistics, linear regressions and ANOVA analyses were calculated with JMP 6.03 (SAS Institute). We also used General Linear Models (GLMs) in SYSTAT 12 (Systat Software 2008) to examine within-season and between-year effects in Hg data for each sampled compartment, using different combinations of potential interactions as terms in the model.

Our previous work showed that Hg blood concentrations of both individual birds and the sampled population significantly declined during the breeding season (Rimmer et al. 2005). We therefore modeled blood Hg levels for all thrushes sampled in more than one year using a GLM, in which the interaction between year (2004-2007) and date were used as terms in the model. Because the interaction was significant ($F_{3,98} = 5.126, p = 0.002$), we examined each year separately and found 2004 to be significantly different from 2005-2007. A GLM excluding 2004 was not significant for the year term ($F_{2,72} = 0.141, p = 0.869$). We then examined blood Hg in a GLM using sex, age (second-year and after second-year), date, and an interaction between sex and date as terms, with data pooled for 2005-2007 and repeated for 2004 alone. We included the sex-date interaction because females can depurate Hg through egg laying (e.g., Thompson 1996, Monteiro and Furness 2001, Evers et al. 2005), which occurs primarily during the first three weeks in June (Rimmer et al. 2001).

There were significant and clear discontinuities in the overall declining trend of Bicknell's thrush blood Hg during the season with blood levels rising rapidly from day 113 through day 158 and falling fairly rapidly from day 160 through day 165. This period was followed by a steady and slower rate of decline through day 206. For the purposes of statistical analysis, the period prior to day 165 was classified as "Early" and day 165 and afterward as "Late" season. A one-sided t-test was used to evaluate differences in blood Hg levels between Early and Late season.

Classification of invertebrate foraging guilds

We classified arthropod samples in three broad guilds (Detrital, Canopy, Varied) according to the base of their known or suspected trophic web. Detrital arthropods include detritivorous organisms living primarily in the bark of dead and downed trees, as well as in

leaf litter and upper soil layers. Canopy dwellers include herbivorous taxa inhabiting most structural forest layers from the forest floor to the uppermost tree canopy. We considered Varied arthropods to be those that are primarily carnivorous and feed on either Canopy or Detrital organisms.

We further classified arthropods within each guild (primarily by order) as Carnivorous, Omnivorous, Herbivorous-Detrital, Herbivorous-Canopy, and Varied. Carnivores included arachnids (spiders and harvestmen) and blood-sucking Diptera. Herbivorous-Detrital included organisms that feed on plants and fungi in the detrital layer, while the Herbivorous-Canopy class included organisms that feed on above-ground plant structures (generally live plants). The Varied class captured organisms such as some Diptera that are typically considered omnivorous. For ants, our personal observations suggested that early season foraging occurs primarily in the detrital layer (i.e., Herbivorous-Detrital), while late season ants were more often seen feeding in the canopy (i.e., Herbivorous-Canopy). For other Hymenoptera (e.g., wasps, bees, sawflies), our field observations and literature searches suggested that all were Herbivorous-Canopy foragers.

Finally, we classified arthropods as early- or late-season based on the dates on which they were sampled in each year (1-27 June = early, 28 June – 21 July = late). Although little information exists on the dietary composition of Bicknell's thrush during its breeding period, the species is reported to be a "versatile" feeder in both microhabitat and behavior (Rimmer et al. 2001). Under the assumption that thrushes are opportunistic foragers, taking available prey in proportion to their abundance and ease of capture, we further assumed that our opportunistic sampling constituted a first-order proxy for foraging success, and that the within- and between-year composition of our arthropod samples reflected the prey items available to Bicknell's thrush. We therefore lumped all orders in our analyses of date and year effects on Hg concentrations, rather than comparing individual orders, which were subject to small sample sizes, high variance and disparities in total biomass or species composition among sampling events. This sample compositing should reflect the Hg signal in food items available to the focal species Bicknell's thrush.

Results

Overall, Hg concentrations showed a generally increasing trend by trophic level (Fig. 1, Appendix). Leaf litter deviated markedly from this pattern, with Hg levels elevated above those in any biotic compartment except sharp-shinned hawk, the top trophic level consumer in our samples (Fig. 1, Appendix). This is not unexpected as leaf litter has lost much of its original mass via decomposition while retaining most of its original Hg content in addition to binding additional Hg deposited via rain, snow, and canopy throughfall (Grigal 2003). Mean litter Hg concentrations differed among years ($F_{2,15} = 6.46, p = 0.01$), but not sampling location ($F_{1,15} = 0.02, p = 0.88$), being significantly higher in 2006 than in 2004 and 2007, which did not significantly differ. Although sampling dates were not uniform among years, they appeared to be no seasonal bioaccumulation of Hg in leaf litter, as evidenced by the relatively high mean value of 0.323 ± 0.09 SD on 6 June 2006 and the lack of significant

difference in mean values between samples collected on 13 June and 15 July 2007 (0.228 ± 0.102 SD ppm [$n = 6$] and 0.292 ± 0.031 SD [$n = 2$], respectively; $t = 0-1.836$, $df = 5.954$, $p = 0.12$).

Hg concentrations in balsam fir branches with aggregated needle samples (2-3 years of growth) were higher than those in the three deciduous tree species, both individually and combined (Fig. 1, Appendix). Single-year needle samples consistently increased in Hg content with age at an annual rate of 0.0142 ug/g ($R^2 = 0.94$, $p < 0.0001$). Seasonally, deciduous leaves showed significantly increasing Hg levels with date ($F_{1,50} = 4.92$, $p = 0.03$), accumulating 0.00001 ug/g per day during the growing season. Aggregated fir needles showed no between-year or within-season temporal trend, but Hg tissue concentrations were significantly higher in fir branches sampled in the forest interior than on the ski area edge ($F_{1,17} = 2.69$, $p = 0.001$).

Hg concentrations in arthropods ranged widely but were lowest in herbivorous insects, highest in predatory taxa (Araneae [spiders], Neuroptera [lacewings], and Opiliones [harvestmen]; Fig. 1, Appendix). The single gastropod sample showed relatively high Hg burdens, while the Diptera sample was elevated in part by an outlier value of 0.982 ppm in a single bloodsucking tabanid (deer fly). Among the three habitat-based foraging guilds, Detrital and Varied arthropods had significantly higher Hg levels than Canopy foragers (ANOVA: $F_{2,173} = 10.42$, $p < 0.0001$), but were not significantly different from each other. Carnivorous, Omnivorous and Herbivorous-Detrital foraging classes showed significantly higher Hg concentrations than Varied or Herbivorous-Canopy arthropods (ANOVA: $F_{4,171} = 32.8$, $p < 0.001$). Although not significantly different, Hg in Carnivorous arthropods was higher than in Omnivorous foragers, which in turn had higher Hg levels than Herbivorous-Detrital arthropods.

We found no significant year effect in Hg levels within any of the six arthropod orders (Araneae, Opiliones, Coleoptera, Diptera, Hymenoptera, and Lepidoptera [larvae]) that yielded sufficient sample sizes for analysis among years. However, combining all arthropods from each sampling event yielded a marginally significant effect of year, with 2004 significantly lower than 2005-2007 (Tukey-Kramer HSD $p=0.05$, ANOVA $p=0.06$). This year effect is interpreted as a combination of differences in Hg concentrations and differences in orders represented in the samples from each year. Due to the opportunistic nature of the sampling, the different representation of orders probably represents a differential food-item availability between 2004 and 2005-2007. No within-season effects of date were found for either individual orders or all arthropods combined in 2005 or 2007, the two years in which early- and late-season sampling was conducted.

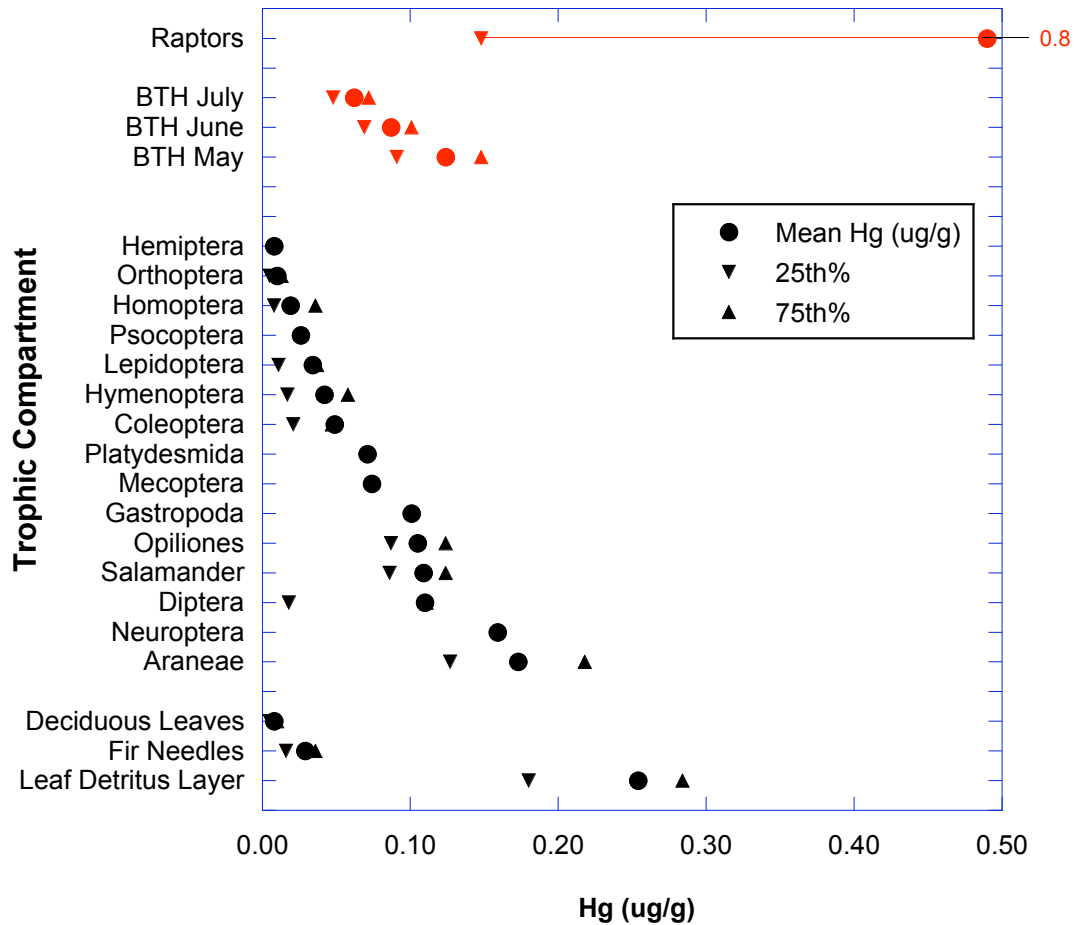


Figure 1. Mean, 25th, and 75th percentile Hg concentrations for leaf litter and biota sampled on Stratton Mountain, Vermont in 2004-2007.

Among the three foraging guilds, we found a significant temporal shift in the proportions of arthropods sampled, from Detrital (63% of total) dominant in early season samples to a more even distribution between Detrital (36%), Varied (33%), and Canopy (32%) foragers in late season samples ($\chi^2 = 15.16$, $df = 2$, $p = 0.0005$). Similarly, foraging subclasses showed a shift between early and late season samples, with Carnivorous (19% early, 14% late) and Herbivorous-Detrital arthropods (7% early, 5% late) declining in proportional abundance and Herbivorous-Canopy invertebrates (6% early, 16% late) increasing ($\chi^2 = 1.99$, $df = 4$, $p = 0.018$).

Among vertebrates, Hg burdens in red-backed salamanders were comparable to those in several invertebrate groups on which they reportedly prey, including Opiliones, Gastropoda, and Diptera (Fig 1; Appendix). For the 151 blood samples from adult Bicknell's thrushes, a marked year effect was evident, with Hg concentrations in 2004 (0.071 ± 0.006 ug/g) significantly lower than in 2005-2007 (0.093 ± 0.004 ug/g; ANOVA $p=0.0002$, Tukey-Kramer HSD $p=0.05$), which did not differ. Bicknell's thrush blood Hg concentrations showed no effects of sex or age classes in 2004 or 2005-2007, nor any interaction between sex and date. However, for the sample population, blood Hg concentrations showed a significantly decreasing linear trend with date across all years ($r^2=0.36$, $p<0.0001$, $n=150$). Although statistically significant as a linear trend over the season, the temporal pattern of Hg blood concentration was actually a rapid increase followed by a rapid decrease, followed by a more steady decline through the end of the season (Figure 2). Early season (prior to day 165) blood levels were significantly different from late season levels ($p<0.00001$, one-sided t-test). Blood Hg concentrations in the two predatory bird species, northern saw-whet owl and sharp-shinned hawk, were elevated above those of Bicknell's thrush, markedly so in the latter species (Fig. 1, Appendix).

Discussion

Although specific trophic relationships within the montane forest food web are not well documented, the Hg concentrations we report here appear to reflect biomagnification from lower to higher trophic levels. Although Hg levels within each compartment or biotic group did not invariably conform to known or suspected patterns of trophic transfer, the general progression was consistent with expectations: food web base (foliage < litter), herbivorous arthropods < detritivorous arthropods < predatory arthropods < insectivorous vertebrates < carnivorous vertebrates (Figure 1, Appendix). The congruence of year effects in leaf litter, arthropods and Bicknell's thrush blood further suggests the existence of dietary linkages across trophic compartments at this montane forest site.

Foliage and leaf litter

Our results conform to those of other studies that show high leaf litter Hg concentrations relative to those in live foliage (e.g., up to 60% greater), due to the accumulation of Hg over time, and the concentration of Hg relative to nutrients that leach and are translocated out of foliage during senescence (Lindberg 1996; Rea *et al.* 1996, 2002; Tyler, 2005). Hg foliar concentrations in the three deciduous species on Stratton were slightly higher than those reported from five hardwoods species at mid-elevations in north-central Vermont (Rea *et al.* 2002). Aggregated balsam fir needle Hg concentrations were higher than those of deciduous leaves; current-year needle Hg levels were almost identical, while those of 2- and 3-year old needles progressively increased and were higher than deciduous leaf Hg levels. This was an expected result, because our aggregated fir needle samples were composed of 3 years of growth, and thus accumulated Hg sequestration, while deciduous leaves reflected Hg uptake only since leaf-out 0.5-1.5 months prior to sampling (Grigal 2003).

Softwood-dominated leaf litter at Stratton Mountain showed relatively high Hg concentrations compared to those of most biotic compartments. Hg in litter is derived both

from litterfall, rain, snow, and throughfall (Grigal 2003). Litter Hg concentrations reflect deposition, retention and release, but these mechanisms and their relationship to bioavailability of Hg in montane forest litter need further investigation. Demers et al. (2007) found that litter Hg accumulated during the growing season. Hall and St. Louis (2004) also reported that both MeHg and total Hg concentrations in softwood-dominated litterfall of Canadian boreal forests increased over time (800 days).

Arthropods

Although few published data exist on Hg concentrations of terrestrial arthropods, our data conform to those of others in which primary consumers (herbivores and detritivores) show lower Hg levels than secondary consumers (predatory species). Zheng et al (2008) studied three arthropods in a Hg-contaminated grassland of China and found Hg concentrations of 0.043 and 0.037 ug/g in two primary consumers (*Locusta* sp. and *Acrida* sp.) and “higher” (no value given) Hg concentrations in a secondary consumer, *Paratenodera sinensis*. Cristol et al (2008) sampled orthopterans, lepidopterans, and spiders in Virginia upland habitats adjacent to Hg-contaminated rivers and at uncontaminated reference sites. Mean Hg concentrations of all three orders were “negligible” at reference sites, and lower than values we obtained on Stratton Mountain, while Hg levels at contaminated sites were dramatically higher (spiders = 1.24 ± 1.47 ug/g, lepidopterans = 0.38 ± 2.08 ug/g, orthopterans = 0.31 ± 1.22 ug/g; Cristol et al. [2008]). In the Catskill region of New York, preliminary data, based on small sample sizes, suggested spiders have Hg levels 2-3 times higher than those of other arthropods (Evers and Duron 2008).

Red-backed salamander

Although the diet of red-backed salamanders in montane forests is not well known, Burton (1976) found that the species preyed primarily on mites, spiders, snails, and numerous insect families at the Hubbard Brook Experimental Forest in New Hampshire. The relatively high levels of Hg in our salamander samples suggest that they are feeding at a high trophic level within the invertebrate community, or that their preferred prey accumulate relatively high amounts of Hg due to micro-habitat preferences, soil strata, or other variables. Red-backed salamanders live and forage in moist soils, often near stream edges where total sediment Hg and MeHg levels are highest (Morel et al. 1998). Although our sampling effort was limited, we found salamanders only along stream edges on our study site. Since they rarely move away from these moist micro-habitats, their prey may consist of a disproportionate number of invertebrates found only along stream edges. Salamander densities in the montane forest appear to be quite low, possibly due to predominantly shallow, acidic soils. These soils have been shown to disrupt sodium balance in red-backed salamanders, which are rarely found on soils with a pH ≤ 3.7 (Frisbie and Wyman 1991).

Birds

Blood Hg concentrations in Bicknell’s thrush (breeding season average 0.088 ± 0.003 ug/g) were lower than previously reported in this species on Stratton Mountain (0.12 ± 0.04 ug/g; Rimmer et al. 2005). There was an initial increase in blood Hg level from 0.1 ug/g to 0.13 ug/g during the first weeks on the breeding ground (days 113-158, Figure 2). Blood Hg levels then declined rapidly from days 160-165 after which a more steady but lower rate of decline persisted through the last samples on day 206 (Figure 2). Although data on dietary

composition of this species are scant, owing to the difficulty of direct observation and sampling known food items, our data strongly suggest that a seasonal shift in diet accounts for the initial increase followed by declining Hg blood levels during June and July.

As a long-distance migrant, Bicknell's thrush spends 7-8 months per year away from its northeastern U.S. breeding sites (Rimmer et al. 2001). Previous research has shown that blood Hg concentrations of thrushes sampled in January and February on their Caribbean winter grounds averaged 2-3 times higher than in birds sampled on breeding sites (Rimmer et al. 2005). An exponential decay model was constructed to estimate the carry-over effects of Hg burdens obtained on the wintering grounds on Hg observations during the breeding season. Although there appears to be no information on the half-life of MeHg or total Hg in passerine blood, published data exist for non-molting adults of three primarily aquatic birds. The half-life of blood MeHg is 31.5-63 days for great skua (*Catharacta skua*; Bearhop et al. 2000), 40-60 days for Cory's shearwater (*Calonectris diomedea*; Monteiro and Furness 2001), and 74 days for mallard (*Anas platyrhynchos*; Heinz and Hoffman 2004). Because Bicknell's thrushes are much smaller than these three species, with higher basal metabolism and presumably lower absolute rates of Hg ingestion, we conservatively estimate 30 days as a probable half-life of MeHg in Bicknell's thrush blood. Furthermore, due to the higher than normal metabolic demands of migration, the loss of Hg obtained on the wintering grounds is likely further accelerated during transit from wintering to breeding grounds. Nearly all individuals depart their wintering sites for northward migration before 1 May and arrive at Vermont breeding sites before 1 June (authors' unpubl. data). Using parameters of blood Hg at time of wintering ground departure equal to 2.5 times the average breeding ground concentration, a 30-day wintering-breeding ground transit time, and a 30-day half-life, an exponential decay model successfully predicted the initial breeding-ground blood Hg observations (0.101 ppm, n=4 on day 113; Figure 2).

There was a significant difference ($P < 0.00001$, 1-sided t-test) between Early and Late season blood Hg concentrations in Bicknell's thrush. Birds return to their breeding grounds during the very early stages of leaf-out and prior to the emergence of most folivorous arthropods. At this time, spiders are relatively numerous (pers. obs.), and we suspect that this group constitutes a significant portion of the species' diet. As a primarily ground-foraging species, Bicknell's thrush likely feed disproportionately on spiders, harvestmen, and ants early in the growing season. Snails may also be taken by females to supplement calcium mobilization for egg production. As new coniferous and deciduous foliage emerges during June, Bicknell's thrush likely shift to a higher proportion of folivorous arthropods, such as adult and larval lepidopterans, hymenopterans (sawflies and ichneumons), and hemipterans. The change in food item availability and lower Hg burdens in late-season potential prey items likely account for the drop in thrush blood concentrations between early and late summer on the breeding grounds (Figures 2 and 3).

Arthropod data corroborate an apparent seasonal diet shift by Bicknell's thrush along the Hg contamination spectrum of potential prey items (Figure 3). Arthropods showed declines in abundance of Carnivorous and Herbivorous-Detrital classes (those highest in Hg) between early and late season samples, and a preponderance of lower trophic order organisms (with lower Hg concentrations) later in the season (Figure 3).

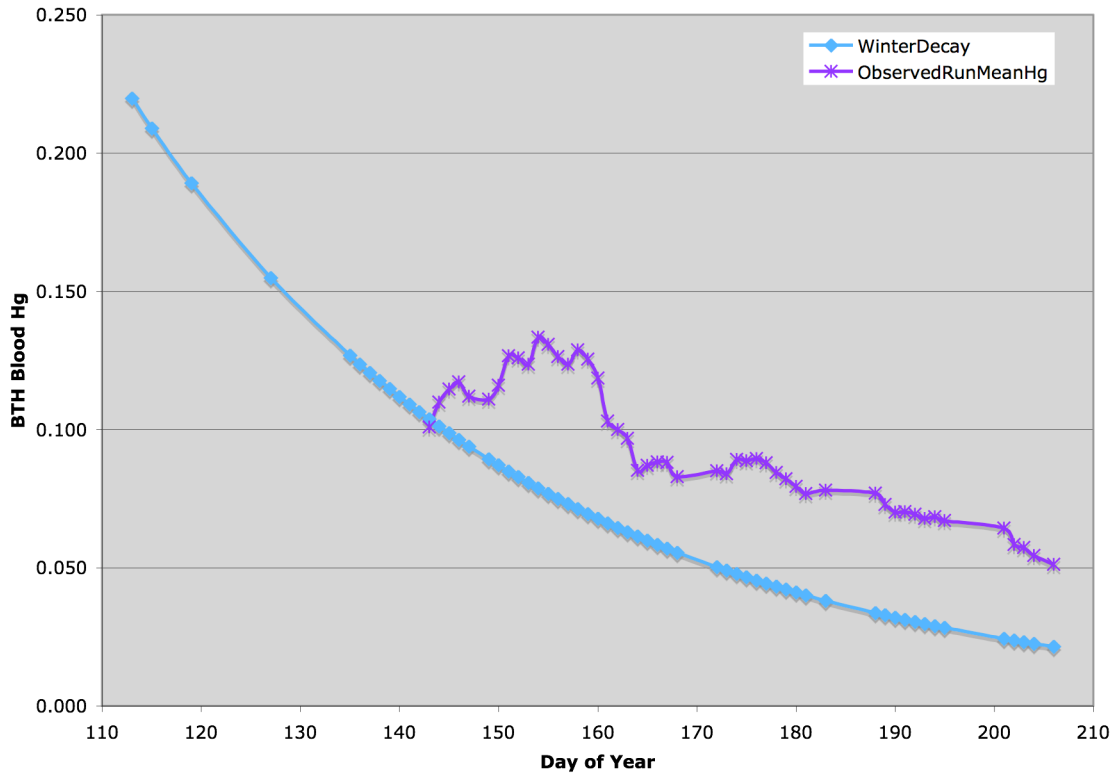
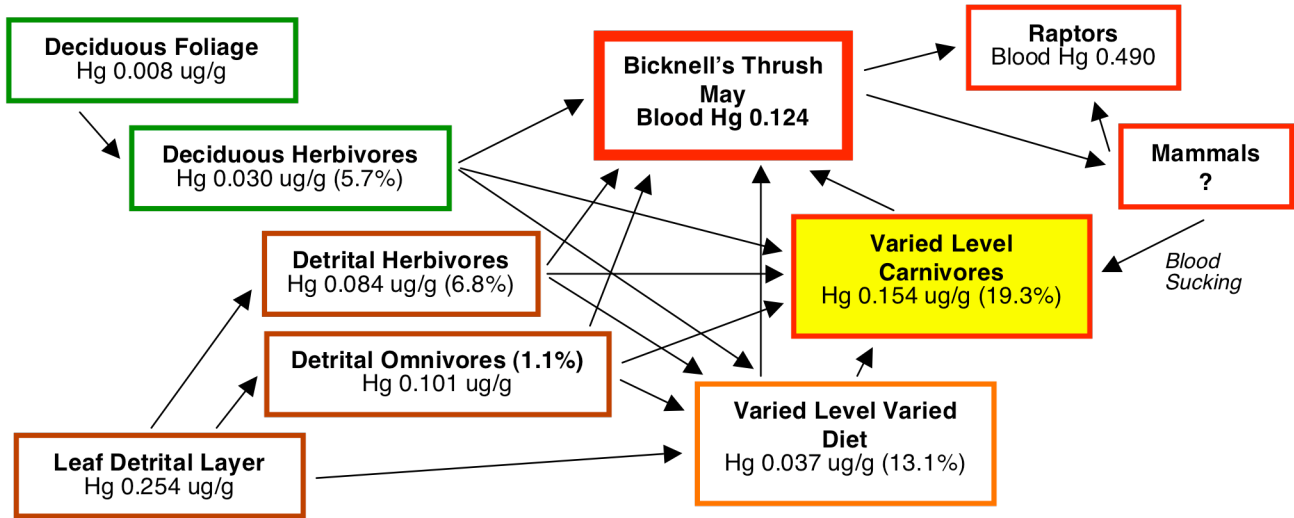


Figure 2. Exponential decay model (light blue) of the dissipation of wintering ground Hg burden and observations (purple) of Hg blood concentrations on the breeding grounds in Bicknell’s thrush. Due to the fluctuations in number of birds captured and sampled daily, the observed blood levels are presented as the 10-day moving average.

The Hg level in Bicknell’s thrush blood at the end of the breeding season is 1.6 times the level of residual wintering-ground Hg burden predicted by the exponential decay model. This suggests that Hg in the breeding ground diet provides a significant component of the total Hg burden of the birds during the breeding season. Still, the Hg burden carried from the wintering grounds is substantial. Further study is warranted into sources of Hg in the winter diet of Bicknell’s thrush and other co-occurring migratory birds in the same wintering areas.

The two predatory bird species, sharp-shinned hawk and northern saw-whet owl, showed elevated blood Hg from Bicknell’s thrush and red-backed salamanders (Fig. 1, Appendix). Reflecting its exclusive diet of small songbirds, including Bicknell’s thrush, sharp-shinned hawk blood Hg was expected to be higher, and was likely accounted for by trophic biomagnification. The order of magnitude increase above Bicknell’s thrush was surprising; however, variance was large. Northern saw-whet owls showed Hg blood concentrations that likely reflected this species’ dietary specialization on small mammals, most of which feed on seeds and vegetation. In contrast to Bicknell’s thrush, one individual sharp-shinned hawk captured on 5 June and again on 13 July 2006 had nearly identical blood Hg on the two dates, 0.967 and 0.975 ppm, respectively. Hawks are unlikely to switch prey items within a summer, and this finding reinforces the likelihood that seasonal declines in thrush blood Hg signal a dietary shift from carnivorous to herbivorous arthropods.

Early Season Food Web



Late Season Food Web

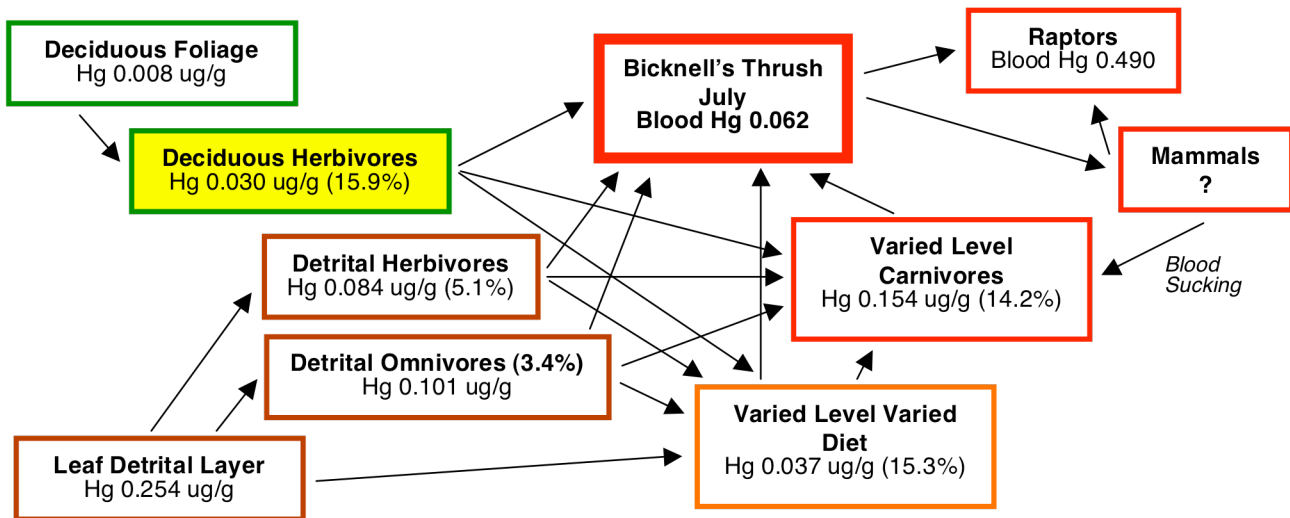


Figure 3. Shifts in food web structure from early to late summer in a montane ecosystem. The relative abundance of different arthropod feeding guilds (as percents in parentheses) and each compartment's mean Hg level are indicated. A detrital-based food web dominates the early season, while a canopy-based food web increases in importance during the late summer season. Bicknell's Thrush (red) is the focal species in this study.

Year effects in Hg concentrations

Significantly lower Hg concentrations in three sampled compartments (litter, arthropods, Bicknell's thrush) during 2004 versus 2005-2007 provide compelling evidence for dietary linkages and trophic transfer in the terrestrial montane forest community. Bioavailability of Hg, as reflected through uptake by Bicknell's thrush, has been shown to correlate to modeled atmospheric deposition patterns (Rimmer et al. 2005). Our results further corroborate this link, in that nearby (Underhill, VT) Hg deposition data were relatively lower from 1999-2003 (mean 9.3 ug/m²/year) and relatively higher from 2004-2007 (mean 11.6 ug/m²/year) (E. Miller, manuscript in preparation). As the early season food items are dependent on the detrital-based food web, there is likely at least a 1-year lag between deposition changes and changes in the Hg burdens of the detrital-based food web. This shift from a lower to higher mercury deposition regime could have accounted for the lower Hg levels on Stratton Mountain in 2004 and relatively higher levels from 2005-2007.

Summary – Overall, Hg concentrations showed a pattern of biomagnification at successive trophic levels in the montane forest food web (Fig. 1, Appendix 1). The within-season changes in Bicknell's thrush blood Hg levels were consistent with a diet switch from more Hg-rich detrital-based prey abundant in the early summer food-web to prey relatively lower in Hg content that were more abundant in the foliage-based food web of mid to late summer (Figures 2 and 3). The significant and consistent year effect among the trophic compartments of litter, arthropods and thrush blood strongly suggests that avian dietary differences are reflected in blood concentrations. These observations provide clear evidence that Hg bioaccumulates and biomagnifies in the montane forest biotic community.

Acknowledgments

We gratefully acknowledge funding support from the U.S. Environmental Protection Agency through the University of Vermont for this study. Our ongoing avian research on Stratton Mountain was supported by the Stratton Mountain Resort, Thomas Marshall Foundation, Vermont Monitoring Cooperative, and friends of the Vermont Center for Ecostudies. We thank the many dedicated field biologists who assisted with collection of these data under frequently difficult conditions. We are indebted to staff of the Texas A&M Trace Element Research Laboratory for conducting all aspects of the mercury analyses. Jason Townsend provided constructive reviews of an early draft.

Literature Cited

- Bank, M. S., C. S. Loftin, and R. E. Jung. 2005. Mercury bioaccumulation in northern two-lined salamanders from streams in the northeastern United States. *Ecotoxicology* 14:181–191.
- Bank, M. S., J. Crocker, B. Connery, and A. Amirbahman. 2007. Mercury bioaccumulation in green frog (*Rana clamitans*) and bullfrog (*Rana catesbeiana*) tadpoles from Acadia National Park, Maine, USA. *Environmental Toxicology and Chemistry* 26:118-125.
- Bennett, R. S., J. B. French, Jr., R. Rossmann, and R. Haebler. 2009. Dietary toxicity and tissue accumulation of methylmercury in American kestrels. *Arch. Environ Contam Toxicol* 56:149-156.
- Borror, D. J. and R. E. White. 1970. A field guide to the insects of America north of Mexico. Houghton Mifflin, Boston, MA.
- Borror, A. J., D. M. De Long, and C. A. Triplehorn. 1981. An introduction to the study of insects. Saunders College Publishing, Philadelphia, PA.
- Burton, T.M. 1976. An analysis of the feeding ecology of salamanders of the Hubbard Brook Experimental Forest, New Hampshire. *Journal of Herpetology* 10:187-204.
- Chen, C. Y., R. S. Stemberger, N. C. Kamman, B. M. Mayes, and C. L. Folt. 2005. Patterns of Hg bioaccumulation and transfer in aquatic food webs across multi-lake studies in the northeast US. *Ecotoxicology* 14:135-147.
- Collier, B. and G. E. Wallace. 1988. Aging *Catharus* thrushes by rectrix shape. *Journal of Field Ornithology* 60: 230–240.
- Demers, J. D., C. T. Driscoll, T. J. Fahey, and J. B. Yavitt. 2007. Mercury cycling in litter and soil in different forest types in the Adirondack region, New York, USA. *Ecological Applications* 17:1341-1351.
- Driscoll, C. T., Y-J. Han, C. Y. Chen, D. C. Evers, K. F. Lambert, T. M. Holsen, N. C. Kamman, and R. K. Munson. 2007. Mercury contamination in forest and freshwater ecosystems in the northeastern United States. *BioScience* 57:17-28.
- Ericksen, J. A., M. S. Gustin, D. E. Schorran, D. W. Johnson, S. E. Lindberg, and J. S. Coleman. 2003. Accumulation of atmospheric mercury in forest foliage. *Atmospheric Environment* 37:1613-1622.
- Evers, D. C. and M. Duron. 2008. Assessing the availability of methylmercury in terrestrial breeding birds of New York and Pennsylvania, 2005-2006. BRI Report 2008-15.
- Evers D.C., O. P. Lane, L. Savoy, and W. Goodale. 2004. Assessing the impacts of methylmercury on piscivorous wildlife using a wildlife criterion value based on the Common Loon, 1998–2003. Gorham (ME): Maine Department of Environmental Protection, BioDiversity Research Institute. BRI Report 2004-05.
- Evers D. C., N. M. Burgess, L. Champoux, B. Hoskins, A. Major, W. M. Goodale, R. J. Taylor, R. Poppenga, and T. Daigle. 2005. Patterns and interpretation of mercury exposure in freshwater avian communities in northeastern North America. *Ecotoxicology* 14: 193–221.
- Evers, D. C., L. J. Savoy, C. R. DeSorbo, D. E. Yates, W. Hanson, K. M. Taylor, L. S. Siegel, J. H. Cooley, Jr., M. S. Bank, A. Major, K. Munney, B. Mower, H. S. Vogel, N. Schoch, M. Pokras, M. W. Goodale, and J. Fair. 2008. Adverse effects from environmental mercury loads on breeding common loons. *Ecotoxicology* 17:69-81.

- Frisbie, M. P. and R. L. Wyman. 1991. The effects of soil pH on sodium balance in the red-backed salamander and three other terrestrial salamanders. *Physiological Zoology* 64:1050-1068.
- Hall, B. D. and V. L. St. Louis. 2004. Methylmercury and total mercury in plant litter decomposing in upland forests and flooded landscapes. *Environmental Science and Technology* 38:5010-5021.
- Hammerschmidt, C. R. and W. F. Fitzgerald. 2005. Methylmercury in mosquitoes related to atmospheric mercury deposition and contamination. *Environmental Science and Technology* 39:3034-3039.
- Iowa State University. 2009. BugGuide.Net. Iowa State University Entomology Department, Ames, IA. <http://www.bugguide.net>
- Lindberg, S. E. 1996. Forests and the global biogeochemical cycle of mercury: the importance of understanding air/vegetation exchange processes. Pp. 359-380 in Baeyens, W., R. Ebinghaus, and O. Vasiliev (Eds.), *Global and regional mercury cycles: sources, fluxes, and mass balances*. Kluwer Academic Publishers, Dordrecht, Netherlands.
- Miller, E. K., A. VanArsdale, J. G. Keeler, A. Chalmers, L. Poissant, N. C. Kamman, and R. Brulotte. 2005. Estimation and mapping of wet and dry mercury deposition across northeastern North America. *Ecotoxicology* 14:53-70.
- Monteiro, L. R. and L. W. Furness. 2001. Kinetics, dose-response, and excretion of methylmercury in free-living adult Cory's shearwaters. *Environmental Science and Technology* 35:739-746.
- Morel, F. M. M., A. M. L. Kraepiel, and M. Amyot. 1998. The chemical cycle and bioaccumulation of mercury. *Ann. Rev. Ecol. Syst.* 29, 543–66.
- Rasmussen, J. L., S. G. Sealy and R. J. Cannings. 2008. Northern Saw-whet Owl (*Aegolius acadicus*). *The Birds of North America Online* (A. Poole, Ed.). Ithaca: Cornell Lab of Ornithology; Retrieved from the Birds of North America Online: <http://www.bna.birds.cornell.edu/bna/species/042>
- Rea, A. W., S. E. Lindberg, T. Scherbatskoy, and G. J. Keeler. 2002. Mercury accumulation in foliage over time in two northern mixed hardwood forests. *Water Air and Soil Pollution* 133:49-67.
- Rich, T. D., C. J. Beardmore, H. Berlanga, P. J. Blancher, M. S. W. Bradstreet, G. S. Butcher, D. W. Demarest, E. H. Dunn, W. C. Hunter, E. F. Iñigo-Elias, J. A. Kennedy, A. M. Martell, A. O. Panjabi, D. N. Pashley, K. V. Rosenberg, C. M. Rustay, J. S. Wendt, and T. C. Will. 2004. *Partners in Flight North American Landbird Conservation Plan*. Cornell Lab of Ornithology. Ithaca, NY.
- Rimmer, C.C., K.P. McFarland, W.G. Ellison, and J.E. Goetz. 2001. Bicknell's Thrush (*Catharus bicknelli*). In *The Birds of North America*, No. 592 (A. Poole & F. Gill, eds.). The Birds of North America, Inc., Philadelphia, PA.
- Rimmer, C.C., K.P. McFarland, D.C. Evers, E.K. Miller, Y. Aubry, D. Busby, and R.J. Taylor. 2005. Mercury concentrations in Bicknell's Thrush and other insectivorous passerines in montane forests of northeastern North America. *Ecotoxicology* 14:223-240.
- Scheuhammer, A.M., Meyer, M.W., Sandheinrich, M.B. and Murray, M.W. 2007. Effects of environmental methylmercury on the health of wild birds, mammals, and fish. *Ambio* 36:12-19.
- Sheehan, K. D., I. J. Fernandez, J. S. Kahl, and A. Amirbahman. 2006. Litterfall mercury in two forested watersheds at Acadia National Park, Maine, USA. *Water, Air, and Soil Pollution* 170: 249–265.

- Systat Software, Inc. 2008. SYSTAT 12. Systat Software, Inc., Chicago, IL.
<http://www.systat.com/SystatProducts.aspx>.
- Wolfe, M., Schwarzbach, F.S. and Sulaiman, R.A. 1998. Effects of mercury on wildlife: a comprehensive review. *Environmental Toxicology and Chemistry* 17: 146-60.
- Yates, D. E., D.T. Mayack, K. Munney, D. C. Evers, A. Major, T. Kaur, and R. J. Taylor. 2005. Mercury levels in mink (*Mustela vison*) and river otter (*Lontra canadensis*) from northeastern North America. *Ecotoxicology* 14:263-274.
- Zheng, D.-M., Q.-C. Wang, Z.-S. Zhang, N. Zheng, and X.-W. Zhang. 2008. Bioaccumulation of total and methyl mercury by arthropods. *Bull. Environ. Contam. Toxicol.* 81:95-100.

Appendix.

Means, standard deviations, and ranges of Hg concentrations (ug/g) in leaf litter and biotic compartments sampled on Stratton Mountain, Vermont in June and July of 2004-2007.

| Compartment | Mean | SD | Range | N |
|--|-------------|-----------|--------------|----------|
| Leaf litter (all years) | 0.254 | 0.091 | 0.141-0.492 | 20 |
| Leaf litter (2004) | 0.199 | 0.04 | 0.141-0.259 | 6 |
| Leaf litter (2006) | 0.323 | 0.09 | 0.254-0.492 | 6 |
| Leaf litter (2007) | 0.217 | 0.058 | 0.149-0.314 | 7 |
| Deciduous leaves (all species) | 0.009 | 0.004 | 0.003-0.02 | 44 |
| Paper birch | 0.007 | 0.003 | 0.002-0.13 | 25 |
| Mountain ash | 0.009 | 0.005 | 0.005-0.22 | 26 |
| Pin cherry | 0.007 | 0.003 | 0.003-0.01 | 6 |
| Balsam fir branches | 0.029 | 0.014 | 0.009-0.058 | 22 |
| Balsam fir needles (new) | 0.006 | 0.001 | 0.005-0.008 | 4 |
| Balsam fir needles (1-year) | 0.019 | 0.002 | 0.018-0.021 | 4 |
| Balsam fir needles (2-year) | 0.035 | 0.02 | 0.034-0.037 | 3 |
| Araneae (spiders) | 0.173 | 0.081 | 0.02-0.334 | 19 |
| Coleoptera (beetles) | 0.048 | 0.067 | 0.004-0.391 | 36 |
| Diptera (flies) | 0.11 | 0.17 | 0.002-0.984 | 50 |
| Gastropoda (snails) | 0.101 | | | 1 |
| Hemiptera (true bugs) | 0.008 | 0.002 | 0.006-0.009 | 2 |
| Heteroptera (assassin bugs) | 0.016 | 0.17 | 0.004-0.04 | 4 |
| Hymenoptera (ants, wasps, sawflies) | 0.04 | 0.033 | 0.004-0.12 | 20 |
| Lepidoptera (adult) | 0.05 | 0.07 | 0.006-0.13 | 3 |
| Lepidoptera (larvae) | 0.29 | 0.28 | 0.007-0.108 | 13 |
| Mecoptera (scorpionflies) | 0.074 | | | 1 |
| Neuroptera (lacewings) | 0.159 | | | 1 |
| Opiliones (harvestmen) | 0.105 | 0.029 | 0.056-0.142 | 7 |
| Orthoptera (grasshoppers) | 0.01 | 0.005 | 0.003-0.014 | 4 |
| Platydesmida (millipede) | 0.071 | | | 1 |
| Psocoptera (barkflies) | 0.026 | | | 1 |
| Red-backed salamander | 0.11 | 0.02 | 0.085-0.131 | 4 |
| Bicknell's thrush (early June 2004) | 0.091 | 0.04 | 0.051-0.199 | 13 |
| Bicknell's thrush (late June 2004) | 0.063 | 0.022 | 0.035-0.107 | 12 |
| Bicknell's thrush (early July 2004) | 0.072 | 0.028 | 0.055-0.105 | 3 |
| Bicknell's thrush (late July 2004) | 0.03 | 0.012 | 0.014-0.046 | 12 |
| Bicknell's thrush (May 2005-07) | 0.123 | 0.047 | 0.05-0.267 | 35 |
| Bicknell's thrush (early June 2005-07) | 0.098 | 0.031 | 0.046-0.201 | 37 |
| Bicknell's thrush (late June 2005-07) | 0.083 | 0.022 | 0.046-0.132 | 30 |
| Bicknell's thrush (early July 2005-07) | 0.065 | 0.014 | 0.046-0.095 | 25 |
| Northern saw-whet owl | 0.164 | 0.059 | 0.107-0.251 | 6 |
| Sharp-shinned hawk | 0.989 | 0.501 | 0.393-1.62 | 4 |

Atmospheric Mercury in Vermont and New England: Measurement of deposition, surface exchanges and assimilation in terrestrial ecosystems

Final Project Report – Additional Project Activities – 1/16/2009

PI: Melody Brown Burkins, University of Vermont (UVM)
Co-PIs: Eric K. Miller¹, Ecosystems Research Group, Ltd.; Gerald J. Keeler, University of Michigan; and Jamie Shanley, US Geological Survey
Collaborators: Sean Lawson, VTANR-VMC; Jen Jenkins, Mim Pendelton, Carl Waite and Alan Strong, UVM; Rich Poirot, VTANR-APCD; Alan VanArsdale, USEPA; Mark Cohen, NOAA; Chris Rimmer, Kent McFarland, and Steve Faccio, Vermont Center for Ecostudies; and Robert J. Taylor, Texas A&M.
Project Officer: Eric Hall, USEPA

Coordination with national, regional, and state mercury research

The project personnel successfully coordinated with other mercury research efforts at local, regional and national levels. We used the new Hg information from the Underhill site and this project to estimate mercury deposition not only to the forested watersheds of Vermont, but also specifically to Lake Champlain in collaboration with researchers supported by the NOAA funded, Lake Champlain Research Consortium. More broadly, Drs. Miller and Keeler participated in the Northeast Mercury Research Group, a regional research group funded by the USDA Forest service (www.briloon.org/mercury). The three-way, west-east (WA-VT), precipitation mercury collector intercomparison was a collaboration designed to inform the national MDN program on potential improvements to collector design as well as to facilitate Underhill's transition from the UMAQL to the MDN system.

Observations and analyses of mercury concentrations and fluxes at Underhill are providing benefits to several mercury research groups working to model emissions-transport-deposition cycles at regional, national and global scales. The results of our trend analysis (no trend detected) for wet deposition and our source identification efforts for wet and dry deposition have informed state, regional, national, and international air-quality planning bodies about the identity of sources contributing mercury to the biologically sensitive New England region. Our pioneering assessment of mercury in a terrestrial food-web has highlighted the need for expanded consideration of the risks posed by atmospheric mercury deposition to terrestrial environments.

Dr. Miller participated in the technical working group designing protocols and operations standards for the proposed MTN (Mercury Trends Network), a new mercury dry deposition network being established by NADP. Dr. Miller provided detailed information on our operating procedures and data management process for use in developing the network SOP. Underhill served as demonstration site for the network and we hosted a field trip for NADP personnel to observe our operations in 2007. The Underhill site was one of the initial four sites funded by EPA-OAR-CAMD for start-up of the network in January of 2008.

¹ Corresponding author for the final project report. Email: ekmiller@ecoystems-research.com Voice: 802-649-5550

Scientific communication and public outreach

In addition to the research coordination activities described above project personnel made numerous presentations about project activities and results at regional and national meetings. Dr. Miller produced a public-outreach overview document describing mercury research activities at Underhill in conjunction with the VMC. Interviews were granted to print and radio media to convey project results to the public. Several peer-reviewed scientific publications were prepared, accepted and published that made use of project data. Additional manuscripts are currently being prepared for submission by the project team. The final results of the project (which are the subjects of these manuscripts) will be presented at national meetings and communicated to the air-quality management community.

Meetings, Public Presentations, and Publications (chronological)

- Dr. Keeler presented results from a coordinated, long-term event wet-deposition study (funding sources including NESCAUM and NOAA) at the October 2004 Vermont Monitoring Cooperative Research Symposium in Burlington, VT.
- Dr. Miller presented preliminary results from the air-concentration and flux measurement activities at the October 2004 Vermont Monitoring Cooperative Research Symposium in Burlington, VT.
- Dr. Miller presented regional mercury deposition estimates based, in part, on the Underhill observation record at the 2004 NADP/MDN meeting in Halifax, Nova Scotia.
- Dr. Miller attended the 2005 NADP meetings and presented preliminary results from the 2005 mercury speciation studies, and 2004 vapor phase exchange measurements. He also described the 3-way precipitation Hg collector comparison study, but no preliminary results were presented at that time.
- The precipitation event mercury record was analyzed and published as part of three different manuscripts:

Keeler, G.J., Gratz, L.E, and Al-Whali, K. (2005) Long-term Atmospheric Mercury Wet Deposition at Underhill, Vermont. *Ecotoxicology* 14, 71-83.

Miller, E.K., VanArsdale, A., Keeler, G.J., Chalmers, A., Poissant, L., Kamman, N., and Brulotte, R. (2005) Estimation and Mapping of Wet and Dry Mercury Deposition across Northeastern North America. *Ecotoxicology* 14, 53-70.

VanArsdale, A., Weiss, J., Keeler, G.J., Miller, E.K., Boulet, G., Brulotte, R., Poissant, L., and Puckett, K. (2005) Patterns of Mercury Deposition in Northeastern North America (1996-2002). *Ecotoxicology* 14, 37-52.

- Initial Bicknell's thrush blood mercury data were analyzed and published in:
Rimmer, C.C., McFarland, K.P., Evers, D.C., Miller, E.K., Aubry, Y., Busby, D., and Taylor, R.J. (2005) Mercury Levels in Bicknell's Thrush and Other Insectivorous Passerines in Montane Forests of Northeastern North America. *Ecotoxicology* 14, 223-240.

- Dr. Miller gave an informal presentation to the NESCAUM/EPA Region 1 Mercury working group at the NESCAUM offices in Boston on January 11, 2006. He presented preliminary results from the 2005 mercury speciation studies, and the 3-way precipitation Hg collector comparison study.
- Drs. Shanley, Miller, and Keeler were coauthors of a study published in *Environmental Science and Technology*.

Gao, N., N.G. Armatas, J.B. Shanley, N.C. Kamman, E.K. Miller, G.J. Keeler, T. Scherbatskoy, T.M. Holsen, T. Young, L. McIlroy, S. Drake, B. Olsen, and C. Cady. (2006) A mass balance assessment for mercury in Lake Champlain. *Environ. Sci. and Technol.* 40: 82-89.

This study used data from the Underhill site and other sites in the region to estimate atmospheric deposition to Lake Champlain as part of a mass-balance assessment for mercury in the lake.

- Dr. Miller gave a presentation at the New England Interstate Water Pollution Control Commission 2006 Mercury Science and Policy Conference in Newport, RI. The presentations from the conference can now be found online at: http://www.neiwppcc.org/hgconference/hg_archives.htm
- Dr. Miller attended a scoping meeting for the NADP proposed Mercury Trends Network (MTN) in 2006. The MTN is being proposed within NADP with support from USEPA Air Markets. The MTN is proposed to provide measurements of speciated ambient air mercury concentrations and estimates of mercury dry deposition. The Underhill site is considered to be an example of how the network sites could be configured and operated.
- Dr. Miller gave a presentation at the Lake Champlain Research Consortium annual meeting on September 29th, 2006. This presentation reviewed the atmospheric mercury research of interest to the LCRC members.
- Dr. Miller gave a presentation at the NADP annual meeting in October, 2006. This presentation reviewed the latest atmospheric mercury research at Underhill. Dr. Miller also presented a poster at the October NADP meetings describing the results of the 3-way mercury collector comparison. An identical poster was also presented at the VMC Annual Meeting, October 30th, 2006. Eric Miller and Sean Lawson gave a presentation on the Atmospheric Mercury Research project to members of the International Society of Environmental Journalists. The society held their annual meeting in Burlington, VT. Approximately 40 journalists participated in a field trip to UVM's Proctor Maple Research Center.
- The project team and the Vermont Monitoring Cooperative participated in hosting the spring 2007 NADP meeting in Burlington, VT. Dr. Miller made a presentation on operational considerations to a session of the meeting. Miller, Lawson, and Pendleton led a field trip to the Underhill Atmospheric Mercury Site as part of the meeting

Manuscripts in Preparation

1. Comparison of precipitation mercury samplers (Miller and others – target journal : *Environmental Monitoring and Assessment*)
2. Possible explanations for the lack of trend in wet deposition of mercury at Underhill, Vermont during a period of significant estimated mercury emissions reductions. (Miller, Poirot, Shanley, Cohen, Gratz, Pendelton, Lawson, Burkings, and Keeler – target journal: *Environmental Science and Technology*)
3. Climatology and Potential Sources of GEM, RGM, and Particulate Mercury at Underhill, VT (Miller, Poirot, Cohen, VanArsdale, others – target journal: *Environmental Science and Technology*)
4. Climatology and Potential Sources of Methyl-Mercury in Precipitation at Underhill, VT (Miller, Poirot, Shanley, others – target journal: to be determined)
5. Wet- and Dry-Deposition of Speciated Mercury at Underhill, VT (Miller, Poirot, Shanley, others – target journal: to be determined) *speciated wet = methyl and total, speciated dry = GEM, RGM, HGP.
6. Mercury Bioaccumulation in the Terrestrial Food Web of Montane Forests (Rimmer, McFarland, Miller, Faccio, and Taylor - target journal *Ecotoxicology*).

Summary of Project Results and Benefits

This project achieved the extension of the longest continuous record of event-based mercury deposition in the world. The collector comparison study facilitated a successful transition from the UMAQL network to the national MDN network. Results from the comparison study provided critical guidance for collector improvements and interpretation of the data collected by various networks. As has been clearly demonstrated through analysis of the impact of reduced sulfur emissions, long-term records are invaluable for trend detection and confirmation of the efficacy of emissions controls. The long-term record of atmospheric mercury levels at Underhill, VT represents one of the few opportunities for this kind of assessment with respect to mercury emissions reductions. Initial results from the period 1993-2007 show no measurable impact of the substantial reductions in municipal-waste and medical-waste incinerator emissions that occurred regionally and nationally during this time period. Instead, the long-term record and studies of potential source contributions using air-mass back-trajectory methods and the observations at Underhill demonstrated that northern New England receives the majority of its mercury deposition from long-range industrial and EGU sources that have not reduced emissions over the observation period.

The project's measurements of bi-directional GEM exchanges over New England forests helped to close the gap in understanding of the magnitude and driving factors for bi-directional GEM fluxes in forests. As new anthropogenic mercury emissions continue to be curtailed, the importance of diffuse sources of re-emission of prior mercury pollution will become more important to the atmospheric mercury burden. Understanding the magnitude and processes governing the canopy re-emission flux is essential to accurate modeling of the persistence of mercury pollution in the environment.

Previous studies at Underhill, VT demonstrated that significant amounts of Hg accumulate in the foliage of forest trees. Investigators speculated that this represented assimilation of atmospheric mercury. The GEM flux measurements conducted in this project confirmed that this process is occurring and represents a large annual transfer of Hg from the atmosphere to the landscape, roughly equal in magnitude to wet deposition.

Given the substantial accumulation of mercury in terrestrial ecosystems due to wet and dry atmospheric deposition, it was imperative to assess the extent to which mercury enters the terrestrial food web. Our measurements of mercury levels in foliage-eating insects and the birds that feed on those insects provided new insights into the magnitude of mercury bioaccumulation and biomagnification in terrestrial ecosystems. Our study has provided the most comprehensive and compelling evidence that biota at the mid- and top-levels of the terrestrial food web are at significant risk from atmospheric deposition of mercury.

Taken together, the results of mercury studies accomplished by the project greatly enhanced the scientific community's ability to assess current and future mercury deposition, re-emission, net ecosystem retention and risk to terrestrial biota across New England.

In-kind and Leveraged Funding and Companion Projects

The scope of project activities described above is broad. The funding provided by EPA-ORD for this project was substantially augmented with in-kind contributions from investigators and collaborators as well as by funds directed toward this research effort as a result of the leverage created by the cooperative agreement. Below we highlight major additional sources of support that will permitted the realization of the full scope of the research described above. The leveraged funds and in-kind support amounted to over \$250,000. The leveraged funding and many companion projects would not have been feasible with out the foundation of support for atmospheric mercury research provided by the EPA-ORD cooperative agreement.

- NOAA Sea Grant – LCRC – (\$40,000) support for analysis of archived ambient Hg samples
- VTANR-DEC-AQD-Air Toxics Program – (\$20,000) support for Tekran RGM system
- VTANR-DEC-WQD – laboratory services and analytical support
- VMC –VTANR-FP&R – targeted research funds (\$60,000) supporting E. Miller’s time
- VMC – UVM– in-kind support: facilities and sampling operations at PMRC
- ERG – in-kind support: micrometeorological flux measurement system, reduced indirect rate
- VINS/VCE – in-kind support: use of facilities and sampling equipment
- NOAA – (\$20,000) intercomparison study
- NOAA Sea Grant – LCRC – Funding for MDN event wet-deposition at Underhill, VT
- NOAA Sea Grant – LCRC – Lake Champlain Mercury Mass-Balance Study
- VTANR-DEC-AQD – Ticonderoga Mill Test Burn Study
- VTANR-DEC-AQD / EPA Region 1 – Mobile Mercury Facility Grant